Analysis and valorization of new thermal management systems for a vehicle powertrain application

Hanna Sara

UNIVERSITE BRETAGNE LOIRE

CENTRALE NANTES

Thèse de Doctorat

Hanna SARA

Mémoire présenté en vue de l'obtention
du grade de Docteur de l'École Centrale de Nantes
sous le sceau de l'Université Bretagne Loire

École doctorale : Sciences Pour l'Ingénieur, Géosciences, Architecture

Discipline : Energétique, Thermique, Combustion
Unité de recherche : Laboratoire de recherche en Hydrodynamique, Énergétique et Environnement Atmosphérique

Soutenue le 20 Septembre 2017

Analysis and valorization of new thermal management systems for a vehicle powertrain application

JURY

Rapporteurs :	**LEMORT Vincent**, Professeur, Université de Liège **PERILHON Christelle**, Maître de Conférences HDR, Conservatoire National des Arts et Métiers
Examinateurs :	**DELACOURT Eric**, Maître de Conférences, Université de Valenciennes et du Hainaut-Cambrésis **LANZETTA François**, Professeur des Universités, Université de Franche-Comté
Invité :	**CORMERAIS Mickaël**, Docteur, MANN+HUMMEL, Laval
Directeur de thèse :	**CHALET David**, Professeur des Universités, Ecole Centrale de Nantes
Co-directeur de thèse :	**HETET Jean-François**, Professeur des Universités, Ecole Centrale de Nantes

Acknowledgements

The PhD research work was carried out within the Thermodynamics of internal combustion engines team (TSM) of the research laboratory in hydrodynamics, energy and atmospheric environment (LHEEA) at Ecole Centrale de Nantes in a joined international teaching and research chair with MANN+HUMMEL entitled "Innovative Intake and Thermo-management systems".

Foremost, I would like to express my sincere gratitude to Pr. David CHALET, my thesis supervisor, to put his trust in my potential and capacities. Pr. Chalet's skillful guidance, precious advices and immense knowledge about the internal combustion engines were really appreciated and helped me to progress in the engine field as well as the time and task management. I would also like to acknowledge the support of Pr. Jean-François HETET, which accepted to contribute to this work.

I am very thankful to Dr. Mickaël CORMERAIS, the manager of the thermo-management competence center at MANN+HUMMEL France for his valuable input to this work. He contributed to the different discussions, and with his skills and expertise he helped to shape this project.

I would like to thank Pr. Vincent LEMORT and Dr. Christelle PERHILHON, Pr. François LANZETTA, and Dr. Eric DELACOURT to be part of the PhD committee. Thank you for accepting to review and examine this work as well as for your constructive remarks during the PhD defense.

Moreover, I am thankful for the technical support of my colleagues especially: Mr. Matisse LESAGE, Mr. Quentin MONTAIGNE and Mr. Antoine BOUEDEC and for their contributions to this work. In addition, I appreciate the support, help and good humor of Deepak KUMAR and Mohamad YASSINE. My further thanks go to TSM team for accepting me to be one of them, and to all the friends that encouraged me during the last three years.

Last but not least, I would like to express my genuine gratitude to my beloved parents for the unwavering support, love and sacrifices. They have been always a great motivation for me in every step in my life. As well, I would like to thank my two sisters, their families and my brother for all their encouragements. Thank you.

Table of contents

Nomenclature

Latin symbols

A	Area (m²)
a	Nusselt correlation constant
B	Cylinder Bore (m)
BMEP	Break mean effective pressure (Pa)
C	Coefficient
c_p	Specific heat capacity (J/Kg/K)
D	Diameter (m)
FMEP	Friction mean effective pressure (Pa)
g	Gravity = 9.81 m/s²
h*	Dimension less heat-transfer coefficient
h	convection coefficient (W/m²/K)
H	Heating value (MJ/kg)
HE	Heat exchange coefficient (W/K)
k	Heat exchange coefficient constant
L	Length of the Duct (m)
$\dot{m}$	Mass flow rate (kg/s)
N	Rotational engine speed (rpm)
Nu	Nusselt number
p	Pressure (Pa)
P	Power (W)
Pr	Prandtl number
$\dot{Q}$	Thermal power (W)
R	Radius
Re	Reynolds number
Sp	Instantaneous speed of the piston (mm/s)
T	Temperature (K)
v	velocity (m/s)
w	Local average gaz velocity in the cylinder (m/s)

Greek symbols

α	Exponent
λ	Air fuel equivalence ratio/thermal conductance (W/m/K)
μ	Dynamic viscosity (kg/m/s)
ν	Kinetic Viscosity (m²/s)
ρ	Density (kg/m^3)

τ	Torque (Nm)
φ	Heat (W)

Subscripts

a	Nusselt number constant
b	Brake
c	Engine's coolant
cold	Cold fluid
cr	Crankpin
cst	Constant
cv	Closed valve
ducts	Ducts in which oil circulates
f	Friction
fuel	Fuel
G	Global
gas	Gas
hot	Hot fluid
hyd	Hydraulic
i	Element i
in	Inlet
jet	Jets
m	Exponent
max	Maximum pressure in cylinder during current cycle
misc	Miscellaneous
oil	Engine's lubricant
out	Exit
ov	Opened valve
p	Piston
ref	Reference
th	Thermostat
wall	Combustion chamber walls
wall_losses	Cylinder walls

Acronyms

AH	Artemis Highway
AU	Artemis Urban

CAC	Charge Air Cooler
CADC	Common Artemis Driving Cycle
EGR	Exhaust Gas Recirculation
EU	Europe
HF	High Frequency
HP	High pressure
NEDC	New European Driving Cycle
NUT	Number of Transfer Units
TPA	Three Pressure Analysis
VGT	Variable Geometry Turbine
WLTC	Worldwide Harmonized light duty driving Test Cycle
WLTP	Worldwide Harmonized light duty Test Procedures

Introduction

Greenhouse gases trap heat in the atmosphere. Carbon dioxide (CO_2) is the primary greenhouse gas emitted through human activities. Fossil fuel use is the primary source of CO_2. Europe part of the global CO_2 emissions is 10% by 2011 [1]. Moving to CO_2 emissions by sector, a study done in 2010 in the world development report stated that the transportation sector contributes 13% of the global CO_2 emissions [2]. However, in 2010, an analysis of the final end use of energy in Europe shows three dominant categories: the transportation with the highest rate at 33.2% [3]. Figure 0-1 shows the equivalent of greenhouse gas emissions by type of transport. Some vehicle equipped with an internal combustion engine have the possibility to produce almost as same as flights.

Statistics done by Bosch reveal that the internal combustion engine dominates over the hybrid and electric new cars markets in 2015. Cars running on Diesel and gasoline engines reduced from 98% of the total cars sold in 2012 to 96.5% in 2015 [4]. In Europe, one fifth of the carbon dioxide comes from road transportation sector [5]. Moreover, trends showed that up to 2030 for the total transportation sector, oil products would still represent about 90% of the EU transport [6]. However, the activity of passenger cars and vans will always be ruled by internal combustion engine with around 67% in 2030 [7].

Table 0-1 shows the importance of the road transport sector in emitting the greenhouse gas CO_2, classified as the second source of emissions. Furthermore, highest oil prices pushed different countries to be less dependent on the fossil fuel and reduce their consumption. Consequently, legislations decided to limit the carbon dioxide of the different passenger cars by applying some emissions laws.

Table 0-1 - CO_2 emissions from fuel combustion by sector in 2014 (million tons of CO2)[8]

	Total CO_2 emissions	**Electricity and heat production**	**Other energy industry own use**	**Manuf. Industries and construction**	**Transport**	**Of which: road**	**Other sectors**
World	32381.0	13625.0	1683.1	6230.1	7547.3	5659.8	3295.5
North America	5731.0	2222.9	372.5	514.9	1905.1	1611.8	715.6
Europe	2609.0	868.1	135.8	338.4	778.7	738.8	488.1
China	9134.9	4415.7	364.2	2890.0	787.9	638.8	677.0
Asia Oceania	1593.6	765.2	91.4	277.7	315.0	277.7	144.3

In Europe, from 2005 to 2015, average CO_2 emissions decreased by more than 26% from new cars [9]. To meet the 2020/21 target of 95g CO_2/km [10], car manufacturers should keep on the same pace in decreasing the CO_2 emissions. Once the target is not achieved, excess emission premium varies from 5€/vehicle for the first exceeding gram, to 95€/g/vehicle if it exceeds by more than 3 grams [11]. From 2012 until 2018, the excess emissions premium shall be calculated using the following formulae:

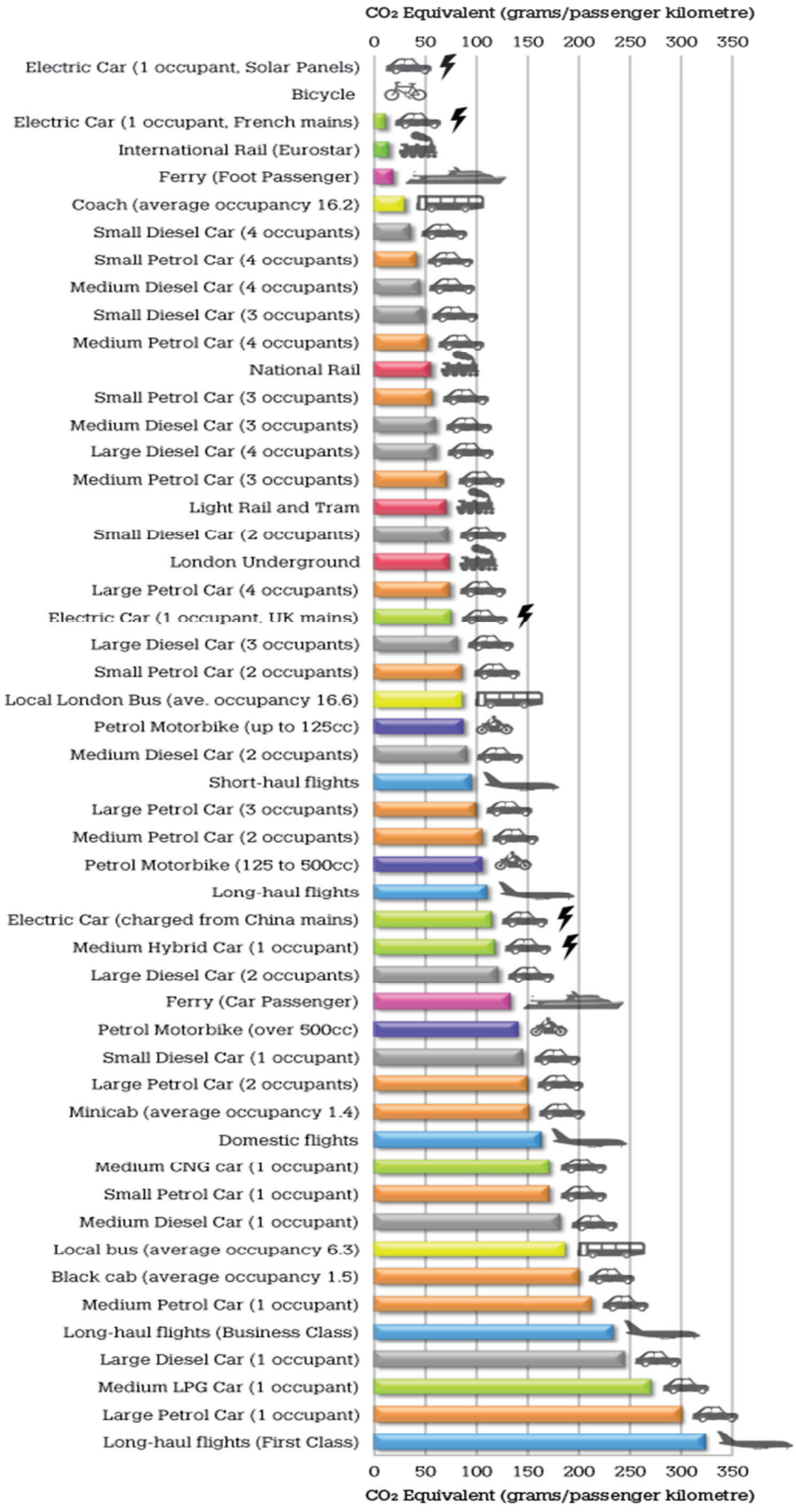

Figure 0-1 - Transport carbon emission [12]

((Excess emissions – 3g CO_2/km x 95 €/g CO_2/km + 1g CO_2/km x 25€/g CO_2/km + 1 g CO_2/km x 15 €/g CO_2/km + 1 g CO_2/km x 5 €/g CO_2/km) x number of new passenger cars. (0-1)

Starting 2019, any gram exceeding the target will be charged by 95€ per vehicle sold [13], [14]. Other countries as the United States of America and Japan had their own regulations with different limits.

To assess the CO_2 emissions on a vehicle, the latter should be run on a homologated driving cycle. New European Driving Cycle (NEDC) was chosen for the first regulations in Europe from Euro 1 to Euro 5. However, this driving cycle will be replaced by another more representative to the real life called Worldwide harmonized Light duty driving Test Cycle (WLTC). The latter will not be applied only in Europe with the Euro 6 but in Japan and other parts of the world. These driving cycles impose a cold start of the engine.

Moreover the statistics presented in Table 0-2 shows that the average length of travel in Europe is around a maximum of 10 km and for a short period of time while in the United States of America it is less than 15 km [15]. This leads to an engine always running in transient conditions.

Table 0-2 - Average trip length [16]

Country	Average trip length (km)
Cyprus	10.4
Germany (MiD)	11.5
Italy (ISFORT)	12.2
Latvia	8.7
Sweden	15.8
Switzerland	7.2

Furthermore, Rouaud *et al.* [17] shows in their study the difference between a cold start-up and an engine running in a steady-state thermal level. The engines were run on a NEDC with a cold engine with water and oil at 20°C which is the standard test and with a hot engine with the water and the oil at 90°C. For 8 vehicles equipped with a Diesel engine, the fuel consumption difference ranges from 8.9% to 12.8% between the two cases.

First research studies to reply to the emissions laws focused on the engine efficiency by improving its combustion efficiency, filling efficiency, different valve openings, different stages of turbocharging, etc … Thus, on one hand those strategies will help the engine to better function in steady-state or to reduce its losses to the coolant and lubricant. The latter will lead to a slower warm-up of the engine's fluids: the coolant and the lubricant. Hence, a higher level of heat losses to the coolant and higher friction power are obtained.

Finally, to answer the emissions laws that impose a cold start test of the engine, studies shifted to thermal management. Thermal management proved itself as one of the main field in minimizing the engine fuel consumption. Thermal management consists in the study of energy flows in the engine starting from the chemical energy of the fuel injected in the combustion chamber to every energy flow: either to the chamber walls, the exhaust gases or the work produced by the engine.

Thermal management target is, as shown in Figure 0-2, to improve the warm-up phase of the engine without any electrical components. The latter is done by improving its temperature during the transient phase and to reach the regulating temperature in advance comparing to a reference case, the engine without any thermal management strategies applied. Also, thermal management consists to let the engine works at a higher temperature during the steady-state phase to improve its efficiency. The latter is applied with a reliability respect especially to the different thermal stresses resulting from this higher temperature.

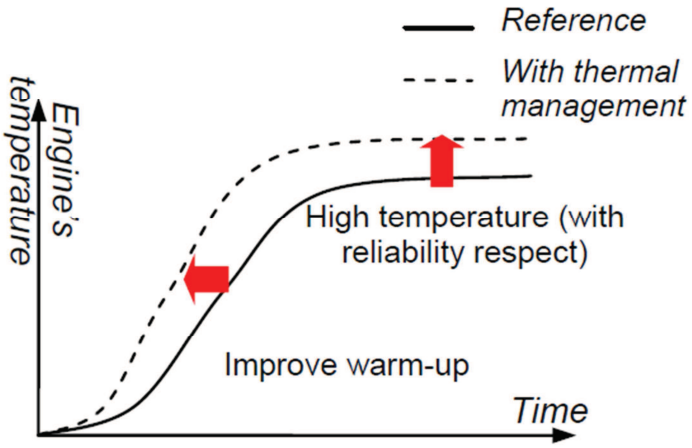

Figure 0-2 - Thermal managemnt target

Application of the thermal management consists to find a new product (hardware or software) to let the different components present in Figure 0-3 work at their regulation temperature.

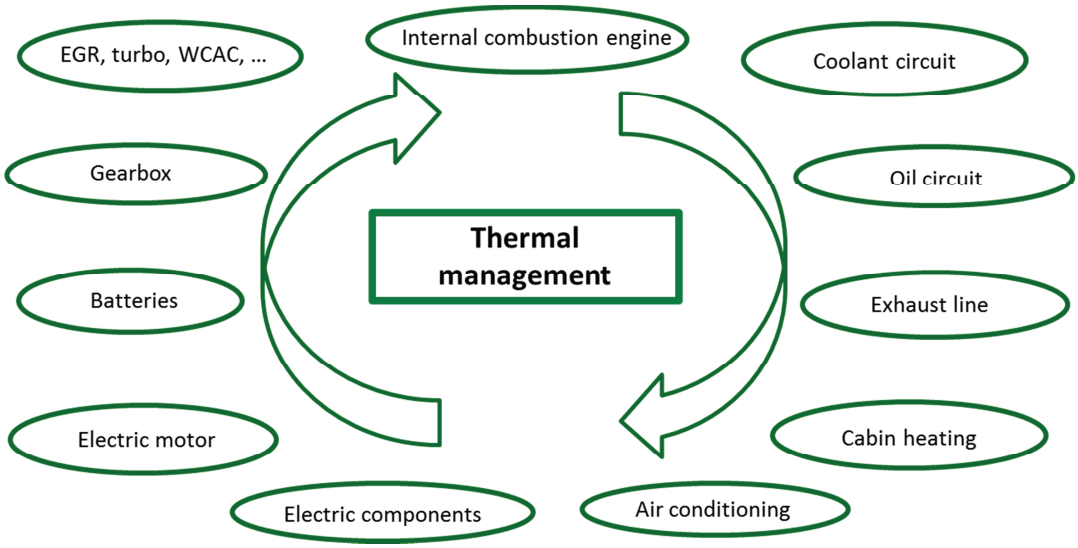

Figure 0-3 - Thermal management in a product point of view

However, making prototypes and testing them on different experimental benches are time consuming and cost effective. Different prototypes should be designed then produced and moved on to different tests. It starts by product test bench to study its endurance, then engine test bench to evaluate its influence on the engine environment. Finally, it ends with a vehicle test bench to assess the different influences on a vehicle environment taking into consideration much more realistic approach than the engine test bench.

This thesis aims to valorize the different thermal management strategies applied on internal combustion engine in terms of fuel consumption by the means of numerical simulations. To attend the target, different engine tests were made upon to calibrate a GT-Suite model and then different strategies were proposed to be evaluated over different driving styles and under different conditions.

The first chapter of this thesis consists of a literature survey. It allows understanding the physics behind the different aspects of thermal modelling covering the heat transfer correlations as well as the heat source in the engine. In addition, energy and exergy balances are introduced highlighting the main results over the years. Finally, thermal management products as well as strategies over the past years were mentioned. The chapter explains the different strategies and covers their main potential as stated through the previous studies.

Chapter two is the first of the thesis. It covers the basics and the essentials used in the study. It covers the experimental setup done to build up a complete engine model with its hydraulic circuits. Then, the GT-Suite model were described and presented. Once it was calibrated and the different driving cycles and the different conditions were presented, an energy balance of the engine and its coolant and lubricant circuits was done. The aim of the energy balance is to highlight the importance of the different losses in the engine, and thus to define the best thermal management strategies as solutions for these losses.

Once, the energy balance and the different thermal management strategies are defined. Chapter 3 covers the application of the first strategy: Heat storage. It is divided into two parts. The first one is using the hot coolant in the system to store heat for a further use. The study covers the different steps to define the right volume, initial temperatures and heat loss during the soak period. The second part concerns hot oil storage. Both parts were applied on different driving cycles at different ambient temperatures and in different configurations.

Chapter four focuses on the exhaust gas heat recovery. A heat exchanger was characterized and integrated in the model. Indirect and direct oil heating were tested and results for different driving cycles were issued.

Chapter five consists of the study of different minor thermal management strategies such as: engine insulation, changing the oil’s grade, by-passing EGR cooler and the charge air cooler, and high temperature set point.

Finally, the conclusion covers the main results of the different driving cycles as well as presenting new perspectives for an upcoming work.

I. Literature survey

Internal combustion engine main losses are within the exhaust gases or transferred to the coolant circuit at the combustion chamber walls. Global warming becoming a worldwide concern pushed toward lowering greenhouse gas emissions. Road transportation is one of the main sources of CO_2. Reducing CO_2 is done by lowering the fuel consumption. Thermal management made a big step in improving the engine thermal efficiency and thus leading to fuel consumption savings. However, new thermal management ideas should be tested and its potential should be valorized before it is applied on different engines. For that purpose, modelling and numerical simulations are important nowadays. This literature survey covers the different aspects of heat transfer and heat sources modeling. Then, it focuses on the different energy balances done over different internal combustion engines. These energy balances underline the important losses in the engine and highlight their variation in function of different conditions and operating points. Finally an important part of this study covers the different thermal management products and strategies in the previous years. Control valves as well as new electrical and variable speed pumps are introduced. Thermal management strategies such as: zero flow, split cooling, high temperature set point, engine insulation, heat storage, exhaust heat recovery, oil application were evaluated through the previous years and the main results are presented in this chapter. A small part was conserved to the li-ion battery thermal management as the hybrid vehicles are the new trend and the promising solution for city travel.

I.1. Modeling

Internal combustion engine optimization is based on understanding and improvement of the combustion and monitoring the thermal process. Heat transfer does not only affect the engine performance, fuel consumption and emissions but also the cooling system architecture, under-hood thermal management and the passenger thermal comfort.

By modeling the heat transfer in the engine, modifications can be easily evaluated with a minimum construction of prototypes and experiments. This allows a better and faster engine design, more efficient with an improved thermal management. Despite the fact that engine simulations are faster and cheaper than prototypes, modeling needs more input parameters, faster computing systems …

At first, numerical simulation is used as a tool to obtain results and to assess different system potentials. In a second phase, it becomes an analysis tool. At the end, it develops and enters the phase of model reductions. This reduction allows highlighting and having simplified models which are used for real time process control, diagnostics …

The model is made from a series of equations introducing a constraint between different parameters of the system. In case of thermal management, those parameters are generally temperature and pressure. The model has to be calibrated and validated by experimental results.

To define a good thermal management model, this part covers the state of art of modeling the heat source of the coolant and the lubricant circuit, the interactions between the latters at the oil cooler, the heat transfer for both fluids and the management of the both circuits. To assess the effect of the thermal management on the engine efficiency, one of the crucial parts is the combustion model. It defines the heat released from the burning fuel depending on all the physical parameters surrounding the combustion chamber. Finally, a dynamic coupling between the combustion model and the fluids circuits, as done by Luptowski *et al.* [18] leads to assess and valorize the different new thermal management strategies.

I.1.1 Heat sources

The heat source in the engine is not exclusive for the combustion process but a part of it comes from different mechanical parts friction.

I.1.1.1. Combustion

An important amount of power produced by the combustion process is lost in form of heat transferred to the coolant. Two types of heat transfer take place in the combustion chamber: forced convection and radiation. They take place between the combustion gases and the cylinder block, the cylinder head, and the piston. They occur also between the cylinder head walls and the inlet and exhaust gases.

Heat transfer between the gas and the walls is composed of a convective term and radiative one. The convective part depends on the aerodynamics conditions of the combustion chamber. Other than the gas movement resulting from the piston translation, there is the swirl and squish movement. It should be noted that the radiative part is negligible in spark ignition engine since it presents only 3 to 4 % of heat transfer. In contrary, because of the particles,

carbon dioxide and water vapor, the radiative part in Diesel engine is about 7 to 23% of the total heat transfer in the combustion chamber [19].

Heat transfer fluctuates greatly through the cycle. Temporal fluctuations could be ignored by imposing a mean and a constant temperature and convective heat exchange coefficient averaged over the four phase of the cycle [20].

Studies were made to define the global exchange coefficient. The most used one is elaborated by Woschni [21] based on turbulent forced convection. Throughout the studies, the authors modified the correlation based on their engine tests and experiments [19], [20], [22], [23] [24]. For example, Douxchamps [22] correlation is as follows:

$$h_G = 3.26\, B^{-0.2}\, p^{0.8}\, T^{-0.55}\, w^{0.8} \tag{I-1}$$

The characteristic velocity w is dependent on the cycle's phase.

Other formulas exist for the global convective heat exchange.

Nusselt correlation

$$h_G = 0.99\left(pT_{gas}\right)^{\frac{1}{3}}\left(1 + 1.24\, v_p\right) + 0.362\,\frac{\left(\frac{T_{gas}}{1000}\right)^4 \left(\frac{T_{wall}}{1000}\right)^4}{T_{gas} - T_{wall}} \tag{I-2}$$

Eichelberg correlation

$$h_G = 2.1\left(pT_{gas}\right)^{\frac{1}{2}} v_p^{\frac{1}{3}} \tag{I-3}$$

Pflaum correlation

$$h_G = cst\left(pT_{gas}\right)^{\frac{1}{2}}\left(3 \pm 2.57(1 - e^{1.5-0.416 v_p})\right) \tag{I-4}$$

Annand correlation was different; it considers the convective and the radiative part with the following correlations.

$$Nu = a\, Re^{0.7} \tag{I-5}$$

$$\phi_{gas \to wall} = A_{gas-wall}\, c\,(T_{gas}^4 - T_{wall}^4) \tag{I-6}$$

"a" is a constant between 0.35 and 0.8.

"c" is a constant worth $3.3 \cdot 10^{-8}$ for the Diesel engine and $4.3 \cdot 10^{-9}$for the gasoline engine during combustion and expansion phases. In other cases, "c" equals zero [19].

Woshcni correlation was compared to those of Eichelberg, Nusslet, Annaud and Pflaum in Figure I-1. The disparity of the coefficient is due to its dependence on the combustion chamber and the cylinder geometry.

The heat transfer between the intake/exhaust gases and cylinder head walls is described by considering two cases: one while the specific valve is opened and one while it is closed [25]. The global exchange coefficient is as follows:

$$h_G = 0.25h_{ov} + 0.75h_{cv} \quad \text{(I-7)}$$

The developed calculation can be found in the work of Alexander *et al.* [19] and Jarrier *et al.* [20].

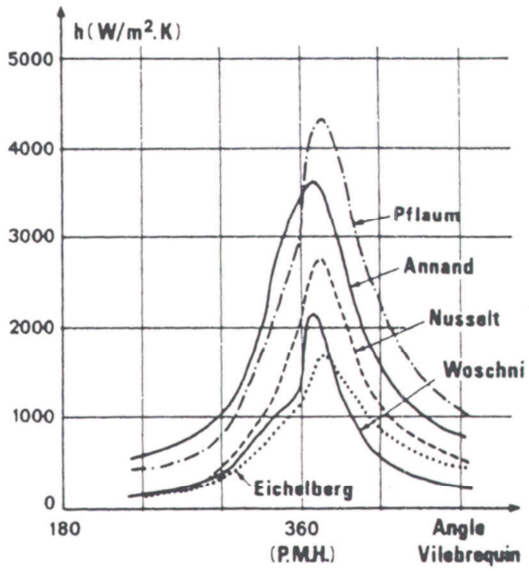

Figure I-1 Global convection coefficient variation with the crank angle [22]

I.1.1.2. Friction

The second major source of heat in the engine is friction. Studies show that the friction mean effective pressure (FMEP) is proportional to the viscosity of the lubricant (function of temperature) and to the engine speed and little influenced by the engine load. According to Jarrier *et al.* [26], for a transient state after a cold start, in function of oil viscosity, the FMEP is calculated for each component i by:

$$FMEP_i = \left[a_i\left(\frac{N}{1000}\right)^2 + b_i\left(\frac{N}{1000}\right) + c_i\right].\left(\frac{\nu_{oil}(T_{oil})}{\nu_{oil}(90°C)}\right)^{d_i} \quad \text{(I-8)}$$

$a_i, b_i \; and \; c_i$ are coefficients identified by the mean least square method for oil temperature of $90°C$. The exponent d_i takes into account the lubrication regime in the component and differs from one to another. For the crankshaft, the Petrroff's law supposed that FMEP evolves proportionally with the oil viscosity ($d_i = 1$). For the pistons and its rings, the friction is elasto-hydrodynamic ($d_i = 0.5$) [27]. For other components, they have a small contribution of the engine friction and are independent from its temperature ($d_i = 0$).

Millington and Hartlés in their work proposed a correlation for the steady state running conditions [28] (I-9) , then Shayler proposed a correction for the transient conditions [29].

$$FMEP = cst(96.5 \cdot 10^3 + 48.3\ N + 400\ v_p^2) \quad \text{(I-9)}$$

cst takes into consideration the recent progress in the friction field.

Chalet *et al.* [30] defined a system for three equations of FMEP based on experimental tests. In their study, the internal combustion engine was powered by an electrical motor. Its power estimates the friction losses. Their model consists of a total friction power that is the sum of the friction power at the crankshaft, valve train and pistons.

Once the friction power is defined, it needs to be transmitted to the different part of the engine. Most of the studies proved that the friction coming from the piston is the highest during the transient phase (around 58%) [19] and is 45% of the total friction power when the oil's temperature is 30°C [26]. Thus, when the engine is cold, the friction power is entirely transmitted to the metal masses. The share of friction power going to the oil progressively increases until it reaches 40-50% [31]. However, some assumed to divide the friction power created between two masses separated by a thin oil film to: 30% for each metal mass and 40% to the oil [30].

I.1.2 Heat transfer

High temperature will cause thermal stress, and thermal stress will lead to material fatigue. The three main ways to evacuate heat in engine are:

- Coolant circuit
- Lubricant circuit
- Direct exchange with the ambient by convection and radiation

I.1.2.1. Engine walls and coolant

Different architectures of the coolant circuit exist for the internal combustion engine. The most common architecture leading to a better thermal homogeneity of the engine is the diagonal architecture. The coolant flows on both faces of the cylinder, go up to the cylinder head and then get out at the opposite side of the coolant inlet.

The heat exchange coefficient is calculated using the correlation of a turbulent flow forced convection of Dittus and Boelter [19], [20], [22]:

$$Nu = 0.023\ Re^{0.8} Pr^{0.3} \left(\frac{\mu(T_c)}{\mu(T_{wall})}\right)^{0.14} \quad \text{(I-10)}$$

This correlation does not take into account nucleate boiling. A phenomena appearing when the surface temperature is hotter than the saturated fluid temperature by a certain amount called overheating degree. The phenomena influence on the heat transfer is studied by Alexandre *et al.* [19]. The coolant circuit architecture as well as the coolant flow, temperature and the pressurized system are dimensioned to prevent nucleate boiling from happening.

I.1.2.2. Oil cooler

The main aim of the lubricant in the engine is to reduce its friction. However, the dissipation of the friction power to the oil leads to increase its temperature. To maintain a good performance of the oil and to prevent its deterioration, hot oil needs to be cooled during the

cycle. At the oil cooler, the oil is cooled by the coolant. The transfer between the engine's fluids can be modelled by the NUT method. An application of this method on different heat exchangers was made by Umekar *et al.* [32]

The method proceeds by calculating the heat capacity rates of the two fluids, then by identifying the minimum and the maximum of the two capacities. The global heat exchange between the cold and the hot fluid is defined as following [22] [33]:

$$HE = \frac{1}{k_1 \dot{m}_{cold}^{0.6} + k_2 \dot{m}_{hot}^{0.8} + k_3} \quad \text{(I-11)}$$

With $k_1 = 4.737 \cdot 10^{-4}$, $k_2 = 8.416 \cdot 10^{-4}$ and $k_3 = 7.418 \cdot 10^{-4}$.

I.1.2.3. Oil and Metallic components

Three different heat exchanges between the oil and the metallic components can be distinguished.

The first type is the convective effect between the pressurized oil and the ducts in which it circulates. It takes place in the engine block and the cylinder head. Some authors used the same correlation as for the coolant, described by equation (I-10) [20]. Other researchers [19], [22] considered the ducts smooth enough to ensure laminar flow despite the running conditions and used the following equation with a Nusselt number equals to 4:

$$h_{ducts} = \frac{Nu\ \lambda_{oil}}{D} \quad \text{(I-12)}$$

The second heat transfer occurs when the oil streams back to the crankcase along the cylinder head and the engine block. For an horizontal stream, authors used the correlation established by Danno [34] that is the same of Pohlhausen as presented in Welty *et al.* [35]:

$$Nu = 0.664\ Re^{0.5} Pr^{0.33} \quad \text{(I-13)}$$

For the vertical stream all along the return duct from engine block to oil sump, Hausen proposed the following correlation as presented in Incropera *et al.* [36]:

$$Nu = 3.66 + \frac{0.00668X}{1 + 0.04\ X^{0.66}}\ with\ X = \frac{D_{hyd}}{2L}\ Re\ Pr \quad \text{(I-14)}$$

The return by gravity was defined by Fujita and Ueda [37] as follows:

$$Re = \frac{4\dot{m}}{\mu D}$$
$$h^* = 2.27\ Re^{-0.33} \quad \text{(I-15)}$$
$$h = h^* \lambda \left(\frac{g\rho^2}{\mu^2}\right)^{\frac{1}{3}}$$

The third heat transfer is between the oil jets and the piston. Seale and Taylor [38] considered it as a forced convection and proposed the following correlation:

$$h = 68.2 \sqrt{R_{cr} N \frac{\rho_{oil} D_{jet}}{\mu_{oil}}} \quad \text{(I-16)}$$

Pirotais [33] proposed a correlation independent from the temperature. The correlation considers a reference coefficient of $1000\ W/m^2.K$ with a corrective term that takes into consideration the rotational engine speed. The same correlation was used by Bohac *et al.* [39] with the reference coefficient of $900\ W/m^2.K$.

$$h = h_{ref} \left(\frac{N}{4600}\right)^{0.35} \quad \text{(I-17)}$$

I.1.2.4. Ambient

Under hood flow velocity is in the range within 5-10 m/s. Thus, the resulting convective heat exchange coefficients are in the range within 10-50 W/m².K. The following values are retained [19]:

- Oil pan 50 W/m².K
- Engine block 20 W/m².K
- Cylinder head 20 W/m².K

The radiative part is too complex to be modeled, surface emissivity is considered around 0.7-0.8. This complexity calls for a 3D simulation. It is considered that external heat transfer, convective or radiative, has little influence on the internal temperature of the engine and on the combustion chamber energy loss.

The coolant heat evacuation to the ambient takes place at the radiator. The fins are the most sensible part of the radiator. Different parts of radiators, as well as its modelling were studied by Bontemps [40].

I.1.3 Nodal modeling

Nodal modeling is one of different types of modeling. It is largely used in different applications, and it is based on the thermal/electrical analogy. The engine system within this method is discretized into a finite number of nodes, metallic masses, coolant circuit and lubricant circuit, each of which is assumed to be isothermal. Each volume constitutes a node with an energy balance that takes into consideration its interactions: convective, conductive or radiative exchange with the other nodes or with the heat source node. In transient phase, the thermo-physical parameters such as the dynamic viscosity, thermal conductivity vary in function of the intensive variables such as temperature, pressure …

Nodal modeling were found in different authors works [17], [20], [23], [39], [41]–[47], and an application on GT-Suite software is done by Lahuerta *et al.* [48]. For example, Jung *et al.* [49] presented different sub-models such as thermal mass, coolant circuit, lubricant circuit, heat transfer, friction and exhaust linked with the combustion process, and its energy flow to define the different mass temperatures.

The important step in the nodal model, yet it is the first one, is to know how to discretize the system. On one hand, a finite discretization leads to highly accurate and fine results but on the other hand, it leads to high computational time.

Douxchamps [22] developed the nodal modeling in his PhD work. Different formulae of the different types of conductance were presented at first. Then, he developed the hydraulic modeling of the coolant and lubricant circuit by presenting the different formulae of the pressure drops in the different tubes, pumps defining by that the right flow rate in each branch of the fluids circuits. Then, the thermal circuits of the lubricant and the coolant in its different architectures (diagonal and pin circulations) were shown.

I.1.4 Thermodynamic model

The thermodynamics is the heart of the engine model; it provides the heat losses necessary for the prediction of different temperatures. Its inputs are fuel flow rate, pressure and temperature of the intake and exhaust plenum and the rotational engine speed.

There are two types of thermodynamic models: one zone and multi-zones models.

In the one zone model, the first law of thermodynamics is applied. The mass fractions, temperature and pressure are considered uniform throughout the cylinder. This type of model is used by all the engine designers. Correlations of different heat losses and the first law of thermodynamic for the one zone model are developed in Alexander *et al.*'s work [50]. An application can be found in Pirotais *et al.* [51].

In the multi-zone model, the pressure is considered uniform in the cylinder, but the temperature is only uniform in small volumes or zones. The number of zones starts from two. In this case, the cylinder is divided in two zones: burnt and unburnt gases. The number of zones can increase to higher number leading to more finite models. The number of variables and equations is directly linked to the number of zones.

The thermal losses in both models are computed using the following correlation [22]:

$$Nu = \frac{hL}{k} = aRe^{b}Pr^{c} \qquad \text{(I-18)}$$

The velocity used to compute the Reynolds number is a function of the mean piston velocity and the turbulence created by the mixture combustion.

To define the heat loss in the cylinder, the heat source coming from the combustion should be modeled and defined. The burnt fuel mass fraction is defined by a combustion law, the Wiebe law giving the rate of combustion as function of the crank angle. It is determined by a combustion delay and two combustion modes: premixed and diffusion as shown in Figure I-2. Premixed combustion corresponds to a peak in the combustion rate: the fuel evaporates and mixes with air without burning because of a delay set by the chemical kinetics. Once the delay is over, all the mixture prepared during this time interval burns very quickly. Diffusion combustion is defined by the diffusion of the fuel and the flame by the oxygen left in the chamber.

Ignition delay as well as the heat release from the combustion is developed in different authors works for different engine types [22], [26], [50], [52].

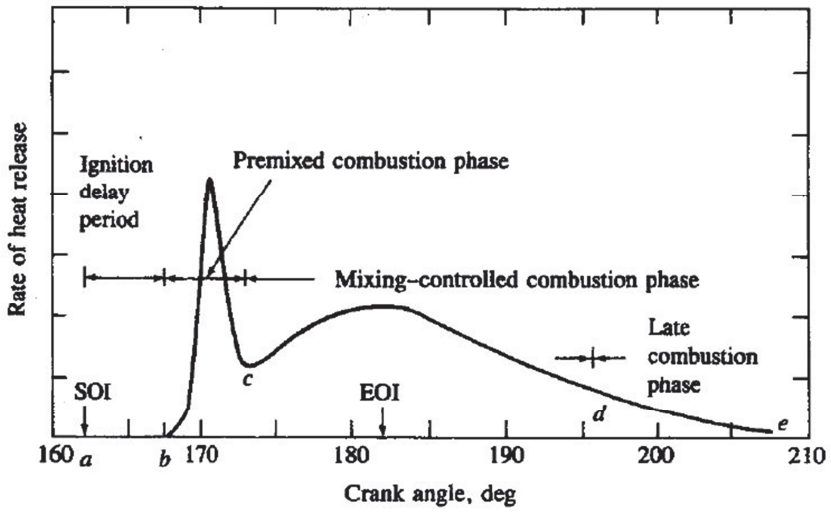

Figure I-2 Heat release rate at the different Diesel combustion phases in function of the crank angle [25]

I.2. Energy balance

Energy is a physical parameter that characterizes the state of a system and it is conserved through transformations. It is measured in Joules. It exists in various forms: mechanical, electrical, magnetic, nuclear, thermal, chemical … Applying the first and second laws of thermodynamics on internal combustion engine helps understanding every form of energy flow, transformation, loss, irreversibility and recovery. The fundamentals of energy is studied by Marty [53], and its well developed in Winterborne book [54].

The creation of entropy has served to measure the degradation of energy by the irreversibilities of energetic transfer and transformations. To directly compare to energy, exergy was introduced [55], [56]. As defined by Lallemand [57]:

Exergy of a certain quantity of material contained in a system is a measure of the ability of production of maximum work by the super-system (system and its ambient), which lets the quantity of material from its initial state to an inert state of equilibrium with the ambient.

Exergy application on the internal combustion engine was found in different researchers studies. The different formulations of the exergetic forms for closed and opened system were developed by Benelmir *et al.* [56] and Sayin *et al.* [58]. Chemical exergy of fuel used in engines was one of the hardest exergy to define in the balance. Some authors did not take it into consideration [59]–[61]. Others used different correlations depending on the fuel type [58], [62]–[65]. Defining the environment, a viral condition to define the exergy, took some important part of their study differing between two types: either taking into consideration the system chemical equilibrium or either not [66]–[68]. Comparison between the two physical quantities: energy and exergy is done by Dincer *et al.*[69] and Caton [70].

Rakopoulos *et al.* [59] presented a detailed exergy analysis for different parts of an internal combustion engine: starting from the chemical exergy of the fuel, to the cylinder, turbocharger, after-cooler, inlet manifold, exhaust manifold to end with the definition of different efficiencies. The exergy balance was applied on a six-cylinder turbocharged Diesel

engine with a charge air cooler at 1800 rpm and 70% load. However, in another work, Rakopoulos *et al.* [71] proved that increased rotational engine speed with constant load reduces heat transfer to the wall. Moreover, cylinder irreversibilites decrease during the transient phase due to the decreased combustion irreversibilities at higher load. Also, exhaust gases exergy increases with the load or speed, thus with the decreasing of the heat transfer losses.

Throughout years, energy balance analysis was coupled with exergy analysis in most of the internal combustion engine applications [72]–[80].

In his review, Caton [70] discussed a result of an energy and exergy balance. As represented in Figure I-3, not all the energy in the heat transfer has the ability to reproduce work. The heat transfer energy is 12.6% while its exergy is only 9.7%. The same difference is obtained with the exhaust gases. An important part of the exergy is destroyed in the combustion process.

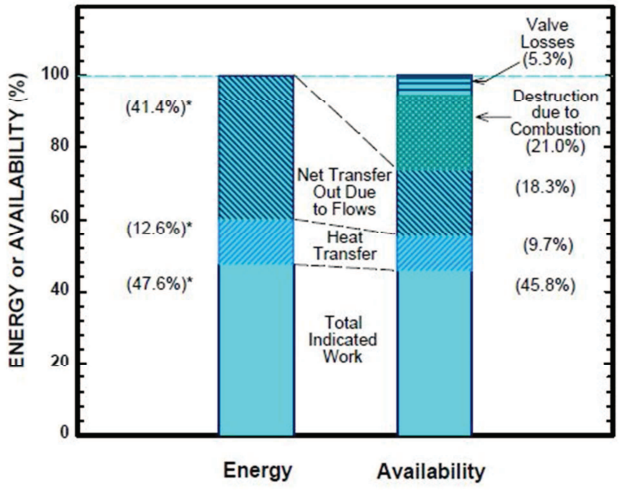

Figure I-3 Percentage of the fuel's energy and exergy (Adapted from Flynn *et al.* [60])

Alkidas *et al.* [75] applied an energy balance on two single-cylinder, water cooled and uncooled Diesel engines. For the same BMEP, the uncooled engine presents a better energetic efficiency. Based on their energy balance, heat transfer loss of uncooled engine was found to range between 50-70% of water cooled engine heat transfer.

The energy balance done by Lipkea *et al.* [55] on a six-cylinder heavy duty, direct injection, turbocharged and intercooled Diesel engine gave an outcome of 35-40% of indicated work, while exhaust gases and heat transfer were around 60% of the fuel energy.

Al-Najem *et al.* [62] applied an energy balance on a turbo-charged, Mercedes-Benz OM422A Diesel engine with a power output of 243 kW and an air/fuel ratio equals to 20. The losses to the coolant circuit were estimated by 25.66% while that to the exhaust gases were 24.12% of the total fuel energy introduced to the engine which is 648.8 kW.

Taymaz [81] compared an energy balance of an engine before and after insulation for different engine load and speed. With the insulation of the engine at high load, the heat loss to the coolant circuit was reduced by 3%. However, the exhaust gases energy increased by 8%. Insulating the engine leads to higher wall temperatures, thus a lower volumetric efficiency.

Energy application was used to valorize the effects of the altitude of a turbocharged Diesel engine [67]. However, the energy balance outputs an indicated work around 45%, while heat transfer and exhaust gases varied each around 25 to 30% depending on the altitude.

Bourhis *et al.* [64] made a study on a Diesel and a gasoline engine. The comparison of each engine was made on two partial loads operating points: 1500rpm, BMEP = 0.3MPa and 2300 rpm, BMEP = 0.8MPa. For the Diesel engine, the effective work increased from 29% to 34%, while the total of the heat losses and the exhaust gases decreased from 57% to 51%. The major losses were transferred to the coolant circuit around 31% that decreased to 19% while the exhaust gases increased from 15% to 25%. For the gasoline engine, the output work was increased from 22% to 32%, the heat losses either to the engine's fluids or the exhaust gases increased from 39% to 45% due to a decreasing of the other energies in the study (air heating under hood, pressure drop, mixing, etc.). Engine output work is less in the case of gasoline engine due to lower engine combustion efficiency. And with engine load increasing, the recoverable energy contains more potential for a re-useable work. Sayin *et al.* [58] made an energy balance as well as an exergy balance on a gasoline engine for different operating points. Heat transfer and exhaust gases losses were presented in different units and not in term of a percentage of the fuel energy.

During the comparison of the Diesel and Biodiesel performance, Sekmen *et al.* [82] made an energy balance on a 4-cylinder Diesel engine. They assessed a heat transfer of 30.09% and exhaust gases losses of 35.36% on an operating point of 100 Nm and 2000 rpm.

To evaluate the energy utilization efficiency of gasoline engine and define the recovery potential for waste heat energy, energy distribution of a naturally aspirated, 4-cylinder, 4 stroke, gasoline water cooled engine has been studied by combining the energetic and exergetic methods by Fu *et al.* [72]. Test speed range was set from 1000 to 5500 rpm with an increment of 500 rpm. The load varies from 0.1 MPa till full load with a 0.1 MPa step. The exhaust gases energy varied between 17% to almost 34% depending on the engine speed and load. Its percentage increases with the speed under most of the operating conditions. Contrary to the exhaust gases, the cooling water energy is high at low operating points and low speed. However, under high load and high speed operating points (especially at full load), it is lower than exhaust gases energy. The coolant energy varies from almost 22% to 50%.

In a recent study, Payri *et al.* [83] made an experimental analysis of the global energy balance in DI Diesel engine. Depending on the engine operating points, its brake efficiency ranged between 30% and 38%, the exhaust gases enthalpy between 18% and 34% and the heat transfer to the coolant was defined around 20%. Moreover, the heat transfer to the oil varied between 4% and 10%, the heat rejection in the intercooler varied between 1% and 7% and the miscellaneous term between 2% and 15%, where the latter high percentage is attended at low speed and load points. Romero *et al.* [84] stated from his experimental studies that more than 30% are accounted as energy losses and for the first third of NEDC cycle, a large part goes to heating the engine masses.

Finally the energy balances throughout the different studies marked a huge amount of heat transferred to the coolant and within the exhaust gases. These percentages highlighted the importance of applying different thermal management strategies either on the coolant circuit or the exhaust line to remedy these losses and increase the engine thermal efficiency.

However, all of the energy balances during the state of art were applied on specific operating points of the engine without taking into consideration complete driving cycles, which is intended to be done in this thesis in order to define the best thermal management strategies to apply on the engine and assess its fuel consumption savings.

I.3. Thermal management systems

In response to strict emissions regulations, extensive researches were made upon developing the coolant and lubricant circuits.

I.3.1 Control valve

The thermostat controls the temperature of the coolant circuit. It blocks the radiator branch while the temperature of the coolant, thus that of the engine, did not reach the regulation temperature. The control valve of the coolant circuit evolved through the years.

The basic configuration is a mechanical wax thermostat that expands with the elevation of the temperature.

The following generation was the smart thermostat or the electronic controlled thermostat. From Cipollone *et al.* [23] point of view, the traditional wax thermostat works by maintaining a stable coolant's temperature, which does not change with the engine load and speed, leading to high variations in metallic masses temperature. However, with the new 'smart' thermostat, the electronic control is made in a way to keep a steady metallic mass temperature and to vary the coolant temperature based on the engine speed and load. The 'smart' thermostat is tested in order to minimize the engine temperature fluctuations [42] [85], its control was bi-dimensional in function of the engine speed and load [43]. A map-controlled thermostat tested on a compact SUV with a 2L 4-cylinder gasoline engine leads to 0.9% of fuel consumption advantage at the end of NEDC [86]. The real effects starts once the thermostat is operating during the steady state stage.

Audi/Volkswagen used a heating resistor to control the thermostat. The resistor was integrated in the wax thermostat. Opening temperature was raised in their study. When energized, the heating resistor heats the wax thermo-couple additionally. The stroke (the displacement of the thermostat) is not only performed in function of the coolant temperature, but as specified by the map stored in the engine control unit [87]. Figure I-4 shows the operating range of the different type of thermostats. With the heated thermostat, the operating range is widened and engine can be operated hotter than usual (at 100°C to 110°C in partial load conditions) leading to an advantage of 1-2% in fuel consumption. The electronically controlled thermostat increases the flexibility to an optimum level [88].

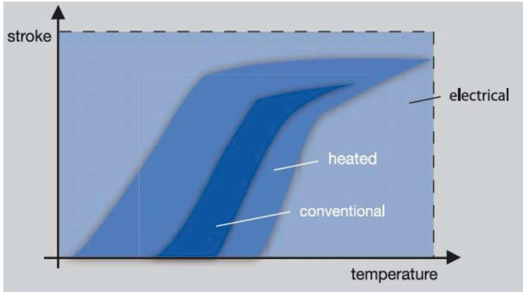

Figure I-4 Operating range of thermostats [88]

The latest innovation is the multi-way valve. It's the concept of the thermostat upgraded in housing able to control the flow proportionally to different branches of the engine such as the by-pass branch, the radiator, EGR loop, and the heater. Multi-way valve can divide the flow to the engine into two (split cooling strategy), or can block any circulation of flow into the system to have a faster warm-up phase (0-flow strategy). The multi-way valve are boosting between car manufacturers because it replaces the smart thermostat and the electrical variable flow coolant pump.

Mitchell *et al.* [89] made a comparison between different thermostat valve configurations: basic wax thermostat, two-way, three way-thermostat and no valve at all. The three way valve configuration provides the most benefits in terms of temperature tracking, warm-up time and power consumption, with very few drawbacks in system design.

Krause *et al.* [90] configuration of a multi way valve consists of a circular housing with a flow restrictor that controls the coolant in the different branches. However, this configuration did not include the EGR branch and did not have a fail-safe characteristic in the case of a malfunctioning of the valve. The model led to lesser temperature fluctuations, a faster warm-up, and a 3% reduction of fuel consumption.

A three way valve controlled electromagnetically was presented in Mohamed's work [91]. It consists of two opposing electromagnets, an armature, two springs and a three way valve. During the cold start-up, a current in the coil of the upper magnet is used to hold the armature up and close the radiator branch, thus open the flow to the bypass. During the steady state stage, a current applied to the lower magnet, attracts the armature to its side and hence opens the radiator branch (Figure I-5). An application over a turbocharged 4-cylinder Diesel engine reduced the warm-up time by 28.5% with an application of zero flow by combining the valve with an electrical water pump. Without mentioning the ambient conditions, a reduction in fuel consumption of 9.7% at transient and 5.2% at steady state were obtained over NEDC.

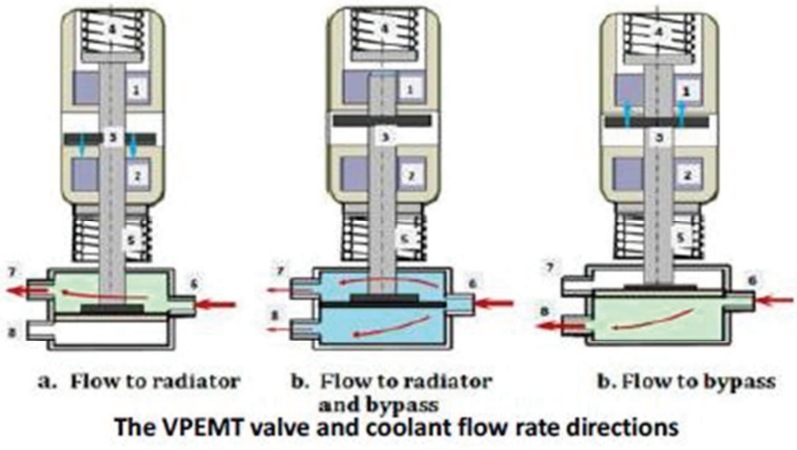

Figure I-5 The Variable Position Electromagnetic Thermostat [91]

More commercial models are present in these days. Valeo was the first to suggest the use of a valve called THEMIS^{TM}. An electric motor together with a position sensor controls the movement of the valve [92]. One of the best features of this valve is its accuracy in controlling the coolant temperature, its fast response, and having the ability of zero flow strategy during the warm-up. An application on different engines led to a reduction of a 5% in

fuel consumption [93], [94]. In 2009, Mann+Hummel introduced the Active Coolant Thermo-management valve (ACT) (Figure I-6). ACT organizes the flow between the three main branches: bypass, radiator and heater of the vehicle cabin. Furthermore, zero flow strategy and split cooling can be provided with this valve [95]. The control between the different branches is provided by a mechanical system based on cam/valve system. The number of circuits to be controlled will define the number of valves and the diameter of the cam [96]. ACT proved its efficiency by reducing the warm up time by 50% and enhanced the cabin comfort while its fuel reduction can reach 2.3%. Audi and Schaeffler worked on their multi-way valve called thermo management module. Its key activation is a plastic rotary slide module which contains two mechanically rotary slides that regulate the flow of the coolant [92]. With this valve, the coolant temperature may vary between 85 and 107°C. This valve offers a faster warm-up with flexibility in coolant routing, a reduction in fuel consumption around 2-4% depending on development stage of the baseline, a precise engine temperature control ($\pm 2°C$) and a unique failsafe thermostat that ensures engine safety outside of normal operating conditions [97], [98]. Finally, Sogefi has developed its own multi-way valve called the Active Multi-Way Coolant Valve or three-way-valve (3WV). It can provide the zero-flow strategy; it is controlled by one actuator and has a fail-safe function. Fuel savings can attend 2% on cold start NEDC [99].

Figure I-6 ACT valve [92]

I.3.2 Pumps

Water pumps transport the coolant through the circuit and build up the pressure. At first, water pumps were belt-driven. Still, this kind of pumps can be found in some passenger cars and trucks. It was designed to cool down the engine at severe conditions. Consequently, an overcooling of the engine happens at partial loads and high rotational engine speed. Roberts *et al.* [100] stated in his review based on others works that a conventional mechanically driven coolant pump can only match 5% of the required flow rate of the vehicle operating time.

Pumps evolved within the demand especially to remedy for the overconsumption at the cold start. Electrical pumps were introduced as well as variable speed pump. The former aims to reduce the parasitic losses by disconnecting the pump from the crankshaft. The latter targets

the warm-up phase. The working concept of the variable speed pump is represented by the following graph as found in the work of Jung *et al.* [49]

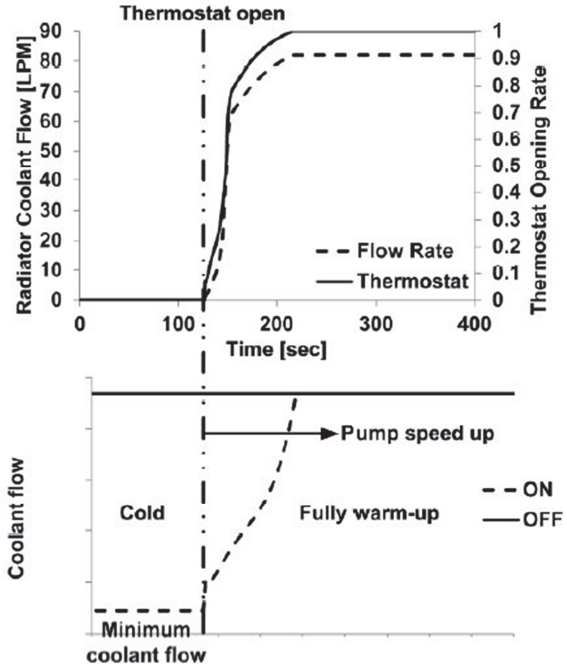

Figure I-7 Working concept of variable speed water pump [49]

On the upper graph of Figure I-7, the dashed line represents the coolant flow rate through the radiator, and the solid line represents the thermostat. A no flow strategy is adapted while the engine is still cold, and once the coolant warms up the thermostat opens and let the flow progressively in the radiator. The lower graph depicts the coolant flow in function of the time for two cases: the first one is the optimal flow rate provided by the variable speed water pump functioning represented by the dashed line, and the second one with the solid line represents the case with no variable speed water pump, thus a mechanical one driven by the crankshaft. The variable speed water pump keeps a minimum coolant flow during the warm-up stage of the engine. In case of a mechanical pump, the flow rate is related to the pump's speed, thus the engine's speed. As a result, the coolant flow rate during the warm-up stage is overestimated. When the thermostat opens, the variable speed water pump's speed increases sharply, followed by an increase of the coolant flow rate.

The study made by Jung *et al.* [49] reported that for an operating point of 2400 rpm and 71 Nm, with the variable speed water pump, a faster coolant warm-up of 21.3% is obtained. Consequently, the fuel efficiency of the engine is increased by 2.49%. A power saving around 4 to 77% depending on the different cases studied is demonstrated by Eberth *et al.*[85] while using a variable speed water pump. Almost each study of the 'smart' thermostat is followed by a study of a coupling with an electrical or variable speed pumps [42], [43], [89], [101], [102]. Fuel consumption and power savings are obtained in a lot of different studies using electrical control of the coolant system: smart thermostat, electrical pump, electrical fan, and boost pump for the cabin heater [103]–[106]. Zhou *et al.* [107] used an oil electrical pump in addition to the coolant electrical pump. Compared to a conventional thermal system, the advanced one showed a more stable temperature during the steady state stage of the engine as

well as the regulation temperature of the both fluids are slightly attended in advance with the advanced system.

I.4. Thermal management strategies

The main problem nowadays is the cold start of the engine. Even the homologated driving cycles impose a cold start of their cycle. Engine, running at transient phase, leads to an overconsumption due to low combustion efficiency. Moreover, low temperature means greater temperature difference between the combustion gases and the chamber walls and the ambient. Hence, lower is the ambient temperature, greater is the heat losses to the coolant circuit and the ambient. Furthermore, friction losses are highly dependent on the lubricant temperature, and their peak is attended with the lowest temperatures of the oil. To resolve these problems, different thermal strategies aimed to improve the warm-up phase of the engine.

I.4.1 Zero-flow

Zero-flow consists to restrain the coolant flow in the engine while the latter is at low temperature. This strategy leads to minimize the heat losses from the combustion chamber to the coolant circuit, and thus accelerate the warm-up phase.

Zero flow strategy was tested with the variable speed water pump that allows controlling the flow rate of the coolant (section I.3.2). Zero-flow strategy does not only lead to higher coolant temperature, but to a higher oil temperature too. The latter permits the engine to run with a lower friction losses level. Rouaud *et al.* [17] reached a 1.5% fuel consumption saving by applying the zero-flow strategy. Chalgren [104] proved that with a low flow rate, the coolant temperature did not show any improvement at the first stage of the warm-up phase, but after 40°C, the coolant temperature of the advanced system rised faster than the basic system. 30% is the improved rate of the warm-up phase attended by Choi *et al.* [101] while applying the zero-flow strategy. Moreover, in the latter work, a study of the influence of the coolant flow rate on the exhaust emissions was done. In the case of decreasing the coolant flow rate to 60%, hydrocarbon and carbon monoxide emissions were reduced by 20%. Cipollone [23] stated that if the pump is stopped the system becomes “warmable” up to a metal temperature of 155°C for many more working conditions and a reduction of 45% in warm up time is obtained.

I.4.2 Split cooling

The split cooling strategy proposes to differentiate between cylinder head cooling and cylinder block cooling leading to a more flexibility in each component’s temperature. Each part can receive a different flow rate of the coolant. In case of two different circuits of cooling, temperature set point can be different between both of the circuits. The main target of the split cooling is to have a cylinder head working at a lower temperature level. Cylinder head low temperature leads to a better filling efficiency enhancing the quality of the combustion. Hence, the emissions are reduced. The risk of knocking is also decreased. High engine block leads to a higher oil temperature, and thus low level of friction. Furthermore, it allows an improvement in the fuel efficiency and has an indirect effect on reducing the temperature and pressure peaks in the cylinder, which are responsible for the nitrogen oxides (NOx) formation.

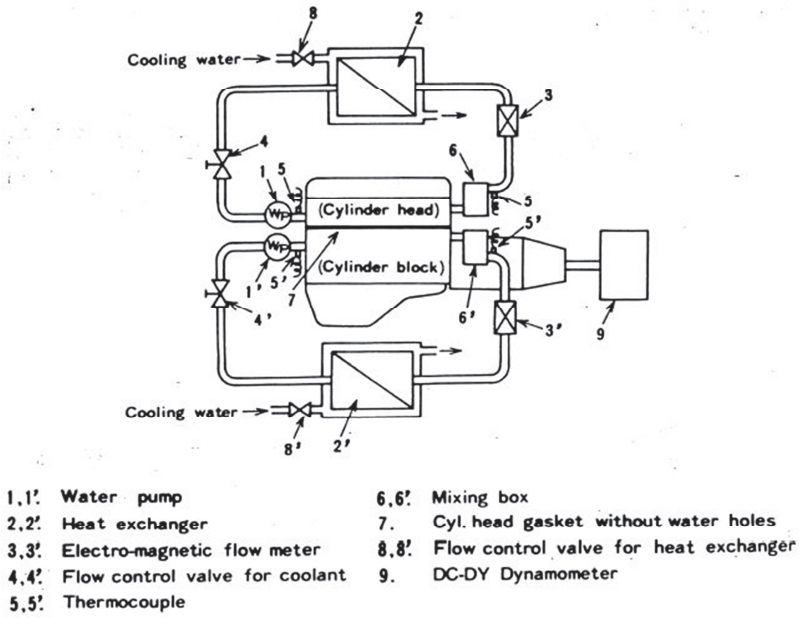

Figure I-8 Split cooling architecture [22]

The first application of the split cooling started with dividing the engine cooling in two different circuits. As depicted in Figure I-8, the cylinder head as well as the engine block have each a different water pump as well as a heat exchanger and controlling valve. Nowadays, the split cooling is provided with the multi-valve (section I.3.1). Cormerais *et al.* [95] presented the split cooling strategy that can be achieved by their Multi-way valve: ACT. As shown in Figure I-9, after applying the zero flow for a short time, the multi way valve allows the coolant flow in the different branches such as the oil cooler, the cabin heater and the radiator. Applying the split cooling strategy, flow rate to the block or the cylinder can be controlled and managed by the controlling valve. An application of this strategy led to 4-6% savings in specific fuel consumption as mentioned by Pang *et al.* [108].

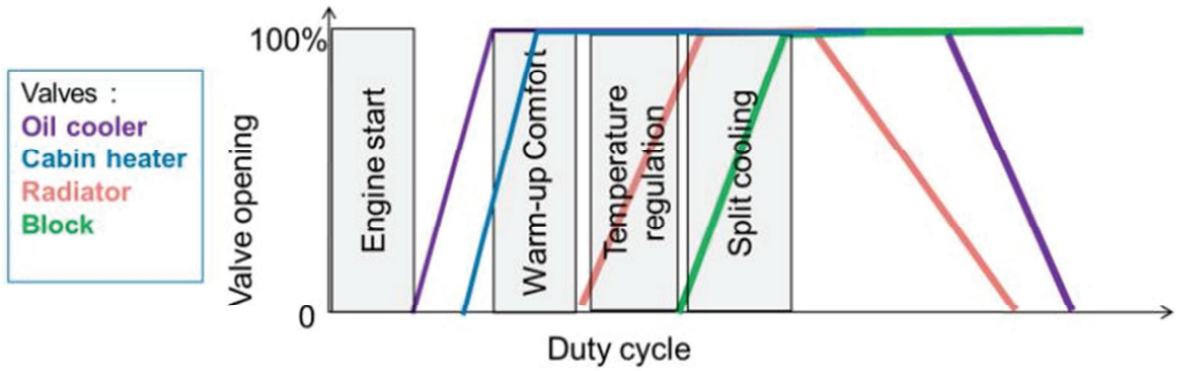

Figure I-9 Split cooling strategy by ACT [95]

Donn *et al.* [109] used a 2010 Audi 3.0L V6 equipped with a split cooling concept. Their study concerned the influence of the coolant temperature in the different compartment on the energy balance. Four coolant temperature levels were proposed as shown in Figure I-10. The main results were as following: the engine head coolant temperature mainly affects the coolant heat input, exhaust gas temperature and external heat rejection while the main

influence of the cylinder block temperature is the friction and the combustion chamber wall heat losses. A 1D/3D simulation to determine the temperature gradient in the cylinder head and cylinder block by using a split cooling was done by Osman *et al.* [110]

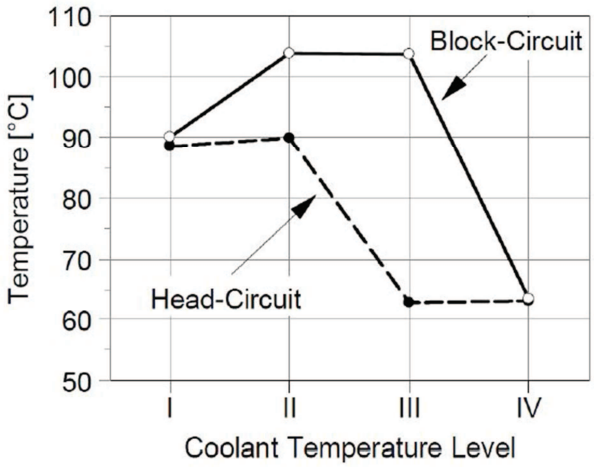

Figure I-10 Coolant temperature different levels [109]

Zhao *et al.* [111] studied in addition to the split cooling, the effect of split oil circuits. In both cases, the circuits separate recirculating flows to the head and the block of the engine. For this study four circuits (two for the split cooling and two for the split oil circuits) were completely separated and no mixing took place. The pumps were driven electrically in all the circuits. The influence of coolant flows and oil pressures were tested on 1500 rpm and 2.5 bar (BMEP) from a cold start. The main outcomes of the study were that: the flow rate of coolant or oil in either head or block circuit influences mainly the rate of heat transfer to the fluid in the circuit. To have the best warm-up of coolant and oil, coolant flow in the block should be minimal at the warm-up phase.

I.4.3 Engine temperature set point

Increasing the engine operating temperature has been one of the most popular strategies to apply on the engine. This high operating set point can be achieved by delaying the opening of the radiator branch. Higher operating set point of the engine leads to higher oil's temperature thus lower friction level. Moreover, with a higher engine temperature, higher is the coolant temperature around the combustion chamber, thus lower is the temperature difference with the combustion gases and lower is the wall heat losses to the combustion chamber walls. Consequently, engine fuel efficiency of the engine will be improved.

Payri *et al.* [83] proved with their engine balance what is stated before. With increasing the coolant and lubricant temperature, wall heat losses were reduced by 3.3% and 1.6% at 2000 and 4000rpm respectively. Couëtouse *et al.* [102] raised the coolant temperature to 115°C and obtained an average reduction in fuel consumption of 3% to 5% corresponding to different driving speeds. Burke *et al.* [112] stated a reduction of friction losses by 2% when increasing the coolant temperature from 86°C to 98°C and 1% in fuel consumption savings. Cormerais *et al.* [95] with the multi way valve (ACT) regulated the coolant temperature of the engine at 105°C and achieved around 1.6% on NEDC compared to a standard regulation temperature of 83°C.

Yousry *et al.* [113] studied the influence of the coolant and oil's temperatures on Diesel engine specific fuel consumption. The latter decreased with increasing inlet oil temperature and it is greater at lower speeds and at higher loads. Similar to the lubricant temperature, the fuel consumption decreases with increasing the outlet coolant temperature, and is higher at higher loads. Influence of the fluids' temperatures was also studied in [114] [115] [47].

I.4.4 Engine insulation

One of the uncontrollable and hardly defined losses in the engine is the thermal radiation to the ambient. To lower these losses and improve the engine fuel efficiency, engine insulation was introduced. In normal states, the engine external convection coefficient ranged between 5-20 W/m²/K. Engine insulation tends to lower this coefficient either by adding some low thermal conductivity layers over the engine or by insulating the underhood compartment or by adding some grill shutters and claps to control the thermal state and environment of the engine. One of the disadvantages of the engine insulation is increasing the radiator size to protect the engine from the overheating and the different thermal stresses. Furthermore adding insulation materials lead to higher engine vibrations.

Bent *et al.* [116] added a 25 mm thick layer of uncompressed Rockwool with a thermal conductivity of 0.04 W/m/K. As depicted in Figure I-11, at an ambient temperature of 20°C, the warm-up temperature of the oil did not show any improvement by applying the engine insulation. However, the improvement is obtained during the soak period. The oil temperature drops less with every mode of insulation. The drop is at its highest with no insulating at all to its lowest with an engine fully insulated. Slowing the engine cool-down from previous running allows it to maintain a warm state for the next start-up. 1.25% fuel savings on NEDC were concluded by starting at a temperature of 25°C, thus 5°C more than the reference case.

Bertolini *et al.* [117] studied the technical requirements needed by the engine bay materials for the encapsulation, followed by a study of the acoustic insulation and absorption of the different components resulting from the encapsulation. A comparison between the different thicknesses of the insulation was made as well as their results. It states better results with the thickest solution.

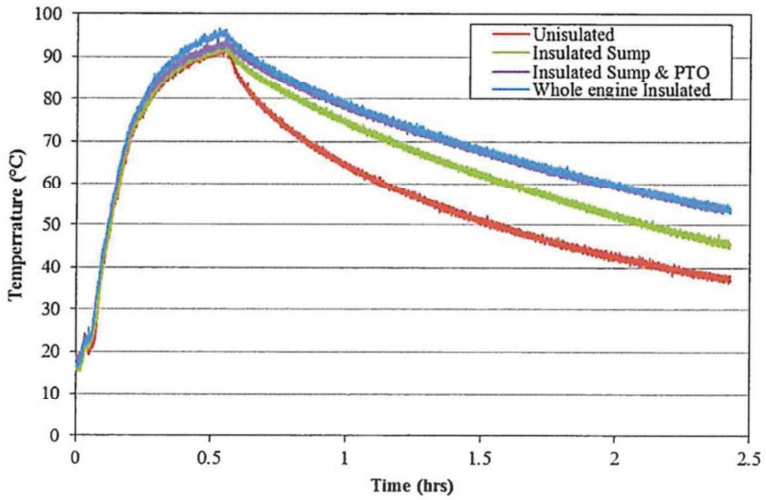

Figure I-11 Experimental sump oil temperatures [116]

In their review paper, Roberts *et al.* [100] showed the following results made by Bürgin. The study consists of applying a 7 mm thick insulation to the external surfaces of the engine. After 15 hours, 16°C temperature rise was obtained with 100% coverage compared to an uninsulated engine. Rouaud *et al.* [17] stated a 1% reduction of the fuel consumption with an engine encapsulation.

Engine oil ways insulation were studied using 2 mm thick nylon 12, a 2 mm thick aluminum and 2 mm stepped aluminum with a 0.5 mm air gap to reduce the transient warm-up of the engine [118]. The highest reduction of energy losses to surrounding metals applied on a 380 mm long oil gallery is 50% with nylon 12.

Makam *et al.* [119] made a study of underhood configurations by introducing active grille shutters and belly pans. Belly pan is a shroud that can covers the underbody of the engine. Grille shutters are devices that open up at the frontal of the car to provide increased underhood air flow. Both increase underhood heat retention as well. Oil attended a higher temperature by 5°C with the belly pan and 20°C with the grille shutters. Grille shutters were added to the vehicle study to help increase the set point of the engine to 115°C [102]. 0.15-0.2 l/100km is stated as reduction in fuel consumption at a constant speed of 120 km/h by applying grille shutters in Huber work [120]. Saab [94] introduced the different flaps in his model and made a developed study over NEDC, WLTC with and without cabin heater stating a fuel saving of 3.1% and 5.2% for the previous cycles cited respectively without cabin heater.

Precision engine cooling is defined as the minimum cooling necessary to achieve optimized temperature distribution [121]. Thermally critical area receives intense cooling, whilst uncritical areas rely on heat conduction through the head and block structures. This is achieved by reducing the cross-sectional area of the coolant ducts in these regions to attain high flow speed [108].

I.4.5 Oil sump and oil's grade

One of the major losses of the engine at cold start-up is the friction. At low ambient temperatures, oil's temperature is at low level, thus viscosity is at its highest hence the friction. Oil thermal management strategies varied throughout the years to improve its viscosity at the cold start-up. As mentioned before, some used an electrical oil pump to control the oil flow rate at the warm-up phase to have a faster increase in temperature. In his review paper, Roberts *et al.* [100] presented Law's work of a split oil sump. The split oil sump used a thermostat that allows isolating a part of it from the oil circuit during the warm-up stage (Figure I-12). Only when the returning lubricant was at temperature around 70°C, the thermostat opened up to increase the oil sump working volume. Applying this strategy on a 2.4l direct injection Diesel engine came up with an increase of the oil's temperature in the main gallery of 5°C relative to the conventional oil sump at an ambient temperature of 20°C, and increased by 12°C with an ambient temperature of -10°C. They stated a reduction of the friction losses by 10% during the first 2 min.

Revereault *et al.* [122] introduced a split oil sump into their work by reducing the oil's volume to 40% and then to 20% of the original state. Applying the strategy over NEDC, savings of around 3-5% are obtained depending on the volume used in the sump. Taylor *et al.*

[123] stated the work of Chisaki in their study where they used a false wall to trap oil's volume in the sump and thus isolated from the circuit. This strategy was applied on Toyota D4-D 2.0L 4-cylinder Diesel engine and had a fuel consumption reduction of 0.8%.

Taylor *et al.* [123] divided the oil sump into three main volumes theoretically: one necessary to fill the oil galleries, one to allow the movement of the oil in the sump during the vehicle acceleration and one to achieve the oil drain interval. The theoretical benefit associated with a reduction in oil fill of 3.1L was 2.2%. By tests, around 0.46% was achieved by reducing the oil's volume.

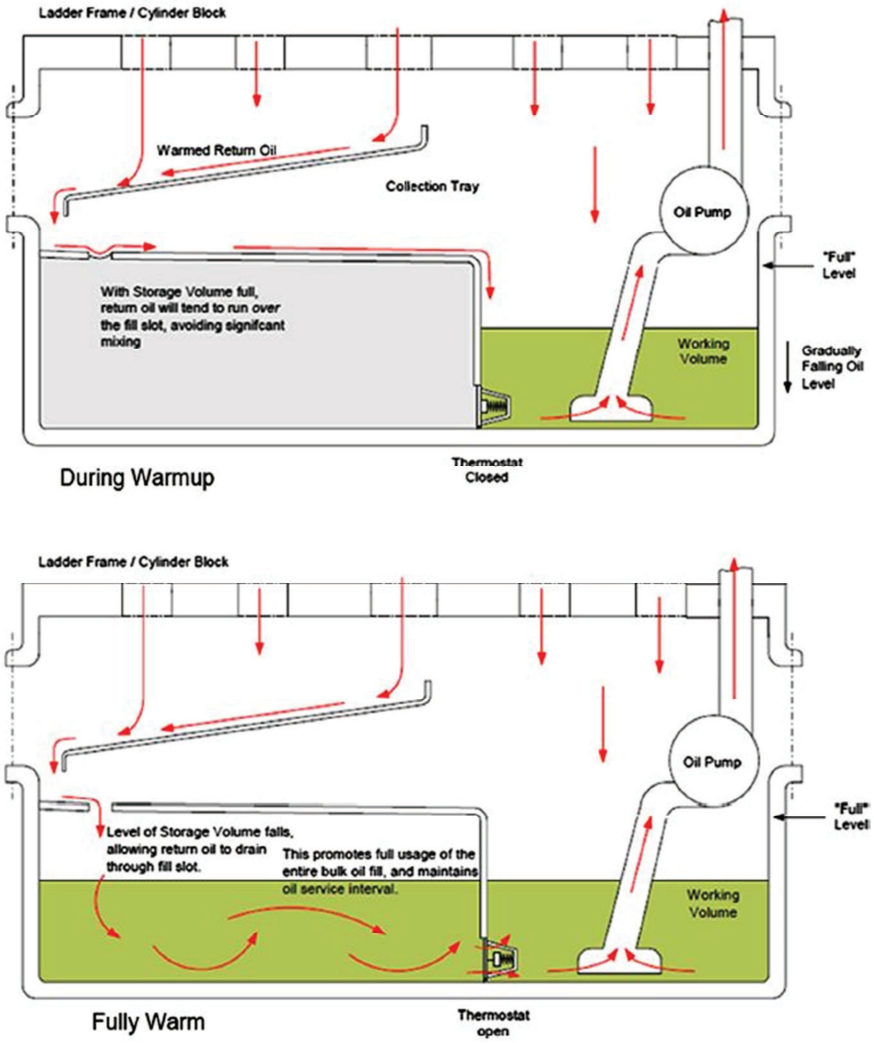

Figure I-12 Split oil sump to have a faster oil warm-up [100]

Zhao *et al.* [124] studied the influence of sump design on oil warm-up and cool down behavior. Five variants of sump design (shape, material and inserts) were proposed for a 2.0L gasoline turbocharged direct injection engine. A difference of 10°C was obtained between the best and worse design of oil sumps. These 10°C almost disappeared after the oil pump. However, the cool-down of oil after the engine shut down was slowest for the more compact, polyamide sump.

It is known that the current oil used in the engines has a high viscosity at low temperatures. With moving on to lower oil's grades, oil's viscosity decreases at lower temperatures and friction losses can be reduced at the cold start-up. Nouvel *et al.* [125] studied the influence of changing the oil's grade on the engine fuel consumption. 0W-20 and 0W-16 oils were used in the study on different Diesel and gasoline vehicles. The different vehicles had different reference oil types. The main results are shown in the Figure I-13, the fuel consumption economy ranged between -0.22% and 0.01% to 3.99% and 4.32% for 0W-20 and 0W-16 respectively. The reference oil's grade for the lowest economy was 0W-20 and for the highest was 15W-40.

Taylor *et al.* [123] tested the influence of the oil's grade by comparing two oils: 5W-30 and SAE 8 with a kinematic viscosity at 40°C of 55 cSt and 26 cSt respectively. 3.7% of fuel savings was obtained with the lowest viscosity oil. During the test, the coolant/oil heat exchanger was by-passed.

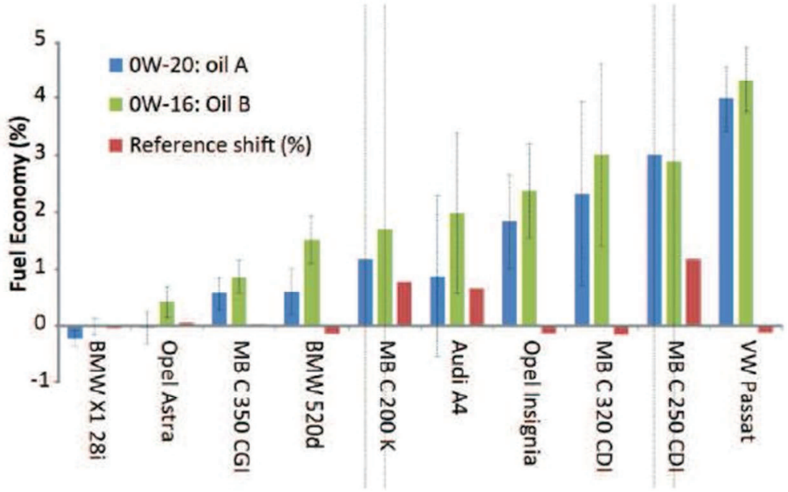

Figure I-13 Results over NEDC of different engine oil's grades on different vehicles with 95% confidence intervals [125]

Other means to reduce the engine's friction in the system by applying variability within the valve train and combustion modes was studied by Altenschmidt *et al.* [126].

I.4.6 Exhaust gas heat recovery

One third of the injected fuel efficiency is lost within the exhaust gases. Studies were focused on recovering the heat evacuated with the exhaust gases. At first, Rankine cycles were applied on the exhaust line to improve the engine efficiency [79]. It transforms the heat energy of the exhaust gases into mechanical energy on the shaft of the engine. Others studied different topologies [127] or developed some new components for this strategy [128]. However, caution must be exercised since exhaust heat recovery may increase the catalyst light-off time and thus the emissions level. To avoid such disadvantages, heat recovery on the exhaust lines should be downstream the after treatment systems.

Agudelo *et al.*[129] made energy and exergy analysis on the exhaust line to define its potential in recovering heat. Temperature measurements were made upon 6 places on the

exhaust line, upstream and downstream of the Diesel oxidation catalyst, the regenerative particle filter, and the muffler. The potential fuel savings are presented in Figure I-14. It is shown that the potential decreases as the gases flow to the atmosphere because of heat losses in the different after treatment systems.

Klopstein *et al.* [86] in their simulation stated a maximum of fuel reduction around 2.5% after 140s of the engine running through NEDC with a heat exchanger on the exhaust line. During the cycle, the fuel consumption reduced due to lower reduction in friction losses and ended up by 0.6% approximately.

Farrant *et al.* [130] tested a heat recovery of the exhaust line by using a coolant/exhaust gas heat exchanger. Fuel savings of 5% over NEDC were predicted compared to the baseline vehicle. Some modifications were made upon the coolant circuit, an electrical pump replaced the mechanical one and the wax thermostat was replaced by an electrically controlled valve. These modifications allowed to control the coolant temperature on the exhaust gas heat exchanger and to maintain the engine from overheating. Dramatically change in the oil's temperature was noticed by their simulations.

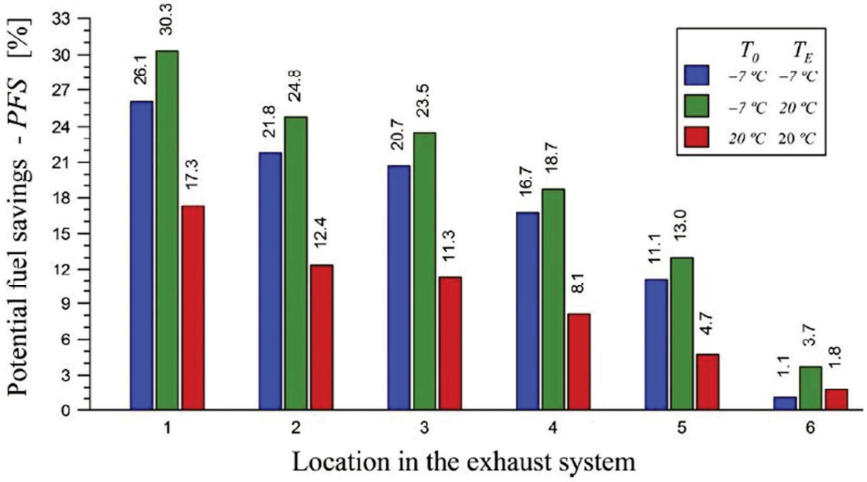

Figure I-14 Potential fuel savings at different location of the exhaust system [129]

An application of exhaust gas to oil heat exchanger was tested by Grimaldi *et al.* [131]. The exchanger was placed at the inlet of the galleries in the oil circuit and downstream the catalytic converter on the exhaust line. To prevent the overheating of the oil, a bypass was added on the exhaust line controlled by a three way valve that operates once the oil has reached its regulation temperature. A faster warm-up by 540s was obtained with the oil's temperature and allowing a reduction of 1.32% in the fuel consumption.

The system depicted in Figure I-15 represents the exhaust gas to oil recovery from Will's work [132]. Downstream the catalyst and upstream the muffler, a heat exchanger with the oil circuit was installed with a bypass controlled by a flap valve. The oil heat exchanger was placed downstream the filter on the oil circuit. The tested vehicle was a Ford Falcon 4.0L I6 engine and automatic transmission. A result of 7% of fuel saving over NEDC was averaged for 5 tests. The most interesting finding with the heat exchanger, as mentioned by Will *et al.* [133], is that the oil temperature rises sharply within the first 100s to reach 80°C and then a

difference of 35°C is spotted during the high speed part of the extra urban cycle at the end of NEDC. A new system configuration is proposed with a bypass that connects the cylinder head oil gallery to the inlet side of the oil pump [134]. At a bypass flow ratio of 70%, the oil temperature increased by 64°C. For low bypass ratio no significant improvements were registered on the oil's temperature.

Barrieu *et al.* [99] introduced their system "Exhaust Heat Recovery System (EHRS)" composed of a heat exchanger similar in principle to an EGR unit, a bypass tube and a bypass flap. Two configurations were tested: indirect oil heating with the engine coolant as a transferring media to warm-up the oil and direct oil heating with oil exchanging heat directly with the exhaust gases. 65°C engine oil temperature can be reached 58 seconds earlier with the first configuration and 122s earlier with the second. The fuel economy saving is about 0.6% on cold start NEDC for the first configuration and 0.9% for the second.

Burke *et al.* [135] tested the oil cooled EGR on 2.4L 4-cylinder euro IV Diesel engine on 25°C cold start NEDC. A variable flow oil pump is introduced in the system. Switching from coolant to oil cooled EGR allowed reducing the heat loss to the coolant by half and consequently the heat loss in the engine is increased. Zammit [31] predicted 0.63% benefits in fuel consumption by changing from coolant to oil cooled EGR and friction reduction of 1.9%.

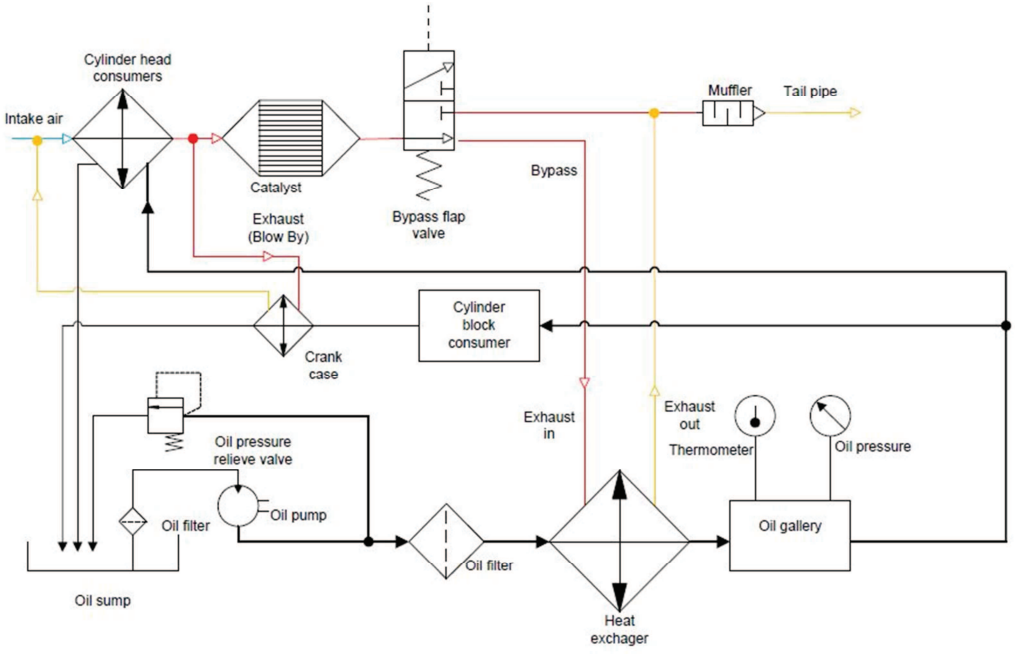

Figure I-15 Exhaust gas to oil heat recovery system [132]

Waste heat recovery by means of storing heat using Phase Change Materials (PCM) is tested by Pandiyarajan *et al.* [136]. Paraffin was used as PCM. The heat exchanger was of a shell and tube type and a castor oil was used to transfer heat from the exhaust line to the storage tank. However, the study focused on the thermal performance of the storage tank and not on the engine. The main results concerned that the best heat extraction is within the high operating points of the engine and nearly 10-15% of total heat is recovered with this system. Moreover, due to its configuration a near uniform temperature was observed throughout the tank.

I.4.7 Heat storage

The main losses of the engine are heat losses to the coolant or heat losses within the exhaust gases. Exhaust gases heat are totally lost to the ambient unless it has been recovered by mean of the different ways described in the previous section. The heat lost to the coolant is used in the first part to warm-up the different metallic parts as well as the engine coolant and lubricant. However, once the engine reaches its regulation temperature, the thermostat opens the radiator branch and almost all the heat transferred to the coolant is transmitted and lost to the ambient via the radiator. Heat storage's principle is to store heat when the engine is running in steady state stage and use it at the next cold start-up.

The stored heat has three primary uses. The first is to heat the engine and reduce its fuel consumption by improving the combustion process. The second is to heat as well the moving parts to reduce the engine friction losses. The third one uses the heat stored for rapid cabin warm-up.

Heat storage exists by two means: either by storing the hot fluid itself or by latent heat and using phase change materials. The second way needs an addition of a heat exchanger, as well as more time for the heat exchange process.

Coolant heat storage systems were tested by Kuze *et al.*[137]. The strategy was applied on the Toyota Prius with THS II (Toyota Hybrid System II). The hot coolant was assumed to 3 Liters at 75°C. The coolant heat storage system consists of a storage tank placed in a new branch with an electrical pump which pumps the hot coolant to the cylinder head and a multi-way valve. The latter controls the coolant flow and isolates the storing system from the traditional circuit during the engine cold start-up if the storage tank is at low temperature. An approximately 3% fuel consumption improvement was stated after 20 minutes at an ambient temperature of 5°C. However, driving conditions were unknown (Figure I-16).

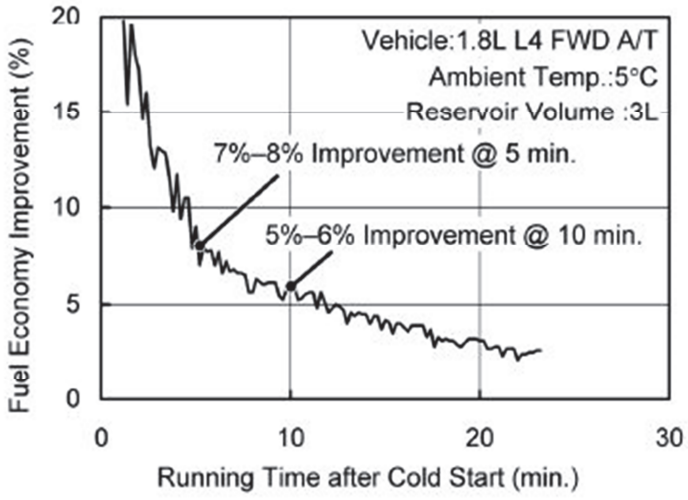

Figure I-16 Fuel savings by applying hot coolant storage [137]

Reverault *et al.* [122] applied this strategy on an Efficient-C hybrid vehicle on three different driving cycles NEDC, Artemis Highway and Artemis Road without mentioning the ambient temperature and showed fuel consumption between around 0.7 and 1.5%. Zammit [31] declared a reduction of 1.3% by applying thermal storage within the exhaust heat.

Bent *et al.* [116] used the same experimental setup and tested two configurations: the first one like those of Kuze *et al.* [137] by returning the hot coolant to the cylinder head and the second by returning it to the cylinder block. A comparison was made between the different configuration preheating the block, heating block from Key-on and preheating the head. Coolant temperature was raised up to 40°C in the first 10s and the regulation temperature was reached earlier, however, no significant effects were observed on the lubricant temperature. A reduction of friction losses by 5% was obtained when the block was heated and 9% when the head was heated. These results were mentioned without any explanations. After 500s running at the operation point of 1500 rpm and 2bar fuel savings were 0.7% when the block was heated from key-on, 1.5% when the block was pre-heated, and 2.3% when the head was pre-heated.

Taylor *et al.* [123] assessed the lubricant thermal energy storage by use of an external oil bath which thermally conditioned the lubricant fill volume during the vehicle soak period. Two start temperatures were tested 60°C and 90°C. Fuel savings were 0.41% for the 60°C case and 1.04% for the 90°C case over NEDC. However, 40-60°C of temperature loss were registered between the sump and oil gallery for the cases of initially temperature of 60 and 90 °C respectively.

Latent heat storage is based on the heat absorption or release when a material undergoes a phase change from liquid to solid or vice-versa. The PCM chosen should have the following proprieties [138]:

- Thermal properties: The PCM should have a matched melting/solidifying temperature, a high latent heat and high thermal conductivity
- Physical properties: Phase stability and small volume changes on phase transformation.
- Chemical properties: PCMs should be non-toxic, non-flammable and non-explosive.
- Economics: Low cost and large-scale availability.

Table I-1 shows the characteristics of four phase change materials provided by SASOL that are adequate with an engine regulation temperature of 83°C. However, Kim *et al.* [139] depicted different types of PCM in a graph (Figure I-17) for different ranges of temperature. The study done by Kim *et al.* covered the response of the storage tank for different configurations.

Table I-1 PCM characteristics

Product	Onset Temperature (°C)	Latent Heat (J/g)
PARAFOL MP 55	50	>190
PARAFOL MP 80	74	>210
NACOL 22-98	69	>250
NACOL Ether 18	62	>215

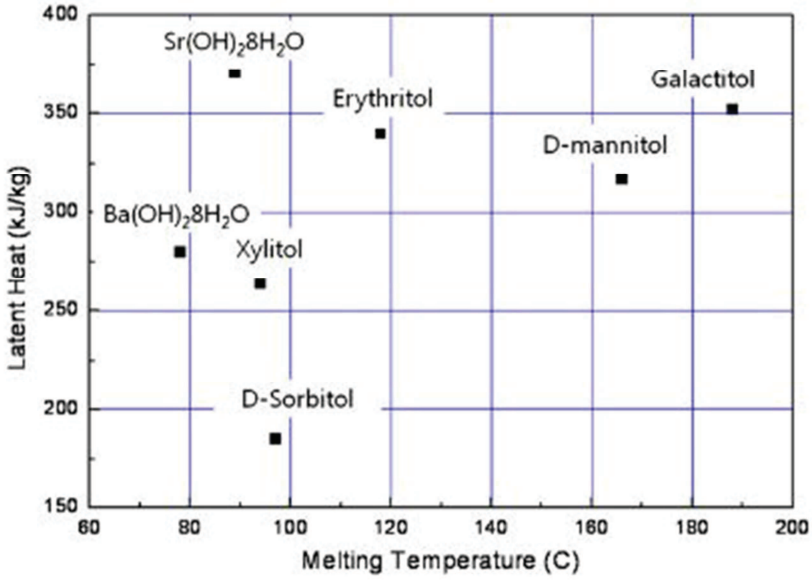

Figure I-17 Latent heat of different PCM in terms of melting temperature [139]

PCM latent heat storage was applied in different studies. Schatz [140] used a water/salt mixture that stores some heat when melting; in his configuration there was an electrical pump either running with the engine start or controlled by a switch linked to the driver's door allowing it to start independently from the engine. The material used has a melting point of 78°C and the heat battery features a heat capacity of 600 Wh when cooled down from 80°C to 50°C. A study of the soak period was done as well as the use of defrost, defogging and warm-up of the cabin. Pandiyarajan *et al.* [136] used the exhaust gases to store latent heat.

Gumus [141] charged the heat battery by using hot coolant; in addition to the storage volume, the author used two valves, an electrical pump and a control system. A detailed presentation of the storage tank was made and it stated that the charging and discharging of the battery is about 500s and 600s respectively. Vetrovec [142] located his storage tank downstream the radiator thus eliminating the use of other valves than the thermostat (Figure I-18).

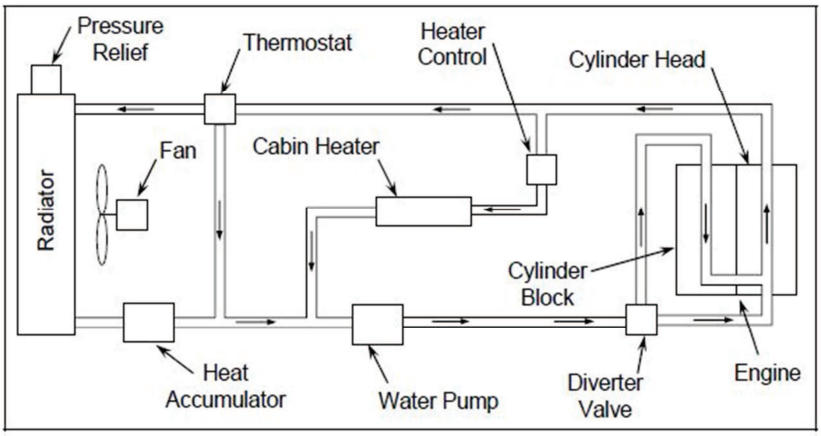

Figure I-18 Coolant circuit with a heat accumulator [142]

Revereault *et al.* [122] assessed the latent heat storage on the coolant and on the oil circuit. The battery was surrounded by vacuum insulation and its volume was 4 L and weighted 8 kg

for the coolant. However, for the oil system it was smaller and it was for 1L to keep the oil volume, hence cost, within a reasonable range. Fuel savings went up to around 6% for Artemis Urban when applied on the coolant. Roberts *et al.* [100] made a developed review over the latent heat storage application on the coolant and lubricant circuits, as well as on the different engine auxiliary systems and the challenges and issues of using phase change materials.

I.4.8 Other systems

The previous mentioned thermal management systems were not the only one existing; the list can go for ever. Here are some others:

- Nucleate boiling: its occurrence in engine acts as an unintentional safety zone for protecting components from excess temperature when the coolant flow velocity is too low to provide the required convective heat transfer [121]. If a metal temperature rises above the saturation temperature of the coolant, local nucleate boiling will occur. Bohac *et al.* [39] modelled the nucleate boiling. Ap *et al.*[93] tested this strategy with two configurations: one with partially filled coolant architecture and the second one with it completely filled. The system is equipped with a small electric water pump. Cylinder head temperature was hotter, lower flow rate was circulated and the oil sump temperature was increased and fuel consumption reduced by 2 to 3% depending on the studied vehicle.
- Thermoelectric exhaust heat recovery: this strategy is based on Seebeck effect to produce electricity by temperature difference. It uses the exhaust gas as a hot source and the water as the cold one. The typical efficiencies of the TEG conversion was stated between 0.5 and 1% depending on the thermoelectric material used [143]. A review of this strategy was performed by Roberts *et al.* [100].

Some studies took into consideration the cabin heater and applied a study on the human body comfort [102], [104], [144]–[146].

I.5. Thermal management on hybrid vehicles

With the new trend, hybrid vehicle are widely known to be the next most promising solution to city driving. However, to have the best efficiency of the battery, it should function in a specific temperature range. Hence, battery thermal management is quite famous around hybrid vehicles. The thermal management system should be compact, light weighted, low cost and adaptable with the vehicle. Thermal management systems can be divided into two main parts: passive one with the air as the working fluid or active one with a fluid, a phase change material or insulation.

The heat generation formulation was presented by Samadani *et al.* [147]. Two commercials Li-ion battery behavior was studied at different ambient conditions. Results agreed with the belief that Li-ion cells have a better performance at higher temperatures. An exergy balance was presented by Hamut *et al.* [148] with an exergy of the battery up to 80% and a destruction rate of 0.04 kW.

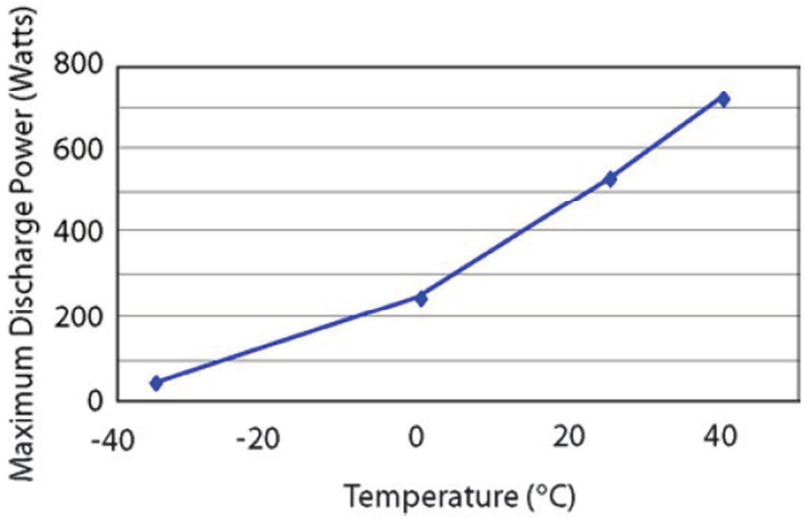

Figure I-19 Maximum discharge power from a battery [149]

All batteries suffer at cold temperatures as shown in Figure I-19. A finite element study done by Pesaran *et al.* [149] proved that battery core heating was the most effective method to warm up the battery quickly with the least amount of energy. Vlahinos *et al.* [150] compared four types of preheating the battery:

- Internal core heating with electric heating of battery core in each cell.
- External jacket heating using electric heaters.
- Internal jacket heating using electric heaters.
- Internal fluid heating using hot fluid around the cell.

The electric heating rises the battery temperature faster than heating with fluids. Internal core heating had the most uniform heating. However, the external jacket heating had the largest temperature spread. Internal core heating is the fastest way between the other electric heaters.

Sabbah *et al.* [151] made a comparison between a forced air cooled and PCM thermal management of high power Li-ion packs. The comparison was carried out for various levels of discharge rate. The same geometry of the different packs were used: firstly an air-cooling system ensures the uniformity of the air flow between the cells, and the second PCM-composite was filling the inter-cell gaps. As presented in Figure I-20, at an ambient temperature of 25°C, to keep the cell temperature below 55°C, both ways succeeded to do it. While at an ambient temperature of 45°C, even with high velocity of the air, PCM showed a clear advantage. An application of PCM is done by Kizilel *et al.* [152]

A new active battery cooling/heating method based on PCS (Phase Change Slurry) was presented by Zhang *et al.* [153]. A heat exchange between the vehicle cabin heater and battery container is done. During the cooling process, PCM with low melting point (28°C) melts down with heat absorption. During the heating process, PCM absorbs heat from the cabin and exchange it at the battery container.

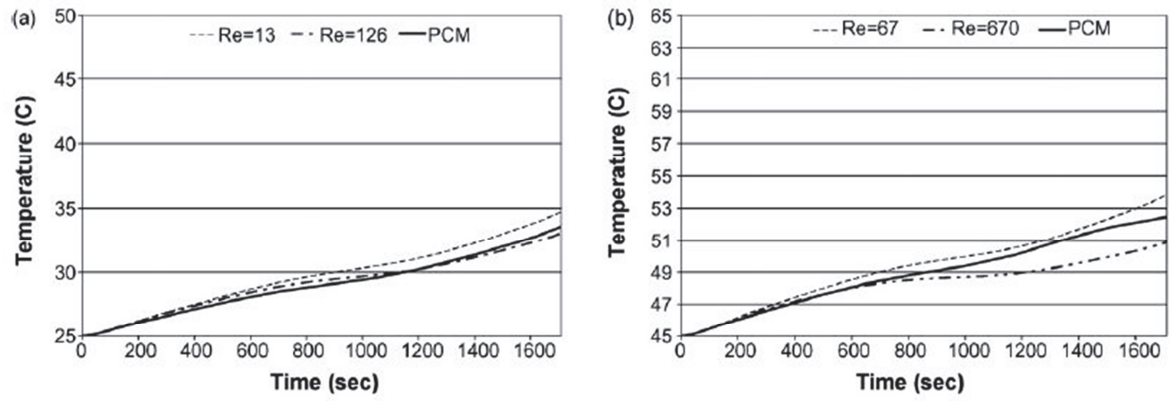

Figure I-20 Volume average cell temperature at 10A: (a) T_{amb}=25°C (b) T_{amb}=45°C [151]

Murashko *et al.* [154] modelled another battery pack thermal management system presented in Figure I-21 . The battery pack has a closed liquid cooling system with a pump and a heat exchanger. The plate heat exchanger is used for heat transfer between the traditional coolant circuit of the internal combustion engine and the battery pack cooling circuit. A three-way valve controls the liquid flow rate in the plat heat exchanger. Another one controls the liquid flow rate in the heat exchanger, hence the battery pack heating time. Fan starts operating once the heat exchanger cannot dissipate the necessary amount of heat.

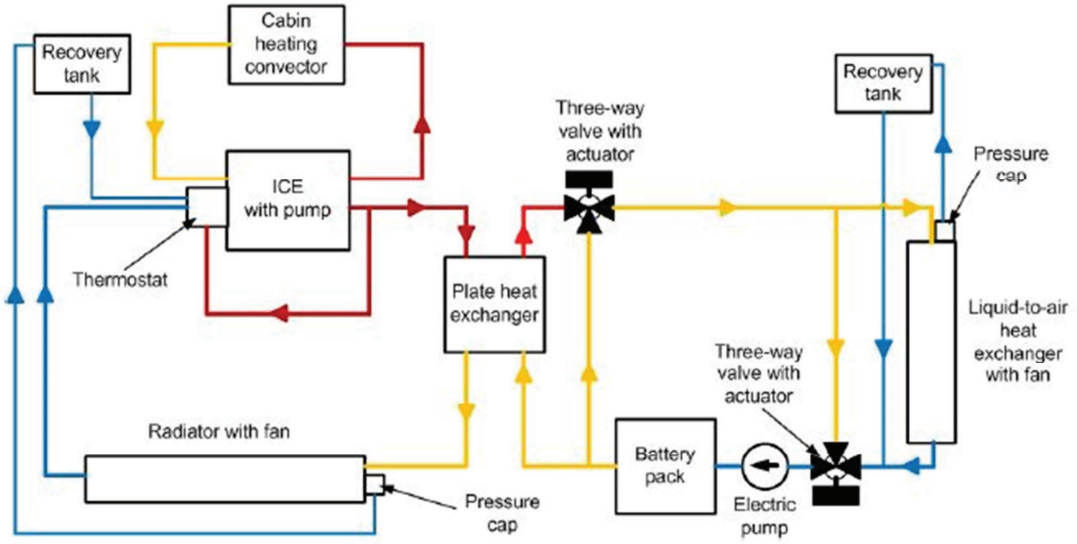

Figure I-21 A schematic presentation of the thermal control system [154]

Some authors covered an underhood study of the hybrid vehicles considering different positions of the different heat exchanger [155] while others were interested in the energy management of the vehicle based on different statistical studies [156]–[160]. Gmeiner *et al.* [161] presented a new multi-way control valve and coupled it with a heat pump and presented different architectures in his study for the winter and summer cases. Heat pump study took another interest in Hopp *et al.* [162] study.

The literature study made covers different aspects of thermal management. The main objective of the thesis is to assess and valorize the different thermal management strategies for a vehicle powertrain application using numerical simulations. For that, the first part of the literature survey covered the different aspects of thermal modelling: from the convective part, passing throughout the different types of heat transfer in the different galleries, to the radiative part and how to simplify it in 1-D models. In addition, heat sources (combustion and friction) modeling was also covered. The different formulation brought closer the physical aspect and helped to explain the behavior of the different components in the different commercial softwares existing nowadays.

The energy balance helped understanding the energy flows through the engine system and its main losses and explaining the reason and the importance of thermal management application. However, most of the energy balances done in the literature survey differ from an engine to another even if the tendencies are always the same. In addition, rare were the energy balance applied on a complete driving cycle and divided into different parts to study the main losses during the warm-up stage as well as during the steady state stage. Consequently, an energy balance of the engine is necessary before any decision in terms of thermal management strategies is taken. Moreover, the energy balances main outcomes will help to compare the tendency of the primary model results.

The thermal management strategies discussed in the literature survey underlined their importance in helping the engine to reach its comfort zone, its high efficiency zone, the steady state stage very quickly. The different applications highlighted the importance of fuel savings that can be reached within these strategies. However, the trend in the last years was with the new multi-valve, a strategy that won't be taken into consideration in this work as it was highly studied before and was put into action. Same as for the electrical equipment used on the engine. Furthermore, thermal strategies can be divided into two main parts: coolant and lubricant application. At cold start-up, lubricant has more influence because of its dependency on the friction power. However, during other operating phases of the engine, where the influence of the oil's temperature on the friction power will be minimal, coolant proved itself. During the thesis, different thermal management strategies will be tested on both fluids to underline the difference between them.

II. Building up the thesis

This thesis consists of assessing the potential of different thermal management strategies with numerical simulations. To do that, a simulation code should be developed based and validated over experimental setup.

The first part of this chapter covers the engine test bench done at Ecole Centrale de Nantes, give an insight over the simulation code and its parts developed on GT-Suite software.

Once the simulation code is calibrated and showed a good agreement, the different driving cycles chosen for this study were presented in details. The second part of this chapter includes the energy balance done on the engine and its main outcomes on its warm-up and steady state stages.

II.1. Engine test bench

The work on this thesis was based on a four cylinder turbocharged Diesel engine. The specifications of the engine are given in Table II-1. The turbocharger has a variable geometry turbine. On the intake line, downstream the compressor, the charge air cooler takes place. The intake air, compressed and then cooled, is mixed with an amount of EGR. EGR rate is controlled by a valve on the High EGR loop. The engine is equipped with a common rail injection system. Downstream the turbine on the exhaust line, a silencer is installed to reduce the engine noise before the exhaust gases are evacuated to the ambient air.

Table II-1 - Engine specifications

Engine type	**Compression ignition**
Compression ratio	15.3
Number of cylinders	4 cylinder in line
Number of valves per cylinder	4
Bore	76 mm
Stroke	80.5 mm
Maximum power	75.4 kW at 4000 rpm
Maximum torque	227 N.m at 2750 rpm

Engine tests were made on a transient dynamometer test bench at Ecole Centrale de Nantes (Figure II-1). Those tests were used to validate the engine model and calibrate it through different operating points. To let the engine fit to the transient dynamometer test bench, some modifications were made. The gearbox was replaced by a direct drive. Some parts were removed such as: the air conditioning compressor, the alternator and many other auxiliaries. For a better control of the engine's temperature as well as the different fluids in the system, heat exchangers based on the ambient air were replaced by water heat exchanger. The charge air cooler was replaced by an air/water heat exchanger and the radiator was substituted by a water to water heat exchanger. The EGR cooler was not modified.

At first, tests were used to calibrate the engine performances, the combustion model and the heat fluxes in the engine cylinders. At a second time, the hydraulic circuits were calibrated. Finally, the different models were validated by the experimental setup. Test varied over different operating points and cold start engine tests were taken into consideration. The engine torque lies between 20 N.m and 200 N.m with a 20 N.m step size and the engine speed between 1000 rpm and 4200 rpm with a 100 rpm step.

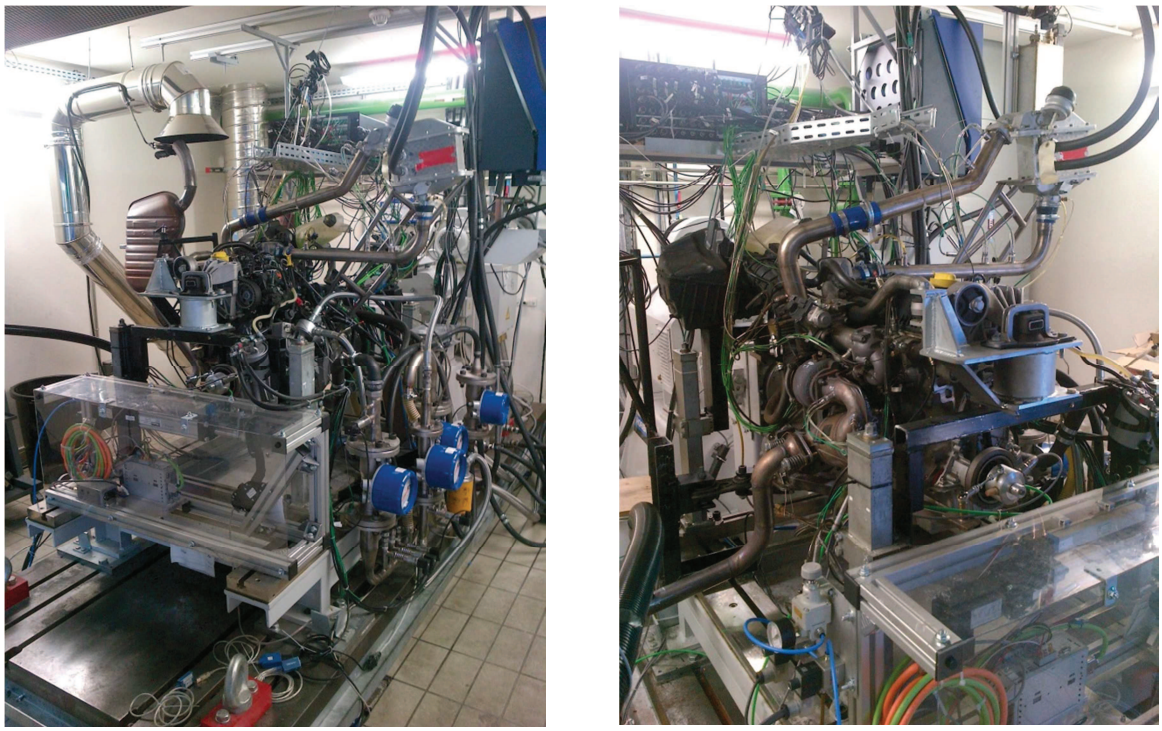

Figure II-1 Transient dynamometer test bench

Pressure, temperature and air flow rate for different fluids (air, coolant and lubricant) were measured along the intake and exhaust line as well as in the different parts of the coolant and lubricant circuits. K-Thermocouple sensors were used for the temperature measurements. Rotational engine speed, torque, fuel consumption and turbocharger speed were also recorded. Air-to-fuel ratio calculation is based on the feedback of a lambda sensor. Kistler pressure sensor (6056A41) measured the in-cylinder pressure, allowing calculating the engine heat release. To tune the combustion model, the injection time and angle as well as the different emissions of the engine were registered (Figure II-2). All details concerning the measurements techniques, calibrated ranges and accuracy are presented in Table II-2.

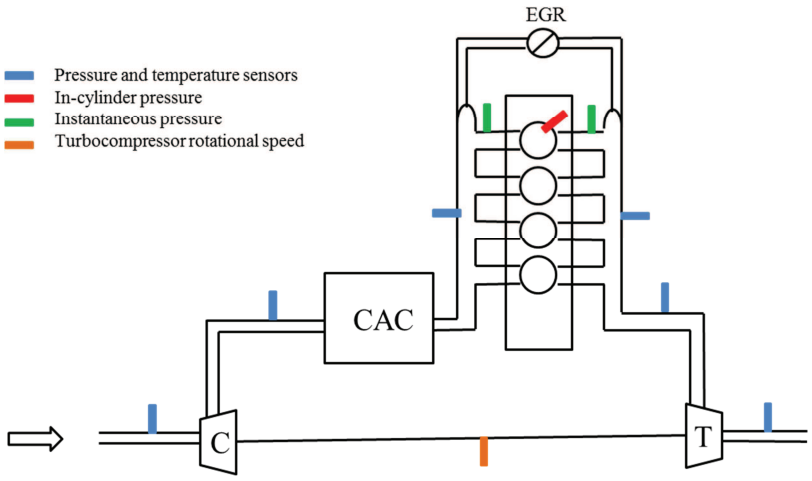

Figure II-2 Engine description and sensors location

Table II-2 - Sensors characteristics

Sensor	Calibrated range	Accuracy
Gas, Coolant and Lubricant temperature (K-type thermocouple)	0-1000 °C	± 1°C
Gas pressure (piezoresistive relative pressure sensor HMA Sensor Technics)	0-2.5 bar	± 1.5%
Coolant pressure (Khrone Optibar P 1010 C high temperature)	0-5 bar	± 0.25%
Lubricant pressure (Khrone Optibar P 1010 C high temperature)	0-10 bar	± 0.25%
In-cylinder pressure (Kistler 6056A41)	0-250 bar	± 0.5 bar
Instantaneous gas pressure (Kistler 4049A)	0-10 bar	± 10 mbar
Coolant mass flow rate (Khrone H250)	16-160 l/min	± 1.6%
Lubricant mass flow rate (Khrone H250)	6-60 l/min	± 1.6%
Fuel consumption (AVL 733)	0-150 kg/h	± 0.12%
Rotational turbocompressor speed (Inductive sensor Picoturn)	0–200 000 rpm	±200rpm

II.2. Simulation Code

The model developed in this study can be divided into two parts. A high-frequency (HF) engine model simulating the air flow through the intake and exhaust line and the engine. Its time step is set to 1° of crank angle. The second is the hydraulic thermal code presenting the coolant and lubricant circuits of the engine. It runs with a 0.1s time step. Those models were developed using GT-Suite software.

II.2.1 GT-Suite software

GT-Suite is a product of Gamma Technologies, a platform for engine and vehicle simulation for concept and system detailed design analysis. It handles in a single software tool, a wide variety of vehicle and engine technical applications such as:

- Engine performance modeling (GT-Power)
- Engine cooling
- Vehicle thermal and energy management
- Lubricant circuits
- Fuel injection systems

and many other applications. Different libraries exist in the software divided between flow, acoustics, thermal, mechanical, electrical, chemistry and control. In addition, GT-Post is a post processor specifically designed for GT users. Once a simulation is complete, results are viewed in GT-Post. The latter allows collecting data for different cases, simulations or tests and performs various mathematical operations on data in all plots.

This work evaluates different thermal management strategies, which are always functioning in an engine environment. GT-Suite was the software chosen to build the model.

II.2.2 Engine model

The engine model (high-frequency) has its time step set to 1° of crank angle. This model is mainly developed on GT-Power based on different engine tests. An overview of the model is given in Figure II-3.

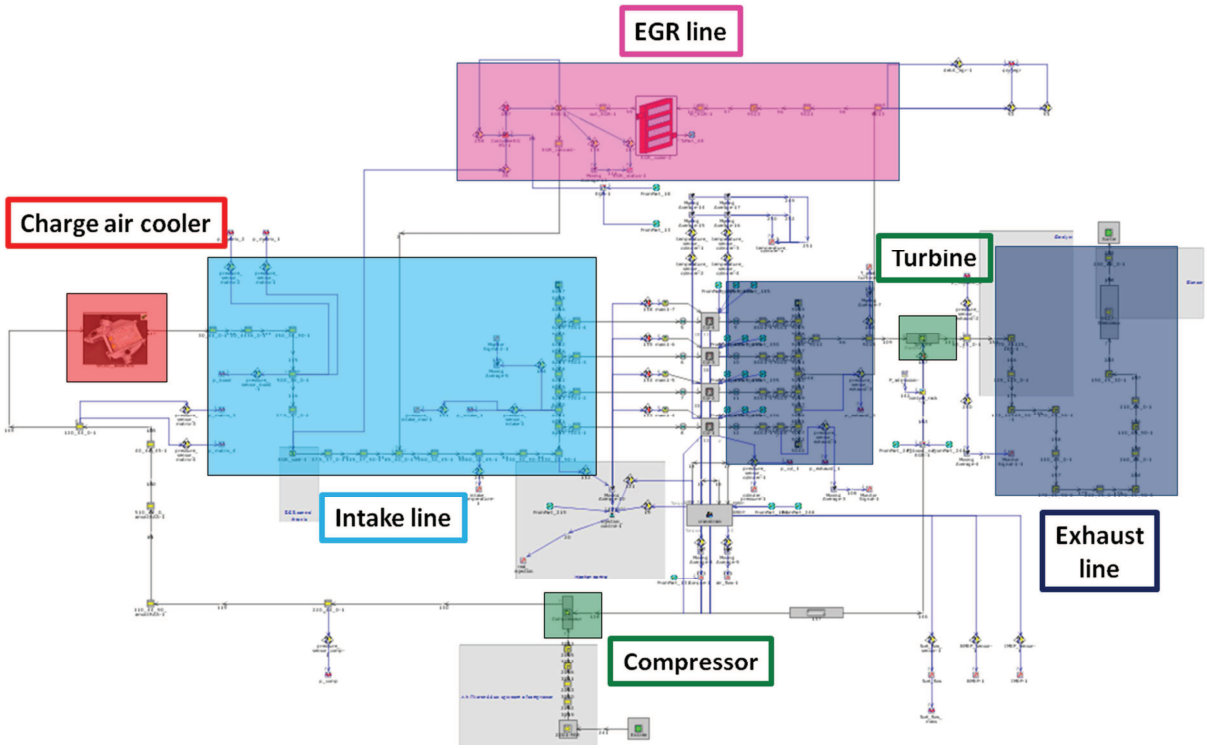

Figure II-3 GT-Power engine model

Largely, it covers the air flow through the engine. It starts by sucking air from the ambient environment via the compressor. The mass flow rate, outlet temperature and consumed power of the compressor are calculated by use of different maps. The pressurized air is cooled by the charge air cooler, before being mixed with the EGR HP. The EGR rate is defined by an EGR valve controlled by the engine speed, its torque and the air flow rate of the intake line. The intake line is modelled to have the best filling efficiency. It takes into consideration the unsteady characteristics of the pressure pulsations and remains close to the model's original wave action.

To define the right amount of injected fuel, the injection controller takes into account the air flow rate, the targeted torque, the engine speed, the torque feedback from the crank train as well as the fuel energy and engine size. The controller gives the calculated amount of injected fuel to four sequential injectors connected each one to a cylinder.

In-cylinder heat transfer is calculated based on the classical Woschni correlation (equation (II-1)) [21] [25] but with some modifications. They consider the treatment of heat transfer coefficients during the period when the valves are opened. At that moment, the heat is increased by inflow velocities through the intake valves and by backflow through the exhaust valves. Furthermore, a map of a convection multiplier is added based on the engine tests in function of the engine speed, torque and crank angle.

$$h_c = CB^{m-1}p^m w^m T^{0.75-1.62m} \quad \text{(II-1)}$$

It is known that the combustion process is dependent on different global engine parameters like variable valve timing, lift, throttle … [94] [95] and the Wiebe laws do not guarantee the prediction of the combustion phenomena when the operative engine conditions are different from tested ones. In GT-Power, the Wiebe laws used are calibrated for full operation power. In most of the normalized driving cycles, the engine mostly operates in part load. And, the Wiebe laws do not guarantee a well prediction of the combustion outside its range. Therefore, the GT-Power combustion profile and burn rate were upgraded and calibrated to cover all different operating points of the engine based on the engine tests. All the engine maps have been calibrated with the Three Pressure Analysis method (TPA) (inlet instantaneous pressure, in-cylinder pressure, and exhaust instantaneous pressure). TPA is a simulation based method to analyze test data to determine quantities that are difficult to measure directly. It is valid only for steady state operating points. It consists of determining three pressures for 1 cylinder, the inlet, the in-cylinder and the exhaust pressure, then running the system will generate different profiles such as the burn rate. Verification is done by running the cylinder with the different burn rate and verifying its pressure.

A part of the exhaust gases evacuating from the engine flows to the EGR HP branch, while the rest flows through the exhaust line to the Variable Geometry Turbine (VGT). The latter's rack position is controlled based on different physical parameters of the engine and its turbocharger system to have a specific boost pressure. The turbine model will define the output power and outlet temperature based on different maps that describes the turbine performance concluded from different engine tests.

II.2.3 Hydraulic and thermal model

The aim of this thesis is to assess the fuel consumption benefits of different thermal management strategies. A model representing the coolant and circuit model was developed using GT-Suite. The global layout of the coolant and lubricant circuit is given in Figure II-4.

At the outlet of the engine, the coolant is divided between three branches, the heater branch including the EGR cooler, the bypass and the radiator branch controlled by a conventional thermostat. Through the warm-up phase, the classical thermostat blocks the radiator branch, and the coolant flow is redirected to the inlet of the engine. Once the regulation temperature is reached, set in this study to 83°C, the thermostat opens the radiator branch, and the heat transferred to the coolant circuit is evacuated to the ambient air via the radiator. Downstream the radiator, an expansion tank takes place. Upstream the water pump, the oil cooler leads to a heat exchange between the two engine fluids.

In the simulation code, every element of the hydraulic circuits was modeled in exception of the cabin heater. It was considered inactive through all the study, and it was modeled only as pressure losses.

Pumps in the system were linked to the engine speed with different gear ratios. The water one is based on measured performance data that correlates speed, flow rate, pressure rise and total efficiency. Those data were given as a map provided with the pump used on the test bench.

However, the oil pump is modeled as a displacement pump which was proposed by GT libraries as the best template to represent the oil pump in the hydraulic system.

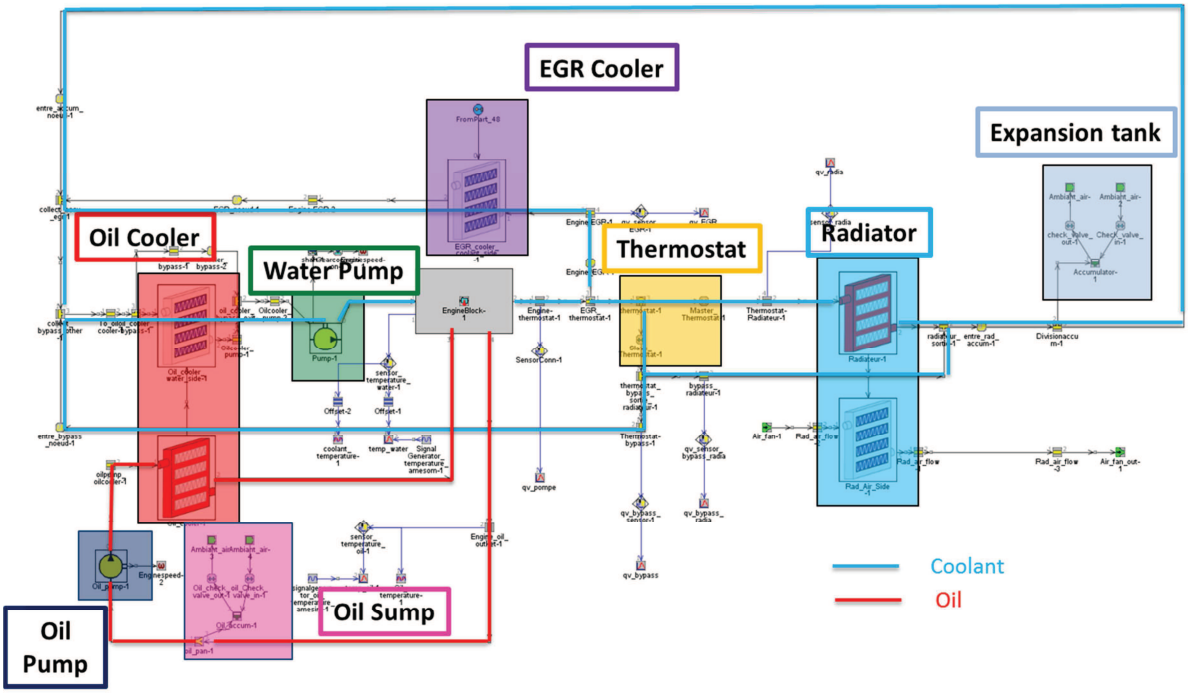

Figure II-4 GT-Suite hydraulic and thermal model

The master-slave notice developed in GT was used for the thermostat and heat exchangers modeling. This notice divides the defined element to model in two parts: a master that is in charge, and a slave that follows the master in its behavior. The main characteristics are given to the master part such as geometrical specifications, heat transfer data and pressure losses.

The thermostat is divided between two valves, the slave one following its master valve. The master valve takes in charge the radiator branch and it is given all the main characteristics as its initial state, the time needed for thermostat to react to its surrounding temperature. Furthermore, the master part gets the opening and closing position of the thermostat in function of its temperature, thus the thermostat hysteresis. The Slave part, which controls the by-pass branch, will be following the master and it will open and close regarding the position of the main part.

For heat exchangers, different engine tests helped to approach the different models to the reality. They are modeled within the same notice as the thermostat. The master part of the heat exchanger already takes in charge most of the exchanger specifics. It covers the geometry specifications such as the different types of exchanger, and its dimensions, the performance maps and the pressure losses of the system. The performance maps are a steady-state operating conditions in function of the inlet pressure, temperature and the mass flow quantity of the two fluids, the master and the slave one. It is valorized by the power or the heat exchanged between the two fluids. For the pressure losses, two types were used. The first consists of a profile of different pressure losses in function of the fluid flow rate. However, for the second type, data are entered in a tabular form taking into consideration the flow rate, inlet and outlet temperatures and pressures. Then, an option is chosen where the simulation pre-processing the solver will perform an optimization to find an orifice discharge coefficient.

The later will be located at the outlet of the exchanger and a pipe friction multiplier that minimizes the error between predicted and measured pressure drops over all of the entered data points. Those coefficients determined during the pre-processing routine do not vary during the simulation. The master part contains pressure drops profile for both the master and slave fluid. Pressure drops profile for the radiator slave part (the ambient air) was ignored in this model, in contrary to the coolant at the oil cooler and at the EGR cooler. Radiator was modeled as a tube-fins heat exchanger. However, the oil cooler and the EGR cooler were presented as a generalized heat exchanger demanding more geometrical characteristics. The slave part contains the type of the slave fluid. Dividing the heat exchanger into two parts that are connected to each other reduces the complexity of the overview of the model, and it allowed the EGR cooler to be integrated in the engine model directly on the EGR HP loop.

An engine block of five masses was used from the software library to model the heat transfer between the engine parts such as the cylinder head, walls and piston and the different fluids. As shown in Figure II-5, two inner masses representing the coolant and the oil are connected to a volume of coolant and oil. These two masses receive direct heat input resulting from the engine combustion model. The input heat is divided between heat to the coolant inner mass and to the oil inner mass. Those two inner masses are connected to three outer masses representing the engine block, head and crankcase. The latter are connected to the ambient environment by a convection coefficient. The model calibration was made upon the different engine masses and the different heat transfer coefficients to approach the engine behavior at the test bench.

The expansion tank is modeled with an accumulator block that already exists in the software where there is a constant volume of two fluids separated by a mass less membrane. The same notice were used and linked to the oil sump to model the existence of the air in the oil sump.

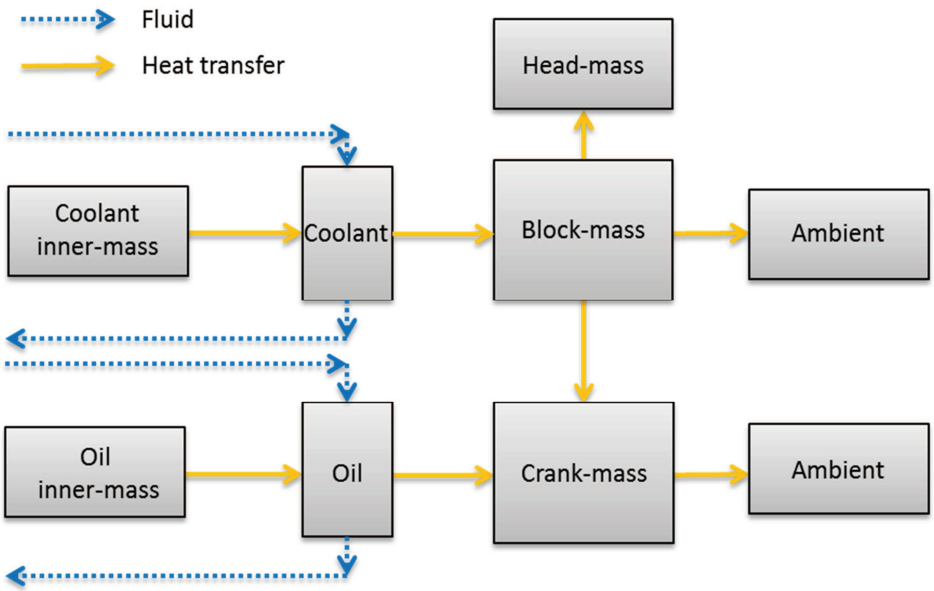

Figure II-5 Engine block 5-Mass

The engine model and the hydraulic thermal model run together. They are linked in a way the HF engine model provides the heat input (coming from the combustion and the friction losses) necessary to the good functioning of the coolant and lubricant circuits. As a feedback,

the latter send the different engine mass temperatures necessary to the good functioning of the engine cylinder template. The friction model existing in the GT-Suite is represented by the equation (II-2) depending on the instantaneous speed of the piston and the maximum pressure in each cylinder during current cycle. This friction model shows no dependency on the lubricant viscosity that represents a crucial parameter and primordial one in defining the level of friction power in the engine. Thus a correction of the friction model has been made depending on the lubricant temperature, thus its viscosity based on the law defined by Shayler *et al.* [29]. To better represent the friction losses on the engine test bench, the reference temperature T_{ref} is set to 90°C and the exponent α is set to 0.35 (equation (II-3)).

$$FMEP = \frac{\sum_{i=1}^{number\ of\ cylinder} C_1 + C_2(p_{\max}) + C_3(Sp_i) + C_4(Sp_i^2)}{Number\ of\ cylinders} \quad \text{(II-2)}$$

$$FMEP(T_{oil}) = FMEP(N, BMEP) \times \left(\frac{\nu(T_{oil})}{\nu(T_{ref})}\right)^{\alpha} \quad \text{(II-3)}$$

For this study, the vehicle mass is equal to 1430 kg. The coolant used in the study contains 40% of ethylene glycol already defined in the library with all its physical characteristics (Density, enthalpy, evaporation, viscosity …). Its volume is around 6.35 L. The lubricant is of type 15W40 with a volume of 4.7L which characteristics are already defined in the library. Once all the different parts were calibrated in a steady-state phase, they were linked to each other, respecting the fluid volume in each branch. Then, pressure drops were regulated in the different branches before the model was tested and calibrated for transient conditions. As cold start and transient conditions were registered during the engine tests, they were used to finally validate the model. The coolant temperature evolution is studied for a static engine operating point 50 N.m, 1500 rpm. Figure II-6 shows a good agreement between the model developed and the engine test bench. The coolant temperature showed a maximum error of 3°C during the transient phase. Regarding the lubricant, the results are acceptable even if the curves are not as close as the coolant. Lubricant temperature can be improved by more detailing the lubricant circuit especially the friction losses at the crank shaft bearings. However, these approaches will result in significantly increasing the computational time and will be less interesting in a thermal view of the different strategies tested during this work.

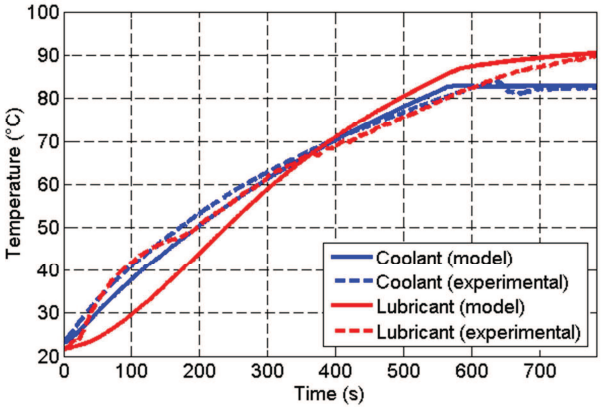

Figure II-6 Comparison between the engine model and test bench results

II.3. Driving cycles

Pollutant emissions as oxides of nitrogen (NOx), carbon monoxide (CO), and particulate matter (PM) as well as fuel consumption, (thus CO_2 emissions) are regulated by European directives. Various laws were set to regulate the limits of a standard vehicle. In order to compare all the commercial vehicles; driving cycles were defined and normalized over different part of the world.

Driving cycles are a profile of vehicle speed in function of time. They varied over each part of the world, describing their driving conditions similar to the way of living. Light-duty vehicle are tested over a chassis dynamometer bench, where a driver controls the vehicle following a speed driving profile and gear ratio versus time. For some commercial vehicles, the driving cycle is not evaluated over a vehicle test bench but on an engine test bench where the cycle is given in term of engine speed and torque [165] [166].

In this study, different driving cycles will be taken into consideration to assess the different thermal management strategies. Those driving cycles used are chosen for different purposes; mostly because they are more related to European driving applications.

II.3.1 New European Driving Cycle (NEDC)

NEDC (Figure II-7) is the first cycle chosen for the study because it is the current homologated driving cycle in Europe used to assess the different emissions and legalize vehicles over Euro6 norm. NEDC consists of four repeated ECE-15 urban driving cycles with a maximum speed of 50 km/h and one Extra-Urban driving cycle with a maximum speed of 120 km/h. The total cycle time is 1180s and runs a distance of around 11 km. This driving cycle has an average driving speed of 33.6 km/h. It has 14 stops consisting 20.42% of the cycle time. However, a lot of critics accuse NEDC to be a non-representative of the real-life driving conditions. With its low accelerations (0.528 m/s² as an average positive acceleration), constant speed cruises and many idling events it is considered as stylized driving speed pattern [167]. For that reason, talks are about changing from NEDC to WLTC with the new norms.

Applying this driving cycle on the simulation model gives the results in terms of temperature presented in Figure II-7. As shown, the coolant temperature reaches its regulation temperature around the end of the driving cycle, leaving the engine to run only few seconds in the steady state stage. Moreover, the lubricant temperature is still increasing at the end of the cycle. These temperature profiles back up the idea that NEDC is a non-representative of the real-life driving cycle.

II.3.2 Worldwide harmonized Light duty driving Test Cycle (WLTC)

WLTC (Figure II-8) or as known too as WLTP (Worldwide harmonized Light vehicles Test Procedures) is the driving cycle globally harmonized; the reason this cycle is the second on the list. WLTC will be the replacement of the NEDC in Euro7 norm. WLTC has three applied test cycles based on the vehicle class defined by power-weight ratio (the engine's power output being divided by the mass of the vehicle). Most of the light duty vehicles or commercial vehicles belong to the WLTC class 3. The latter can be divided into four parts: low, medium, high and extra high depending on the average speed of the vehicle. This driving

cycle is longer than NEDC, as it goes for 1800s and 23 km and it reflects more the driving cycle of the average world where you have multiple velocity changes as well as gear ratios. It reaches its maximum speed of 131.3 km/h in the extra high speed part, the last part of the driving cycle; while the average driving speed is 46.5 km/h. Less stop phases are found in WLTC (12.6% stop share) in comparison with NEDC (23.7%) [168].

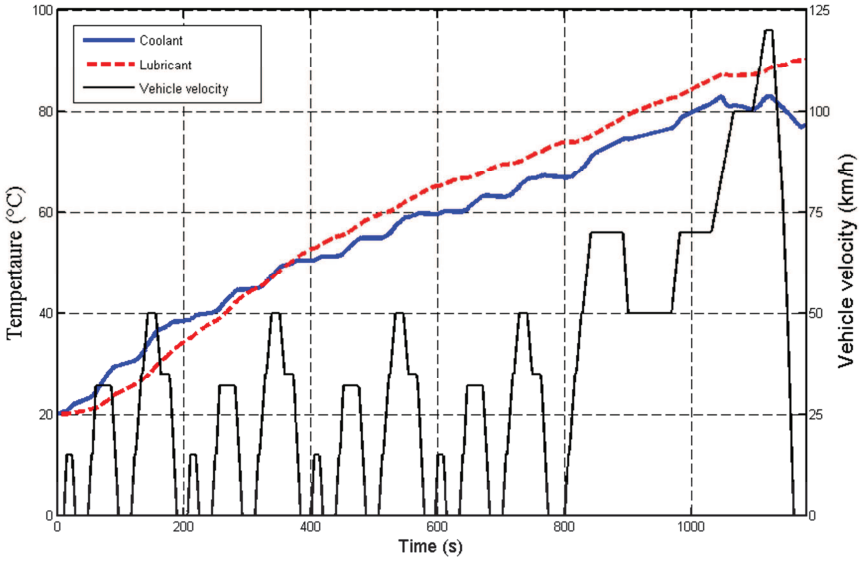

Figure II-7 NEDC

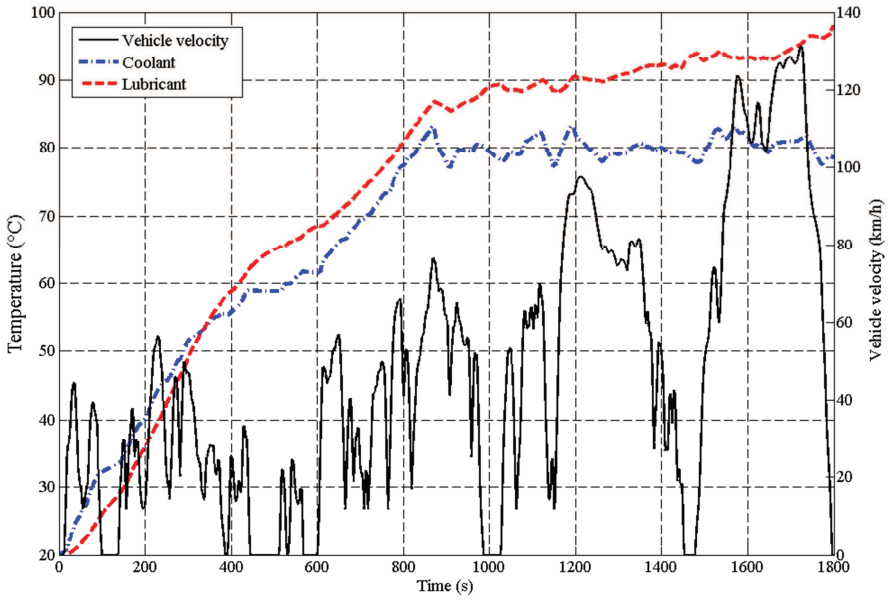

Figure II-8 WLTC

Temperature profile depicted over the vehicle velocity in Figure II-8 shows that the engine reaches its regulation temperature almost at the half of the driving cycle. Lubricant temperature shows a quasi-steady state around 1000s when it reaches 90°C. Then, it starts to increase again at the high vehicle velocity at the extra high velocity part of WLTC.

II.3.3 Common Artemis Driving Cycles (CADC)

CADC are cycles based on statistical studies done in Europe with the Artemis project (Assessment and Reliability of Transport Emission Models and Inventory Systems). There are three different configurations of the CADC: the urban cycle, the rural cycle and the motorway cycle which has two variants: a maximum speed of 130 km/h and 150 km/h. CADC is not a legalized cycle and is not used to officially measure the pollutant emissions of a vehicle or its fuel consumption. It is used by the manufacturers to assess the fuel consumption of their new technologies on vehicles in a more realistic use because CADC reflects real driving conditions. Two configurations are used in this study: the Artemis Highway (130 km/h) and the Artemis urban cycle [169].

II.3.3.1. Artemis Motorway 130 – Artemis Highway

AH (Figure II-9) – Artemis Highway – is the next driving cycle on the list. It was chosen because it is representative of real severe driving conditions, vehicle taking the highway and reaching high vehicle speed in a short amount of time. This driving cycle forces the engine to operate at high load operating points in transient conditions. Additionally, during steady state stage, the engine is at its full power, under high load. The average driving speed is 97.6 km/h; it heats the peak of 131.43 km/h only after 300s from the engine start. This cycle goes for 1068s and the engine runs a distance of 28.7 km and presents only three total stop over the whole cycle. The severe acceleration on the early stages of the cycle leads the engine to its regulation temperature quickly, leading to steady state stage domination during the cycle. The latter is one drawback of the Artemis Highway driving cycle; it does not highlight the importance of the different thermal management strategies during the transient phase. The latter will be underrated by the steady state phase and the length of the driving cycle. However, this cycle is interesting to highlight the improvements of the regulation temperature.

The temperature profiles depicted in Figure II-9 proves the severity of this driving cycle. The coolant reaches its regulation temperature around the first quarter of the driving cycle, while the lubricant reaches 100°C slightly before 900s.

II.3.3.2. Artemis Urban

AU (Figure II-10) – Artemis Urban – is a driving cycle from CADC also reflecting the urban European average real world driving. It is for 993s, covering 4.8 km with an average speed of 17.7 km/h. It is a reflection of a city driving with a maximum speed reaching 57.32 km/h and total number of 14 stops for 14.71s. Hence, it is a driving cycle where the engine is most of the time at part load, thus in transient conditions almost through all the cycle. Furthermore, one of its characteristics is having a lot of acceleration and deceleration. It has 48 accelerations through the whole cycle. This cycle was chosen to highlight the importance of the different thermal management strategies during a cycle in which the steady state stage, if existing, won't be dominating the driving cycle.

Figure II-10 shows an engine running all the cycle during a transient phase. The coolant temperature does not reach 83°C, engine's regulation temperature, at the end of the cycle. The lubricant temperature increases in a softer slope than the other cycles to end with a temperature around 80°C at the end of the AU cycle.

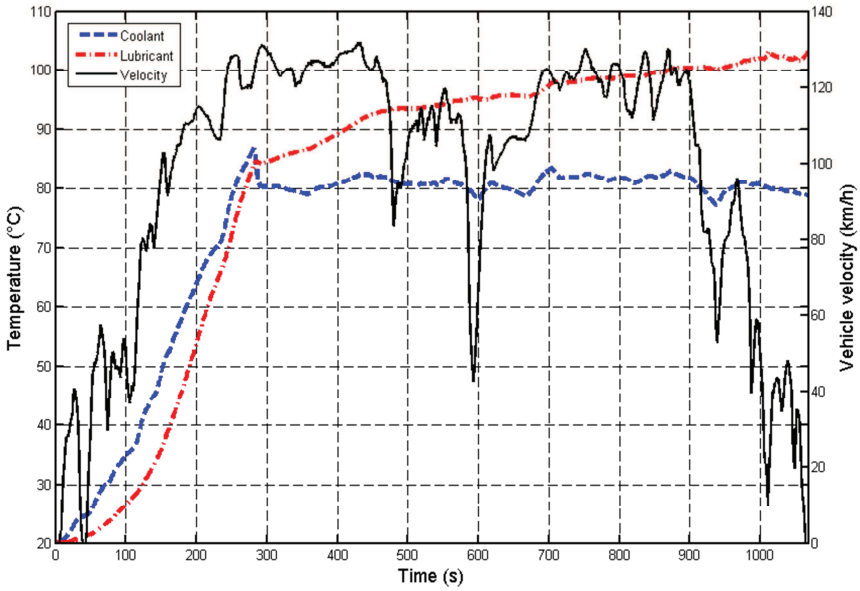

Figure II-9 Artemis Highway

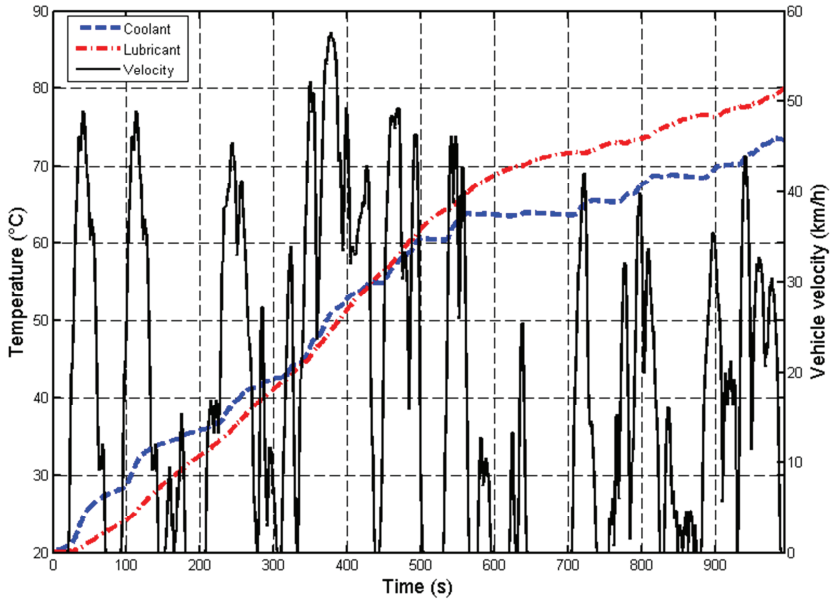

Figure II-10 Artemis Urban

II.3.4 In-House Developed driving Cycle (HDC)

After the common driving cycles chosen to be tested, an in-House Developed driving Cycle (HDC) was proposed. The last two driving cycles had their own drawbacks: one does not highlight the importance of thermal management strategies and the other is a representative of a city travel and limited by an average low speed. HDC reflects a suburban driving style, leaving around the city and not confronting the city traffic jam and allowed to go higher in speed in a short amount of time. The idea was to combine the high speed part of the Artemis highway and a short cycle to take the advantage of a dominated transient cycle as the Artemis

urban. HDC is a short cycle of 254s, for about 2 km with no stops; it's a representative of driving style of a suburban French worker situated in Nantes, West France, taking his car in the morning from its home to the work allowing reaching 90km/h in 50s (Figure II-11). This driving cycle will highlight the importance of different thermal strategies on engine working on higher load than most of the driving cycles proposed and still in transient conditions through all the cycle. It will focus on the benefits of the applied thermal strategy on the engine performance.

Identically to the previous cycle, HDC has the engine running in transient phase throughout the cycle; coolant is still increasing at the end of the cycle (Figure II-11). The lubricant temperature stays lower than the coolant during the whole driving cycle.

The different temperature profiles shown for the different driving cycles are the reference cases to which all the thermal management strategies temperatures will be compared in the upcoming sections.

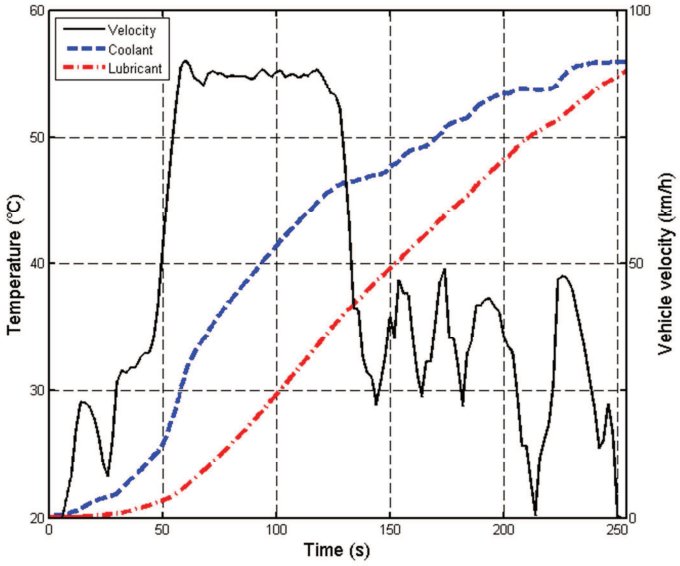

Figure II-11 In-House developed driving cycle

II.4. Energy Balance

In this part an energy balance of the engine is done in addition to an energy balance of the coolant and lubricant circuit. These energy balances were applied on the different driving cycles mentioned before. The energy balance is divided as shown in the Figure II-12.

II.4.1 Formulation

The energy flow entering the engine comes from the chemical energy of the fuel, which is transformed into different forms: the brake power, the heat transferred to the cylinder walls, the sensible energy of the exhaust gases downstream the turbine, the heat dissipated to the coolant at the EGR cooler, the heat flow in the charge air cooler (CAC), the friction power that is dissipated later to the oil circuit, and different miscellaneous losses such as the incomplete combustion, radiation to the ambient air, etc.

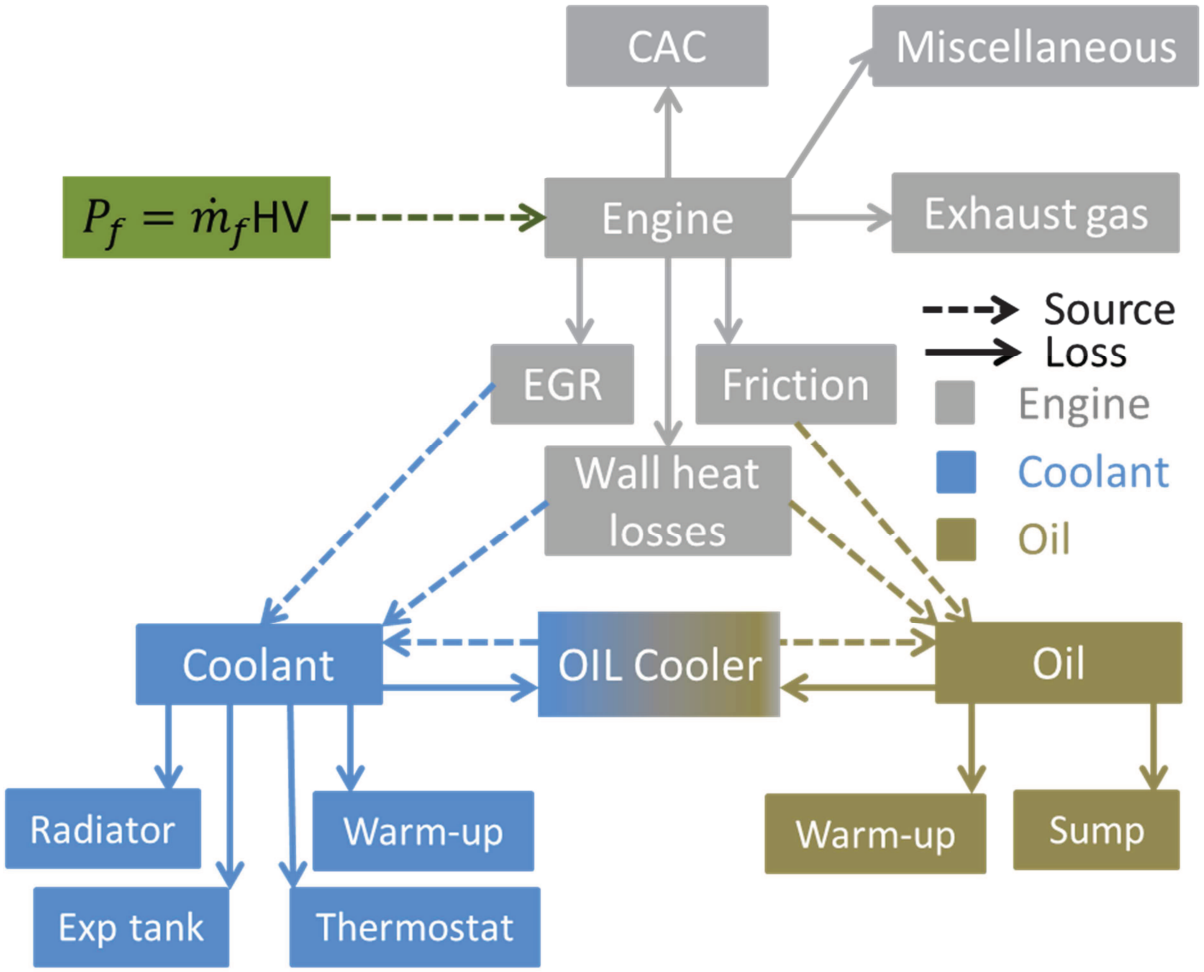

Figure II-12 Energy balance

The chemical power of the fuel is determined by measuring the fuel mass flow and knowing its heating value (43.07 MJ/Kg).

The indicated power is simplified in this work and divided between the brake power and the friction power. The brake power is considered as an output of the engine and calculated using the rotational engine speed N (rpm) and the engine torque τ (Nm) as follows:

$$P_b = \frac{2\pi N\tau}{60} \qquad \text{(II-4)}$$

The friction power P_f is transferred mainly to the oil circuit, but a part is dissipated to the coolant circuit at the piston/cylinder block.

The heat transferred to the cylinder walls is associated to the power $\dot{Q}_{wall\_losses}$, and is mainly dissipated to the coolant circuit but as the oil passes in the cylinder head and lubricates the piston, some of this heat is transferred to the oil circuit at those points.

The heat power rejection at the charge air cooler ($\dot{Q}_{CAC}$) and at the EGR cooler ($\dot{Q}_{EGR}$) are obtained from the following expression

$$\dot{Q} = \dot{m}\, c_p (T_{out} - T_{in}) \quad \text{(II-5)}$$

$\dot{m}(kg/s)$ is the mass flow rate of the air in the charge air cooler and of the EGR in the EGR cooler. T_{out} and T_{in} are the fluid temperatures respectively at the outlet and inlet of the exchanger. The EGR mass flow rate can be obtained from the EGR rate that was imposed into the model in function of the engine speed and torque; issued from the engine tests. $c_p\ (J/kg/K)$ is the specific heat of the air or the EGR.

For the exhaust gases downstream the turbine, the equation (II-5) is used to calculate the exhaust power $\dot{Q}_{exhaust}$. The specific heat of the exhaust is calculated by the following equations depending on the temperature and the air-fuel equivalence ratio [53]:

For $T \geq 326.85°C$

$$c_p = \left(166.3 + \frac{24.5}{\lambda}\right) \cdot \log\left(T - 70 - \frac{120}{\lambda}\right) \quad \text{(II-6)}$$

For $T < 326.85°C$

If $\lambda < 8$, then:

$$c_p = (975.5 + 0.28 \cdot T) - \log(\lambda) \cdot (11.92 + 0.06 \cdot T) \quad \text{(II-7)}$$

Else

$$c_p = 1000 + 2.85 + e^{0.0088 \cdot (T - 273.15)} \quad \text{(II-8)}$$

The miscellaneous losses $\dot{Q}_{misc}$ are computed from the general energy balance equation:

$$\dot{m}_{fuel} H_v = P_b + \dot{Q}_{wall\_losses} + \dot{Q}_{exhaust} + P_f + \dot{Q}_{EGR} + \dot{Q}_{CAC} + \dot{Q}_{misc} \quad \text{(II-9)}$$

To define the coolant and oil circuit energy balance, a definition of their heat sources should be done.

On one hand, the main heat source of the coolant comes from the combustion where the coolant cools down the cylinder head and the cylinder block, in addition to a small part of the friction. On the other hand, the coolant cools down the EGR, making the latter a secondary heat source for the coolant circuit. For the oil circuit, the main heat source is the friction, then the combustion. The oil is cooled down by coolant making the oil cooler a heat source to either one of the systems, hence the necessity of dividing the energy balances during the transient phase.

The thermal power dissipated to the coolant circuit $\dot{Q}_{c,heat}$ will be divided between losses to the ambient air at the radiator $\dot{Q}_{rad}$, thermal power transferred to the oil at the oil cooler $\dot{Q}_{oil-cooler}$, a minor part at the thermostat $\dot{Q}_{th}$ and at the expansion tank $\dot{Q}_{exptank}$, while the rest is used to warm-up the water ($\dot{Q}_{c,warm-up}$).

$$\dot{Q}_{c,heat} = \dot{Q}_{rad} + \dot{Q}_{oil-cooler} + \dot{Q}_{th} + \dot{Q}_{exptank} + \dot{Q}_{c,warm-up} \quad \text{(II-10)}$$

For the oil energy balance, the main source $\dot{Q}_{heat\_oil}$ is dissipated at the oil cooler $\dot{Q}_{oil-cooler}$, the oil sump $\dot{Q}_{o,sump}$ and to warm-up the oil $\dot{Q}_{o,warm-up}$.

$$\dot{Q}_{o,heat} = \dot{Q}_{oil-cooler} + \dot{Q}_{o,sump} + \dot{Q}_{o,warm-up} \quad \text{(II-11)}$$

II.4.2 Application

The energy balance will be applied on different driving cycles in the order defined in paragraph II.3. The ambient temperature is set to 20°C.

II.4.2.1. NEDC

The temperature profile of the coolant and the lubricant are presented in the Figure II-7. It can be noticed that the coolant temperature takes the lead over the lubricant at the start of the driving cycle, when the heat source is much important to the coolant system. However, the heat capacity of the oil is lesser than of the coolant, the former will take the lead starting from the 368th second of the cycle. Additionally, the regulation temperature of the engine is reached around 1016th second of the cycle, very close to its end. For more insight of the energy balance during the different parts of the cycle, the latter will be divided into four parts: three of them in the transient phase of the cycle and one in the steady state stage. Energy balance will be applied on the different phases of the cycle highlighting the importance of each one. Phase A will cover the driving cycle from 100s to 200s, having the coolant temperature higher than the oil's. Phase B ranges from 400 to 600s, shifting to the oil temperature as the leader. Phase C covers the end of the transient phase from 800 to 900s and the phase D gives an insight during the steady state phase covering the cycle from 1050 to 1150s.

The main heat sources for the coolant and the lubricant comes from the combustion and the friction. These two sources are divided as seen from the plot of the phase A in Figure II-13(a) into around 1.7% only to the lubricant circuit and 10.2% to the coolant circuit. The big amount of the combustion heat and the friction losses are used to heat up the global mass of the engine. Consequently, a decrease of the total engine mass is considered primordial at the start of the cycle. Light weighted materials as aluminum cylinder head can be proposed. Moreover, a thermal insulation of the engine or any under-hood management as flaps helps to improve the engine efficiency from the start-up. However, it will lead to a bigger radiator to maintain the engine optimal phase and protect the different engine parts from the thermal stresses as well as maintaining the right temperature of the oil film around the different moving parts of the engine. As described before, during phase A, the coolant temperature takes the lead over the lubricant so it contributes to its heating. Thus, in addition to the combustion heat and the friction losses, the coolant at the oil/water heat exchanger is another heat source of the oil circuit. It is 52.6% of the total heat transferred to the oil during phase A (Figure II-13(b)). This 52.6% of additional heat to the oil circuit is considered as a loss to the coolant circuit, and it is around 22.3% of the total coolant circuit energy balance. The latter defines the energy used to warm-up the coolant about 77% of its total energy (Figure II-13(e)). However, all the energy dissipated to the oil circuit is used to heat up the lubricant (Figure II-13(c)).

Moving on through the NEDC cycle, to phase B when the oil temperature takes the lead over the coolant temperature. The only heat source to the oil circuit is now the combustion heat and the friction losses. Despite that almost all the heat given to the oil during phase A was used to warm the oil; in phase B this amount is reduced to 55.4% and 39.3% is transmitted to the coolant circuit via the oil/coolant exchanger. From this phase, the oil cooler is considered another heat source for the coolant circuit in addition to the engine and the EGR cooler. During this phase, almost all the heat given to the coolant is used to increase its temperature. In phase C, the heat used to warm-up the oil keeps on decreasing because the heat transmitted to the coolant circuit increased because of higher temperature difference between the two fluids at the heat exchanger. From the coolant heat source point of view (Figure II-13(d)), the percentage of the heat coming from the oil circuit hits its peak in this phase. On one hand, the difference between the two fluids grows bigger. On the other hand, with the coolant temperature growing and the radiator branch still closed the heat transferred to the coolant circuit from the combustion heat will be minimized in percentage. Not to forget, in phase C, the engine runs at higher operating points, increasing its speed, thus the flow rate in the heat exchanger, hence the heat transfer between the two fluids.

The regulation temperature during NEDC is reached around 1016s, opening the radiator branch and start evacuating heat to the ambient air. This is the main changing happening during the steady-state phase. After 10.2% of the total heat of the combustion and the friction were given to the coolant in the phase A, it increases to 46.4% during the steady state phase D. Furthermore, the main losses in the oil circuit energy balance are at the oil cooler. 89% of the entire heat source given to the oil circuit is transmitted to the coolant (Figure II-13(c)). This is due to an increase between the two fluids temperature. The oil temperature increases while the coolant stays constant during the regulation phase. Moreover, the heat evacuated at the radiator increases the transfer between the two fluids. Despite the huge amount of the heat transferred from the oil to the coolant, it is only 13.8% of the total heat of the coolant circuit. 46.4% of the combustion and the frictions losses constitute 82.1% of the total heat of the circuit. However, this quantity of the heat coming either from the engine, the oil circuit or the EGR cooler is 95.5% lost to the ambient air, as depicted in the plot of the coolant circuit energy balance (Figure II-13(e)).

The engine energy balance plot (Figure II-14) offers an insight of the evolution of the main losses of the engine through the driving cycle. The friction is proportional to the oil viscosity, and the latter is inversely proportional to the oil temperature. The oil temperature increases during the driving cycle; the oil viscosity decreases and thus the friction losses. The friction losses during the phase A, the beginning of the driving cycle are at its highest level around 19% of the fuel power injected in the engine. These friction losses decrease through the different phases to reach 6.6% in phase D. The exhaust gases losses increase with time. On one hand, their level is related to the coolant temperature. When the latter increases, the temperature difference between the coolant and the combustion gases decreases thus the heat loss to the walls. By decreasing the heat loss to the walls, the combustion gases stay at higher temperature level, leading to higher temperature exhaust gases and higher losses. On the other hand, at the fourth phase of the engine energy balance, the engine is operating at high operating points, extra-urban part of NEDC. At this state the engine turns at a faster rate, leaving less time for the combustion gases to exchange heat with the chamber walls, so higher

exhaust gases temperatures. The exhaust losses grow from 16% in phase A to 27% in phase D.

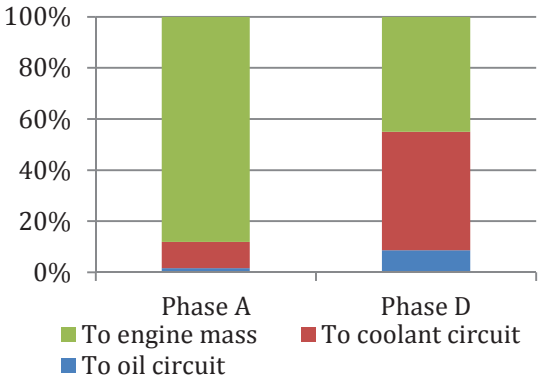

(a) : Engine thermal power source destiny

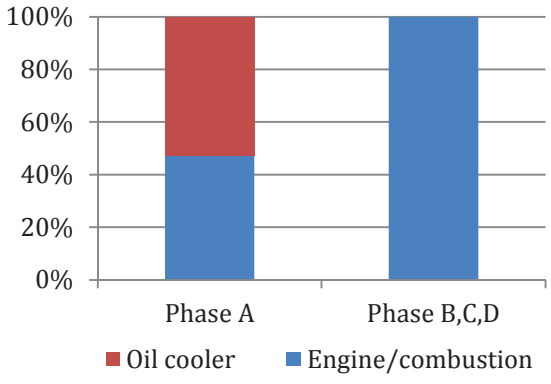

(b) : Oil thermal power source

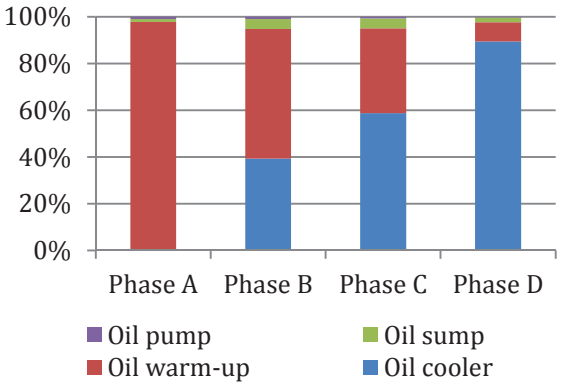

(c) : Oil circuit energy balance

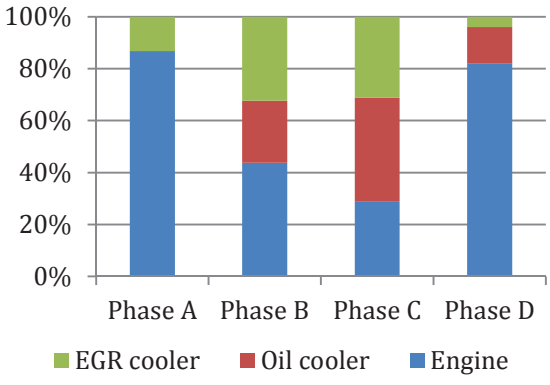

(d) : Coolant thermal power source

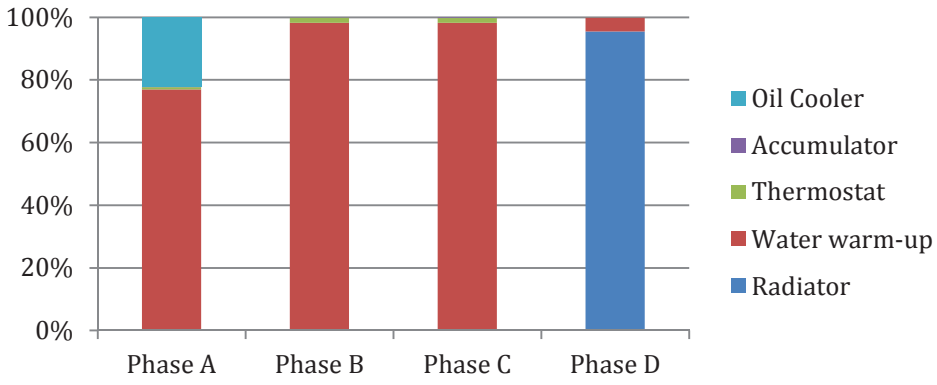

(e): Coolant circuit energy balance

Figure II-13 Coolant and lubricant energy balance over NEDC

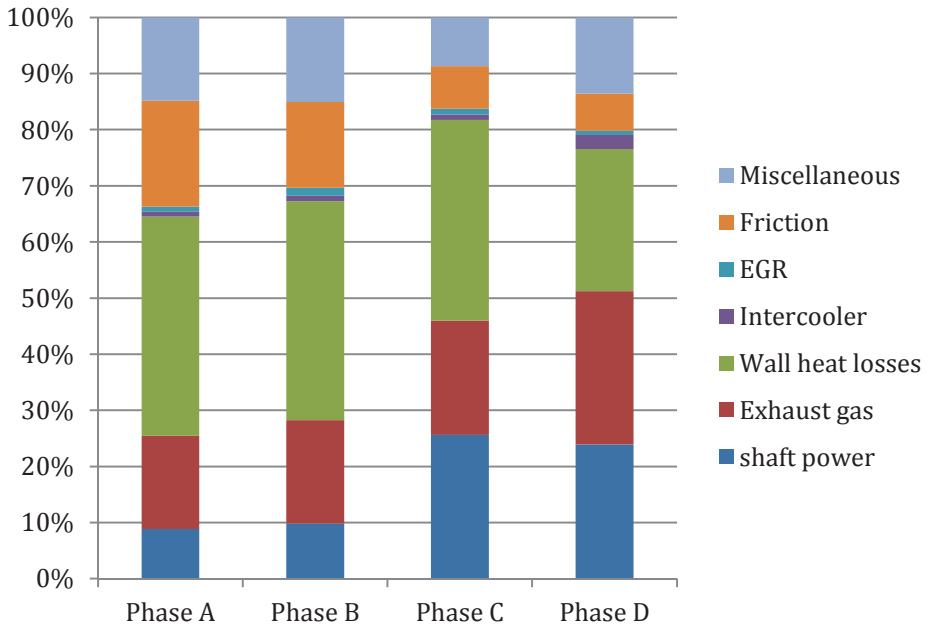

Figure II-14 Engine energy balance over NEDC

II.4.2.2. WLTC

As shown in the temperature profile plotted in Figure II-8, the coolant temperature takes the lead over the lubricant until the 334th second of the driving cycle. After that, the oil rises over the coolant. The regulation temperature of the engine (83°C) is reached around the 870th second of the cycle. Hence, the steady state phase dominates the cycle with 51.6%. To always highlight the transient phase, it was divided into three parts for the energy balance. The first phase A consists of the first 100 seconds of the cycle. Phase B was chosen in order to have the meeting point of the two fluids temperature in its interval, thus its covers the cycle from 200th to the 400th second. The end of the transient phase (600-800s) is covered by the third phase C. And one final phase to cover a part of the steady state stage, chosen around the halfway of this stage. Phase D gores from the 1200th to the 1400th seconds of the cycle.

Considering that the total heat source of the engine comes only from the combustion heat and the friction losses, during phase A friction losses are around 37% of this total heat source (Figure II-15(a)). Moving to the oil heat sources plot (Figure II-15(b)), it can be noticed that the heat coming from the engine directly to the oil circuit is around 47% while 53% is the indirect transfer of the engine heat to the oil circuit by the coolant via the oil/water exchanger. The total heat given to the oil circuit in this phase is used to increase its temperature. This oil temperature increment is primordial at this phase, because the friction portion of the total energy of the fuel injected in the engine is about 23.2% (Figure II-16). Friction losses percentage at the beginning of WLTC is higher than that of the NEDC because of the highest rotational speed of the engine at the first driving cycle and highest torque demand. It is known that the friction is a result of two parts in contact sliding at each other's. And, as the moving part's speed of the engine is proportional to its rotational speed, thus with higher rotational speed and torque demand higher are the friction losses.

As mentioned before, the phase B is characterized by including the meeting point of the two fluid temperatures in its interval. By analyzing the lubricant and coolant heat sources, the oil cooler takes part in both of the plots. At first it was considered as a heat source for the oil circuit while the coolant temperature was higher than the lubricant's. Later it becomes a heating source for the coolant once the latter goes back to cooling down the lubricant. Because the meeting point is close to the end of this phase, the amount of the oil cooler heat source for the coolant circuit is minimized to a 0.8% of the total heat. The major part comes from cooling down the engine block and the cylinder head and it is for 80.7% while the rest of the heat comes from the EGR cooler (Figure II-15(d)). This 0.8% contribution to the coolant warm-up is considered as a loss of around 3.7% of the lubricant circuit (Figure II-15(c)). The total heat transferred to the lubricant during this phase is used to warm it up and to contribute more in diminishing the friction losses. Basing on the coolant energy balance during this phase, the biggest amount of its total heat is used to heat it up. In addition to minor losses in the different parts of the circuit, 15% of this heat is transferred to the oil circuit to help in increasing the latter temperature (Figure II-15(e)).

At the end of the transient phase, phase C, and before reaching the regulation temperature, the lubricant temperature takes the lead, and all the heat transferred to the coolant is used for its warming (Figure II-15(e)). The amount of the heat transferred indirectly from the engine to the coolant either by the oil/water exchanger or the EGR cooler in this phase takes the lead over the engine direct heat (the combustion heat and the friction losses) with an amount of 65.5% (Figure II-15(d)). The main heating source of the coolant in phase C is the oil circuit. This huge transfer between the two fluids goes back to higher temperature difference between both of the fluids and a higher coolant flow rate due to a higher engine rotational speed, thus higher pump speed.

The steady state stage presented by phase D, is the phase in which the radiator branch is opened, and the heat transferred to the coolant circuit will be evacuated to the ambient air. Consequently, the heat coming directly from the engine to the coolant will hit its peak. It is called the regulation phase, the temperature of the coolant stays quasi-constant. Hence, higher is the dissipation of the heat at the radiator; higher is the amount of heat transferred to the coolant either by any source: the engine, the EGR or the oil cooler. As shown in Figure II-15(c), 94% of the oil heat is transmitted to the coolant, 66.5% of the total heat of the coolant comes from the engine (Figure II-15 (d)) and almost all of that heat is evacuated at the radiator (Figure II-15 (e)).

The engine energy balance of the WLTC highlights the importance of the oil temperature and its viscosity on reducing the friction losses during the driving cycle. As shown at the start of the cycle, the friction losses are at their summit with 23.2%, then reducing to almost 8% during the final phase. A reduction of around 65% of the friction losses is obtained between the start and the end of the driving cycle. Identically to the friction losses, the wall heat losses reduce all along the driving cycle from around 40.2% to 29.4%. These two major losses underline, on one hand, the importance of improving the engine thermal efficiency, thus its total efficiency, at the beginning of the transient phase where its friction losses and its wall heat losses are at their peak. On the other hand, the exhaust losses mark its importance in increasing with every second of the driving cycle. As mentioned before, with increasing the

engine rotational speed and increasing the coolant temperature, the exhaust losses hit their summit. Hence, heat recovery at the exhaust gases or during the regulation phase can be applied to improve the earliest phase of the transient state of the engine.

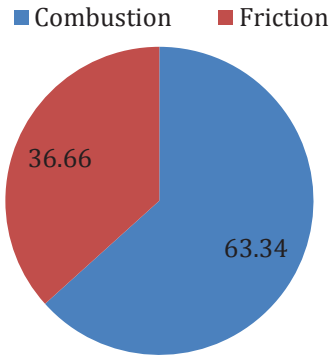

(a) : Engine's thermal power division during phase A

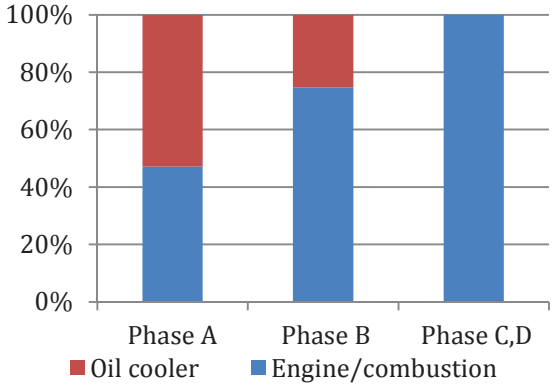

(b) : Oil thermal power source

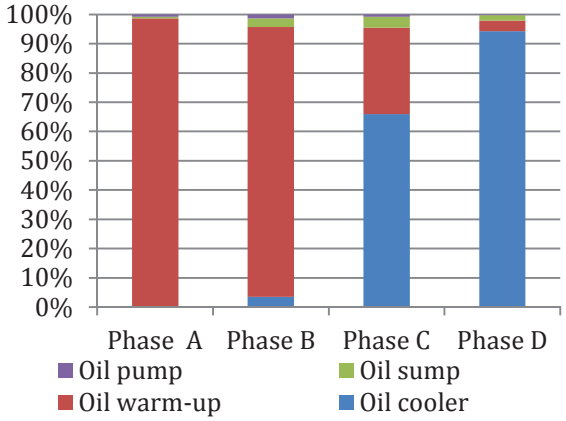

(c) : Oil circuit energy balance

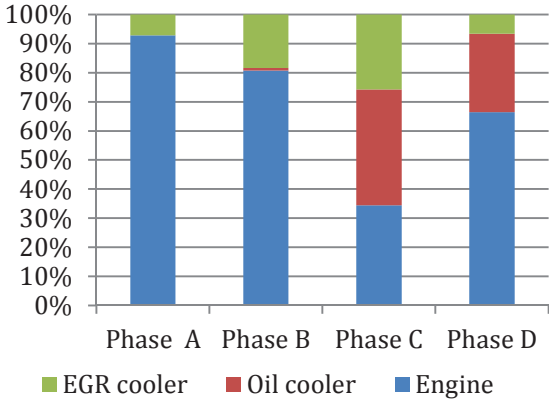

(d) : Coolant thermal power source

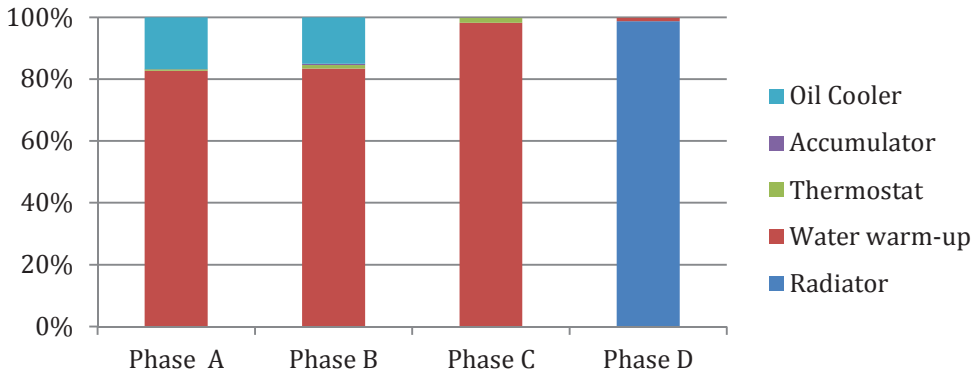

(e): Coolant circuit energy balance

Figure II-15 Coolant and lubricant energy balance over WLTC

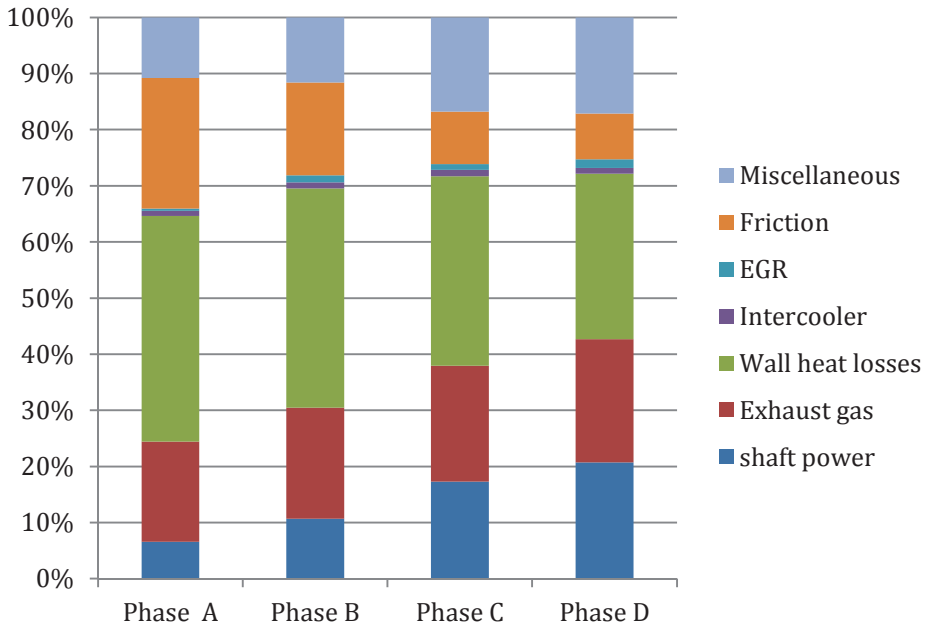

Figure II-16 Engine energy balance over WLTC

II.4.2.3. Artemis Highway

One of the particularities of this cycle is its severity. It pushes the engine to work on high operating points in its earliest stage leading it to reach its regulation temperature after only 281s. The early reach of the regulation temperature leaves the engine to operate on its regulation temperature and its higher efficiency level for around 73% of the total driving cycle.

At the start of the cycle, as it is represented in the plot of the Figure II-9, the coolant temperature is higher than the lubricant's; the latter takes the lead at the 285th second of the cycle. The engine balance for this driving cycle is divided into four parts: the first two covering the transient phase and two in the regulation phase. Phase A and B covers simultaneously the interval 50-150s and 150-250s. Phase C and D covers the beginning and the end of the steady state stage, the former is between the 400th and the 600th of the cycle while the latter's interval is 800-1000s.

Both the transient phases show that the part of the heat transmitted from the engine directly to the oil circuit is insignificant compared to the part transmitted to the coolant or to the engine mass. It equals 0.68% in phase A and increases to 0.85% during phase B. While the heat evacuated to the coolant circuit increased from 9.7% to 13.1%. The rest is considered consumed by the mass inertia of the engine to heat up (Figure II-17(a)). Despite that low percentage of heat transmitted to the fluids in the engine, the latter reached higher temperature faster than any other driving cycle. In Artemis highway, the high operating point of the engine demands more fuel injection in the transient phase, thus more initial fuel energy to start with. Additionally, as mentioned before, the coolant temperature is higher than the lubricant in all the transient phase leading the oil cooler to become a heat source to the lubricant circuit. In phase A, the heat coming from the coolant is 65.9% of the total heat of the lubricant circuit and it rises to 79% due to an increase in the temperature difference of the two fluids and higher flow rate of the two fluids in the oil heat exchanger (Figure II-17(b)). The coolant

circuit energy balance informs that the coolant loses 20% of its heat source to the oil in phase A and 28% in phase B (Figure II-17(e)).

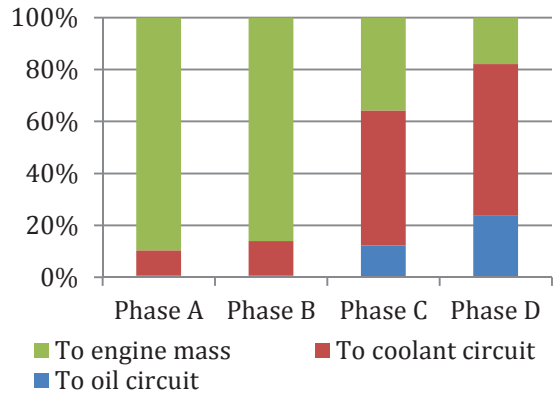

(a) : Engine's thermal power destiny

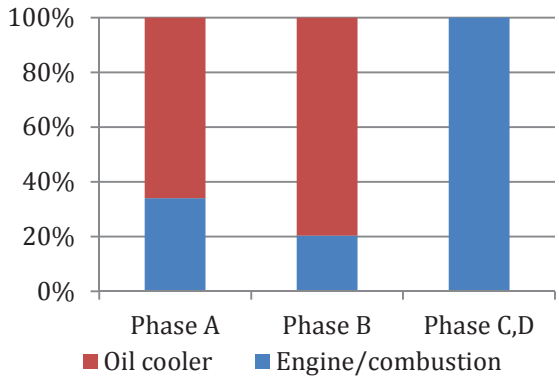

(b) : Oil thermal power source

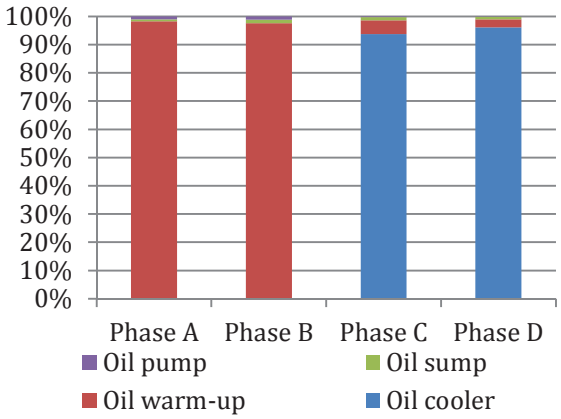

(c) : Oil circuit energy balance

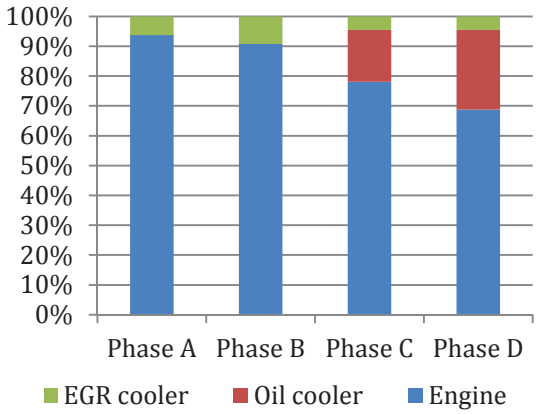

(d) : Coolant thermal power source

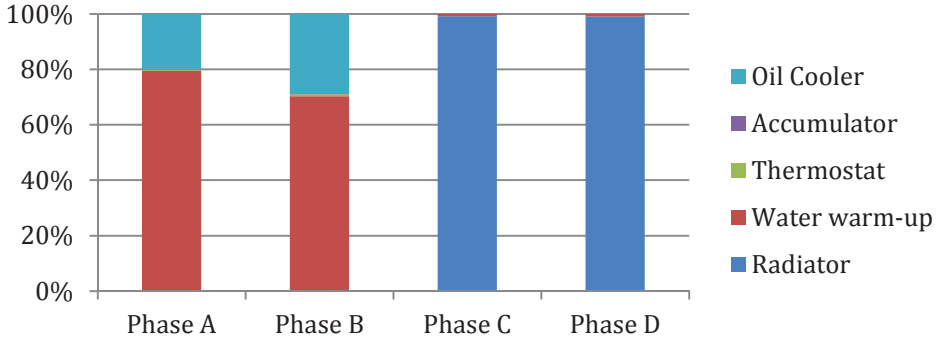

(e): Coolant circuit energy balance

Figure II-17 Coolant and lubricant energy balance over Artemis Highway

Moving on from the warm-up stage to the steady state stage, the first thing to notice is the repartition of the heat source coming from the engine between the different parts. An increase in the part of the two hydraulic circuits is shown in the differing plots. The coolant circuit dominates the use of the engine heat source with an amount of 51.9% in phase C and 58.4% in phase D followed by the oil part that hit the peak in the last phase with 23.7% of the engine

heat source. The oil circuit energy balance shows that most of the heat given to the oil in the engine is transmitted to the coolant via the oil cooler, and still a small amount around 4% and 2% in phase C and D simultaneously is used to continue to warm-up the oil (Figure II-17(c)). And as the radiator branch is opened, most of the heat transmitted to the fluids is evacuated to the ambient air.

Analyzing the engine energy balance through the Artemis highway underlines the small amount of the friction through this driving cycle (Figure II-18). The summit of the friction losses was in the phase A with only 10.9% comparing to 23.2% with WLTC. Consequently, the thermal management focusing on reducing the friction losses will have a higher impact on the WLTC than on the Artemis Highway. The friction losses go down to the point of 6.9% between the 800th and the 1000th second of the cycle. In this driving cycle, the exhaust losses take a big amount of the fuel energy losses as the engine runs most of the driving cycle in high operating points and especially at high speed. The shaft power in this driving cycle shows an important part of the engine balance, as the engine runs most at the time in comfort zone in terms of engine efficiency; while rare is the time it runs in low speed and low charge operating point. Furthermore, the engine idle time during the Artemis highway, which is a representative driving cycle of the highway real driving, are insignificant comparing to the homologation driving cycle and the upcoming one.

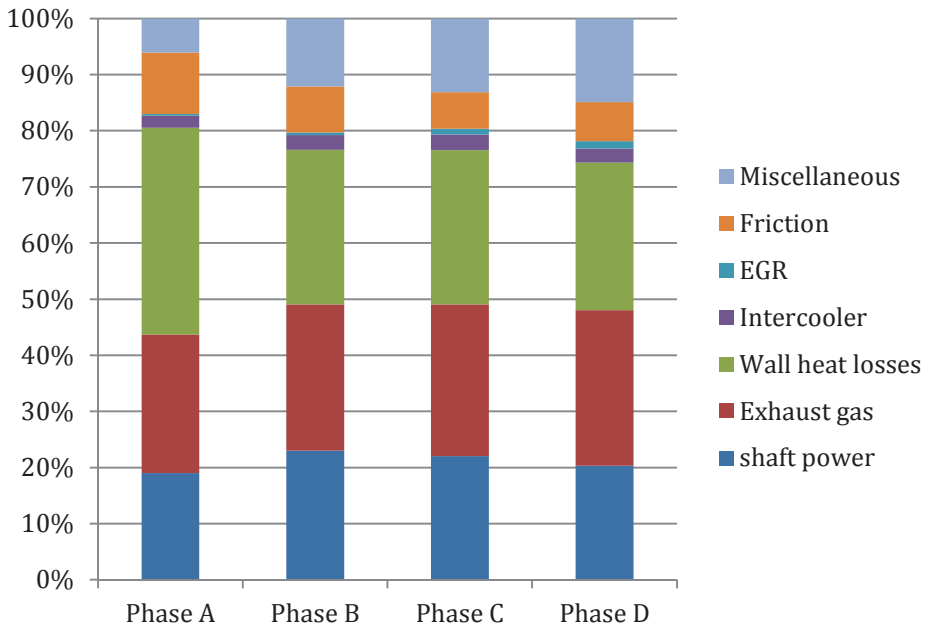

Figure II-18 Engine energy balance over Artemis Highway

II.4.2.4. Artemis Urban

The second driving cycle from CADC is much softer than the former one. In AU, the engine runs with a maximum speed of 57 km/h, leading to an average of 1500 rpm through the whole cycle. During this driving cycle and as the temperature profile shows (Figure II-10), the engine does not reach the regulation temperature, and during the whole cycle it runs in a transient state with lower efficiency. This cycle as mentioned before is a realistic representation of a city driving based on statistical studies. The cycle, thus the transient phase, is divided into three different parts covering the beginning, the middle and the end of the

cycle. 100-200s, 400-600s and 800-900s are the intervals of phase A, B and C simultaneously. The phase B includes the meeting point between the two fluids temperature. The coolant takes the lead over to the oil until the second 434 of the cycle.

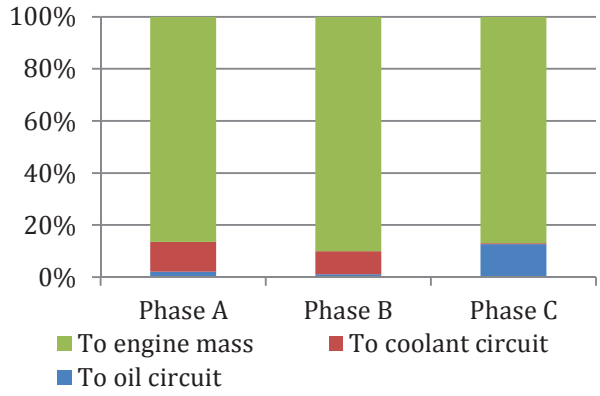

(a) : Engine thermal power destiny

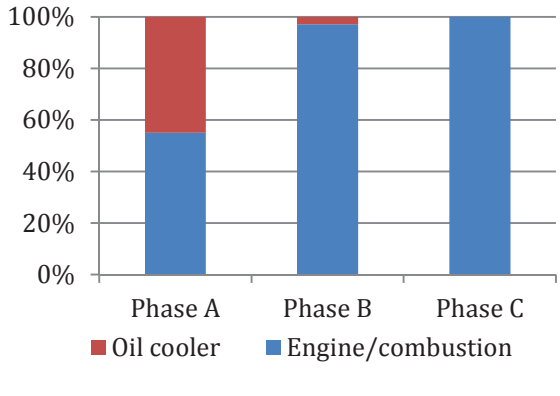

(b) : Oil thermal power source

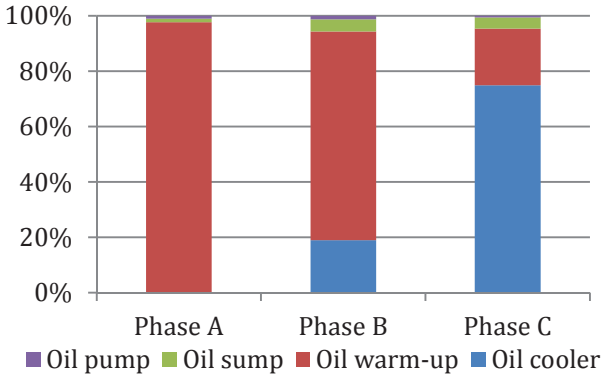

(c) : Oil circuit energy balance

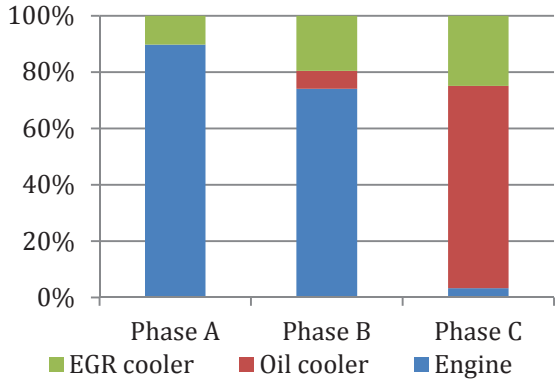

(d) : Coolant thermal power source

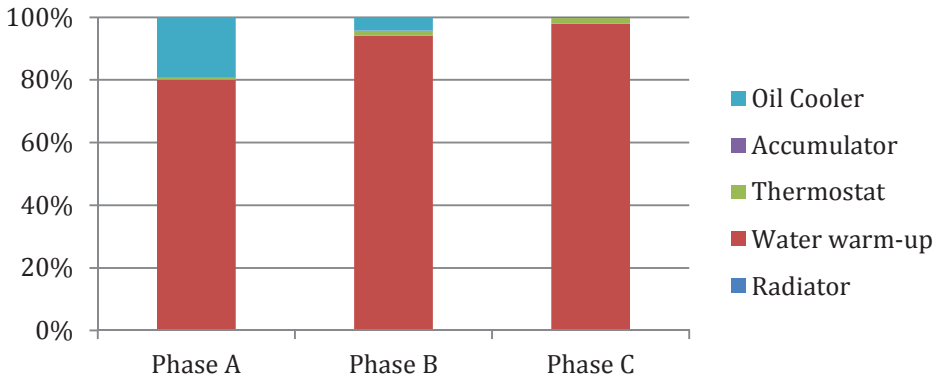

(e): Coolant circuit energy balance

Figure II-19 Coolant and lubricant energy balance over Artemis Urban

Similar to the previous driving cycles, during phase A, the oil receives heat from the coolant in addition to the heat received from the engine. The distribution is 45% from the oil cooler and the rest from the engine (Figure II-19(b)). Almost the totality of the heat is used to warm-

up the engine (Figure II-19(a)). The energy balance of the two fluids changes during the second phase where for the first 34s of the phase B, the oil receives heat from the coolant, before the latter switch to the receiver side and the oil takes the lead in the temperature. During phase B, the oil circuit energy balance shows that 20% of energy is dissipated to the coolant via the oil heat exchanger. The major part is still used for the heating up of the oil (Figure II-19(c)). The heat transfer between the two fluids in AU is not as high as the different cycles, in which the engine is running at higher speed leading to higher flow rate through the heat exchangers, increasing the heat transfer between the two fluids. The oil dominates the coolant by its temperature for almost three quarter of this phase. Despite that, the heat transmitted to the water represents only 6.4% of the total heat source of the coolant circuit (Figure II-19(d)). Most of it is used to warm it up (Figure II-19(e)).

During the last phase, the heat dissipated from the combustion chamber is still in its major part seeded to the engine mass inertia, and only 0.42% of it is connected to the coolant circuit while 12.6% to the oil circuit. In this phase the vehicle is stopped for more than half of the time, thus the engine is at idle and the injection at it lowest, while most of the other part of the vehicle is decelerating, thus moving. Examining the water heat sources energy balance, the heat coming from cooling down the lubricant dominates the different heat sources with 71.8%, followed by the EGR cooler with 24.9% and the rest comes from the engine (Figure II-19(d)).

The engine energy balance highlights the low energy efficiency during the city driving cycle as the shaft power is at their lowest during this cycle with a peak of 13%. The friction losses are important with 21.33% in the earliest stage of the driving cycle. The huge wall heat losses underline the importance of applying different thermal management strategies leading to lower these losses during the transient phase of the engine. Exhaust losses stays quasi-constant during the cycle with an important amount of an average of 22% (Figure II-20).

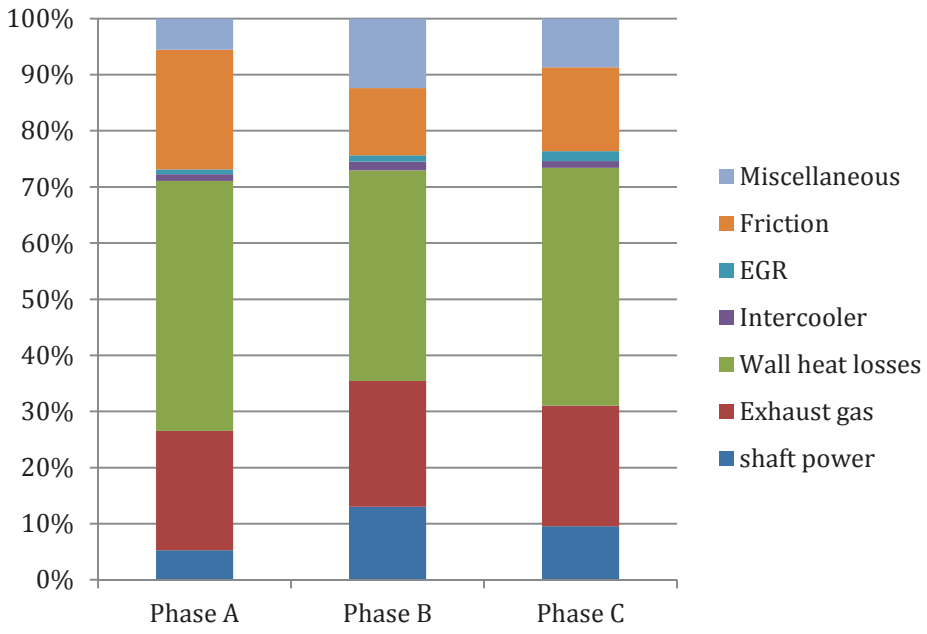

Figure II-20 Engine energy balance over Artemis Urban

II.4.2.5. HDC

This short driving cycle for 254s is similar to the previous one where the engine does not reach its regulation temperature at the end of it. The engine runs for 254s in transient phase with a maximum speed of 90 km/h. This driving cycle isn't decomposed into different parts. The temperature profile of the coolant and lubricant shows that the coolant takes the lead through all the cycle (Figure II-11).

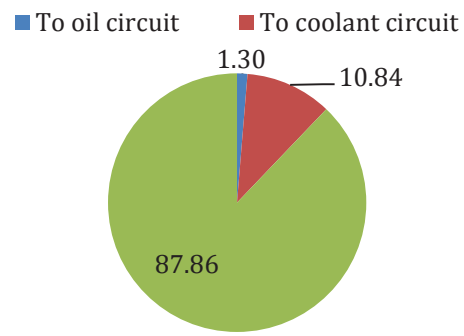

(a) : Engine thermal power destiny

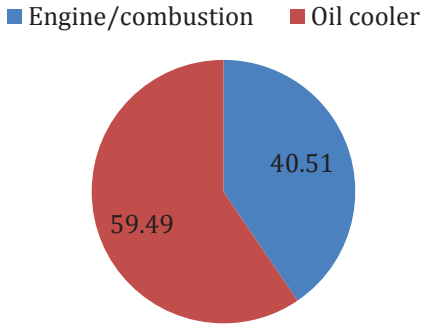

(b) : Oil thermal power source

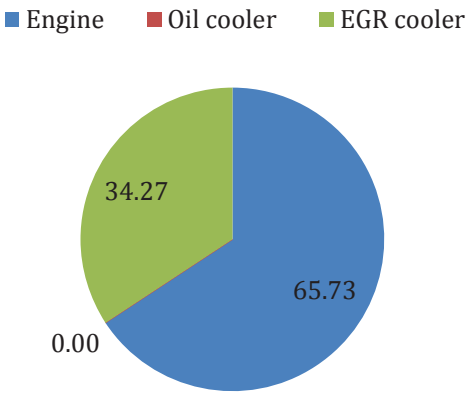

(c) : Coolant thermal power source

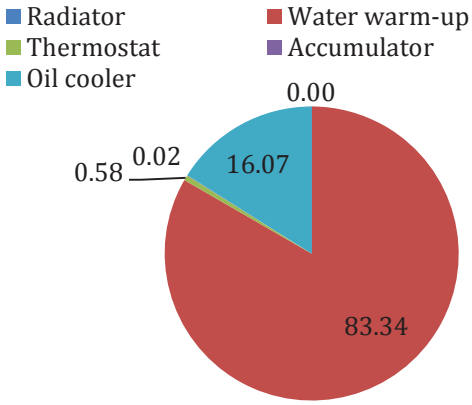

(d) : Coolant circuit energy balance

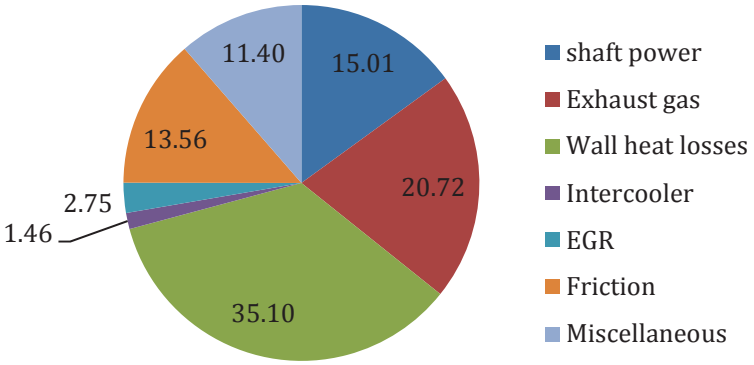

(e): Engine energy balance

Figure II-21 Engine and both fluids energy balance over HDC cycle

This cycle is highlighting the warm-up stage of the engine where most of the energy losses through the chamber walls or the friction are transmitted to the engine mass inertia. Still 10.8% of the total heat is communicated to the coolant and 1.3% to the oil circuit (Figure II-21(a)). Those 10.8% of the heat communicated to the coolant are 65.7% of the total heat to the coolant circuit. The other part comes from the water cooling down the EGR at the heat exchanger situated in the EGR HP loop (Figure II-21(c)). The coolant circuit energy balance shows that only 83.8% of the heat given to the coolant is used to warm it up while around 16% is seeded to the oil circuit at the oil heat exchanger (Figure II-21(d)). The heat received from the coolant dominates the total oil heat sources with 59.5% (Figure II-21(b)). In contrary to the coolant, all the heat given to the oil circuit is used to heat up the oil and contributes in decreasing its viscosity, thus the friction losses.

The energy balance of this short driving cycle supports the first phase of the different driving cycles shown before as the main losses of the injected fuel energy into the engine are the wall heat losses, the exhaust gases and the friction losses. This energy balance shows that the engine during HDC was running in more comfort zone than in Artemis Urban. The shaft power is 15% of the fuel power, supporting the hypothesis that the highest overconsumption of the engine is within the city driving styles (Figure II-21(e)).

II.4.2.6. Outcome of the energy balance

The different energy balances of the engine throughout different driving cycles give as an outcome the following points:

- Reducing the friction losses in the early stages of the driving cycle is primordial. With the friction peaking to 23.2% in the phase A and reducing to 8% during phase in WLTC highlights the importance of the oil's temperature. Moreover during the last phase, the heat transferred from the oil circuit to the coolant circuit is then evacuated to the ambient air. This leads to the thermal management idea of storing heat from the oil circuit during the steady state stage to reduce the friction losses in the upcoming cold start of the engine.
- The major losses in the engine are the wall heat losses in the combustion chamber. These losses cannot be managed completely. The heat transfer in the combustion chamber is essential for the good functioning of the different components of the engine. It allows maintaining a good combustion rate and a good filling efficiency necessary to obtain the best combustion efficiency. From a thermal efficiency point of view, in the earlier phases, the heat evacuated to the combustion walls is used to heat up the different parts of the engine. But once the steady state stage is reached, this energy evacuated to the ambient air is, on one hand, extremely important to keep the engine from overheating and protecting its different parts from the thermal stresses. However, on the other hand, it is a pure loss of energy. The exergy of the heat transmitted to the coolant is still important once it is not evacuated to the ambient air. It should be stored or used in a way to improve the engine efficiency in thermal or total terms. One thermal management strategy is to store this heat during the steady state stage and use it in an upcoming driving cycle. This leads to reduce the heat losses to the walls in the first stages of the engine, where the latter efficiency is at its lowest while it is in his cold states. The storage process can be done in different ways either

by storing hot coolant directly and pumping it in the engine circuits in the next start up, or by latent heat storage. While with the latter, heat is transmitted to phase change materials which can store it for further use.

- The second major losses that increase when advancing in the driving cycle are the exhaust gases. They are considered as pure losses of the engine. Evacuating the combustion gases is one major role of the 4 stroke engine. It cannot be eliminated from the process. Hence, it is good to find a solution to the heat release at the exhaust line. Heat exchanger can be used to transfer the heat from the exhaust gases to the engine fluids to improve warm-up time. Not to forget, the heat exchanger at the exhaust line should be installed downstream the post treatment systems, to not influence their light off time.
- Wall heat losses and friction losses' main destination is the mass inertia of the engine. Reducing the engine mass is one of the different solution for the drawback of this losses. Insulating the engine is another thermal management strategy. It minimizes the dissipation of the heat to the engine's mass by minimizing the heat radiation and convection to the ambient air.
- Oil heat exchanger control is necessary to manage the heat transfer between both fluids. Controlling the fluid temperature, either to reduce the friction losses during the transient phase or to have a faster warm-up of the coolant, can be done by controlling the flow rate at the oil heat exchanger.
- EGR cooler and the charge air cooler are minor losses to the engine total energy balance. EGR heat is dissipated to the coolant and helps its temperature ascent. However, warming up the combustion chamber to reduce the wall heat losses can be tested by introducing hot air into the cylinders. It can be done by by-passing the EGR cooler or the charge air cooler. As a drawback the filling efficiency of the engine will be deteriorated during this strategy. Other strategies propose an EGR cooler with oil. One of its drawbacks is the oil leakage into the EGR high loop.

The energy balance applied on the engine outlines the main losses during the different stages of the engine and shows an agreement with those of the literature survey (main losses with exhaust gases, wall heat losses and friction).

The energy balance highlights the importance of the lubricant temperature at the first stages of the engine, as it is of direct influence on the friction losses. Friction losses that showed high level in some driving cycles (23% at WLTC) reduce to around 8% at the steady state stage when the lubricant temperature is at its highest level. Reduction in friction losses leads to a direct fuel savings.

The coolant showed an importance because of a direct influence on the engine's temperature, thus a direct influence on the wall heat losses that are huge during the warm-up stage. However, reducing wall heat losses won't affect directly the fuel consumption savings. Wall heat losses reduction will lead to a better combustion efficiency, thus fuel consumption savings, but a part of the improvement will lead to higher exhaust gas losses as the latter will have higher temperature. Consequently, exhaust gas heat recovery will be studied. However, different applications of it will lead to different fuel savings.

But at first, to reduce wall heat losses and improve the coolant and lubricant temperatures warm-up phase, heat storage application will be tested. The latter will benefit from the steady state stage of the engine, when the heat losses to the ambient at the radiator are almost all the heat transferred to the coolant circuit. During this stage, the heat recovery from the coolant and lubricant circuit won't have any influence or any fouls on the fuel consumption of the system.

III. Heat storage

Heat storage application will be tested in this chapter. The study is divided in two parts: Coolant and lubricant applications.

For the hot coolant storage, the principle of the strategy will be presented, followed by the primary studies done to choose the tank's volume, the ambient temperature, the initial temperature of the storage tank and the thermal behavior of the latter during the soaking period. Later on, the results of the application of the strategy on the different cycles were presented. Based on the first results, different configurations for the strategy were proposed and applied on different driving cycles. At the end, the influence of the oil's grade was studied.

The second part consists of the study of hot oil storage, where the main conditions of the ambient temperature were taken from the first study. Similar to the first part, the principle of the strategy is introduced followed by the application on the different driving cycles, different configurations and oil's grade influence.

III.1. Hot coolant storage

III.1.1 Hot coolant storage principle

As the new studies and researches to optimize the engine fuel consumption shifted from its optimization to the thermal management, heat storage idea was created. The fuel power injected in the engine is not totally used to propel the vehicle. Major losses of this energy are dissipated to the coolant circuit such as heat through the wall of the combustion chamber, or evacuated to the ambient air within the exhaust gases.

This part will focus on the reutilization of the heat dissipated to the coolant circuit to improve the fuel consumption. As shown in section II.4.2, one of the hugest losses during the warm-up phase is the wall heat losses. To minimize those losses, on one hand, the initial temperature of the coolant should be increased, thus the temperature difference between the combustion gases and the chamber walls should be reduced to its minimum. On the other hand, a zero flow strategy applied to the engine can help to solve this problem. On the same time, the energy balance of the different driving cycles that attended the steady state stage proved that during this phase all the heat dissipated to the coolant circuit is evacuated to the ambient air via the radiator. Based on this idea, the heat storage was chosen to be tested in this study.

Hot coolant storage idea consisted on storing the lost energy to the coolant while the engine is running at its regulation temperature to use it at the next cold start-up. During the next engine use, the stored heat will be released to the engine to warm it up. This allows reducing the temperature difference between the combustion gases and the chamber walls, hence the heat losses to the coolant circuit at the first running stages of the engine. With a higher engine temperature at the early stages, friction losses will be also reduced.

To apply this strategy during the steady state stage, an isolated volume of coolant was placed downstream the thermostat and upstream the radiator. The placement of the storage tank in the radiator branch has a lesser impact on the transient phase. The added volume of the coolant is isolated while the thermostat is closed, thus no addition volume of coolant is needed to be heated. Once the regulation temperature is reached, the thermostat opens the radiator branch and hot coolant flows into the storage volume and its temperature starts to rise. The storage tank is controlled by three different valves in addition to the thermostat as shown in Figure III-1.

The control and the functioning of the hot storage tank are divided into three parts as following:

First start-up: For the first start-up, the coolant in the storage volume is considered at ambient temperature. With the thermostat closed, the storage volume is isolated from the engine and the latter functions normally during the warm-up stage. The coolant flows into the engine, then to the bypass branch and the EGR branch before entering the oil heat exchanger and back to the pump. During this crucial phase, the total volume of the engine coolant does not change.

Storing heat: Once the regulation temperature of the engine is reached, the thermostat opens the radiator branch and hot coolant flows to it. The valve number 3 opens and closes with the

thermostat. With the hot coolant entering the radiator branch, the storage volume starts to be filled with hot water. Valve 1 and 2 stay closed.

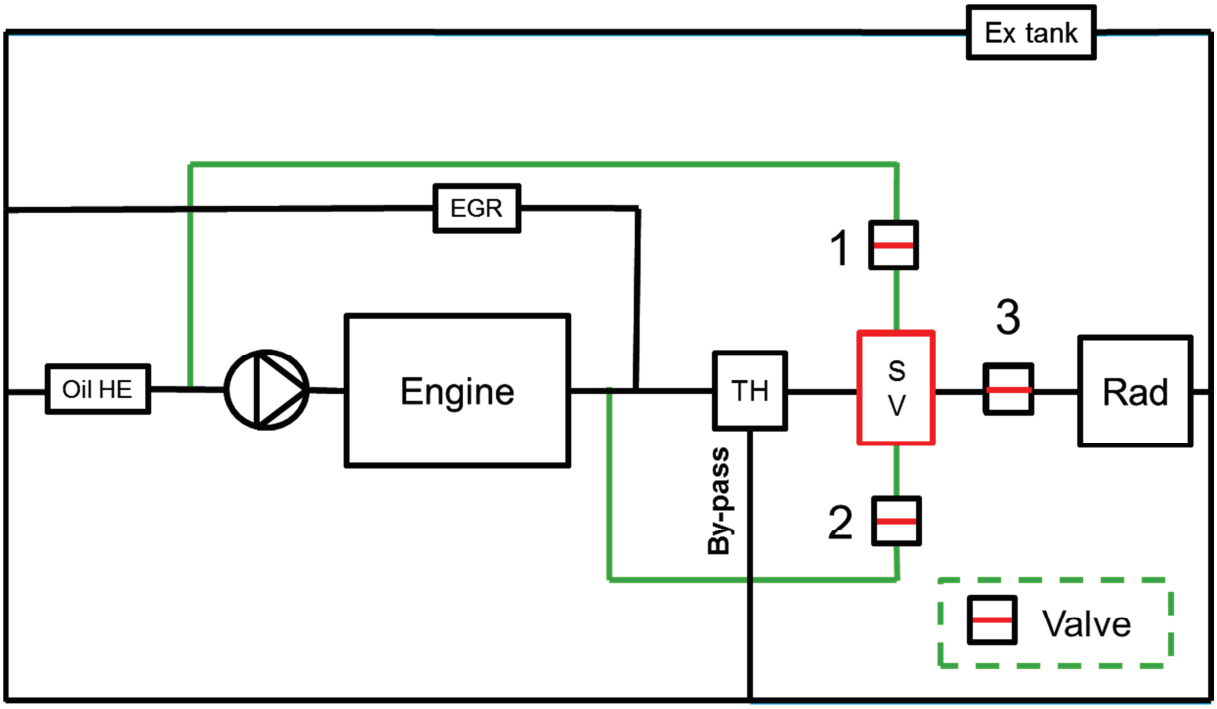

Figure III-1 A schematic presentation of the hot coolant storage strategy (SV: Storage volume; TH: Thermostat; Oil HE: Oil heat exchanger; Ex tank: Expansion tank; Rad: Radiator)

Next start-up: At the next cold start-up, hot coolant stored in the tank will be used to warm-up the engine. As the regulation temperature has not been reached yet, the thermostat is closed, thus the valve number 3. Valves 1 and 2 operate as follows:

If the temperature of the engine is lower than the storage volume temperature **and if** the thermostat is still closed (regulation temperature (83°C) is not reached, hence engine operates in transient conditions), valves 1 and 2 open and the hot stored coolant is sucked by the pump, pressurized and sent to the engine to warm it up. If one of the two conditions is not met, the two valves close and the engine goes back to the traditional architecture until the regulation temperature is reached and the hot coolant is being stored again.

III.1.2 Storage tank volume

To define a storage tank volume suitable for the study of the hot coolant storage thermal strategy, tests were first made on NEDC at an ambient temperature of 20°C. The storage tank volume was varied between 1L, 2L, 3L, 4L and 5L. To study the ability of heating up the storage volume over NEDC, the initial temperature of the storage tank is fixed equal to the ambient temperature.

Figure III-2 presents the storage tank temperature profiles evolution over NEDC with the different volumes cited before. 1L and 2L storage capacity can be heated up to 80°C with NEDC, while 3L reaches 76°C, 4L reaches 71°C and 5L rises up until 65°C. On one hand, primary studies with the lowest volumes (1L and 2L) did not show a significant interest in faster warm-up engine, or saving in fuel consumption as showed the highest volumes. For example, the highest temperature difference was 5°C at the start of NEDC with a storage

volume of 2L and an initial temperature of 60°C. On the other hand, 5L and 4L are considered big volumes in comparison with the engine's initial coolant volume and in term of space under hood. Consequently, a storage tank of 3L was chosen to be the optimal volume to carry on with the studies.

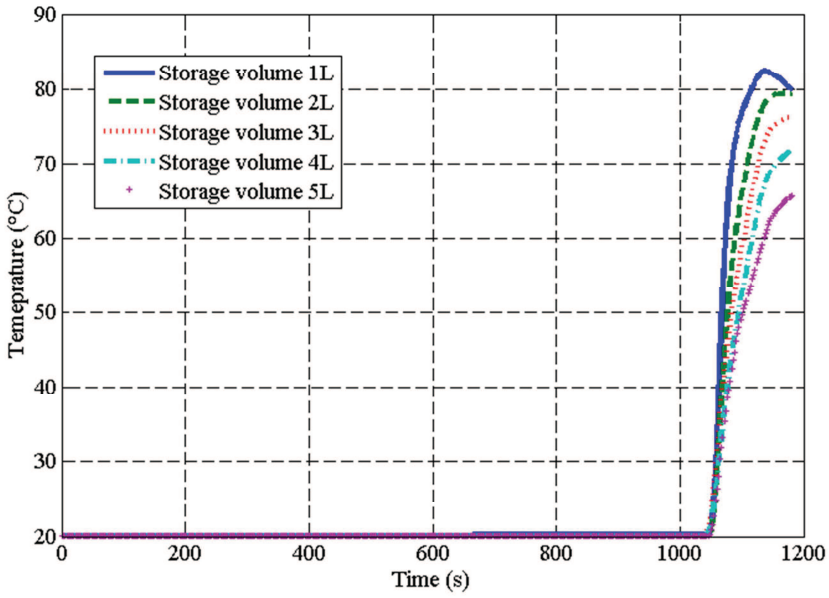

Figure III-2 Storage tank temperature profile over NEDC

III.1.3 Storage tank initial temperature

Different simulations were run varying the storage tank initial temperature after the soak period, between 20°C and 80°C with a 10°C step. The storage tank volume is fixed to 3L. The driving cycle is NEDC and the ambient temperature is set to 20°C.

To highlight the difference between the different initial temperatures, only three hot initial tank temperatures were depicted in Figure III-3: 40°C, 60°C and 80°C in addition to the reference temperature profile (where no heat was stored). The greatest benefit is within the greatest initial temperature of the storage volume. If the preceding driving cycle is NEDC, the storage volume temperature rises to 76°C. For other driving cycles as WLTC or AH, it is possible to obtain a storage temperature equals to the optimal one (83°C). Consequently, 80°C seems to be a theoretical temperature. It presents the case with the coolant temperature stored is at its maximum and is perfectly isolated and no heat losses are occurred during the soak period. 40°C as a starting temperature did not show the same interest as the other superior initial temperatures. Moreover, 40°C is considered too low because it takes into consideration a lot of heat losses during the soak period, an unacceptable behavior of a well isolated storage tank with a low thermal conductivity material. Hence, 60°C seemed to be more reasonable as a starting temperature for this study. It takes into consideration heat losses during the soaking period over a night, it presents a drop of 16°C for the NEDC case, and as it is shown in Figure III-3 it promises good improvements.

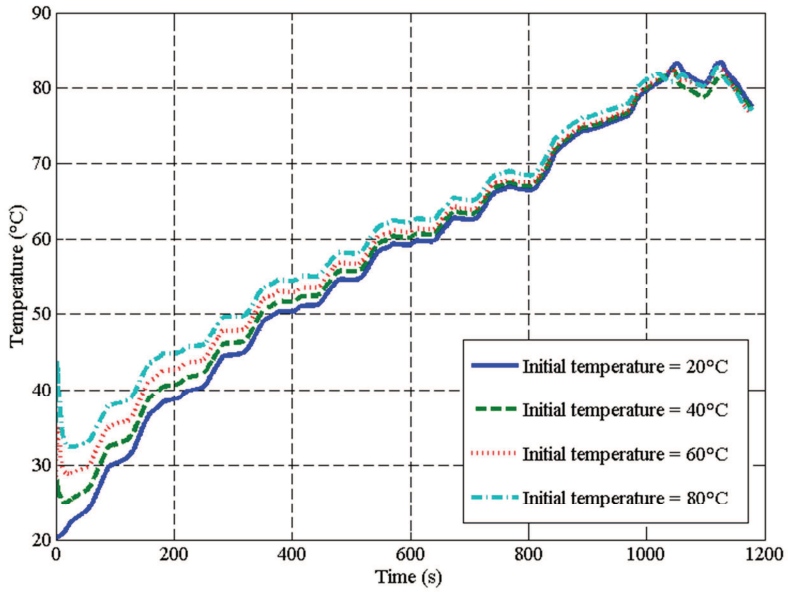

Figure III-3 Engine coolant temperature with a storage tank of 3L

III.1.4 Ambient temperature influence

The ambient temperature is an important factor in the engine performance. The normal average temperature for a warm day in Europe is around 20°C, during winter the ambient temperature can drop to 0°C and even to lower levels. The engine is very sensitive to its temperature; its efficiency grows with its functioning temperature. To assess its influence, the ambient temperature was varied between four values: 20°C representing the warm European day, 10°C representing a lower temperature, 0°C to represent the winter days and -7°C as a coldest winter.

Figure III-4 shows the different plots of the ambient temperature influence on the engine coolant's temperature over the driving cycles. A huge difference between the two extreme cases is seen. For NEDC (Figure III-4 (a)), the temperature of 60°C is reached around 607.5s at an ambient temperature of 20°C, around 741s at 10°C as an ambient temperature, 853s at 0°C. At the coldest temperature of -7°C the engine temperature of 60°C is reached after 960s. Hence, a difference of 353s is obtained between the two extreme cases. The lowest temperature leads to the highest energy losses, because the lubricant viscosity is at its highest, thus the friction losses too. Furthermore, with a colder starting temperature, a bigger temperature difference between the combustion gases and the chamber walls exists. The heat losses to the coolant circuit and to the ambient during a cold day are greater than a warm one. Finally, at an ambient temperature of -7°C, the engine consumes 19.2% more fuel than at an ambient temperature of 20°C.

Examining WLTC response to the ambient temperature variation (Figure III-4(b)), a difference of 312s between the two extreme cases is observed to reach the regulation temperature. 312s is equal to 17% of the length of the WLTC cycle, showing the importance of the influence of the ambient temperature over WLTC. An overconsumption of 9.06% is obtained during the coldest days.

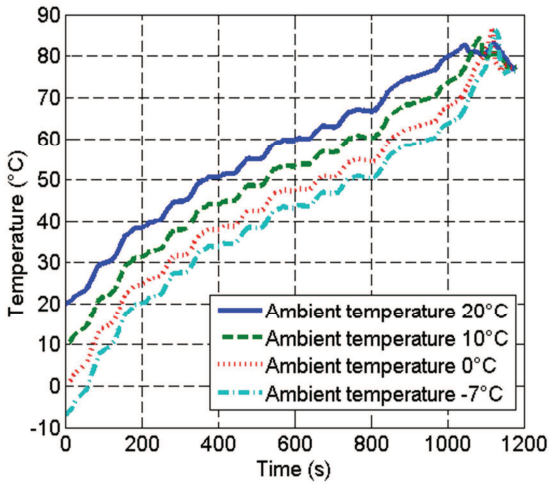

(a): NEDC

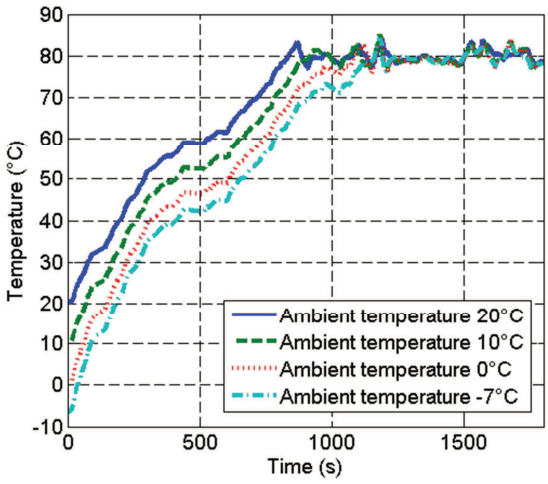

(b): WLTC

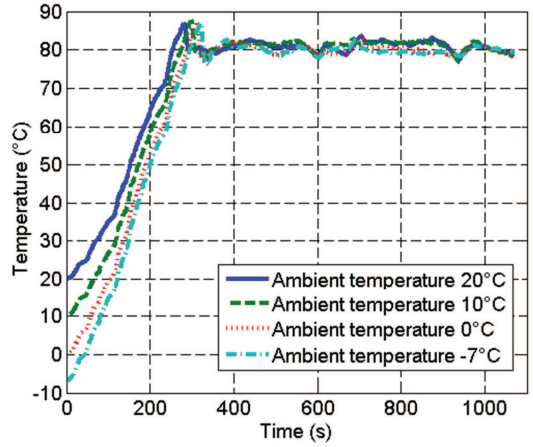

(c): Artemis Highway

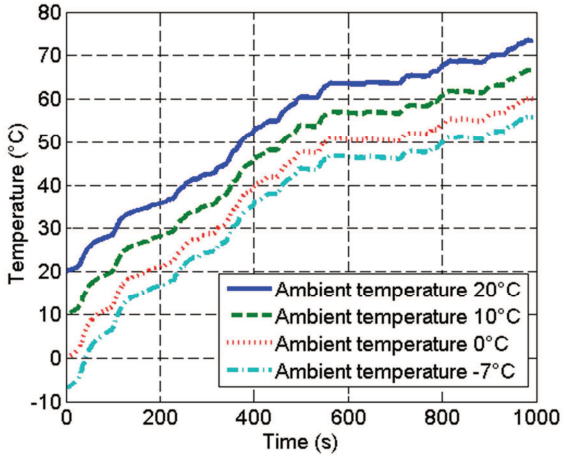

(d): Artemis Urban

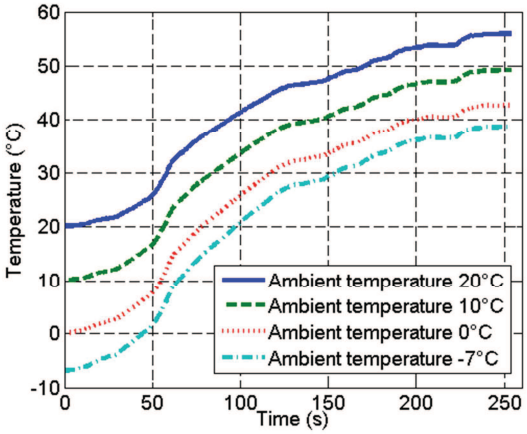

(e): In-House developed Driving Cycle

Figure III-4 Ambient temperature influence on different driving cycles

For Artemis Highway, the influence of the ambient temperature is limited to the first quarter of the driving cycle. Even in the coldest days, with an ambient temperature of -7°C, the

regulation temperature is reached within 340s, only 60s more than a warm day of an ambient temperature of 20°C. Comparing to the 19% of NEDC, at an ambient temperature of -7°C, only an overconsumption of 3.8% is obtained within Artemis Highway. Thus, the ambient temperature and the transient phase do not have a big influence on this driving cycle like the others. Contrary, Artemis Urban verifies the importance of the ambient temperature. During AU, the regulation temperature is not reached throughout the cycle. The influence of the ambient temperature will be as significant as the first two cycles, with an overconsumption of 19.9% at -7°C in comparison with 20°C as an ambient temperature.

The in-House developed Driving Cycle in part (e) of the Figure III-4 demonstrates the importance of the ambient temperature for the short driving cycle with an engine running in transient conditions all the time. The significant influence of the ambient temperature is presented with an overconsumption of 40.33% between the two extreme cases. This huge difference may go back to the idea of the engine operating at high load on low temperature. The friction level will be huge due to lower lubricant temperature and high rotational engine speed.

The simulation for the different thermal management strategies to come will be tested on the two extreme cases of the ambient temperature: 20°C and -7°C.

The last two driving cycles which have an engine running through a transient condition during the whole time will not allow the recharge of the storage tank of the thermal management strategy. These two driving cycles were chosen to test the importance of these applications in short driving cycles, where it represents most of the city travel. It is supposed that these driving cycles are used after an engine running a long driving cycle such as NEDC, WLTC or Artemis Highway. The objective is to have the storage temperature at the start of the cycle equals to 60°C.

III.1.1 Storage volume insulation

The storage volume thermal behavior of the hot coolant storage thermal management is tested in this part. Mann+Hummel provided the characteristic of specific plastic used in their production. The plastic known as PA 66 GF 30 has the characteristic presented in Table III-1 and used in tanks with a thickness of 3 and 3.5 mm.

The storage tank was tested for a soak period of 15 hours. The engine was not running in the simulation code (its rotational speed and torque were set to zero) and no heat supply was taken into consideration. The thickness used for the study was 3mm; the external convection coefficient is set to 20 W/m²/K and the ambient temperature is 20°C. The comparison was made between the different volumes at 80°C as an initial temperature at the starting of the soak period. Results are shown in Figure III-5(a). The plot shows the importance of the thermal inertia of the storage volume in the decreasing temperature. For 5L, the temperature of the tank is reduced to around 74°C after 15 hours, while a tank of 1L shows a drop of around 27.5°C after 15 hours and ended up with a 52.5°C storage tank.

3L storage tank had a temperature of around 70°C at the end of the soaking period. The initial temperature considered in the study of the hot coolant storage thermal management strategy is 60°C, leading to a marge of 10°C. The soaking period for a working day is less than 15 hours. Consequently, all the fuel consumption savings obtained in the following study can be

increased by increasing the initial temperature of the storage tank. With an ambient temperature of -7°C, the storage tank temperature drops to around 66°C after 15 hours of soak period, around 5°C less than the first case (Figure III-5(b)).

Table III-1 Plastic characteristics

Thermal conductivity k	**0.31 W/m.K**
Density	1469 kg/m^3
Specific heat c_p	2000 J/kg.K

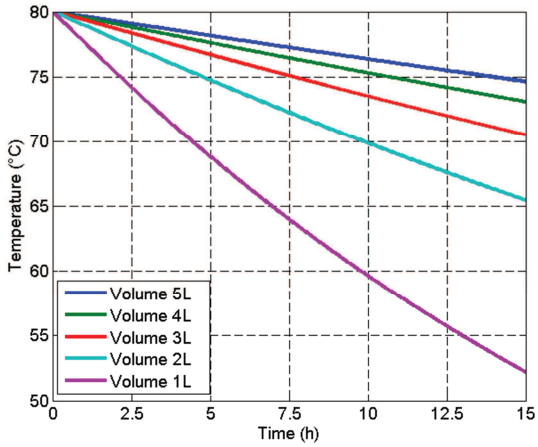

(a): different storage volumes

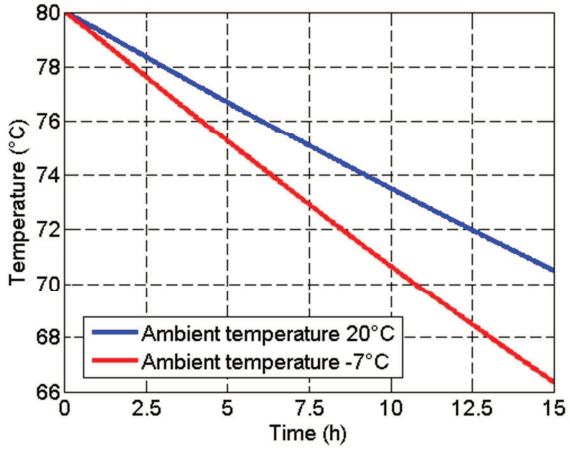

(b): 3L storage tank at different ambient temperatures

Figure III-5 Storage tank temperature profile over 15 hours of soaking period

III.1.2 Application on different driving cycles

The study is carried out on a 3L storage volume of hot water at 60°C, and the strategy will be applied on the different driving cycles and at two different ambient temperatures: 20°C and -7°C.

III.1.2.1. NEDC

Starting with an ambient temperature of 20°C, the results of the coolant and lubricant temperatures are shown in Figure III-6(a). The ref line shown in the figures represents the reference case with the engine traditional coolant circuit without any storage tank as depicted in Figure II-7. At first, the coolant temperature profile shows a faster warm-up of the engine, an advance of 64s to reach 60°C, and the regulation temperature was reached at approximately the same time. This is due to the higher temperature difference between the coolant and lubricant leading to a greater heat transfer from the coolant to the lubricant at the oil/coolant heat exchanger. Also, the heat fluxes from the engine to the coolant are lesser in the case of the hot storage coolant strategy because of the highest temperature of the coolant,

thus lesser temperature difference with the combustion chamber walls as shown in Figure III-7. Hence, the two temperature profiles do not stay parallel through NEDC. The lubricant profile shows an improvement too in the earlier stages of the driving cycle. It reaches the 60°C with an advance of 34s. This strategy reduces the fuel consumption by 0.26% comparing to the reference case without a storage tank.

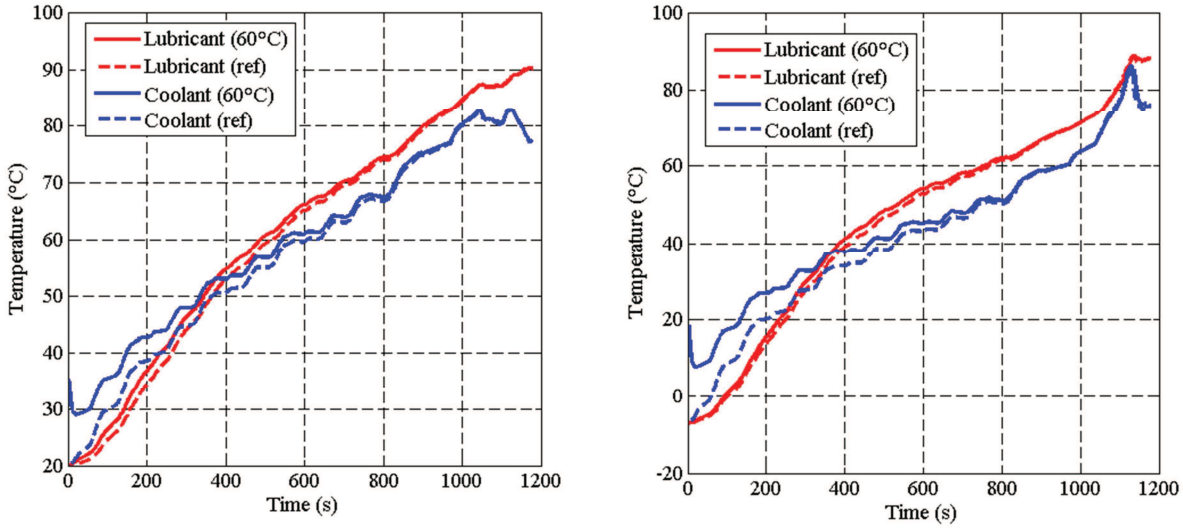

(a) : ambient temperature 20°C (b) : ambient temperature -7°C

Figure III-6 Engine's fluids temperatures with a storage tank at 60°C over NEDC

At an ambient temperature of -7°C, the engine's fluids temperatures are presented in Figure III-6(b). The reference line in the plot presents the engine at its basic configuration without a storage tank at an ambient temperature of -7°C. The coolant temperature, thus the engine temperature with the new thermal management strategy applied is always above 0°C. The 20°C temperature is reached with 61s advance with the hot coolant storage strategy. The lubricant reaches the 50°C with an advance of 19s. 1.17% reducing in fuel consumption is obtained in applying hot water storage strategy on the engine at an ambient temperature of -7°C.

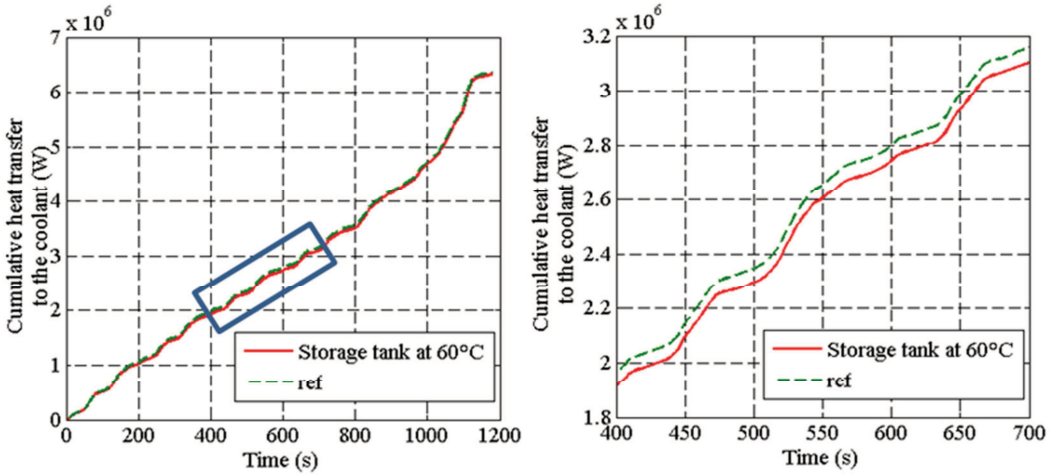

Figure III-7 Cumulative heat transfer to the coolant at an ambient temperature of 20°C

An assessment of the fuel consumption savings at the end of the transient phase was made too in order to highlight the importance of the thermal management strategy during the warm-up of the engine. At an ambient temperature of 20°C, the total fuel savings raised from 0.26% at the end of the cycle to 0.37% at the end of the transient phase. The regulation temperature is reached around 1046.5s, 133.5s before the end of the cycle. However, at the ambient temperature of -7°C, the regulation temperature is reached 51.5s before the end of the driving cycle, leading to an insignificant change in the fuel consumption reduction.

NEDC allows the engine to reach its regulation temperature by the end of the cycle; hence the storage phase will start once the radiator branch is opened (Figure III-8). After 24s of the start of the cycle, the hot storage water has been used by the engine, and then the storage tank has been isolated. The temperature is constant from the 24s until the opening of the radiator branch. Then, the tank's temperature starts rising by storing hot water until it equals to the engine temperature around the end of the cycle.

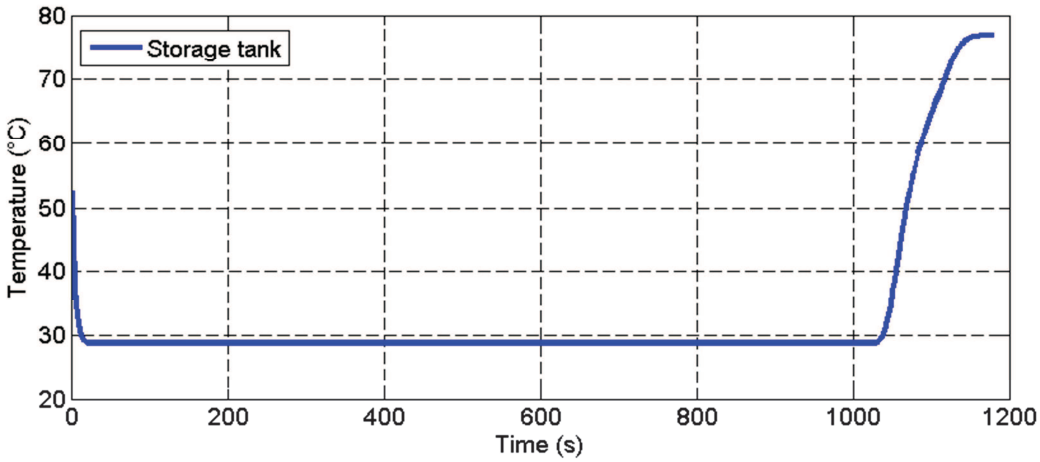

Figure III-8 Temperature profile of the storage tank for NEDC at 20°C

Applying this thermal management strategy may have other consequences. The strategy is based on an addition of 3L volume of water to the system, thus 3 kg of mass. The storage tank and its surroundings are estimated to 1 kg. The mass of the vehicle is a priority factor in the fuel consumption. 4kg to the vehicle mass were added. An updated torque profile of the NEDC was given to the engine's model to take into consideration the added mass of the water volume. Temperature profile of the engine's coolant, thus the engine temperature, at an ambient temperature of 20°C taking into consideration 4 kg added mass to the vehicle is presented in Figure III-9. The reference line in the plot, presents the engine running with a storage tank of 3L of hot water at 60°C, without taking into consideration its weight. As seen in the plot, the coolant temperature does not vary through the cycle in function of the modification of the torque profile. Thus, the influence of the 4kg mass is insignificant over the driving cycle from a thermal management point of view. For that, the added mass study will be dropped and won't be done in the different driving cycles' analysis.

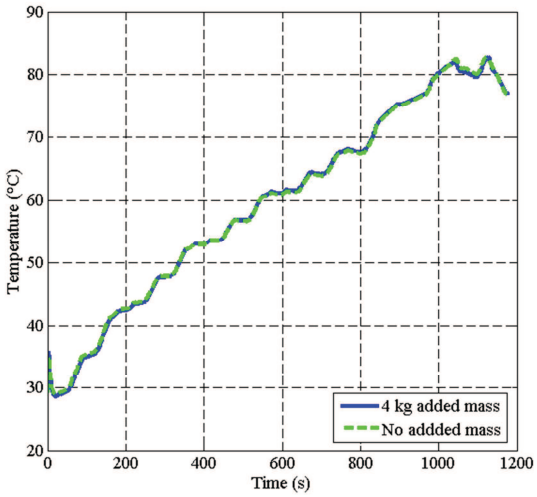

Figure III-9 Coolant temperature profile w/o added mass

III.1.2.2. WLTC

Starting with an ambient temperature of 20°C; the coolant temperature profile shows improvements during the transient stage. An advance of 48s is obtained to reach 30°C and 111s in attending 60°C. The lubricant temperature profile presents an advance of 30s in reaching the 60°C (Figure III-10(a)). The regulation temperature is reached at 870.5s. A comparison of the fuel consumption is made over the transient phase to have a real insight of the gain, and the effect of the thermal management strategy. At an ambient temperature of 20°C, the engine consumes 2.36% less with the new thermal management strategy.

At an ambient temperature of -7°C, the plot (b) of the Figure III-10, an advance of 86.5s to reach 20°C for the coolant, and 24s reaching the 50°C were obtained. With the thermal strategy applied, the coolant temperature starts from above 0°C. Concerning the lubricant profile, 50°C is reached faster by 22s. At the end of the transient stage (1182.5 for the reference case), a fuel consumption reduction of 3.43% is obtained by using the hot water storage strategy. The two savings of the transient phase in the WLTC cannot be compared due to the time difference between the two cases. During both cases, the engine reaches the steady state stage allowing the storage tank to be recharged for a further usage (Figure III-11).

From the plot in Figure III-11, the stored hot water is used for the first 24s of the cycle, then the storage tank is isolated from the system and its temperature is constant during the rest of the transient phase. At 870.5s, the steady-state stage starts and the hot water flows into the radiator branch, thus the storage tank. The latter's temperature rises until it reaches the engine's temperature around 1200s. The temperature profile of the storage tank for this driving cycle proves that if the engine regulation temperature was raised to a higher level, (with new multi-valve technologies where it could attend 100°C) the initial temperature of the storage tank for the following driving will be higher, thus greater fuel consumption reduction.

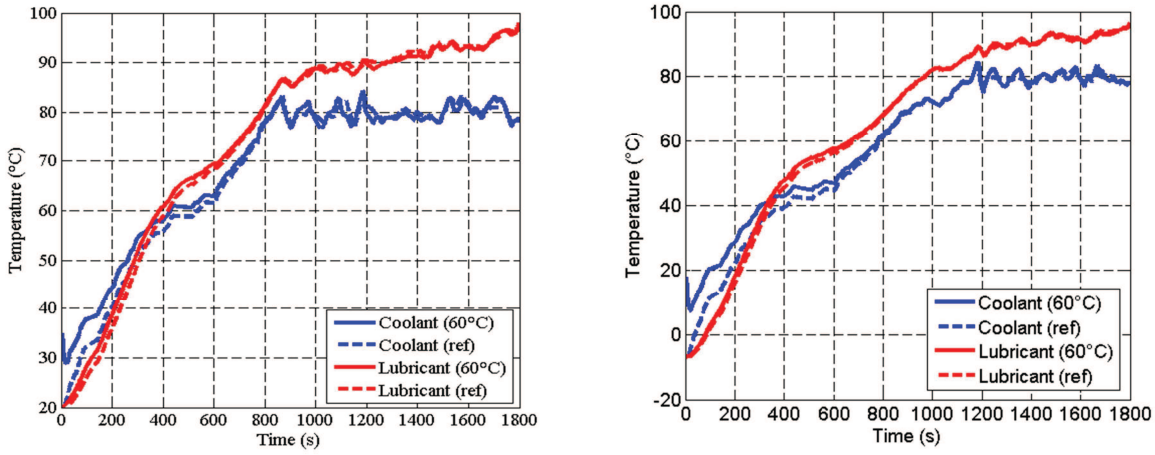

(a): Ambient temperature 20°C (b): Ambient temperature -7°C

Figure III-10 Engine's fluids temperatures with a storage tank at 60°C over WLTC

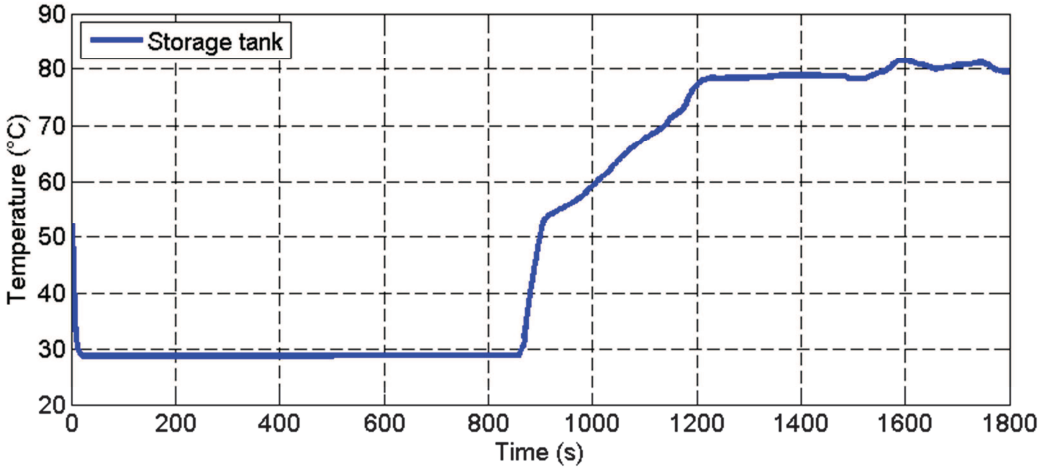

Figure III-11 Temperature profile of the storage tank for WLTC at 20°C

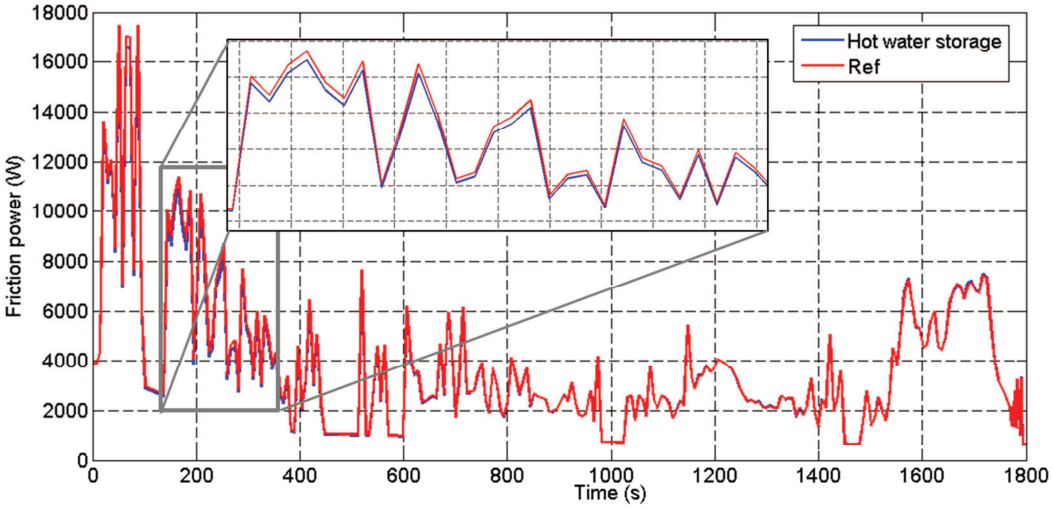

Figure III-12 Friction power profile at an ambient temperature of -7°C during WLTC

Moreover, a study of the friction power showed that using this thermal management strategy led to a reduction of 1.25% at an ambient temperature of 20°C and 1.64% in case of -7°C. As seen in Figure III-12, the profile of the friction power when applying the thermal management strategy is lower of the ref line to around 700s, corresponding to the time where the two lubricant temperature profiles become one. This proves the accuracy of the results and the link between the lubricant temperature and the friction losses. To end the study, the fuel consumption saving at the end of the cycle reduces to 1.83% in case of an ambient temperature of -7°C and to -1.2% in case of 20°C as ambient temperature.

III.1.2.3. Artemis Highway

As mentioned before, while analyzing the influence of the ambient temperature on the Artemis Highway, it appears that the transient phase of this cycle is the shortest and it is only for the first 28% of the cycle in the coldest days. Consequently, the thermal management strategy won't have a significant influence on the fuel consumption over the whole cycle.

While applying the hot coolant storage strategy, the improvement in the transient phase is limited to its earlier stages. For an example, at an ambient temperature of 20°C (Figure III-13) the coolant reaches 30°C in an advance of 41s, and 12s earlier to attend 60°C. With a 4.5s of advance, the lubricant reaches 60°C. The regulation temperature for the reference case was reached at 265s, thus for the transient phase, an assessment of the fuel consumption gave a reduction of 1.09% for the thermal management strategy of a 3L of hot water stored at 60°C. This reduction becomes insignificant over the whole cycle. At an ambient temperature of -7°C, the regulation temperature for the reference case (the coolant circuit architecture without the storage tank at an ambient temperature of -7°C) is reached at 304s, and with an advance of 6s with the strategy applied, the latter shows an improvement of 1.13% of fuel consumption.

The regulation temperature is reached early in this cycle; hence, the storage tank in the two cases is recharged at the end of the driving cycle for an upcoming use. At 20°C, as seen in Figure III-14, the hot coolant is pumped into the system for the first 24s, and then the storage tank is isolated during the rest of the transient phase. The stagnated temperature during the rest of the transient stage is a proof of the well isolated stored tank from the rest of the coolant circuit. The regulation temperature is reached around the 285th second of the cycle, the hot coolant flows into the radiator branch and the storage tank starts recharging for a further use. The storage tank reached the engine's temperature quick enough around 100s in the steady-state stage. For this type of driving cycle, a long one where the steady-state stage is attended early, using a modern multi-valve controls the engine at higher temperature. The higher temperature should always be allowed with reliability. An engine running at higher temperature generates greater thermal stresses around different engine parts. Higher temperature can lead to a higher stored temperature in the storage tank. During the soak period, some heat will be lost to the ambient air, but as the study for the isolated tank showed a maximum drop of 10-15°C depending on the ambient temperature, the initial temperature of the storage tank can be raised to 70°C or even 80°C, generating a greater fuel consumption saving with this thermal management strategy.

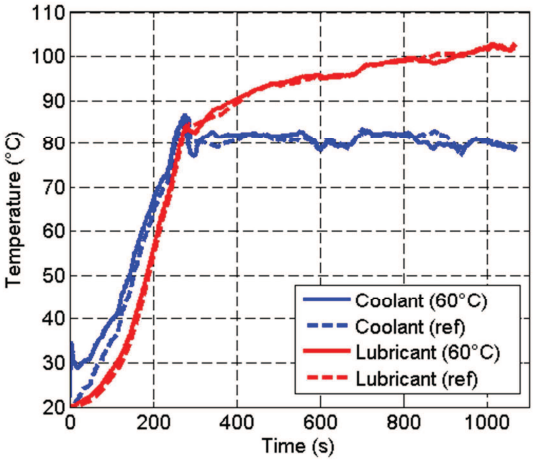

(a): Ambient temperature 20°C

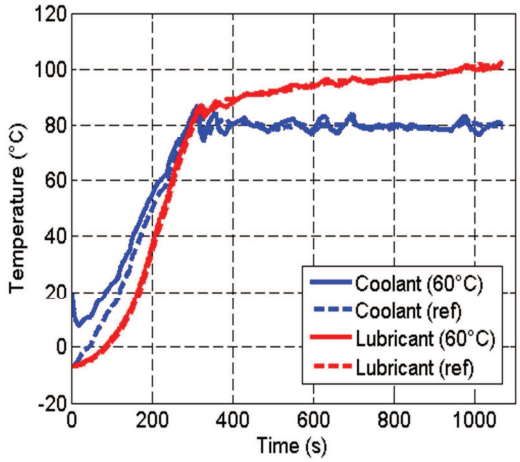

(b): Ambient temperature -7°C

Figure III-13 Engine's fluids temperatures with a storage tank at 60°C over AH

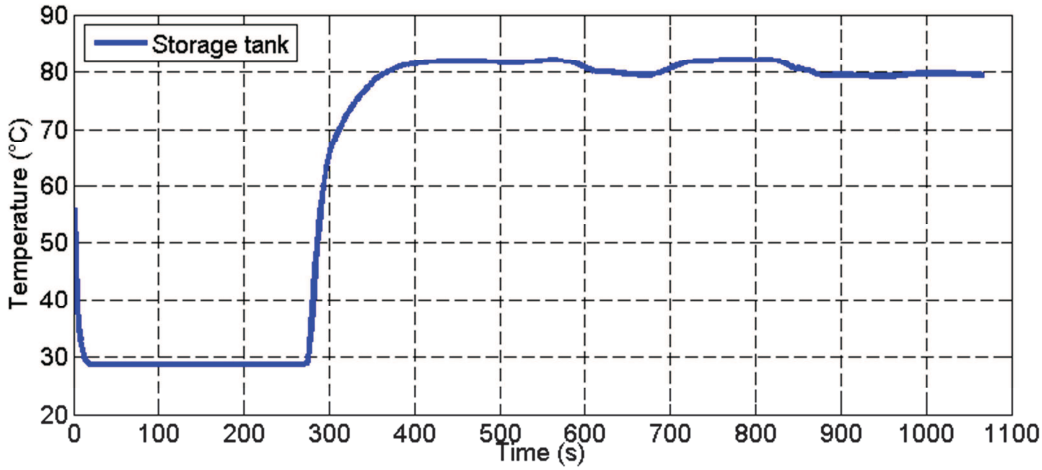

Figure III-14 Temperature profile of the storage tank for AH at 20°C

III.1.2.4. Artemis Urban

The simulation shows that the engine running on the AU cycle, at an ambient temperature of 20°C, stays in the transient phase during the whole cycle. The regulation temperature of 83°C is not reached at the end of the cycle (Figure III-15(a)). This kind of driving cycle highlights the importance of thermal management strategies that acts on the transient phase. One inconvenient of such cycles, it won't lead the storage tank to be recharged at the end of the cycle. This driving cycle is tested in the idea of supposing one person used the car on another driving cycle leading to recharge the storage tank with hot water, and the second day the car is used for some city travelling.

Testing the hot water storage strategy on this cycle at 20°C as ambient temperature leads to a reduction of 0.97% in fuel consumption. The coolant profile shows the greatest advance between the previous driving cycles to attend 30°C which is 69s, and 14.5s to reach the 60°C. The lubricant showed an advance of 23s to reache 30°C and this advanced is reduced to 11s at 60°C (Figure III-15(a)). Moreover, at ambient temperature of -7°C the reduction in fuel consumption rises to 3.04%. This reduction can be observed in the huge difference between

the two temperature profiles of the coolant. An advance of 124s is obtained in reaching 20°C while the lubricant showed an advance of 22s at the temperature of 50°C (Figure III-15(b)).

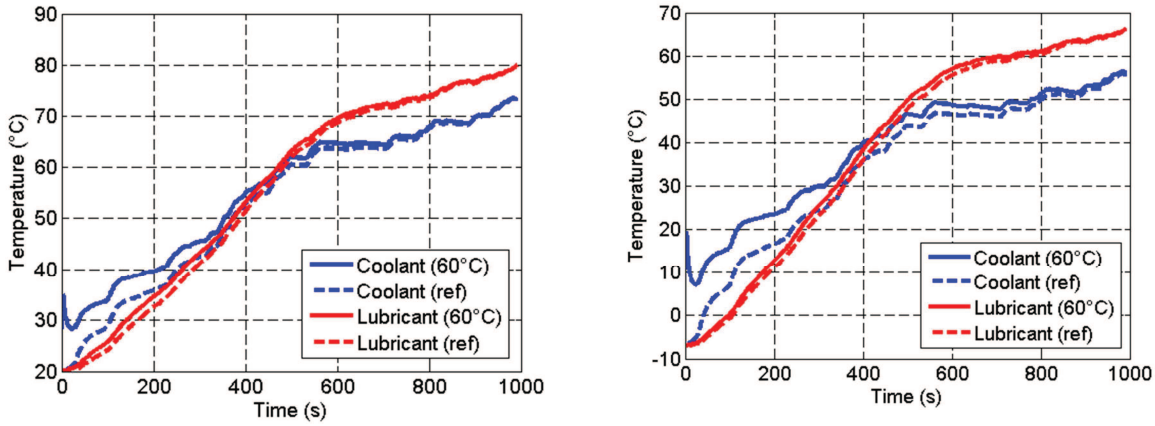

(a): Ambient temperature 20°C (b): Ambient temperature -7°C

Figure III-15 Engine's fluids temperatures with a storage tank at 60°C over AU

III.1.2.5. In-House developed Driving Cycle

Similar to the last case, In-House developed Driving Cycle (HDC) does not allow the engine to reach its regulation temperature as it is represented in the temperature profiles in Figure III-16. The temperature profile exhibits that during the whole driving cycle, using the thermal management strategy of hot coolant storage, the engine runs at a higher temperature in term of coolant temperature and lubricant temperature too. This statement is true for the two ambient temperatures. Unfortunately, comparing to the other driving cycles, at the end of the driving cycle, the engine's temperature reached 58°C (20°C as an ambient temperature) and a maximum of 43°C with an ambient temperature of -7°C. On one hand, the coolant profile attends the temperature of 30°C in advance of 18s while the lubricant reached the 30°C in advance of 9s. On the other hand, at an ambient temperature of -7°C, an advance of 31s is obtained at 20°C for the coolant and 9s for the lubricant.

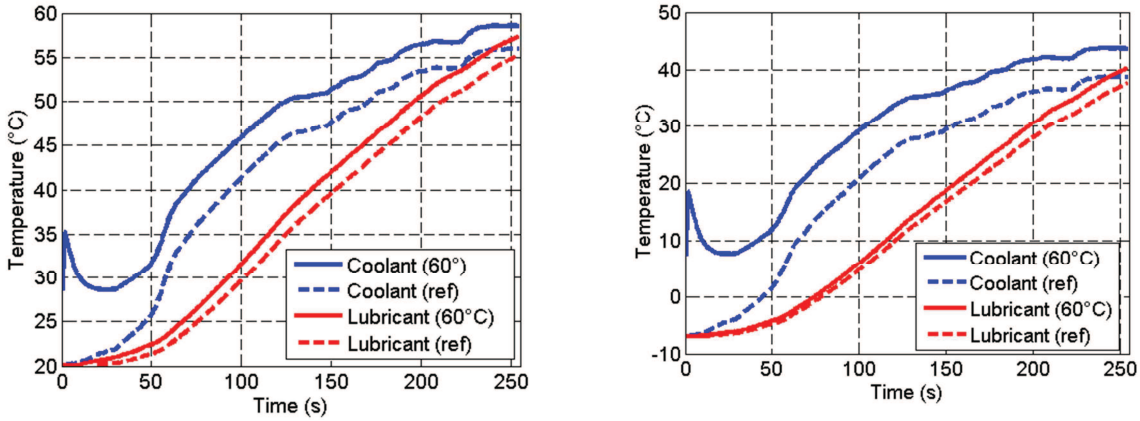

(a): Ambient temperature 20°C (b): Ambient temperature -7°C

Figure III-16 Engine's fluids temperatures with a storage tank at 60°C over HDC

The fuel consumption is reduced by 1.24% when applying the hot coolant storage strategy with an initial temperature of 60°C at an ambient temperature of 20°C. At -7°C, the benefit rises to 1.4%.

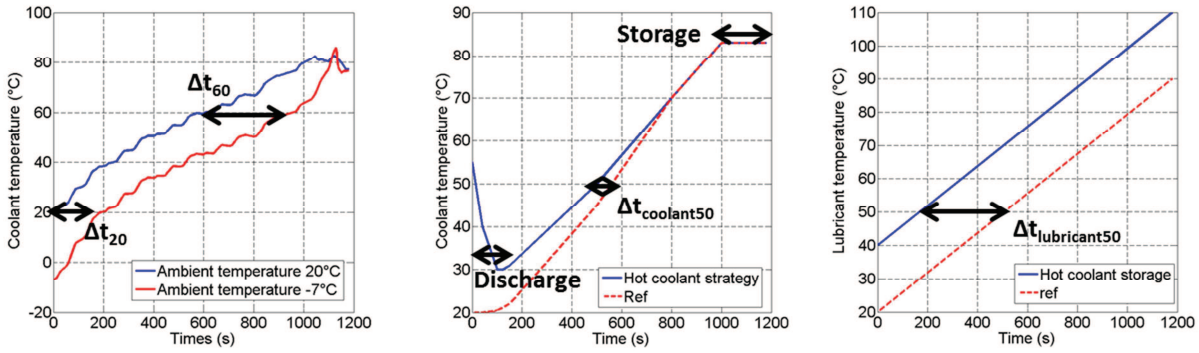

(a) (b) (c)

Figure III-17 Schematic presentation of different profiles

Figure III-17 represents schematic profiles, where part (a) shows the profile of the engine's coolant temperature without having the hot water tank in the coolant circuit, at different ambient temperatures: 20°C and -7°C. Δt_{T_i} is the time difference to attend the coolant's temperature T_i between the two ambient temperatures. Figure III-17(b) represents a comparison of a typical coolant temperature when applying the hot coolant storage strategy over the reference line (dashed lined -Ref-) that presents the engine temperature status at the same ambient temperature with traditional coolant circuit architecture. "Discharge" in Figure III-17(b) is a magnified presentation of the first stage of the cycle where the hot coolant flows in the engine and heats-it up. Its temperature drops from 60°C (initial temperature of the hot storage tank) to a level higher than the ambient temperature taken into consideration, then rises to reach the regulation temperature. At that stage the "Storage" phase starts, and hot coolant flows into the storage tank. $\Delta t_{coolant,T_i}$ displays the advance in time to reach the "$coolant$" temperature T_i obtained by applying the thermal management strategy. $\Delta t_{lubricant,T_i}$ shown in Figure III-17(c) is the advance in time obtained to attend the "$lubricant$" temperature T_i by applying the hot coolant storage strategy over the traditional engine presented by the dashed line entitled ref.

The advance in time for the different cases and driving cycle are summarized in Table III-3. The "-" in the table means that the required temperature is not reached.

Table III-2 summarizes the fuel consumption benefits over different driving cycles at the both ambient temperature 20°C and -7°C by applying the Hot Water Storage thermal management strategy on the Diesel engine chosen in this study in the configuration presented in Figure III-1.

The biggest difference between the fuel consumption savings at the two ambient temperatures were seen for the following two driving cycles: NEDC and AU. These two driving cycles are known for their soft start. It means low vehicle speed, and low operating points at the first stages of the cycle, when the engine is still in its transient conditions. For the other cycles, it

is more severe during the first stages as for AH (comparison made at the end of the transient phase) and HDC, less difference between the two fuel consumption benefits was observed.

Table III-2 Fuel consumption savings at different ambient temperature

Driving cycle	20°C	-7°C
NEDC	0.26%	1.17%
NEDC (at the end of the transient phase)	0.37%	1.17%
WLTC	1.2%	1.83%
WLTC (at the end of the transient phase)	2.36%	3.43%
AH cycle (at the end of the transient phase)	1.09%	1.13%
AU cycle	0.97%	3.04%
HDC	1.24%	1.4%

Table III-3 Warm-up time savings (in seconds) for different cycles and ambient temperatures

Ambient temperature		NEDC	WLTC	AH	AU	HDC
	Δt_{20}	195.5	181.5	121.5	240.5	97
	Δt_{60}	353	244	55.5	-	-
	Δt_{83}	70	312	41	-	-
20°C	$\Delta t_{coolant,30}$	52	48	41	69	18
	$\Delta t_{coolant,60}$	64	111	12	14.5	-
-7°C	$\Delta t_{coolant,20}$	61	86.5	35.5	124	31
	$\Delta t_{coolant,50}$	11	24	17.5	22	-
20°C	$\Delta t_{lubricant,30}$	16	28	10.5	23	9
	$\Delta t_{lubricant,60}$	34	30	4.5	11	-
-7°C	$\Delta t_{lubricant,20}$	18	14	5	15	9
	$\Delta t_{lubricant,50}$	19	22	7.5	22	-

III.1.3 Different architectures

The first architecture proposed for this thermal management strategy consists of a storage tank placed downstream the thermostat in the radiator branch. Once the hot fluid is pumped from the storage tank, it flows downstream the oil heat exchanger. On one hand, the stored

hot coolant does not affect directly the lubricant. On the other hand, the position of this storage tank is safely chosen to protect the engine during the transient phase and it's controlled by some valves. What happens if the volume was added to the configuration without any control?

III.1.3.1. Architecture beta

To study the influence of the hot water storage strategy on the lubricant, the outlet of the storage tank is changed in this architecture to upstream the oil/water heat exchanger as shown in Figure III-18.

The control of the storage volume by three valves stays similar to the first architecture. Valve number 3 opens and closes with the thermostat allowing storing heat during the storage phase and controlling the flow of the hot coolant during the cold start up. It blocks the hot coolant to enter the radiator and the stored heat to be evacuated to the ambient air. Valves 1 and 2 are closed during the storage phase and opens when the regulation temperature is not reached and the storage tank's temperature is higher than the engine's.

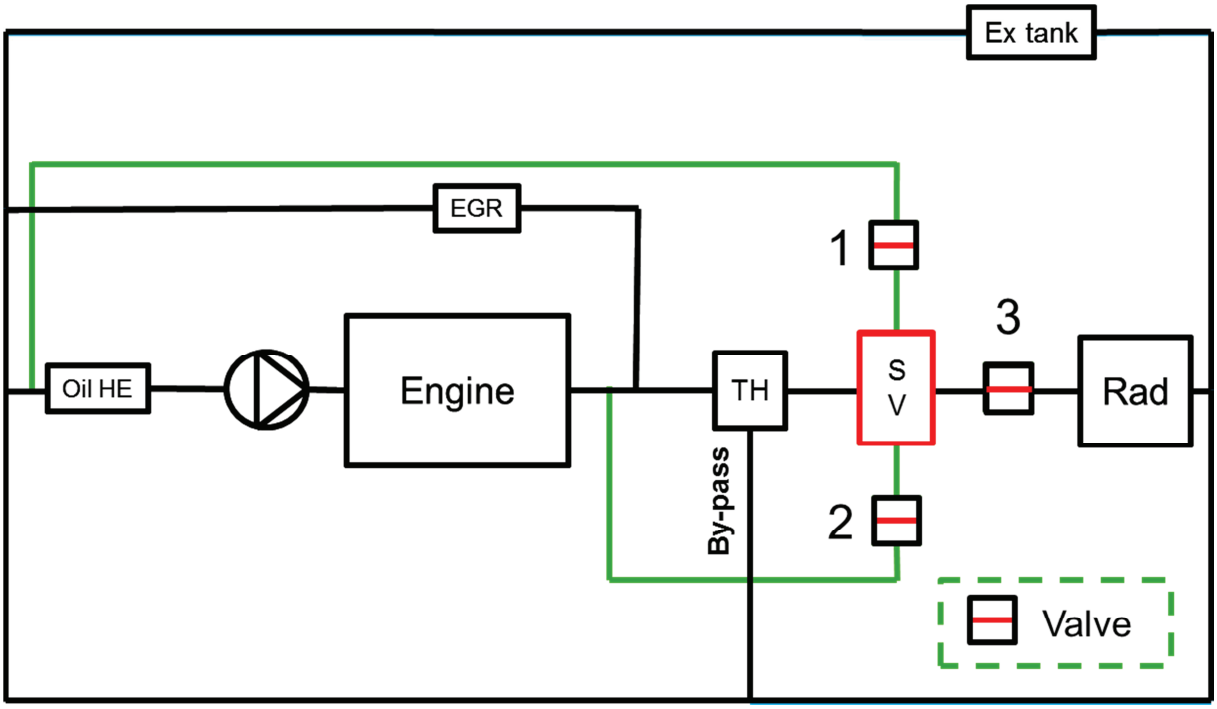

Figure III-18 A schematic presentation of the hot coolant storage strategy architecture beta (SV: Storage volume; TH: Thermostat; Oil HE: Oil heat exchanger; Ex tank: Expansion tank; Rad: Radiator)

The same procedure was done for this architecture; simulations for different driving cycles were run, varying the ambient temperature between 20°C and -7°C. The main results of the fuel consumption savings are presented in Table III-4.

Fuel consumption benefits for the second architecture with the outlet of the storage tank upstream the oil heat exchanger is lower than the first architecture in most of the driving cycles except for HDC. As shown in Figure III-19 for WLTC, the coolant temperature profile for the beta architecture is slightly lower than for the basic storage strategy. It indicates a transfer of heat from the coolant when flowing in the oil heat exchanger. Examination of the lubricant profile does not show an improvement in the lubricant temperature over the transient

stage. It goes back to the heat transferred from the coolant is lost in the heat exchanger mass inertia.

Table III-4 Fuel consumption saving for achitecture beta

	Driving cycle	20°C	-7°C
Architecture beta	NEDC	0.15%	1.42%
	NEDC (at the end of the transient phase)	0.17%	1.43%
	WLTC	0.75%	2.48%
	WLTC (at the end of the transient phase)	2.02%	4.66%
	AH cycle (at the end of the transient phase)	0.7%	1.13%
	AU cycle	0.78%	2.73%
	HDC	1.71%	1.57%

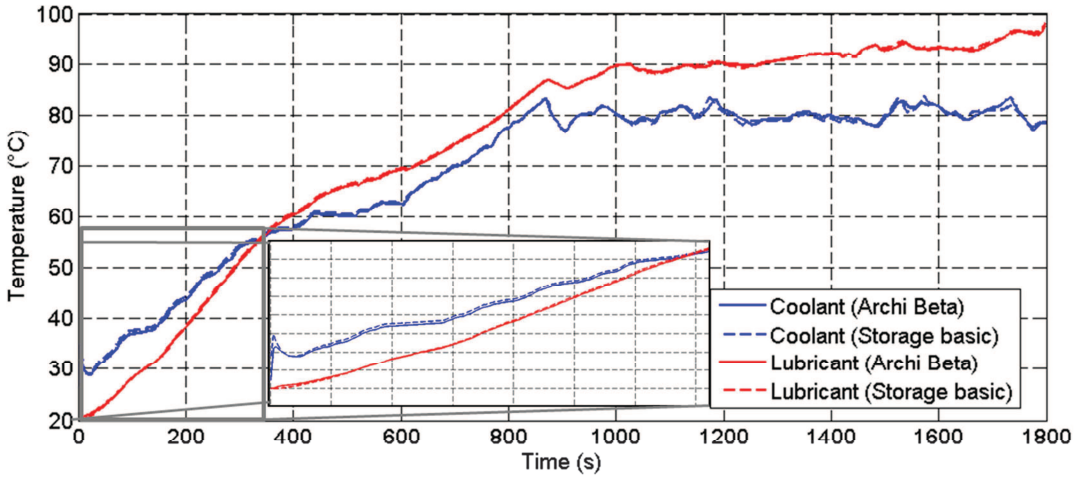

Figure III-19 Fluids' temperatures for beta architecture over WLTC

HDC temperature profile is shown in Figure III-20 at 20°C as ambient temperature. The difference of the coolant temperature at the start of the cycle is noticed. The huge difference compared to that of WLTC allowed the lubricant temperature profile to be higher than the basic profile. This lubricant temperature difference generated a higher reduction in fuel consumption of HDC than the basic architecture of the hot water storage thermal strategy.

III.1.3.2. Architecture gamma

The third proposition was to test the storage strategy without any control. The strategy tends to remove all the valves presents in the former architectures. To manage to flow the hot coolant through the system, the position of the storage tank had to be changed. The storage tank was placed upstream the thermostat, downstream the engine and the EGR branch as shown in the schematic presentation of architecture gamma in Figure III-21. The total volume of the engine's coolant is raised. During the warm-up stage, the engine should heat the

additional storage volume to attend its regulation temperature. Identically to the former architectures, simulations of a 3L hot water storage thermal management strategy were run over the different driving cycles at two ambient temperatures of 20°C and -7°C.

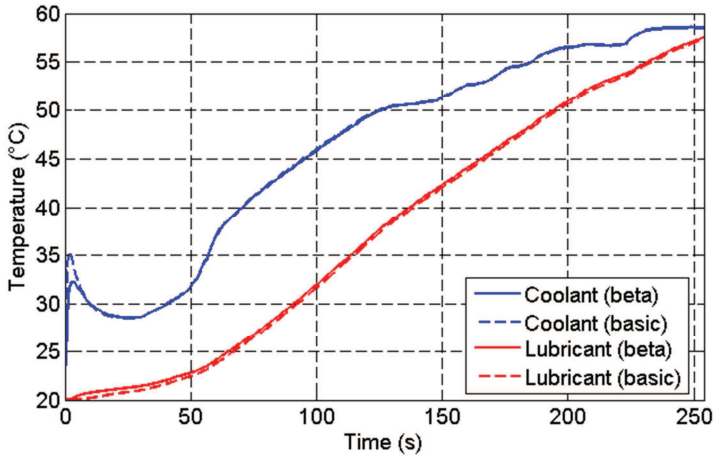

Figure III-20 Fluid's temperatures for beta architecture over HDC

Fuel consumption savings from this architecture are summed up in the Table III-5. The minus sign (-) in the table refers to an overconsumption. As predicted, all the results showed a decrease in the fuel consumption savings comparing to the first architecture. More heat will be lost to warm-up the coolant, the transient phase will become longer and less fuel will be saved. Despite this, architecture gamma interest is in the benefits which can be obtained with the different driving cycles without any control of the storage volume. No valves lead to fewer problems related to the available space under the hood. It should be mentioned that this architecture as well as the one before always used the same material of the storage tank and the same thickness.

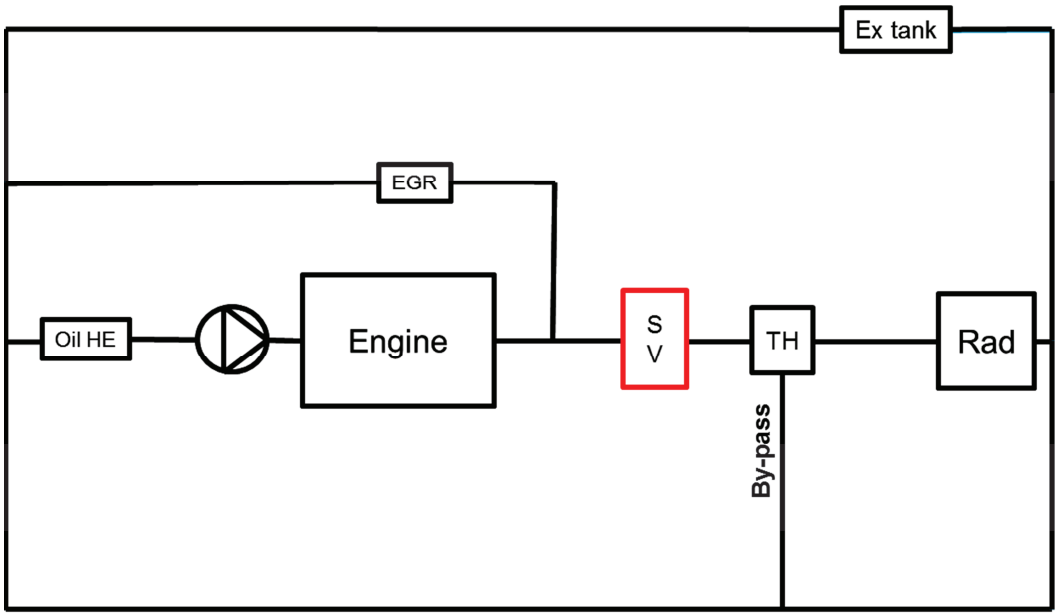

Figure III-21 A schematic presentation of the hot coolant storage strategy architecture gamma (SV: Storage volume; TH: Thermostat; Oil HE: Oil heat exchanger; Ex tank: Expansion tank; Rad: Radiator)

Table III-5 Fuel consumption savings for architecture gamma

	Driving cycle	20°C	-7°C
Architecture gamma	NEDC	-0.45%	0.44%
	NEDC (at the end of the transient phase)	-0.56%	0.44%
	WLTC	0.48%	2.03%
	WLTC (at the end of the transient phase)	1.86%	3.98%
	AH cycle (at the end of the transient phase)	0.7%	1.13%
	AU cycle	0.89%	2.18%
	HDC	1.04%	1.14%

For example NEDC and AU coolant temperature are plotted in Figure III-22 (a) and (b) respectively. The coolant temperature of the gamma architecture represented in the blue line is greater than the ref line which is representing the driving cycle with no storage tank at all. The storage tank was charged and contained hot coolant at 60°C. The coolant temperature, thus the engine's temperature of the architecture gamma increasing slope is softer than the basic architecture. At some point, the coolant temperature of the reference case meets the temperature of the gamma architecture and grows higher during the rest of the driving cycle. The amount of fuel saved at the beginning of NEDC was less than the overconsumption of the fuel resulting from heating up the added coolant volume during the rest of the transient phase. Contrary in Artemis Urban, at first, savings were higher than NEDC, overcoming the drawback at the end of the cycle and leading to save some fuel. Comparing the heat losses to the chamber walls for the Artemis Urban, wall heat losses in case of gamma architecture are 0.8% less comparing to the reference case, the engine without any storage tank. However, gamma architecture wall heat losses are greater than the basic configuration by 0.63%. For NEDC, gamma architecture has wall heat losses greater than the reference case by 1.57%, leading to an overconsumption at the end of the cycle.

The third configuration is the only one that influences badly the transient phase of the engine during the first start-up when the storage tank is at the ambient temperature. Simulations were run for different driving cycles at different ambient temperatures with a cold storage volume of 3L with no control, upstream the thermostat.

Figure III-23 represents the different coolant's temperature profile over the different driving cycles for an ambient temperature of 20°C, with the storage volume initial temperature equals to the ambient temperature. The dashed line representing the reference case is the engine running without a storage tank. As seen in the different plots that the regulation temperature is reached in a delay of 37s for NEDC, 33s for WLTC and 30s for Artemis Highway. As for the last two driving cycles, with an engine always at transient phase, the final temperature reached at the end of the cycle was decreased by around 5°C.

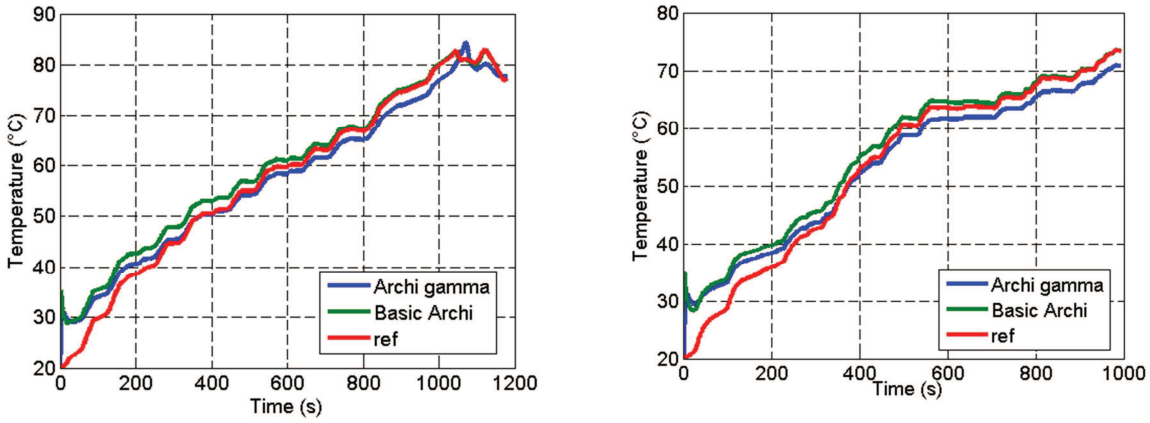

(a): NEDC (b): AU

Figure III-22 Coolant temperature profile for architecture gamma at 20°C

The fuel consumption results are given in Table III-6. Consequently, on one hand, applying the thermal strategy in its gamma architecture over NEDC won't have any benefits. On the other hand, the first cycle to charge the storage tank will have major drawback on the fuel consumption that will be retrieved in the following driving cycles. For Artemis urban and HDC, the storage tank won't be recharged at the end of the cycle. This architecture won't prove its benefits as the other architectures where the storage tank can be isolated from the coolant circuit when its temperature is lower than the engine's.

Table III-6 Fuel consumption for architecture gamma with cold storage tank

Driving cycle	20°C	-7°C
NEDC	-0.45%	-0.7%
WLTC	-0.31%	-1.14%
AH cycle	-0.8%	-0.12%
AU cycle	-0.57%	-0.42%
HDC	-0.35%	-0.64%

Figure III-24 sums up the different fuel consumption savings for the hot coolant storage thermal management strategy.

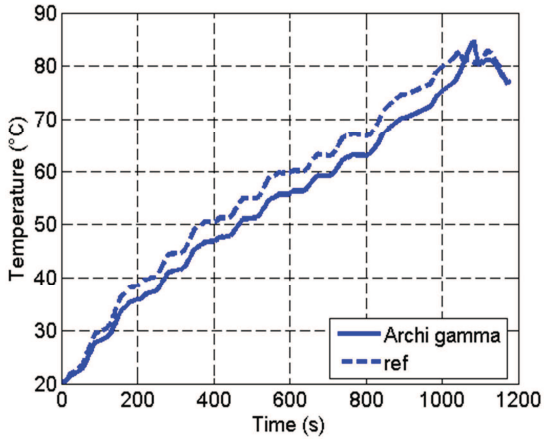

(a): NEDC

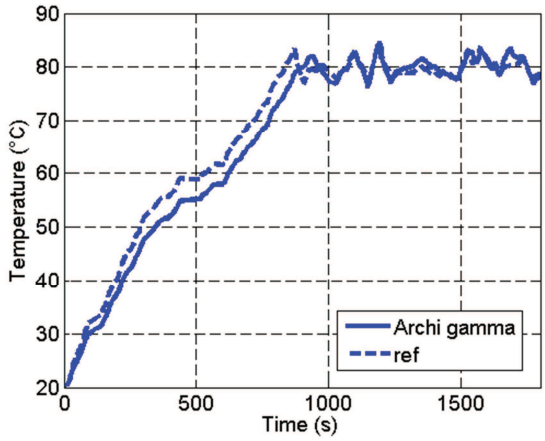

(b): WLTC

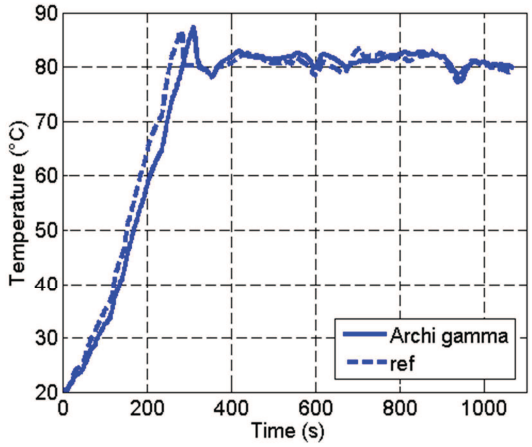

(c): Artemis Highway

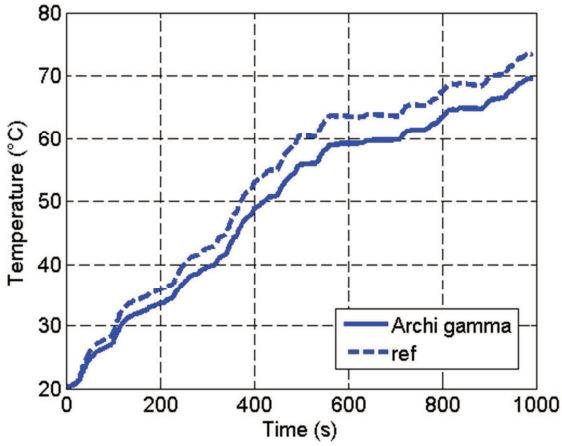

(d): Artemis Urban

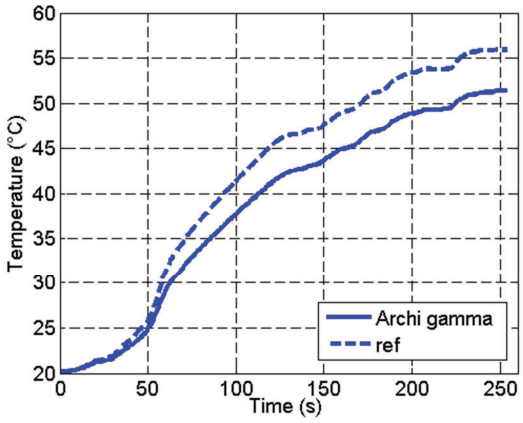

(e): HDC

Figure III-23 Coolant temperature profile over different cycles for a cold storage volume

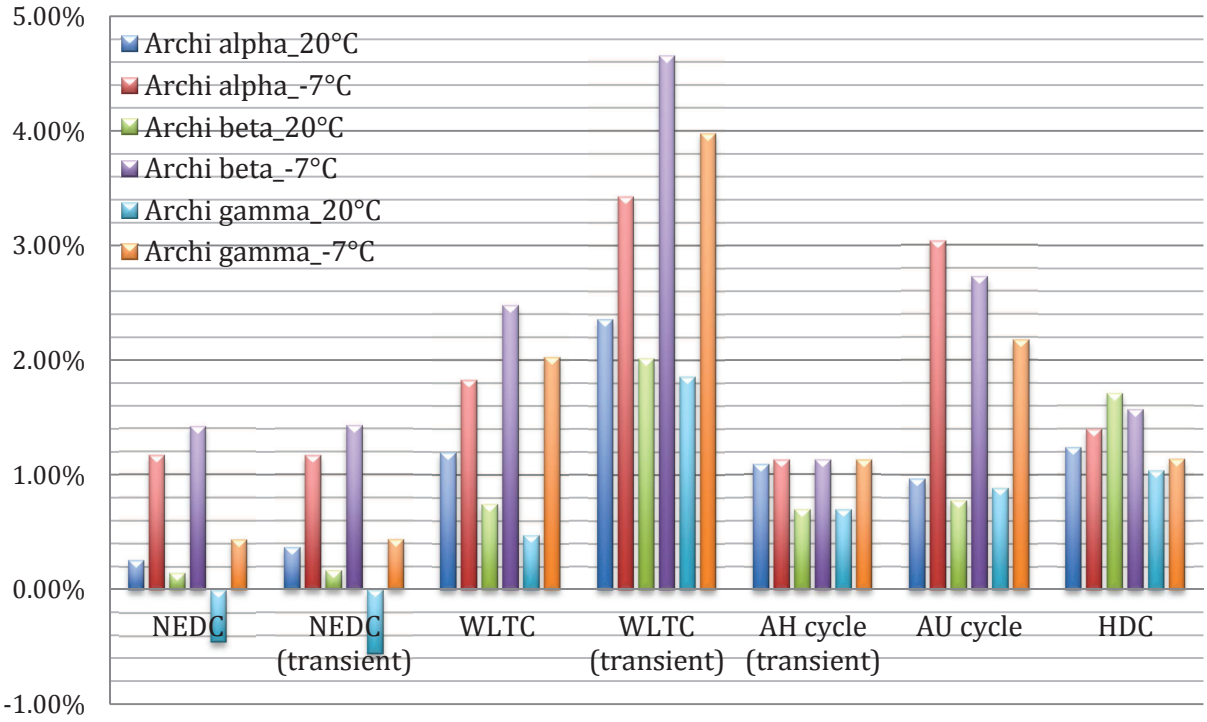

Figure III-24 Fuel consumption savings for coolant storage strategy for: different configurations, driving cycles and ambient temperatures.

III.1.4 Influence of Oil's grade

Most of the automotive manufacturers are converting to changing the oil used in the engine. They are choosing lubricant with a lower viscosity at low temperature to reduce the engine's frictions during the cold start-up. The strategy of changing the oil's grade is studied and compared to the reference engine in an upcoming chapter. To finish the study of the Hot Water Storage strategy, a study of the influence of the oil's grade is done in this part.

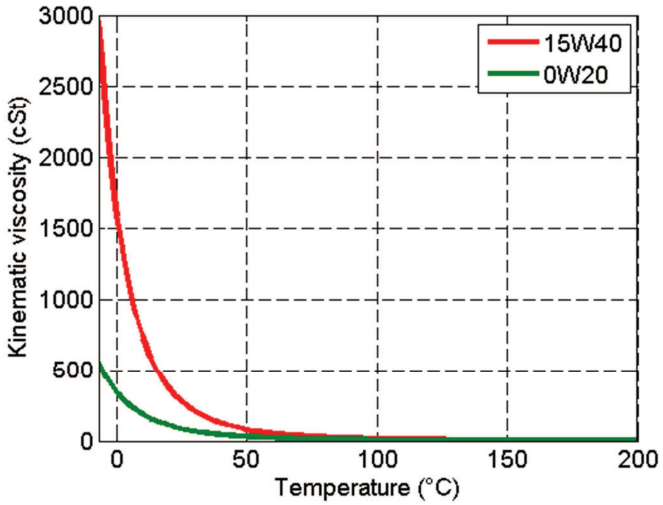

Figure III-25 Oil kinematic viscosity

The engine's oil is changed from 15W40 to 0W20. The engine's oil characteristics are provided by the GT-Suite library. It can be seen in the Figure III-25 that the oil's viscosity is largely reduced by using the new oil. With oil's grade of 0W20, the kinematic viscosity at the start of the driving cycle at -7°C is minimized by 81.25% and at 20°C by 71.32%. The influence of the temperature on 15W40 is greater than on 0W20. At first, the viscosity of 15W40 dropped remarkably with the elevation of the temperature. Then, it almost converged to the same characteristics of 0W20 around the highest temperatures, which is attended by the oil around the steady-state phase of the engine. Hence, the 0W20 oil is less temperature related. And, it is interesting to study the influence of these different thermal management strategies on this kind of oil's grade.

The configuration admitted for this study is the first one with the storage tank located downstream the thermostat and upstream the radiator and controlled with 3 valves. The numerical simulation is done over the five different driving cycles and at both ambient temperatures of 20°C and -7°C. The comparison is made between the thermal management strategy with 0W20 as oil's characteristics and the engine basic configuration with no storage tank but with the oil is changed to 0W20. The fuel consumption savings over the different cycles are given in Table III-7.

Table III-7 Fuel consumption savings with 0W20 as oil's grade

Driving cycle	20°C	-7°C
NEDC	0.52%	1%
WLTC	0.4%	1.45%
AH cycle (at the end of the transient phase)	0.38%	1 %
AU cycle	0.7%	0.72%
HDC cycle	1 %	2.67%

Most of the fuel consumption benefits have dropped by changing the oil's grade, thus its viscosity at the lowest temperatures. With lowest oil's viscosity, friction losses are reduced. Also, with the new oil, the variation of the latter's temperature does not lead to an important viscosity variation that had the first oil in use. Consequently, improvements regarding the engine's friction will be less significant. The hot water storage strategy has less impact on the engine with changing the oil's grade but it still has a significant improvement in fuel consumption.

III.2. Hot Oil Storage

New regulations impose a cold start up for all the driving cycles. Low functioning temperature leads to low oil's temperature. Low oil temperature means higher viscosity level. Higher viscosity generates higher level of friction. The energy balance done in the previous chapter proves that friction losses were high at the first stage of the driving cycle, and then they are reduced to their minimum at the end of the driving cycle.

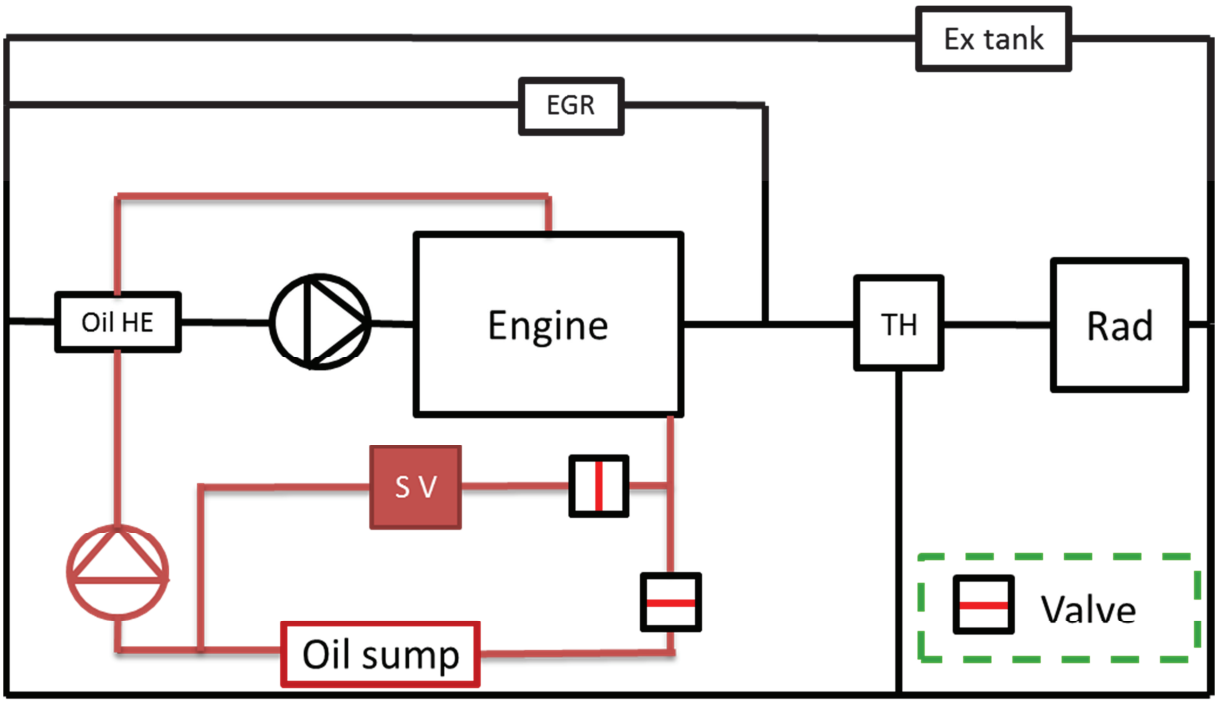

Figure III-26 A schematic presentation of the hot oil storage strategy (SV: Storage volume; TH: Thermostat; Oil HE: Oil heat exchanger; Ex tank: expansion tank; Rad: radiator)

This part of the study will focus on reducing the friction losses at the early stages of the driving cycle. Friction losses are reduced by increasing the lubricant's temperature. Lubricant's temperature can be improved by many ways such as controlling the lubricant's flow rate through the first stages of the driving cycle. Engine friction can be improved by using another type of oil with better grade characteristics. The energy balance of the different hydraulic circuits during the steady state phase of the different driving cycles informs that the oil circuit was seeding heat to the coolant at the heat exchanger. Then, the coolant was transmitting this heat to the ambient air via the radiator. In order to reduce the heat loss from the oil circuit, hot oil storage thermal management strategy was chosen to be tested.

Hot Oil Storage consists on using the heat transferred to the coolant circuit from the oil circuit and evacuated to the ambient air. During the steady state stage, a part of the hot oil is flown into an isolated tank with the same characteristics as that of the previous strategy (Table III-1). At the next cold start of the engine, the stored oil is flown into the engine to replace the cold lubricant. As seen in Figure III-25, the oil's viscosity decreases exponentially with its temperature. Firstly, an important drop of the viscosity is obtained with increasing slightly the temperature. Then, it ends to be almost constant at some temperature level. Flowing hot lubricant from the first seconds of the driving cycle will prevent the engine to run with high viscosity oil and thus reduces its friction losses.

To apply this thermal management strategy and assess the different fuel consumption over the different driving cycles, a first proposition is to place a 1L tank upstream the oil sump. As depicted in Figure III-26, the tank is placed in a branch parallel to the oil sump. Flowing into the storage tank is like bypassing the oil sump. This new branch is controlled by a valve that opens and closes to use the hot oil stored in the tank or to reload the latter with the hot oil at the end of the driving cycle.

The control of the storage tank will be as following:

First start-up: the oil in the storage tank is considered at the ambient temperature. While the storage tank temperature is equal or lower to the lubricant flowing into the engine system, the valve of the storage tank branch is closed. The two valves are always in an opposed position. Once the bypass branch valve is closed the other one is opened and vice versa. By closing the bypass branch, the storage tank is isolated from the lubricant circuit and the engine is considered functioning at its basic configuration with no additional oil's volume. Therefore, the engine transient phase regarding the lubricant temperature won't be disturbed.

Storing hot oil: When the lubricant's temperature reaches 90°C, the storage tank branch valve opens and hot oil flows into the storage tank. In this manner, hot oil will be stored for a further use.

Next start-up: During the next cold start up, the storage tank branch is opened if the stored oil's temperature is higher than that of the engine's lubricant.

To sum up, the valve controlling the storage tank opens **if** the stored oil temperature is higher than that of the engine's oil **or if** the engine's oil temperature exceeds 90°C.

Similar to the previous strategy, numerical simulations will be run over the five different driving cycles at two ambient temperatures: 20°C and -7°C. The initial temperature of the storage tank after the soak period is chosen to be 70°C. Most of the long driving cycles end with oil's temperature higher than 95°C, a drop of more than 20°C is considered enough during the soaking period.

III.2.1 Application on different driving cycles

In this part, the different results of applying the thermal management strategy of hot oil storage at an initial temperature of 70°C at both ambient temperatures are presented.

III.2.1.1. NEDC

The numerical simulation results for the hot oil storage strategy over NEDC at the two ambient temperatures are presented in Figure III-27.

Hot oil storage strategy has no impact on the coolant temperature profile at 20°C (Figure III-27(a)). On the contrary, the lubricant temperature showed an improvement on the first stage of the transient phase with an advance of 12°C at the start of the driving cycle. The lubricant's temperature tends to decrease as the stored oil's temperature in the tank tends to drop. Once the tank's temperature drops to the engine's temperature, its branch will be closed by the control valve. The engine goes back to its basic configuration, running the warm-up stage with the stored tank isolated.

Similar to the first case, with an ambient temperature of -7°C, the temperature of the lubricant at the start of the cycle has an advance of around 20°C. The oil's temperature starts decreasing after having a peak at the start of the cycle. It decreases to a point slightly lower than in the reference case (Figure III-27(b)). At the ambient temperature of -7°C, the coolant temperature profile with the thermal management applied is slighter lower the reference case, and it goes back to the friction losses reduced during this application. Decreasing the friction losses means less heat is dissipated to the hydraulic circuits.

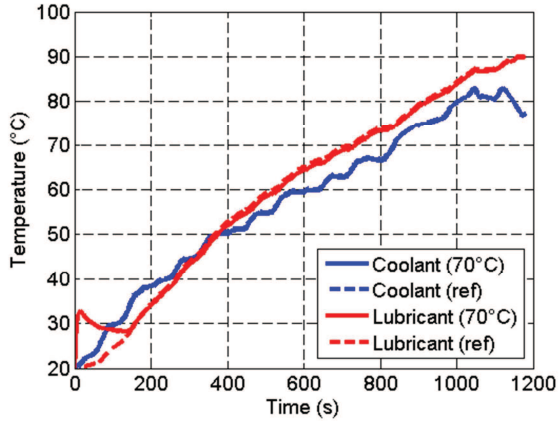

(a): Temperature profile at 20°C

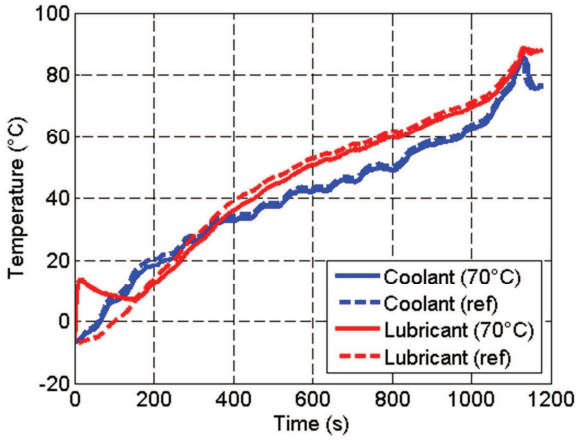

(b): Temperature profile at -7°C

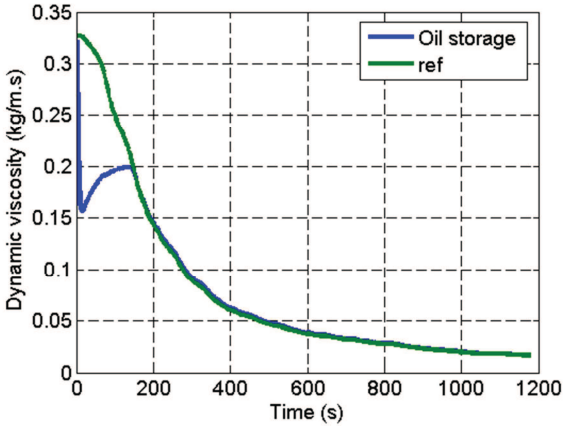

(c): Viscosity profile at 20°C

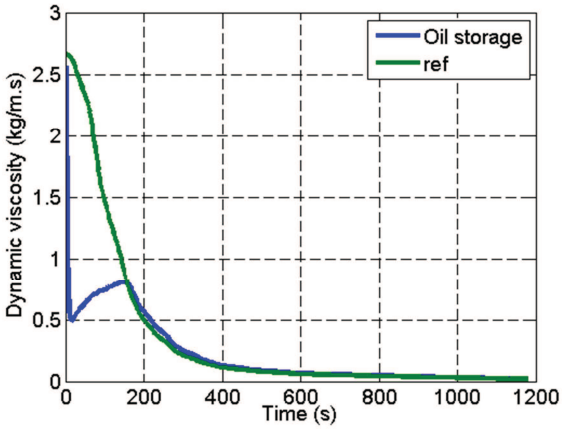

(d): Viscosity profile at -7°C

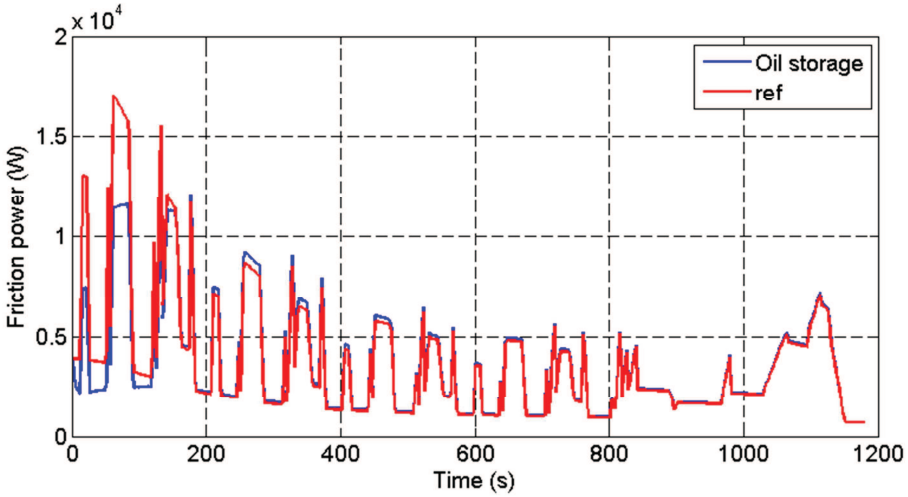

(e): Friction power at -7°C

Figure III-27 Hot oil storage results over NEDC at different ambient temperatures

The increasing in the oil's temperature at the start of the cycle leads to an improvement in the oil's viscosity as presented in Figure III-27 (c) and (d) at both ambient temperatures. During the first 153s of the cycle, with the lubricant temperature of the engine improved, an important drop of the viscosity is obtained. It hits a peak of difference around 51.3% and 81.3% at 16s and 20s of the driving cycle at 20°C and -7°C as ambient temperatures respectively.

The ambient temperature of -7°C highlights the importance of applying this thermal management strategy. The viral changes in the oil viscosity at the lowest temperature are enormously reflected in the friction power profile of the engine. In plot (e) of Figure III-27, the friction power profile at an ambient temperature of -7°C shows an important reduction in the first 150 seconds of the cycle. It corresponds to the time when the oil temperature of the oil storage strategy is higher than in the reference case. At the end of the cycle, at an ambient temperature of -7°C, the friction losses were dropped by 4.9% and by 1.6% at 20°C as an ambient temperature.

NEDC did not allow recharging the tank's temperature at those conditions. The storage tank's control can be changed to start recharging the oil storage tank once the regulation temperature of the engine is reached, thus not altering its transient phase. And as seen in plots (c), (d) and (e) of the Figure III-27, the oil's viscosity variation around the highest temperature is minimal, reflecting no big changes to the friction losses.

Finally, an assessment of the fuel consumption over NEDC with applying the hot oil storage thermal management gives an improvement of 0.03% at 20°C that rises to 6.63% at -7°C as an ambient temperature.

III.2.1.2. WLTC

The results shown in Figure III-28 are obtained from numerical simulations over WLTC at both ambient temperatures. The dashed line in the plot represents the coolant and the lubricant temperatures profile as well as the viscosity and friction power for the reference case (without a storage tank).

At an ambient temperature of 20°C, with the thermal strategy applied, the coolant temperature did not show a big variation in comparison to the basic state (Figure III-28(a)). In contrary, the lubricant profile showed an improvement in the earlier stages of the driving cycle. An increase in the oil temperature was observed at first. It hits a peak of 12.6°C difference, and then it starts to decrease in a soft slope until it reaches the reference curve and then increases in the same manner. Afterwards, the oil temperature for the cycle was slightly lower with the storage volume configuration. The valve for the storage branch starts closing at 74s, and then some opening and closing phases happen until it closes finally at 135s. The valve opens when the storage tank's temperature is higher than the engine's oil or when the engine's oil temperature reaches 90°C. The oil temperature with the strategy applied does not take the lead over the whole cycle but converges to the reference temperature. At the start of the cycle, with the highest oil temperature, the latter's viscosity is lower, leading to less friction losses in the engine. The main oil heat source comes from the friction losses of the engine. Decreasing those losses will lead to a lower heat-up rate of the oil temperature, thus converging to the reference oil temperature.

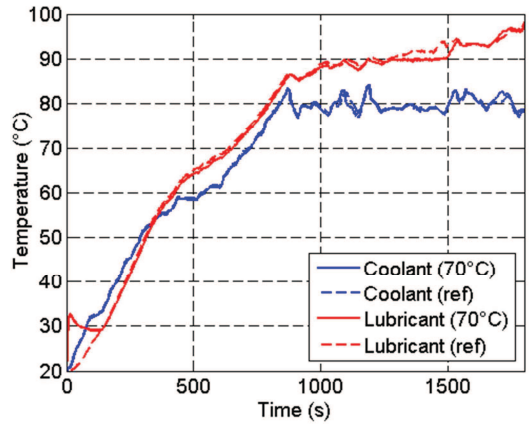

(a): Temperature profile at 20°C

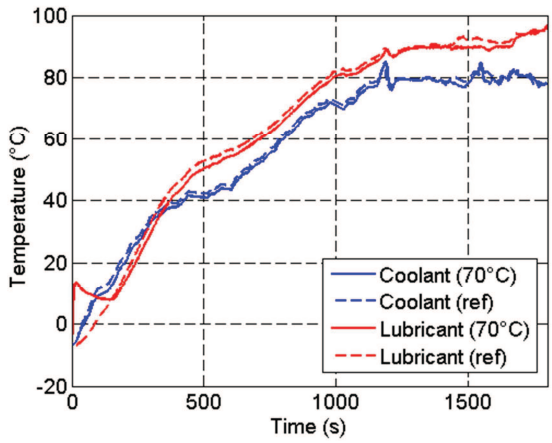

(b): Temperature profile at -7°C

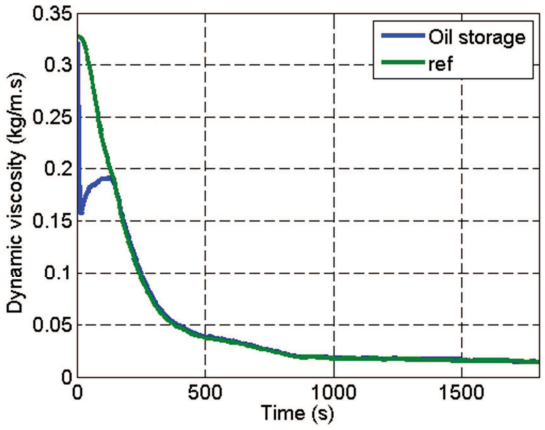

(c): Viscosity profile at 20°C

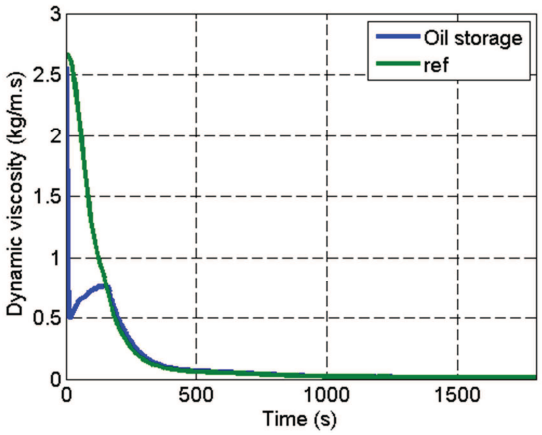

(d): Viscosity profile at -7°C

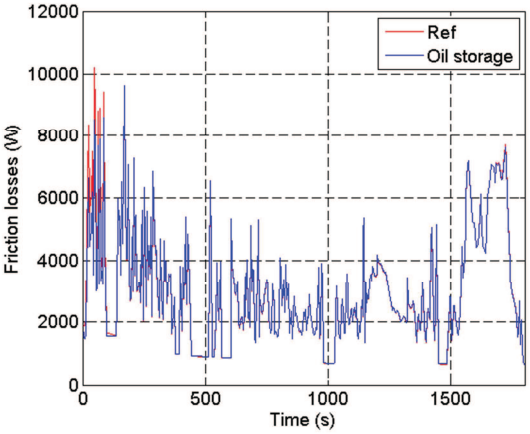

(e) : Friction power at 20°C

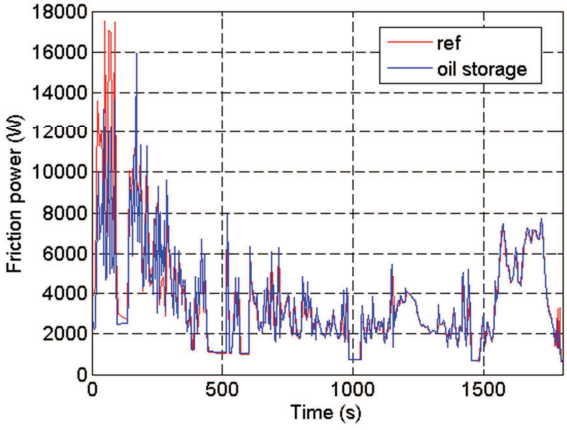

(f): Friction power at -7°C

Figure III-28 Hot oil storage results over WLTC at different ambient temperatures

Similar to the first case, at an ambient temperature of -7°C, the coolant temperature profile did not show any important variation. However, the lubricant temperature showed an improvement in the earlier stages of the transient phase. With a peak in difference around

20°C, the lubricant temperature converges to the reference case temperature afterwards, and the bypass branch is closed at 142s.

The friction power profiles presented in Figure III-28 (e) and (f) shows the important reduction of the losses level at the beginning of the cycle when the hot oil stored in the tank is circulated in the system. This decreasing of the friction losses of 0.9% and 5.85% at ambient temperatures of 20°C and -7°C respectively, goes back to the lower viscosity of the oil as shown in the part (c) and (b) of Figure III-28. As said before, the oil viscosity is inversely proportional to its temperature. The decay of the viscosity is significant at first and attends a certain state of stability afterwards. The applied thermal strategy allows the engine to avoid the highest viscosity part. The cumulative viscosity over the cycle is reduced by 38% and the highest instant decrease peak reached around 81.7% at 16th second of the cycle at ambient temperature of -7°C. At 20°C, the cumulative viscosity over the cycle is reduced by 10.8%, a predictive lower proportion than the lowest ambient temperature and a peak that reached 53% at the 16th second of the cycle.

The temperature profile of the storage tank, at the ambient temperature of 20°C, starts with a decrease in the temperature as its containing is circulated through the lubrication system. It drops from 70°C to around 29°C in 135s corresponding to the closing of the storage tank profile (Figure III-29). The latter's temperature stays constant through the cycle till the engine's oil temperature reaches 90°C at 1184s at the first time, and 1285s for the rest of the cycle. The constant temperature proves that there is no flow through the storage tank during the warm-up stage, thus no drawback in the fuel consumption during this phase. With the opening of the valve at 1285s, the engine oil temperature profile shows a constant temperature around 90s while the reference profile keeps on increasing (Figure III-28(a)). With the opening of the storage tank branch, a flow of oil with lower temperature will be flown into the system, and the hot oil of the engine will enter the tank to be stored for a later use. The engine oil temperature resumes its increment once the storage tank reaches the same temperature, and continues rising to resume the reference line till the end of the cycle.

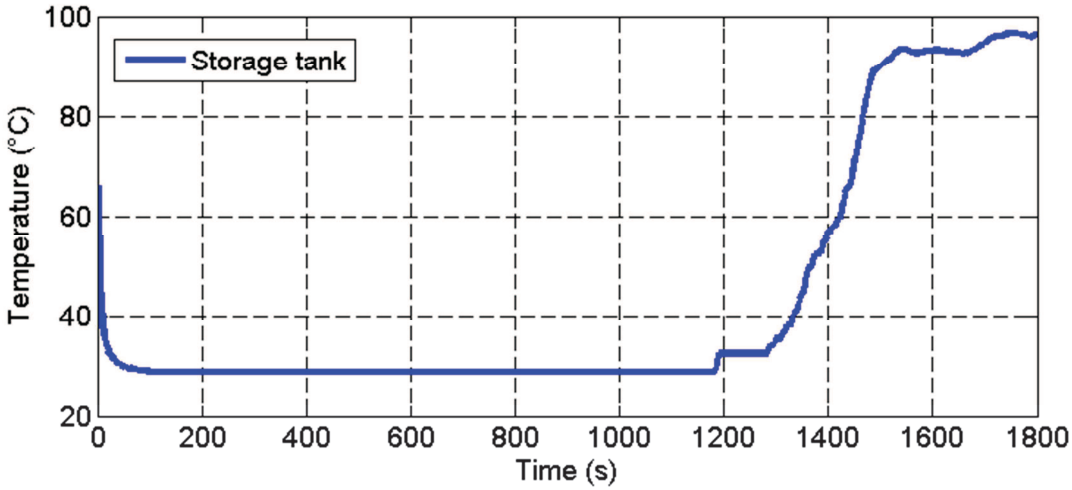

Figure III-29 Storage tank temperature over WLTC at 20°C

Finally, the "hot oil storage" thermal strategy over WLTC at an ambient temperature of 20°C, leads to a reduction in fuel consumption of 1.1%. Running the numerical simulation with the same configuration but at a lower ambient temperature highlights the importance of the hot oil

at the coldest start of the engine. Reducing the initial temperature of the engine generates higher level of friction losses. And at an ambient temperature of -7°C, the thermal management strategy applied provokes a saving of fuel consumption around 5%.

III.2.1.3. Artemis Highway

The results for the Artemis Highway using the hot oil storage strategy to improve the friction losses at the early stages of the transient phase are presented in the Figure III-30.

As mentioned before and seen in the plots, engine warm-up stage during AH is very short. At 20°C, the coolant temperature profile did not show any significant improvement over the reference case presented in dashed line in plot (a) of Figure III-30. During the steady state stage of the cycle and around 800s, the coolant's temperature of the reference case shows an important difference in comparison with the strategy applied. The latter is lower. The lubricant temperature showed an improvement in the first stage of the transient phase, when the hot oil was being circulated. This temperature improvement is reflected in the dynamic viscosity profile with a drop of the viscosity by half at the start of the cycle (Figure III-30(c)). This viscosity drop will lead to lower the friction power losses during the same period. It is represented by the difference between the red line (the reference case) in part (e) of Figure III-30 and the blue line (the engine with the hot oil storage tank). The friction losses are reduced by 0.76% by applying this thermal management strategy. After reaching 90°C, the oil's temperature profile shows a constant temperature corresponding to the time when the valve opens the branch to the storage tank. Once the storage temperature's reaches the oil's engine temperature, the latter continues its increment and follows the reference line.

The storage tank temperature profile in Figure III-31 proves that at end of the cycle, the storage tank is recharged with hot oil. The temperature of the storage tank drops over the first seconds of the cycle as the hot oil is flown into the engine. The constant temperature of the storage tank proves the insulation of the latter from the engine during the transient phase. When the temperature of the oil reached 90°C, the control valve opens the storage tank branch and the latter temperature starts to increase. At the end of the driving cycle, the oil's temperature reaches a temperature of 100°C. Higher is the storage tank final temperature, higher is its initial temperature at the next cold start-up, and higher is the fuel consumption benefits.

The fuel consumption assessment over the whole driving cycle leads to an overconsumption of 0.12% that can be a result of a lower static temperature of the engine with applying the strategy. The fuel consumption saving was also assessed at the end of the transient phase which is reached after 26% of the driving cycle, and a reduction of 0.6% was obtained.

At an ambient temperature of -7°C, the same behavior of the lubricant's temperature was observed throughout the cycle. At first an improvement of the oil's temperature is obtained, then, it is reduced to meet with the reference case. Afterwards, it increases all along the cycle, following the slope of the reference case but slightly lower (Figure III-30(b)). The increase of the oil temperature leads to an important reduction of its viscosity. It avoids the interval of the oil highest viscosity (Figure III-30(d)) as seen in the reference case with the lubricant starting at the ambient temperature of -7°C. Consequently, the friction losses are minimized by 3.5% by the end of the cycle (Figure III-30(f)).

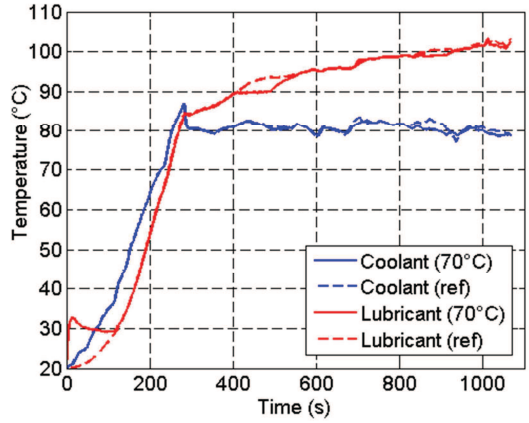

(a): Temperature profile at 20°C

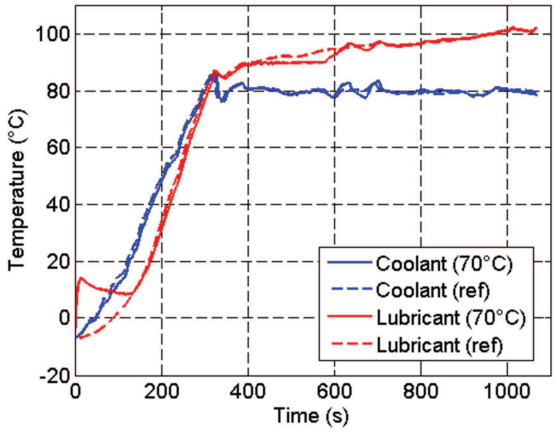

(b): Temperature profile at -7°C

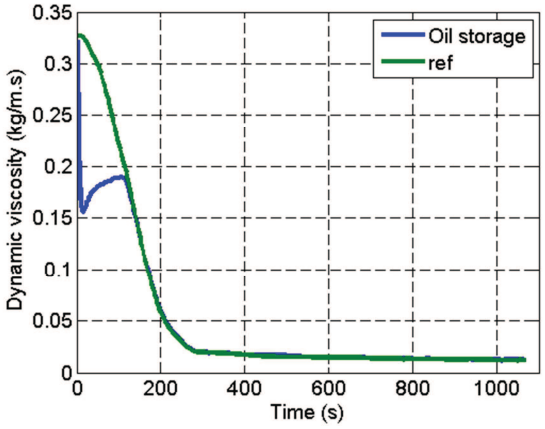

(c): Viscosity profile at 20°C

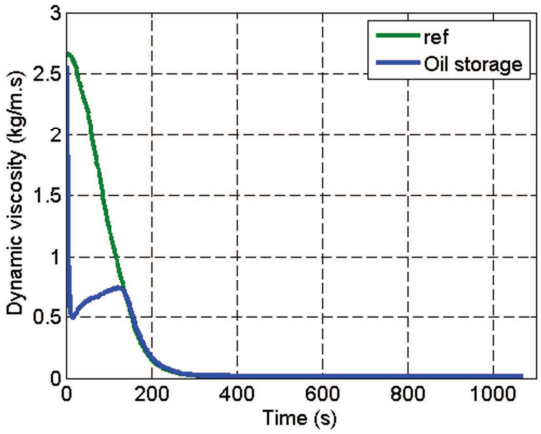

(d): Viscosity profile at -7°C

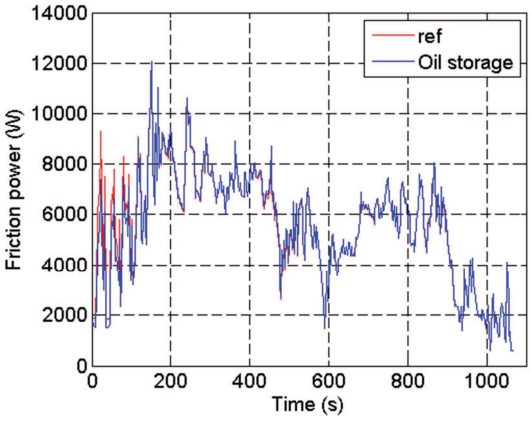

(e) : Friction power at 20°C

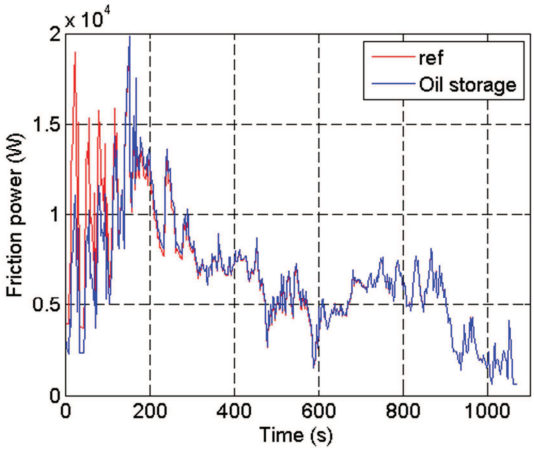

(f): Friction power at -7°C

Figure III-30 Hot oil storage results over AH at different ambient temperatures

Contrary to the warmer day, at an ambient temperature of -7°C, the fuel consumption savings will be more significant. The assessment of the fuel consumption with the hot oil storage strategy over at the end of the transient phase of the AH at -7°C gives a reduction of 2.24% that decreases to 0.12% at the end of the driving cycle.

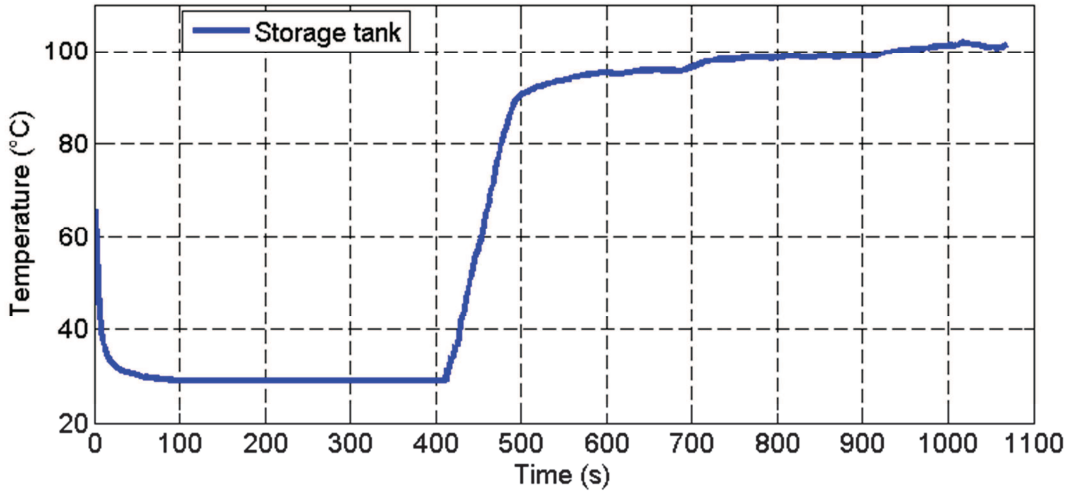

Figure III-31 Storage tank temperature over AH at 20°C

III.2.1.4. Artemis Urban

Artemis Urban is the fourth driving cycle to be tested with the hot oil storage thermal management strategy. The results of the different simulations are summed up in Figure III-32.

The temperature profiles in Figure III-32 (a) and (b) showed the same behavior as the different driving cycles. At -7°C, it is more noticeable the difference between the temperature profiles. With hot oil flown into the system in the early stages, friction losses drop enormously compared to the reference case, the engine running with no storage tank. When the storage tank's temperature drops lower than that of the engine's oil, the oil in the sump is pumped into the system. The sump oil's temperature is still equals to the ambient. Consequently, the oil temperature profile is slightly lower than in the reference case. Also, the main heat source of the oil circuit is the friction losses. However, around 160-180s, as seen in the part (d) of Figure III-32, the friction losses do not vary a lot between the two cases. The main heat source of the oil circuit in both cases (with storage tank and reference case) is quasi-equal. Thus, the oil's temperature profile will follow the one of the reference case, with a slight difference obtained when the oil sump was flown into the system. Friction losses analysis, over the driving cycle, states a reduction of 2.49% and 6.31% at an ambient temperature of 20°C and -7°C respectively.

Applying the hot oil storage thermal management strategy over Artemis Urban driving cycle leads to a reduction in fuel consumption of 1.19% and 5.37% at 20°C and -7°C respectively as ambient temperatures. Contrary to the other driving cycles, the fuel consumption savings are important because the engine operates only in transient phase. Hence, the improvement at the beginning of the cycle is not compensated by the steady state stage of the cycle as was happened in AH cycle.

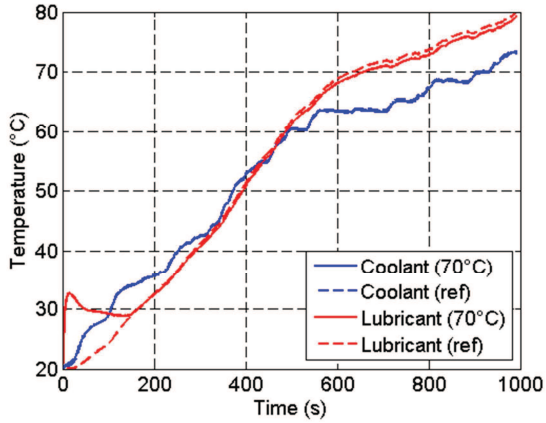

(a): Temperature profile at 20°C

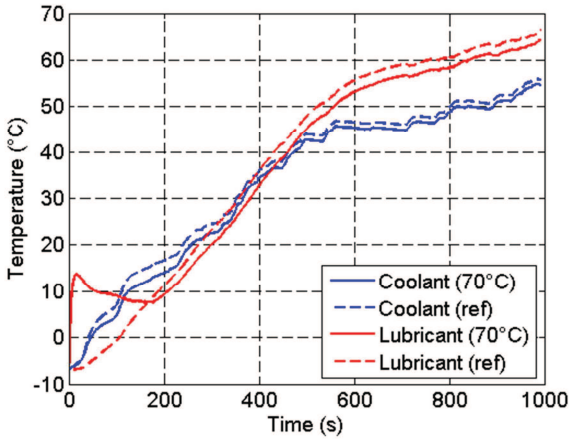

(b): Temperature profile at -7°C

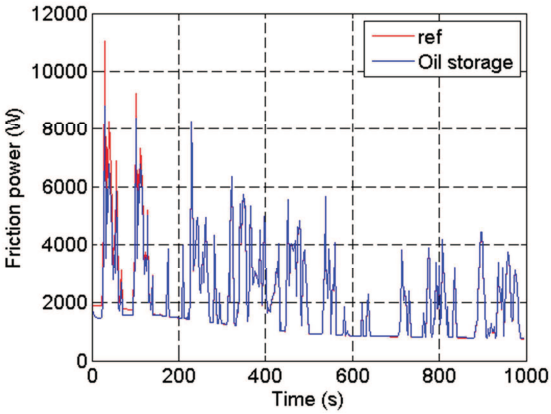

(c) : Friction power at 20°C

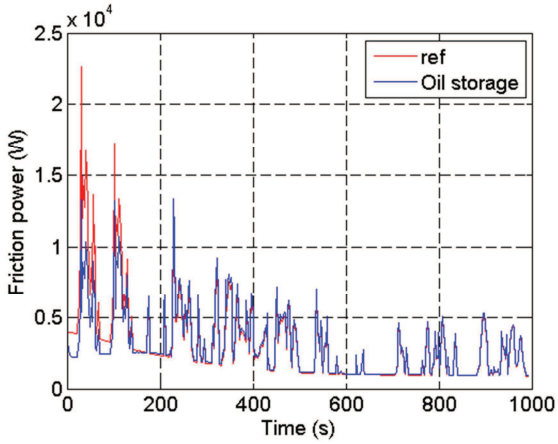

(d): Friction power at -7°C

Figure III-32 Hot oil storage results over AU at different ambient temperatures

III.2.1.5. In-House developed Driving Cycle

The last cycle to be tested is HDC at both ambient temperatures. The results are depicted in Figure III-33.

The temperature profiles of the engine fluids are presented in part (a) and (b) of Figure III-33 at an ambient temperature of 20°C and -7°C respectively. The behavior of the temperature profiles is similar to the previous cycles. During this driving cycle, because it is only for 254s the improvement in the beginning is highlighted, zoomed on. At 20°C, the oil temperature stays over the reference case until the end of the cycle. However, at -7°C, similar to the former cases, the lubricant temperature for the reference case takes the lead around 150s of the cycle. The friction losses are one of the many heat sources to the hydraulic circuits, and not only the lubricant uses this heat to increase its temperature, the coolant circuit benefits also from this heat source. By reducing the friction losses as seen in Figure III-33 (c) and (d), the coolant temperature of the reference case will take the lead over the tested strategy more significantly in the coldest days.

At an ambient temperature of 20°C, friction power was decreased by 6.67%. It hits 16.7% with -7°C. The fuel consumption analysis over the driving cycle gives a reduction of 2.47% for a warm day, and 8.56% for the coldest one.

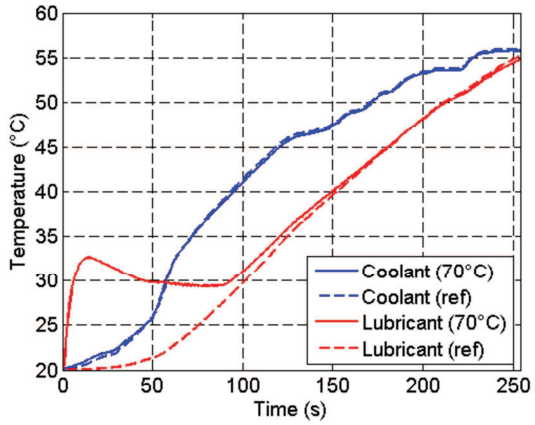

(a): Temperature profile at 20°C

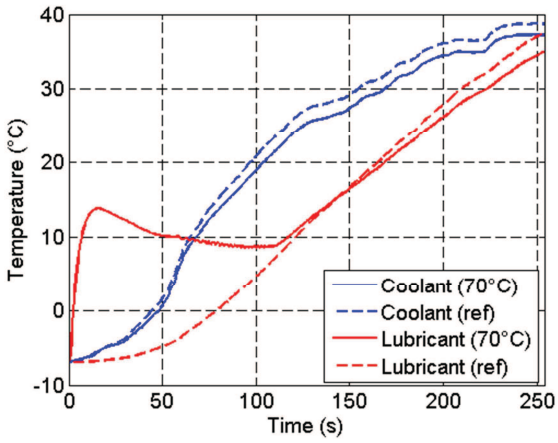

(b): Temperature profile at -7°C

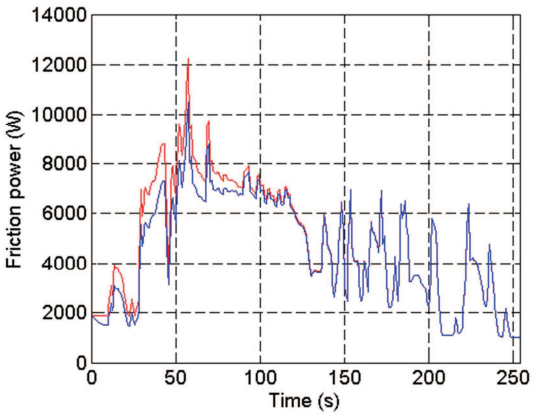

(c) : Friction power at 20°C

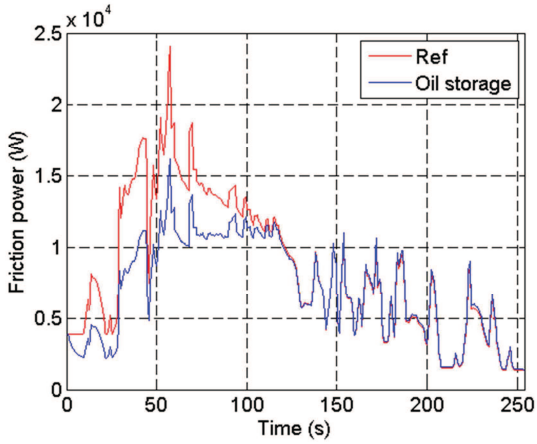

(d): Friction power at -7°C

Figure III-33 Hot oil storage results over HDC at different ambient temperatures

HDC focuses on the benefit of the thermal strategy over the cold start of the engine. For the whole cycle, the engine is in warm-up stage, and normally does not lead the engine to its steady state stage. However, this driving cycle is imagined used back to a long cycle such as Artemis highway or WLTC.

The results obtained for all the simulations are summarized in Table III-8.

The different variation in the fuel consumption goes back to the big dependency between this strategy and the driving cycle. The main profit goes to the reduction of the friction losses and the lubricant temperature in the system. Thus, these two values are related also to the rotational engine speed and torque where at cold temperatures, the highest the rotational speed is, higher is the oil flow rate in the system, and highest is the frictional forces applied to the different moving/rotating parts. Based on this analysis, different configurations for the hot oil storage are proposed and assessed in the following part.

Table III-8 Oil storage results at different ambient temperatures

	Fuel consumption		Friction power	
Driving cycle	**20°C**	**-7°C**	**20°C**	**-7°C**
NEDC	0.03%	6.63%	1.66%	4.9%
WLTC	1.1%	5%	0.9%	5.84%
AH cycle	-0.12%	0.12%	0.76%	3.5%
AH cycle (at the end of the transient phase)	0.6%	2.24%	3.67%	8.24%
AU cycle	1.2%	5.37%	2.49%	6.31%
HDC cycle	2.47%	8.5%	6.67%	16.7%

III.2.2 Multifunction oil sump

In the first configuration proposed, the storage volume was added to the system. The total volume of the engine's oil was increased by 1 liter. To improve this strategy, thoughts were shifted to the oil sump, where the strategy of storage is possible without adding new components to the system and without additional volumes. Based on this analysis, three other configurations were proposed.

III.2.2.1. Configuration A

Configuration A consists to integrate the storage volume in the oil sump. Contrary to the hot oil storage configuration, configuration A will be isolating one liter of oil already existing in the system. As benefits, one less component is proposed, a good thing regarding the lesser free space under hood existing nowadays, and no additional mass to the system. Furthermore, isolating 1L already existing in the oil sump, not only avoid the addition of a supplement 1L of oil to the system but will lead to combine the benefits of two strategies: Hot oil storage, and reducing the thermal mass of the oil. The control of the stored oil will be done as same as the previous hot oil storage strategy, with a valve that opens and closes in function of the engine's oil temperature.

III.2.2.2. Configuration B

Configuration B is based on the previous configuration, where the storage will be done in the oil sump, with addition of neither mass nor oil volume. The difference is in the control, where one criterion will be added. The friction is a result of two parts in contact sliding at each other's, and the moving part's speed of the engine are proportional to its rotational speed. Therefore, the valve of the storage tank will be controlled by the rotational engine speed, in addition to the oil's temperature. This configuration takes in consideration the safety of the moving parts, as with higher rotational speed, higher is the flow rate of the oil pumped into the system. To not isolate 1L of oil during the peak point of flow rate and depending on the different driving cycles used in this study, 2500 rpm is the level when the valve controlling the storage part of the sump opens up to back up the flow of the oil into the system.

III.2.2.3. Configuration C

Configuration C is the simplest among them all, called no valve configuration. The oil sump is equipped with an isolated part where the hot oil should be stored throughout a soak period. While the engine is running, oil flow rate from the isolated part as well as from the other part will be mixed upstream the pump.

III.2.2.4. Application on different driving cycles

In this part, the results for the numerical simulations of hot oil storage for the three different configurations will be presented. Figure III-34 and Figure III-35 represents the oil temperature profile and the viscosity profile respectively at an ambient temperature of 20°C.

For all the driving cycles, “Ref” line in the plots represents the reference case with the engine in its traditional architecture, without a storage tank. Configurations A and B showed the highest initial oil’s temperature, followed by Configuration C. During these two configurations, the oil storage quantity is controlled by different ways. Configuration C takes the lead after around 85s for NEDC, 78s for WLTC, 77s for AH, 98s for AU and 63s for HDC. The last configuration has no control for the hot oil, thus it will be mixed with the cold one in the system once the engine starts running. Consequently, the oil temperature profile for the configuration C has a more stable temperature and rises monotonically compared to Configurations A and B. With the oil’s temperature of the storage tank drops to the engine’s oil temperature, the valve isolates the storage part of the oil sump and lower oil’s temperature of the oil sump flows into system. This functioning leads to a drop of the temperature in the Configurations A and B. However, through the cycle, configurations A and B are circulating a lesser oil’s volume in the engine. Hence, the oil’s temperature for these two configurations retakes the lead. Configurations A and B follow the same behavior for almost all the simulation. The control in Configuration B differs from Configuration A by opening the storage tank once the engine’s speed is higher than 2500rpm. It is shown in NEDC at the end of the driving cycle at 1097s (Figure III-34(a)) a drop of the oil’s temperature is due to the opening of the oil storage volume and low temperature oil is flown into the system. The same behavior is present at different points during the WLTC (Figure III-34). For AH (Figure III-34(c)), 2500rpm is exceeded the first time at 200s, during the warm-up stage of the engine. The oil’s temperature before 200s was higher than that of the reference case, and it presents a slight drawback around 200s, and continues to rise following the ref line.

During AH, rotational engine speed surpasses 2500 rpm two times, the first for 235s allowing the storage volume temperature to be reach 90°C. Hence, during the second opening of the valve, the oil’s temperature profile does not show any temperature drawback. The same behavior occurs with WLTC, with the third opening of the valve, the storage volume temperature is elevated to 90°C and thus no more temperature drops are shown for the Configuration B. However, for configuration A, for WLTC and AH, the recharge of the storage volume with hot oil can be noticed in the plot where the green line shows a constant part during the steady state phase corresponding the opening of the valve when the oil temperature reaches 90°C. This phenomenon is present neither in NEDC nor in AU and HDC because the oil’s temperature does not reach 90°C.

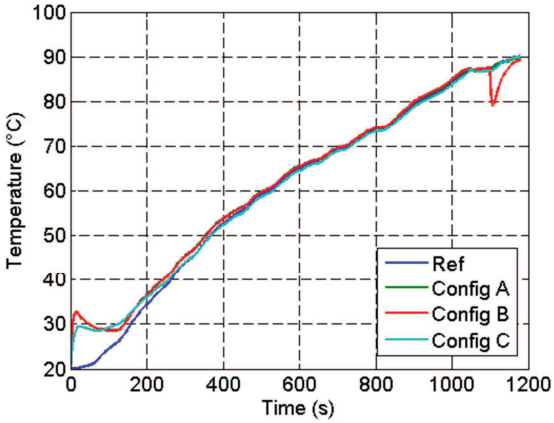

(a): NEDC

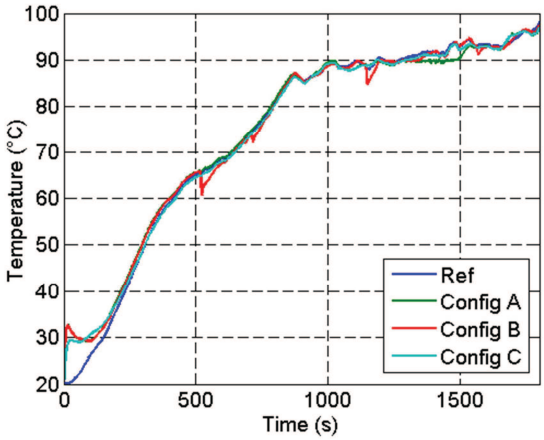

(b): WLTC

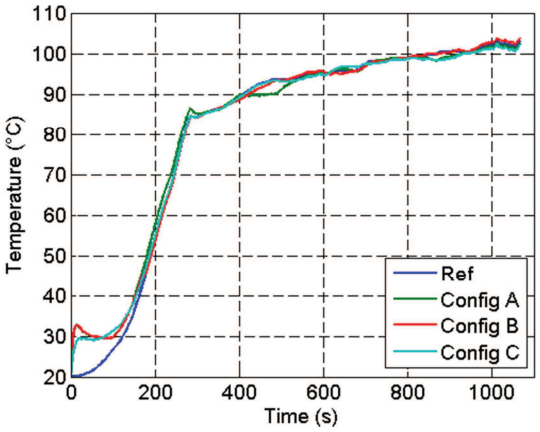

(c): Artemis Highway

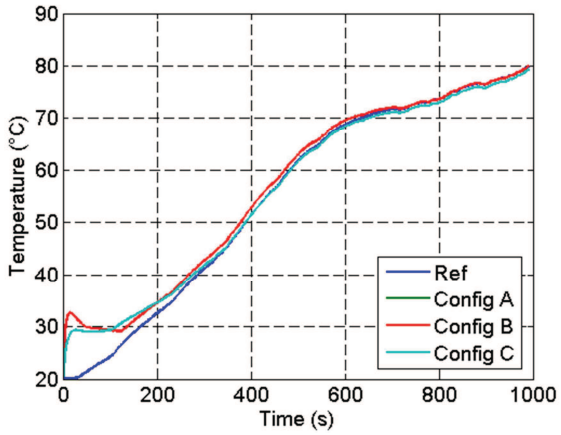

(d): Artemis Urban

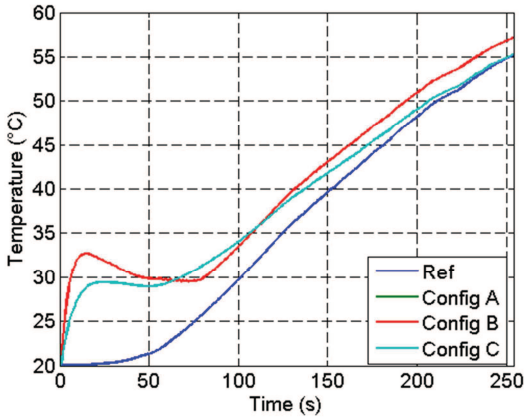

(e): HDC

Figure III-34 Oil temperature profile for different configurations over different driving cycles at 20°C

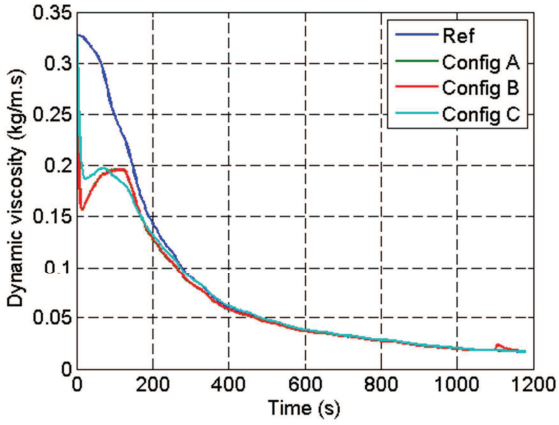

(a): NEDC

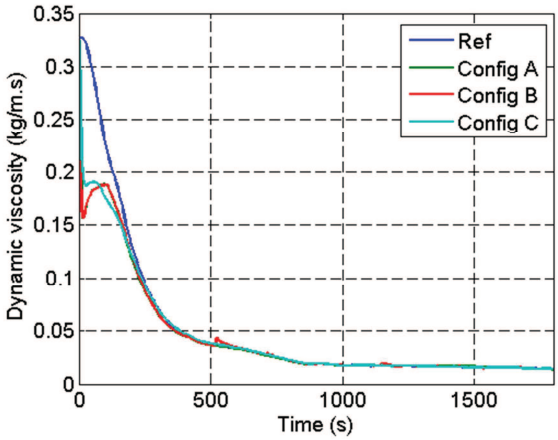

(b): WLTC

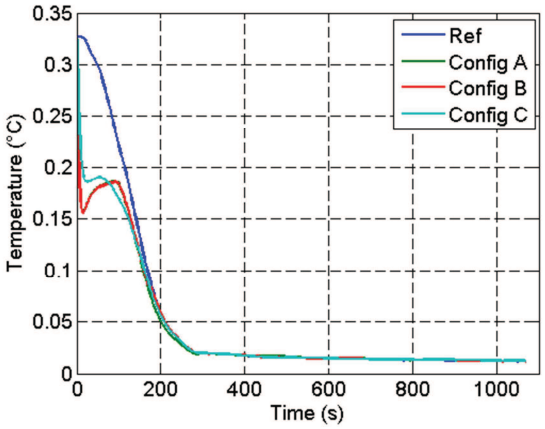

(c): Artemis Highway

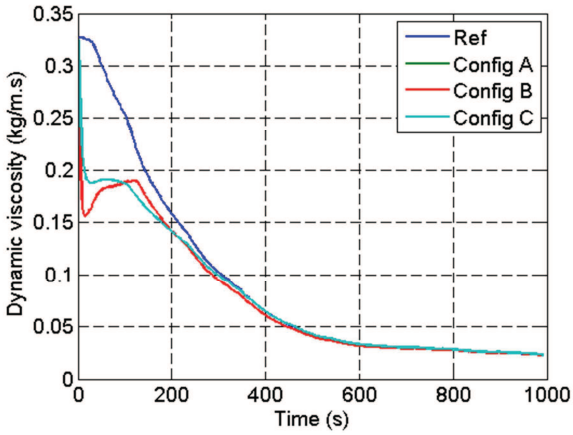

(d): Artemis Urban

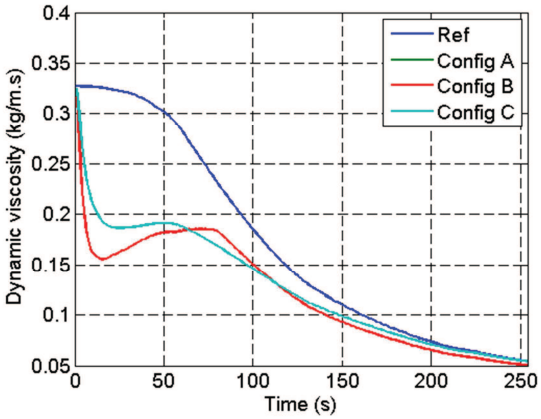

(e): HDC

Figure III-35 Oil dynamic viscosity profile for different configurations over different driving cycles at 20°C

The dynamic viscosity presented in Figure III-35 for the different driving cycles follows the same reasoning of the oil's temperature. Configurations A and B have the highest reduction of viscosity at the start of the driving cycle. Then, the viscosity rises higher than in that in

Configuration C, because the latter has a temperature profile increasing all the time. With lower volume been circulated into the system with Configurations A and B, they retake the lead in the lowest viscosity after some times depending on the driving cycles. Valve opening when surpassing 2500rpm is noticed for NEDC and WLTC with red peaks during the steady-state stage of the viscosity profile, while for AH, the red plot can be seen exceeding the different viscosity profiles around 200s to re-converge and follow the other behavior later on. Charging the storage tank is not noticed during the viscosity profiles and that goes back to the fact to the minimal changes of the oil's viscosity to the changes of the oil's temperature at high level.

Simulations were run for an ambient temperature of -7°C too. Fuel consumption savings for the different configurations, driving cycles and ambient temperatures are depicted in Figure III-36.

Table III-9 sums up the results of the different configurations A, B and C in term of fuel consumption savings and friction power improvements.

The fuel consumption for the configuration B is lower for NEDC and AH where the opening of the valve due to surpassing 2500 rpm has a drawback in comparison to configuration A. On one hand, the oil temperature drop for NEDC was significant, while on the other hand, the first opening for the AH was during the transient phase and for a long duration. Furthermore, the second opening of the valve during AH was insignificant in term of fuel consumption because of the hot oil contained in the storage tank at that time. However, the multiple openings during WLTC, which was for a short amount of time, were insignificant on the fuel consumption. The friction power improvements for WLTC during configuration B in comparison to Configuration A proves the necessity of a greater flow rate of the oil during some operating points of the engine. Artemis Urban and HDC, in which the rotational engine speed does not exceed 2500rpm, did not show any changes in their fuel consumption between configurations A and B.

Configuration C proves that isolating a part of the oil sump to store hot oil from a cycle to another benefits the engine. As presented in the Table III-9 or Figure III-35, all the driving cycles except Artemis Highway at the end of the cycle, show an improvement in fuel consumption. Configuration C does not force a full insulation of the storage tank, thus avoiding an overheating of the engine's oil.

All three configurations studied for the hot oil storage leads to a renovation of the oil sump technology, either to isolate a part of it or to add a controlling valve to manage the flow or the hot oil stored. At the end, the three configuration presented in this part announce a multifunctional oil sump, which is capable to store hot oil, control the oil flow rate through the system, thus the oil mass put into action.

The main outcomes of this study are the importance of the oil strategy proposed on coldest winter days, presented in the ambient temperature of -7°C. Due to the important improvement in the oil's viscosity at lower temperature, friction losses are virally minimized leading to lower fuel consumption through the cycle. This improvement is mostly highlighted with the short driving cycles such as Artemis Urban and HDC in which the engine runs in transient phase.

Table III-9 Oil storage results for different configurations at different ambient temperatures

		Fuel consumption		Friction power	
	Driving cycle	**20°C**	**-7°C**	**20°C**	**-7°C**
Config A	NEDC	0.86%	7.7%	3.25%	7.56%
	WLTC	0.57%	4.27%	-0.39%	7.85%
	AH cycle	-0.06%	1.09%	1.93%	5.99%
	AH cycle (transient phase)	1.61%	3.63%	7.06%	13.4%
	AU cycle	1.44%	6.25%	4.32%	9.52%
	HDC	3.39%	10.78%	9.26%	21.02%
Config B	NEDC	0.33%	7.24%	2.8%	7.01%
	WLTC	1.8%	4.37%	1.61%	7.48%
	AH cycle	-0.19%	0.49%	1.47%	4.98%
	AH cycle (transient phase)	1.04%	6.46%	4.95%	10.79%
	AU cycle	1.44%	6.25%	4.32%	9.52%
	HDC	3.39%	10.78%	9.26%	21.02%
Config C	NEDC	0.71%	4.4%	2.25%	6.17%
	WLTC	1.21%	3.8%	-0.9%	7.04%
	AH cycle	-0.08%	0.89%	1.43%	3.5%
	AH cycle (transient phase)	1.09%	3.28%	5.18%	11.22%
	AU cycle	1.82%	6.9%	3.23%	7.71%
	HDC	3.14%	6.79%	8.14%	19.61%

III.2.1 Influence of oil's grade

Fuel consumption benefits by applying hot oil storage is mainly due to friction losses reduction. The latter is a result of lowering the oil's viscosity at the start of the driving cycle. However, lately, oil with low viscosity at low temperature is being used for engine lubrication. To study the influence of the oil grade on the hot oil storage strategy, simulations were done by replacing the current oil 15W40 by 0W20 which characteristics were depicted in Figure III-25. Configuration A was chosen to be tested on both ambient temperatures 20°C and -7°C.

Results of the different simulations are presented in Table III-10. Fuel consumption savings are reduced with the new oil been tested, because of the less dependency on the oil's

temperature with the low viscosity oil. Despite the reduction of the oil's kinematic viscosity by 81.25% and by 71.32% at -7°C and 20°C as ambient temperature respectively, the thermal management of hot oil storage showed some improvements in fuel consumption especially with the short driving cycles such as Artemis Urban and HDC.

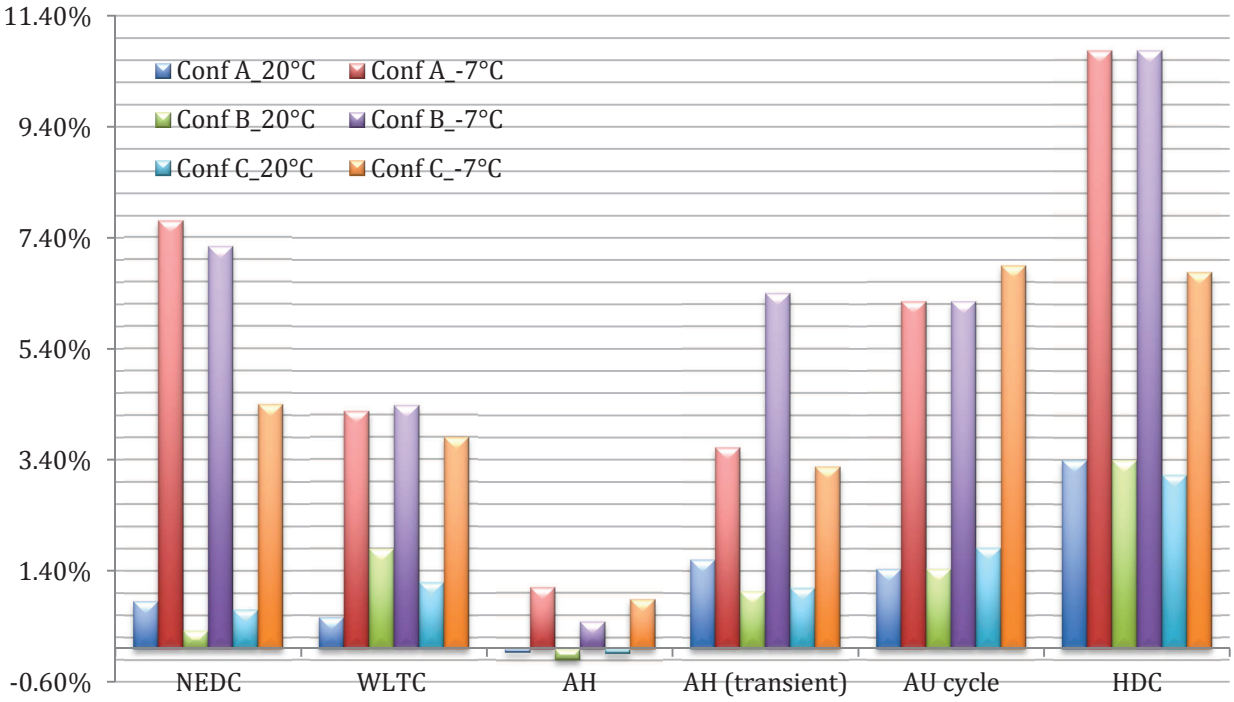

Figure III-36 Fuel consumption savings for oil storage strategy for: different configurations, driving cycles and ambient temperatures.

Table III-10 Fuel consumption savings for hot oil storage configuration A with 0W20 as oil's grade

Driving cycle	20°C	-7°C
NEDC	0.91%	1.37%
WLTC	0.23%	2.43%
AH cycle (end of transient phase)	0.79%	1.99%
AU cycle	0.95%	4.46%
HDC	1.81 %	5.87%

Heat storage strategy is a thermal management strategy that consists of storing heat when an engine is running with the objective to use it during the next cold start. An application of this strategy over the coolant and lubricant was tested.

Hot coolant storage strategy was the first to be tested. A 3L storage tank was proposed to be installed in the radiator branch downstream the thermostat and upstream the radiator. Different valves controlled the flow in and out of the storage tank in function of the engine and the tank temperatures. Initial temperature of the storage tank was set to 60°C and the ambient temperature was set to: 20°C and -7°C. Numerical simulations were made over different driving cycles. Hot coolant storage proved its efficiency in improving the fuel consumption of the engine. It influences the engine's coolant temperature, as the latter started by an elevated temperature by applying the strategy, than converges to the reference case due to the low level of the wall heat losses with the strategy applied. The main influence of this strategy is over the warm-up stage of the engine. Thus, it will have less influence on driving cycles with short warm-up stage such as Artemis Highway. Fuel consumption varied between 0.26% and 3.04% depending on the conditions. However, this strategy did not influence the lubricant. To do so, other configurations were proposed. The outlet of the storage tank was set upstream the oil cooler to have a direct exchange between both fluids. Another configuration consists of installing the storage tank upstream the thermostat and not been controlled by any valves. Fuel consumption savings were reduced in the two latter configurations. The last configuration showed that increasing the coolant mass inertia in the system with an isolated tank with no control at all will lead to improve the fuel efficiency. However, its drawbacks are remarkable for the cold cycle where the storage tank is at ambient temperature. The study was closed by the influence of the oil's grade on the efficiency of the strategy. Switching from 15W40 oil's grade to 0W20 led to lower the fuel savings. For example, over WLTC at an ambient temperature of -7°C the savings from the first configuration decreased from 1.83% to 1.45%.

Hot oil storage consists of storing hot oil when the engine is running under steady state stage in order to use it for the next cold start. This thermal strategy was tested at first by adding a storage tank in a branch parallel to the oil sump and controlled by its temperature. Fuel consumption savings ranged between -0.12% and 8.5% depending on the driving cycles and the ambient conditions. Furthermore, the storage strategy was implemented in the oil sump. It consists of isolating 1L volume of the oil sump combining the hot storage strategy with lower oil mass inertia. Three configurations were proposed. The oil sump isolated part is controlled in function of the temperature at first, then in function of the temperature and the rotational engine speed and at the end with no control at all. Fuel savings varied between -0.19% and 10.78% depending on the various conditions. The main outcome was the importance of such strategy on the cold days, in which the friction power is the highest. A little improvement of the oil's temperature at low temperature leads to remarkable improvement in the friction power. At the end, the influence of the oil's grade was tested. With 0W20, improvement still exists when applying the hot oil storage thermal management strategy especially on the driving cycles where the engine is always in a warm-up stage, thus transient stage.

IV. Exhaust gas heat recovery

Exhaust gas heat recovery is the thermal management strategy studied in this chapter.

An overview of the heat exchanger, the experimental setup and the different tests done at Ecole Centrale de Nantes will be presented first. These tests were used to model the heat transfer between the two fluids in the exchanger as well as the pressure drops on the two sides.

Once that done, numerical simulations were run to assess and valorize the strategy. The application were divided into three parts: an indirect heating of the oil with the coolant as a medium fluid, a direct heating of the oil and direct heating of the oil and the coolant. The different ideas were tested over five different driving cycles and two ambient temperatures. Different configurations were proposed to control the engine's lubricant maximum temperature. Results concerning the temperature profiles as well as the assessment of fuel consumption were stated for each case.

IV.1. Experimental setup

IV.1.1 Heat exchanger

The heat exchanger chosen to be tested during this study is originally an EGR heat exchanger used on Peugeot Boxer 3 with a Turbo Diesel engine F30 (Euro5 175 HP). The heat exchanger is presented in Figure IV-1. The heat exchanger coolant inlet diameter is 14mm, while that of the air is 50 mm. Its section is around 60x60 mm. It can contain 0.415 L of coolant and the air volume is estimated around 0.58L.

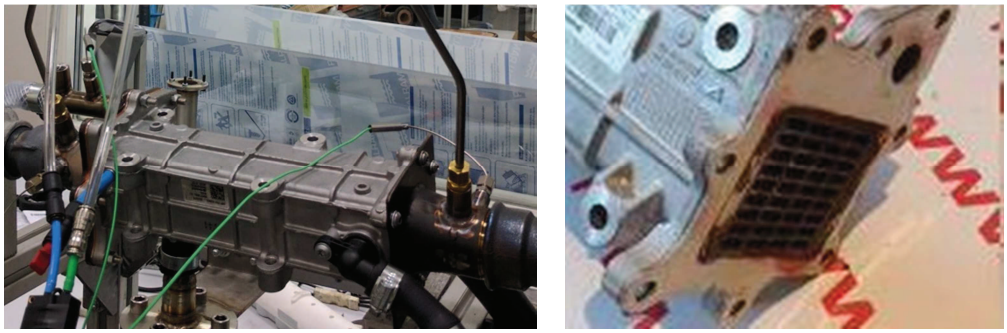

Figure IV-1 Heat exchanger

IV.1.2 Test bench

The heat exchanger was installed on a test bench to characterize its heat exchange as well as the pressure drops on the air and coolant paths (Figure IV-2).

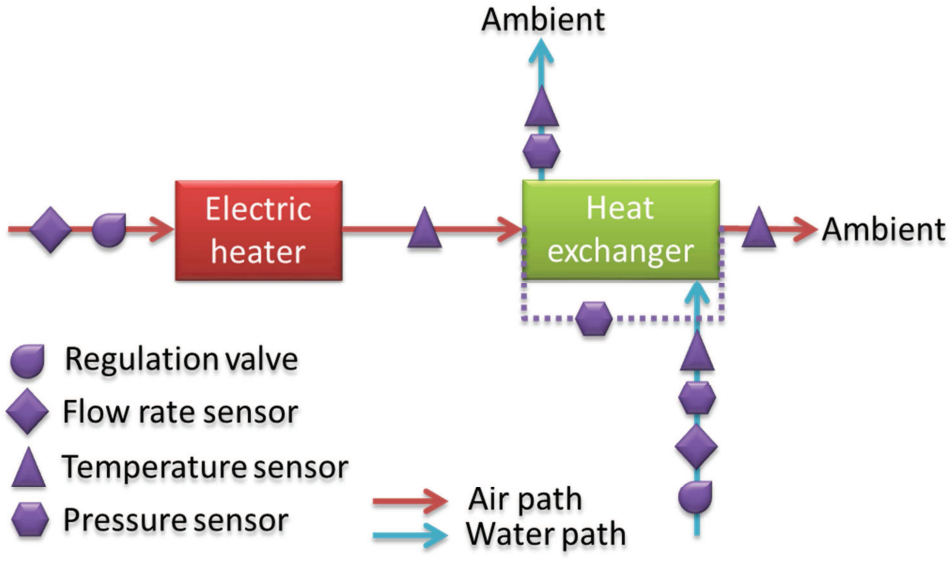

Figure IV-2 Schematic presentation of the heat exchanger test bench

The inlet air mass flow rate of the heat exchanger was controlled by an electro-valve (SCHUBERT & SALZER PSL204AMS) downstream the flow rate meter of type OPTISWIRL 4070C. Then, the air is heated by an electric heater allowing controlling its temperature. Downstream the electric heater, the heat exchanger took place. The outlet of the exchanger is connected to the ambient air. Air inlet and outlet temperatures were registered

using K-type thermocouples. A HCX001 D6V differential pressure sensor is installed between air inlet and outlet to measure its pressure drop.

A variable area flow meter H250 M40 is used for the coolant mass flow rate measurements. An ambient coolant source was used to cool down the hot air. Water inlet and outlet temperatures were also measured using K-type thermocouples. Water inlet and outlet pressures were measured using OPTIBAR P 1010C sensors. Afterwards, the water flows to the ambient. The test bench as well as the heat exchanger and its sensors are shown in Figure IV-3. Water was connected to the exchanger in a way to have a counter flow heat exchanger type.

The acquisition devices were “National Instrument 9205 cDAQ” for the pressure and the flow rate and “National Instrument 9213 cDAQ” for the temperature. Results were registered using LabView software. Different sensors characteristics are presented in Table IV-1.

Figure IV-3 Heat exchanger test bench

Table IV-1 Sensors characteristics

Sensor	Calibrated range	Accuracy
Air and Coolant temperature (K-type thermocouple)	0-1000 °C	± 1°C
Air differential pressure (HCX001 D6V)	0 – 1bar	± 1.5%
Coolant pressure (Khrone Optibar P 1010 C high temperature)	0-2.5 bar	± 0.25%
Coolant mass flow rate (Khrone H250)	6-60 l/min	± 1.6%
Air mass flow rate Vortex Optiswirl 4070C	$10^4 < Re < 2*10^4$ $Re \geq 2*10^4$	± 2.5% m ± 1.5% m

Hence, this test bench gives the possibility to regulate different parameters:

- Intake air temperature.
- Air flow rate.
- Water flow rate.

Various steady state points were registered. The tests were done as following: for each of the four water flow rates, the air temperature was varied over three values. For each air temperature, the air mass flow rate was varied over 8 values. Thus, 94 points were registered (Figure IV-4). Water inlet was at around 16°C. The different operating points were chosen based on the previous simulations of the different driving cycles to cover the operating range of the heat exchanger in terms of flow rate and exhaust gas temperature. Tests covered beyond these ranges to prevent the extrapolation for unexpected behavior.

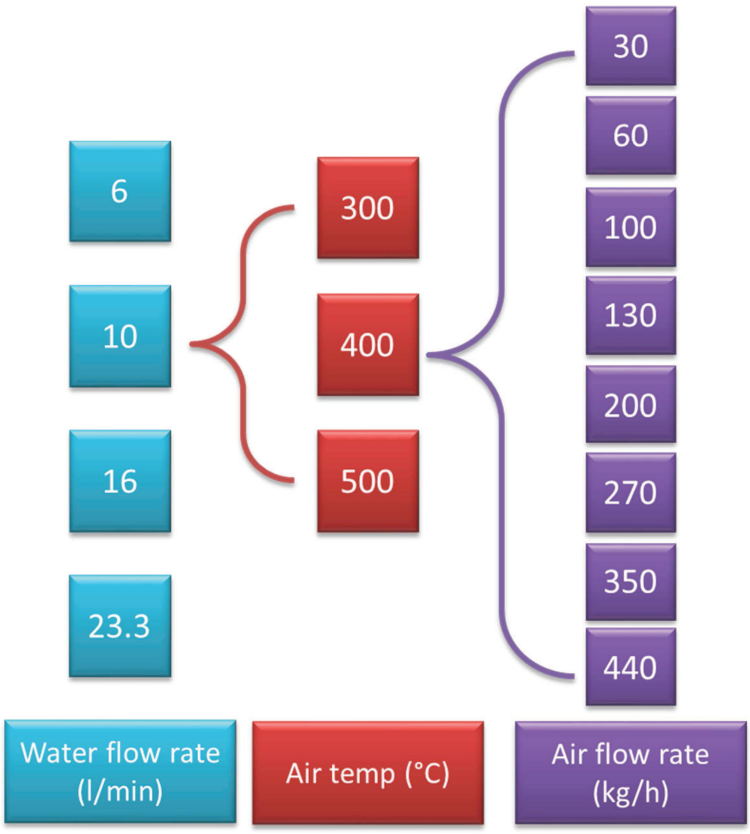

Figure IV-4 Heat exchanger data points

Heat rate between the two fluids was calculated based on the experimental results using equation (II-5). The heat rate exchanged between the two fluids varied from 2 kW to around 48 kW depending on the different main parameters, the air and water mass flow rate and the air intake temperature. The three graphs in Figure IV-5 show the different range of heat rate over the different tested points. The data point “air mass flow rate: 440 kg/h, coolant mass flow rate: 6 l/min and an air intake temperature of 500°C” was not registered because the water rose up to temperature higher than 95°C. Coherent results were obtained as the heat rate increased with the air mass flow rate as well as with the coolant mass flow rate as seen in the different plots in Figure IV-5. The heat exchanger efficiency was highest with the lowest air mass flow rate, and ranged between around 0.75 and almost 1 (Figure IV-6). Three experimental points showed a drop in the heat exchanger efficiency to 0.5. They are within the lowest coolant flow rate 6 l/min for the highest air intake temperature and highest air mass flow rate.

(a)

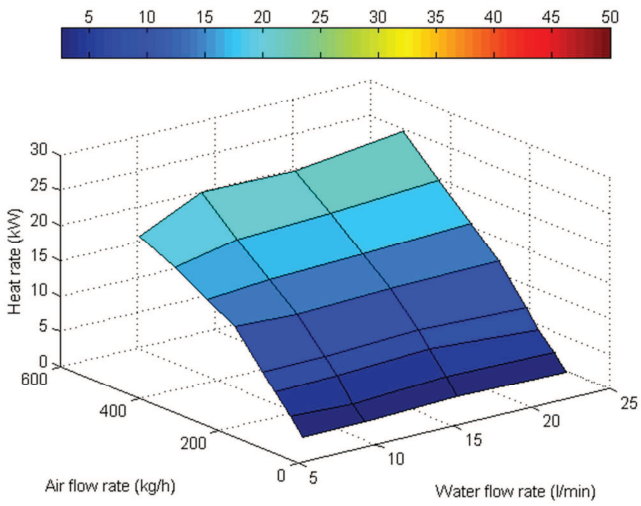

(b)

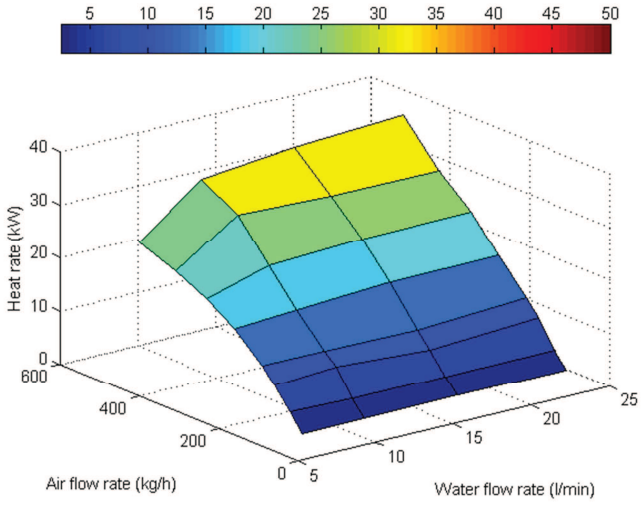

(c)

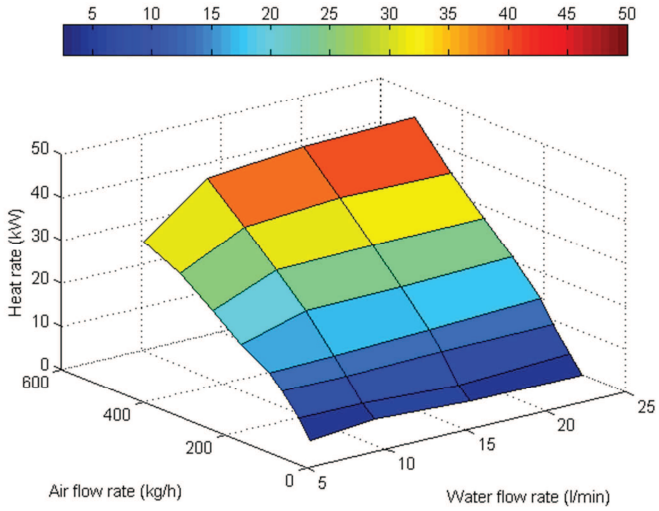

Figure IV-5 Heat rate between the two fluids at the heat exchanger with an intake air temperature (a): 300°C, (b): 400°C and (c): 500°C

(a)

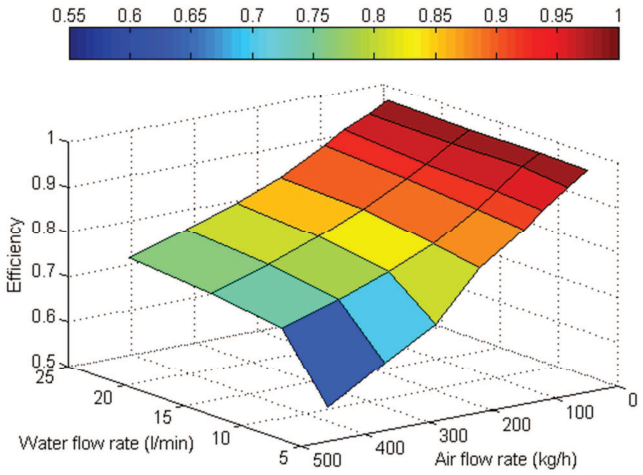

(b)

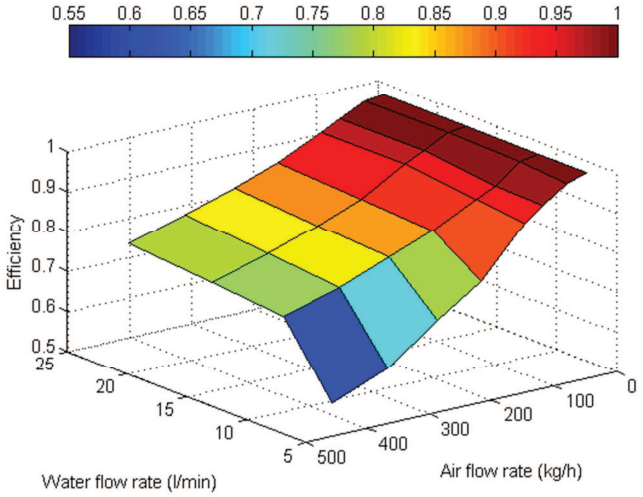

(c)

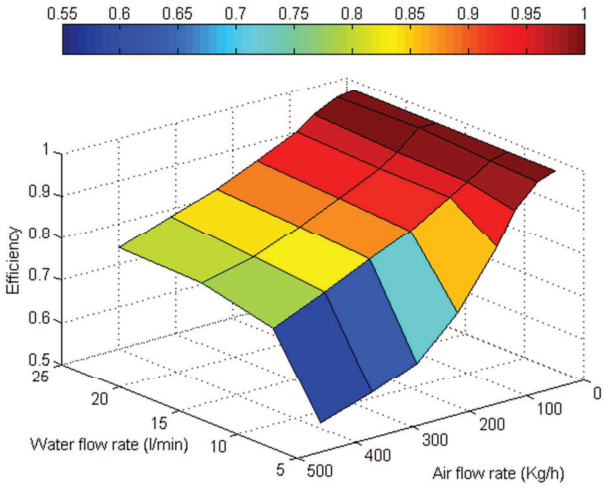

Figure IV-6 Heat exchanger efficency with an intake air temperature (a): 300°C, (b): 400°C and (c): 500°C

Figure IV-7 depicts the air pressure drop in the heat exchanger. It is minimal at the lowest flow rate of a value of around 4 mbar and rises to around 430 mbar at 440 kg/h. The values depicted in the plot are the average of the different 94 points registered during the tests.

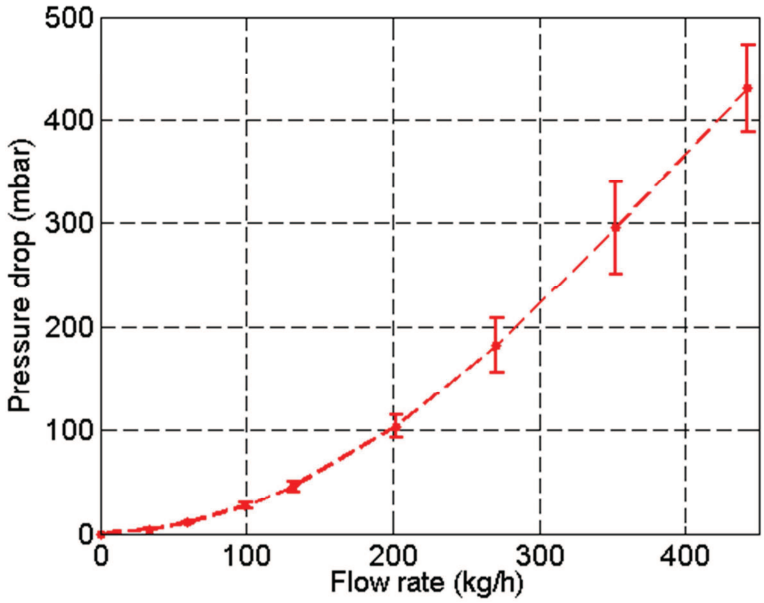

Figure IV-7 Air pressure drop in function of its flow rate

Because of outlet pressure sensor difficulties, water pressure drops tests were done in a different setup as presented in Figure IV-8. The water flow meter and the pressure inlet sensor were the same as the one used in the first setup. The water outlet of the heat exchanger was connected directly to the ambient air preventing any back pressure at the outlet. Water flow rate covered the same ranges as the first setup. However, more points were registered during the test. The pressure drop curve of the water path is presented in Figure IV-9. Pressure drop varied from the lowest values and increased with the flow rate to the maximum of 109.5 mbar at a flow rate of 24.2 l/min.

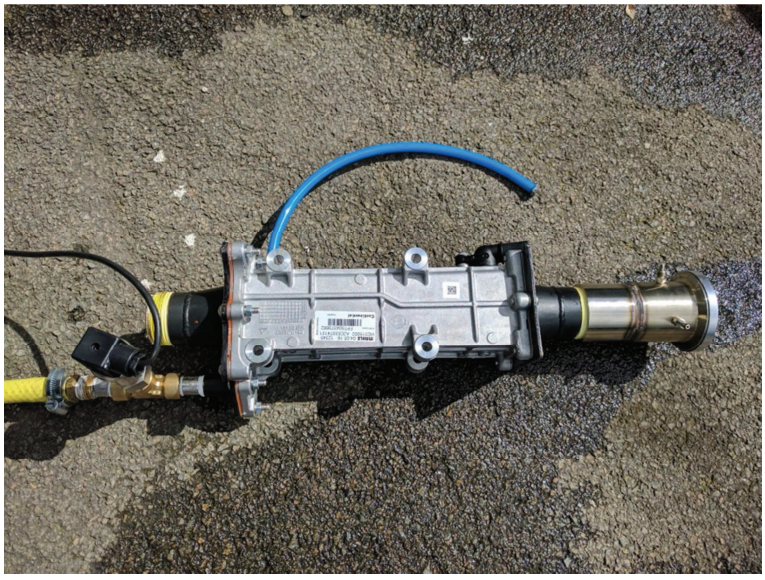

Figure IV-8 Water pressure drop measurements

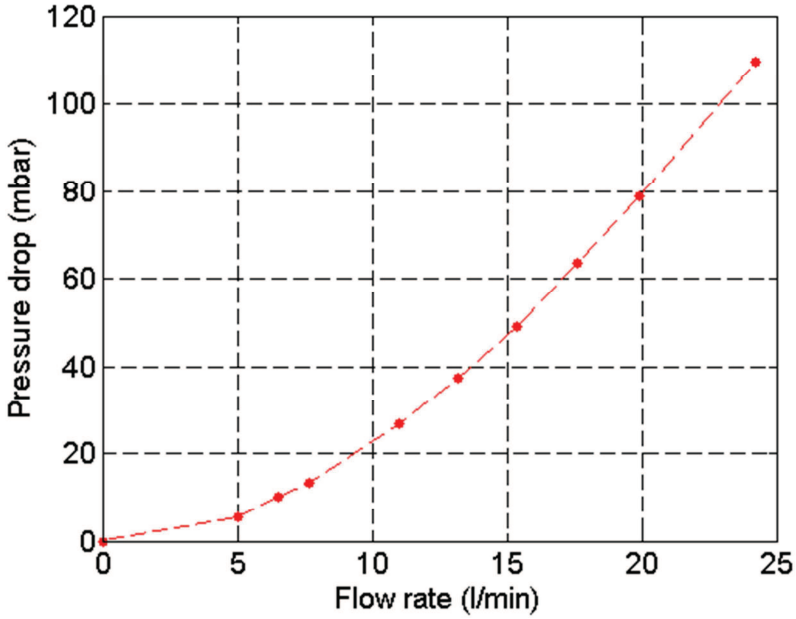

Figure IV-9 Water pressure drop in function of its flow rate

IV.2. Heat exchanger modeling

The exhaust heat exchanger is modeled as the others heat exchangers in GT-Suite software. The Master – Slave notice is used (refer to section II.2.3). The geometrical characteristics were measured and entered in the model. It was supposed that the heat exchanger is iron cast and weights 3 kg. The master fluid is considered hot air during calibration and thus the slave fluid was water. Flow rates were imposed during calibration as well as the inlet temperature and pressure of each fluid. As mentioned before, the heat exchanger is considered of counter-flow type. The outlet of the heat exchanger on both sides: air and water is connected to ambient conditions. Pressure drops were easily calibrated and agreed almost perfectly with the experiments.

The calibration of the thermal behavior took place over 4-5 points in first place, where heat transfer area was varied to have the better agreement with the outlet. Outlet temperatures for the water and the air were examined at the end of the simulations. Then, the 94 data points were tested on the heat exchanger model, imposing the same conditions as the experimental setup. Calibrations were done in a way to have the minimum error on the water side as it is more important during the following study. The increase of its temperature is one of the important thermal behaviors of the engine. However, the error on the air side was of lesser importance as the air exiting the exchanger will be then evacuated to the ambient air and would not influence any behavior of the engine that can affect the results of the study. Over 94 data points, the average error of the outlet water temperature was 1.6°C, while the error of the outlet air temperature was averaged by 7.5°C.

Once the heat exchanger model was calibrated, it was added to the existing model. It was installed on the exhaust line downstream the turbine and the catalyst.

IV.3. Exhaust/coolant heat exchanger

Engine fluids: the coolant and the lubricant are the primordial actors in the engine thermal behavior and efficiency. Based on the energy balance done in section II.4.2, the exhaust gases are one of the main losses of the engine. The state of art study highlights also the potential of exhaust gases heat recovery.

At first an application on the engine's coolant will be tested. As mentioned before, to not influence the catalyst light-off time, the exhaust gas heat exchanger was placed downstream the catalyst. On the coolant side, the heat exchanger was installed on a new branch upstream the thermostat as it is depicted in the Figure IV-10.

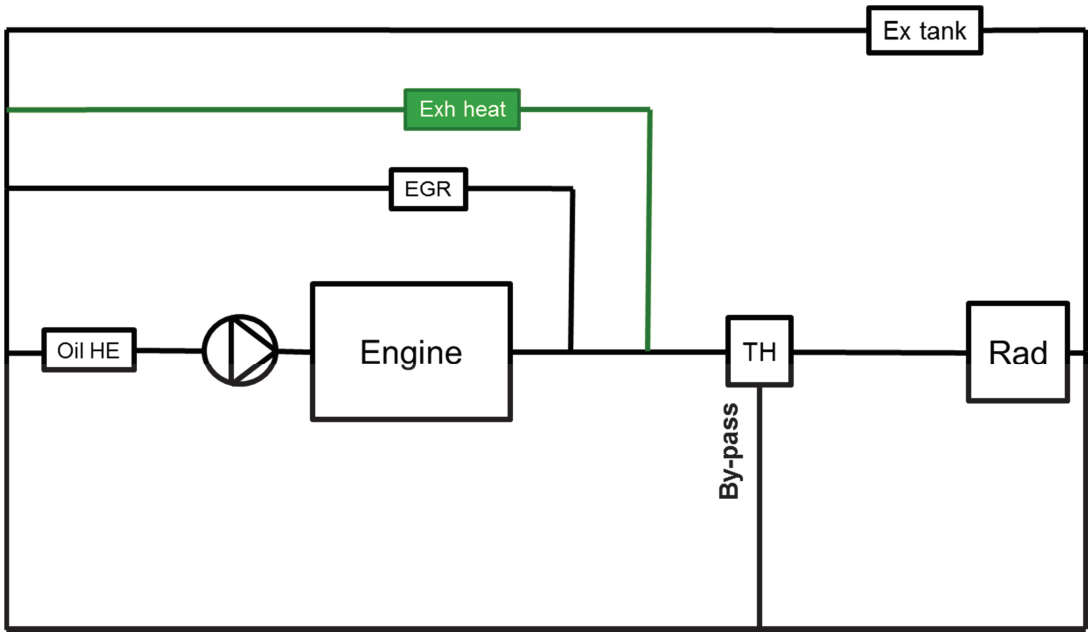

Figure IV-10 A schematic presentation of the exhaust gas heat recovery strategy applied on the coolant circuit (Exh heat: Exhaust heat exchanger; TH: Thermostat; Oil HE: Oil heat exchanger; Ex tank: Expansion tank; Rad: Radiator)

The exhaust gas cooler line was not controlled during the simulations. However, an application with a modern multi-way valve controlling all the different branches: EGR cooler and the cabin heater, and the exhaust gas cooler can be proposed.

IV.3.1 Application

The exhaust gas heat recovery by an exhaust/coolant heat exchanger will be applied on the different driving cycles defined in section II.3 at two different ambient temperatures: 20°C and -7°C.

IV.3.1.1. NEDC

The main results of running numerical simulations over NEDC at both ambient temperatures are represented in Figure IV-11. The reference (ref) depicted in each plots of Figure IV-11, represent the case with the engine simulated without any thermal management strategy. The improvement in the temperature profiles of either the coolant or the lubricant is well remarkable with this thermal management strategy.

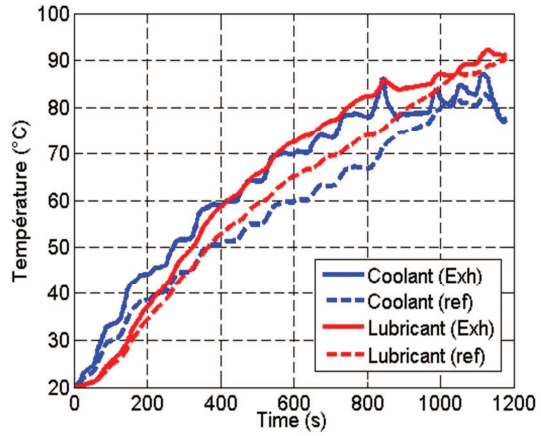

(a): Temperature profile at 20°C

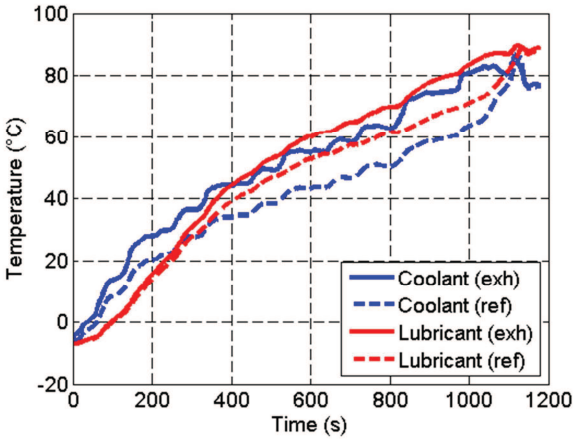

(b): Temperature profile at -7°C

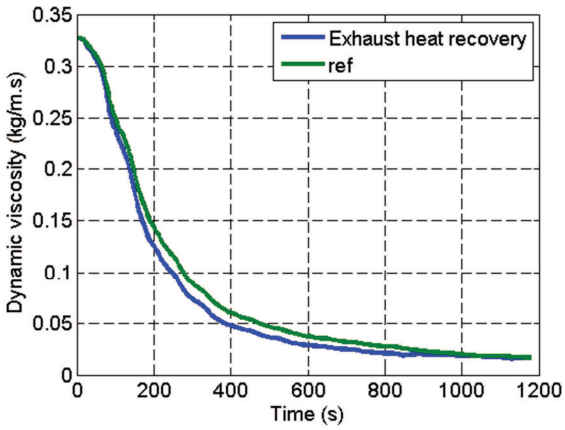

(c): Viscosity profile at 20°C

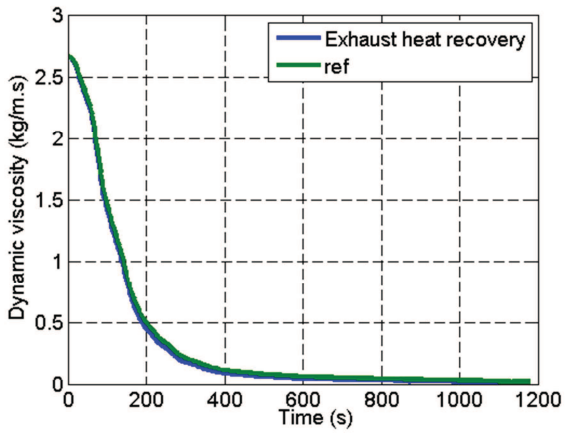

(d): Viscosity profile at -7°C

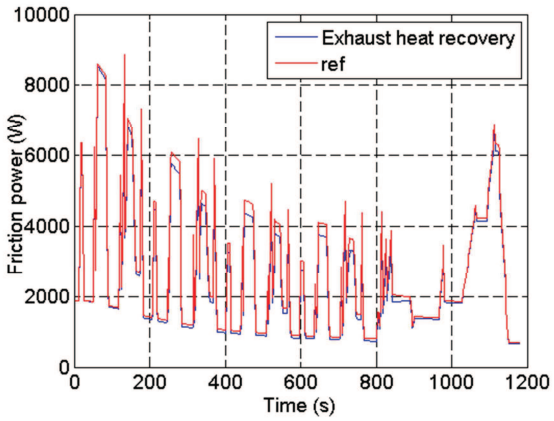

(e): Friction power at 20°C

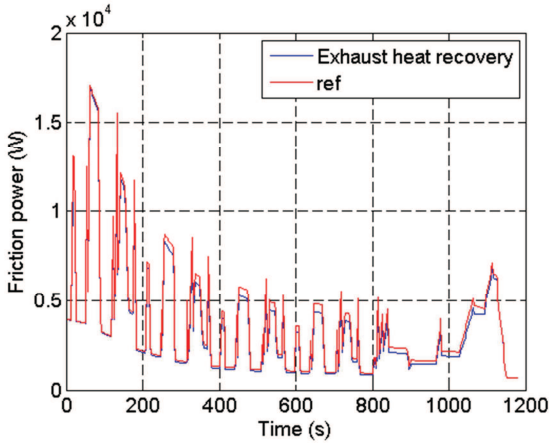

(f): Friction power at -7°C

Figure IV-11 Exhaust heat recovery results over NEDC at both ambient temperatures

At an ambient temperature of 20°C, the coolant temperature profile shows an advance that increased all along the driving cycle (Figure IV-11 (a)). The heat exchange with the exhaust gases is not controlled during this strategy. At the start of the engine, coolant is directly flown into the exhaust gas heat exchanger branch. An advance of 161s to reach the temperature of

the coolant of 60°C, and an advance of 212s to reach the regulation temperature are obtained with the exhaust gas heat recovery directly to the coolant. The regulation temperature of 83°C was reached first time at around 833s where the thermostat opens up the radiator branch. With this modification, the coolant shows a small drop in the temperature to under the optimal one, to reach it for a second time around 981s. The lubricant temperature increases quickly with the new thermal management applied. Although, the reaction of the lubricant to the extra heat of the system started later than the coolant, different advances were noticed for its profile. The lubricant's warm-up procedure is considered indirect with the coolant as a medium. The heat transmitted to the coolant from the exhaust gases led to a bigger difference in the two fluids temperature than during the traditional configuration. The lubricant reaches 60°C in 101 seconds faster than the reference case, and reaches 80°C with an advance of 166s. During the first 400s of the driving cycle, the coolant temperature was higher than the lubricant. After that, the lubricant took the lead. After 400s, the lubricant was not getting any heat from the exhaust gases, but it was cooled down by the coolant. Once the engine's temperature was reached and the thermostat opens the radiator branch, heat transmitted to the coolant is evacuated to the ambient via the radiator. The lubricant temperature showed a softer slope once the peak of the coolant temperature is reached (Figure IV-11 (a)) and it is brought closer to the reference line. The improvement in the lubricant temperature profile leads to an improvement in the lubricant's viscosity (Figure IV-11 (c)) thus the friction losses of the engine (Figure IV-11 (e)). Heating the lubricant indirectly through the coolant does not lead to avoid the high viscosity areas of the lubricant. However, the cumulative dynamic viscosity of the lubricant over the whole driving cycle was reduced by 10.6% leading friction losses decrease by around 4.9%. The benefits of this thermal management strategy over NEDC can be seen by a reduction of fuel consumption around 1.39% at an ambient temperature of 20°C.

At an ambient temperature of -7°C, the same behavior of all the profiles took place. The coolant temperature showed an advance of 240s in reaching 60°C, and an advance of 71s in reaching the regulation temperature (Figure IV-11 (b)). The lubricant showed 172s advance at 60°C and an advance of 135s at 80°C. The lubricant viscosity (Figure IV-11 (d)) did not show the huge difference as seen at 20°C. However, the improvement of lubricant's viscosity at low temperature, thus at high level can be seen in assessing the friction losses (Figure IV-11 (f)). Therefore, over NEDC at an ambient temperature of -7°C, the frictions losses were reduced by 5.9% and the fuel consumption savings were assessed to be 2.31%.

Heat transfer rate at the heat exchanger at both ambient temperatures are illustrated in Figure IV-12. The ambient temperature does not only influence the coolant side of the heat exchanger but also the air side. As the exhaust gas temperature are dependent of the combustion process and its efficiency. At low temperatures, the efficiency is decreased as well as the exhaust gas temperature. However, the instant heat rate during the driving cycle ranged between 0.8 kW to around 25 kW at the high operating points. At the end of NEDC, during the high extra speed part, the engine is running at high rotational speed leading to higher speed of the coolant pump and thus higher flow rate in the heat exchanger. The same behavior will be expected at the air path, with increasing the torque and the rotational engine speed, the air mass flow rate will be increased in the exhaust line.

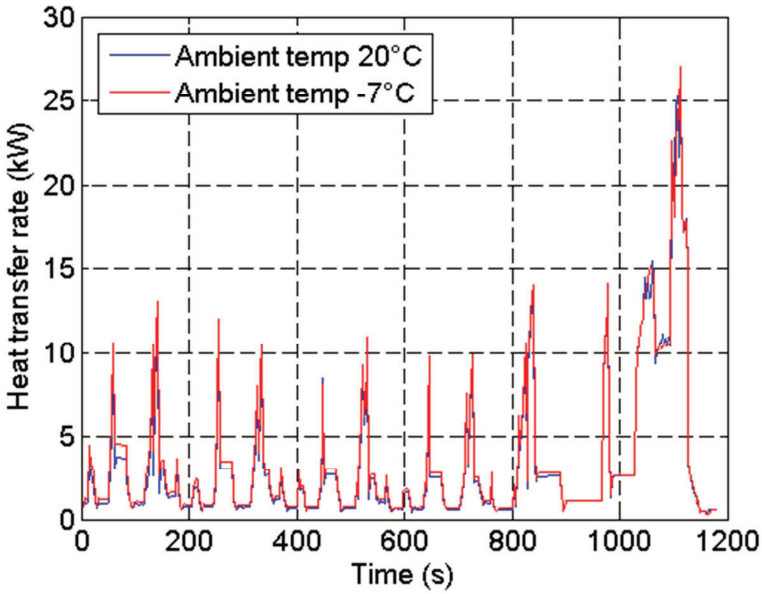

Figure IV-12 Heat transfer rate at the heat exchanger over NEDC at both ambient temperatures

The heat exchanger located on the exhaust line with its pressure drop on the air side creates a back pressure on the engine and it will prevent the latter to reach its high power at the same conditions. However, a bypass of the heat exchanger on the exhaust line can be proposed. The bypass can be functional when the coolant reaches the regulation temperature.

A study over NEDC to evaluate the effect of the pressure drop of the heat exchanger on the fuel consumption was made. The study consists of two simulations with the pressure drops of the heat exchanger at the air side reduced by half in one and set to zero in the other. Air pressure drop profiles used are presented in Figure IV-13.

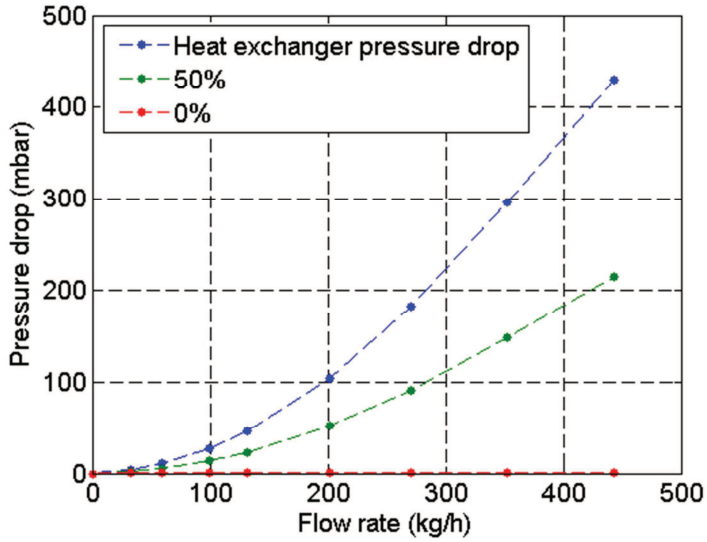

Figure IV-13 Different level of pressure drops

The coolant temperature profile, as well as the lubricant, did not show any significant changes to the one with the exhaust gas exchanger with a full pressure drop. However, the fuel consumption savings were increased. At an ambient temperature of 20°C, and for the same

heat exchanger but with a pressure drop half the original value, the fuel consumption benefits in comparison to the reference case were valued to 1.4% and 1.48% for a heat exchanger without pressure drop. Fuel consumption savings increased by 6.5% compared to the initial exhaust gas heat recovery.

IV.3.1.2. WLTC

Running the exhaust gas heat recovery thermal management strategy over WLTC gave the results depicted in Figure IV-14. Similar to NEDC, the improvement in the temperature profile is easily remarkable on the different graphs.

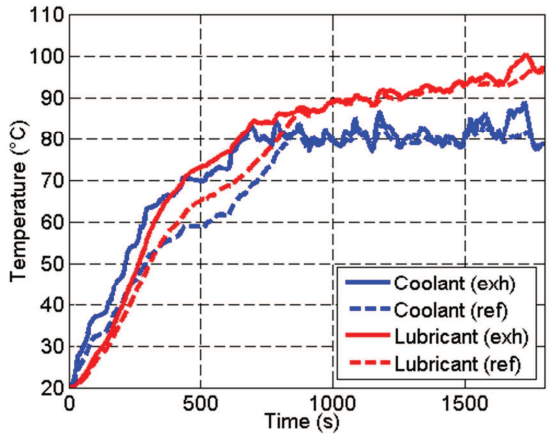

(a): Temperature profile at 20°C

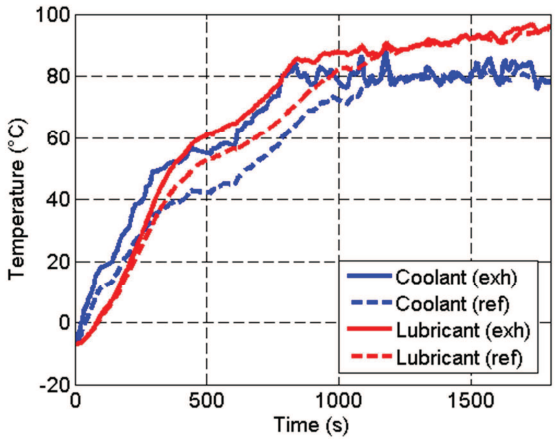

(b): Temperature profile at -7°C

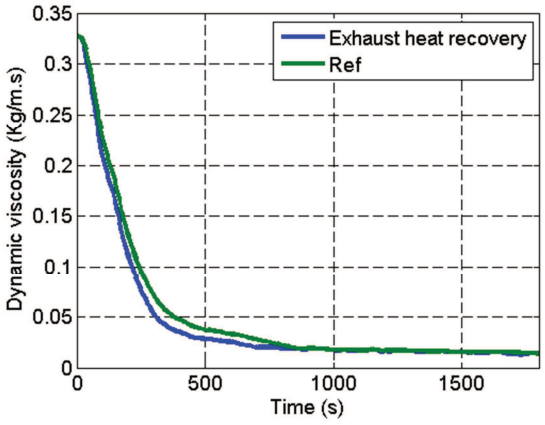

(c): Viscosity profile at 20°C

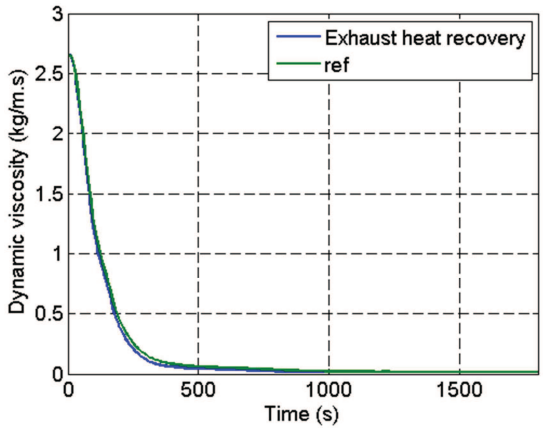

(d): Viscosity profile at -7°C

Figure IV-14 Exhaust gas recovery results over WLTC at both ambient temperatures

The coolant temperature profiles rise quickly in case of the thermal management strategy applied than in the reference case. Increasing the coolant temperature will lead to a higher heat exchange with the lubricant in the part of the cycle where the coolant temperature is higher than the lubricant. The engine's regulation temperature is reached earlier with the heat recovery from the exhaust gases. The lubricant temperature profile shows a faster warm-up rate with the strategy applied. The improvement in the lubricant profile is shown with the viscosity evolution.

At an ambient temperature of 20°C, the coolant reaches 60°C with an advance of 254s, and then reaches the regulation temperature with an advance of 176s. The lubricant temperature reaches 60°C after 326s with the strategy applied, faster in 92s than the reference case. As for 80°C, the lubricant reaches it with a lead of 145s (Figure IV-14 (a)). This advance in the lubricant temperature leads to improve the friction power resulting from lower lubricant's viscosity. The latter represented by Figure IV-14 (c) underlines the difference between both studied cases where the difference in both lines is highlighted at an ambient temperature of 20°C because the range of the viscosity is smaller than at an ambient temperature of -7°C. The difference in the plots of the viscosity agrees with the lubricant temperature profile where it exists only almost for the first half of the driving cycle. Furthermore, it can be noticed at the end of the driving cycle, the lubricant and the coolant profiles show a difference with the reference. During this phase, the vehicle speed increases from almost a 0 km/h to a 125 km/h. The friction losses at the end of the driving cycle were reduced by 3.7% and the fuel consumption savings were assessed by 1.7%.

At an ambient temperature of -7°C, the effects of the strategy will be more valuable because the transient stage of the engine is longer. As seen in Figure IV-14 (b), the coolant and the lubricant reach 60°C with an advance of 172s and 208s respectively. The coolant reaches its regulation temperature at 834s with the strategy applied saving 348s from the reference case. The lubricant reaches 80°C with an advance of 181s. The viscosity plot in Figure IV-14 (d) does not highlight the difference of the two strategies because of the big range; it varies between 2.5 and 0.02 kg/m/s. However, the small difference of the viscosity at lowest temperatures has a bigger influence than a bigger difference at a high temperature. The friction losses were reduced by 7.4% using the exhaust gas recovery strategy. An assessment of the fuel consumption gives a reduction of 3.3%.

To compare with NEDC, the heat exchanger highest transfer rate during WLTC reaches around 29 kW.

IV.3.1.3. Artemis Highway

AH is a representative of a highway driving cycle. The engine operates under high load early in the driving cycle. The regulation temperature, as stated before, is reached almost in the first quarter of the cycle. With the strategy applied and as shown in Figure IV-15 (a) and (b) the regulation temperature is reached even earlier in the driving cycle.

At an ambient temperature of 20°C (Figure IV-15 (a)), the coolant temperature reaches 60°C with an advance of 48s and the regulation temperature with an advance of 82s. The lubricant temperature profile showed an improvement too. It reaches 60°C and 80°C with an advance of 37s and 28s respectively. The coolant temperature showed a rise to around 90°C before it decreases after the thermostat opens. During the steady-state stage, it can be shown that the engine operates at a higher temperature. The lubricant temperature is higher than the reference case contrary to the previous driving cycles. This difference in the regulation temperature can be referred to the size of the radiator. It is not able to release all the heat necessary to the ambient temperature to maintain the regulation temperature fixed for the reference case. This is why it is important to add a control system to by-pass the heat exchanger when the regulation temperature is reached. This temperature difference during the steady state stage is not observed at an ambient temperature of -7°C in Figure IV-15 (b). It is due to, at lower

ambient temperature, the temperature difference with the coolant at the radiator is higher, thus leading to a higher transfer to the ambient.

At an ambient temperature of -7°C, the coolant reaches 60°C and its regulation temperature with an advance of 78s and 96s respectively. The lubricant shows a faster rate of warm-up too. It reaches 60°C and 80°C faster by 43s.

The lubricant temperature during the transient stage of the engine stays lower than the coolant. Friction losses were reduced by 4.9% and 5% at an ambient temperature of 20°C and -7°C respectively. Fuel consumption savings were 1% and 0.76% at 20°C and -7°C respectively. Engine running at a higher temperature during the steady state stage may be behind the better fuel consumption benefits at 20°C.

The heat rate at the exhaust gas heat exchanger hits its peak of 43 kW around 240s of the driving cycle and it has as average of 20 kW between 200s and 500s (Figure IV-15 (c)).

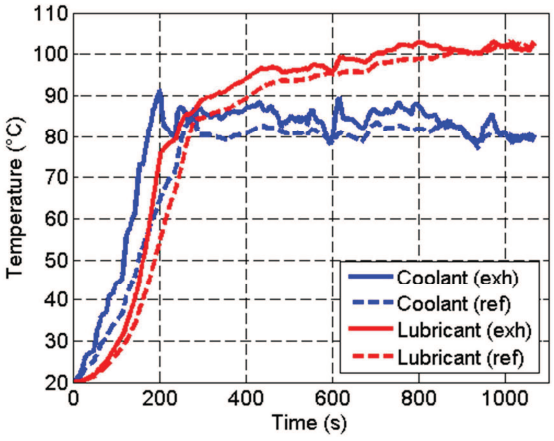

(a): Temperature profile at 20°C

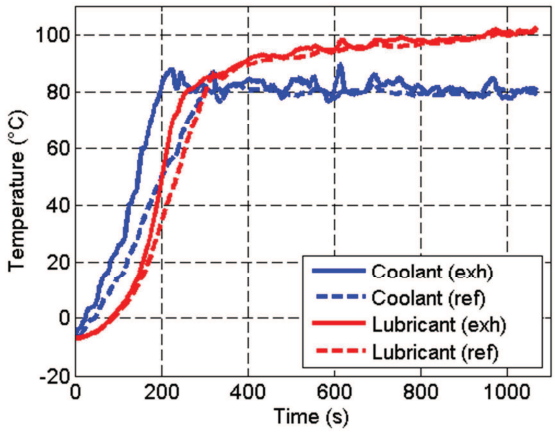

(b): Temperature profile at -7°C

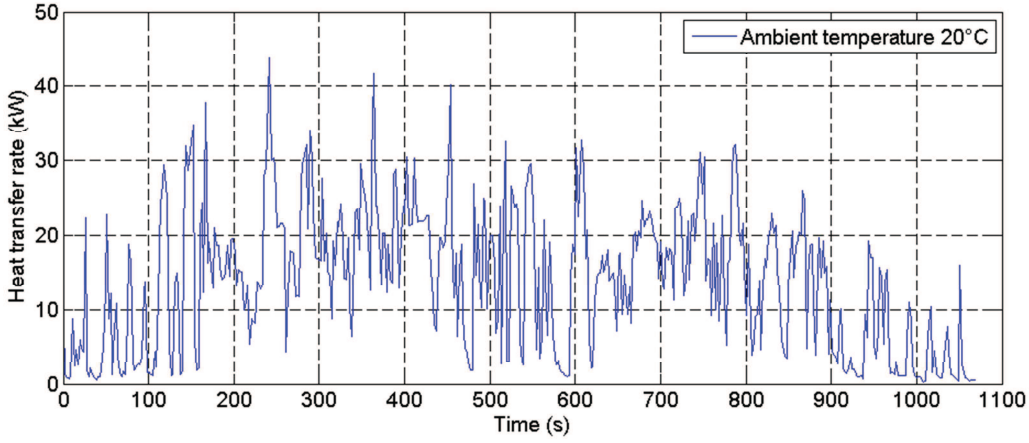

(c): Heat transfer rate of the exhaust gas heat exchanger at 20°C

Figure IV-15 Exhaust gas recovery results over AH at both ambient temperatures

IV.3.1.4. Artemis Urban

Numerical simulations over AU were run and the results are depicted in Figure IV-16. With the heat exchanger at the exhaust line, the engine reaches its regulation temperature at an ambient temperature of 20°C for the first time in the different strategies applied in this work. At an ambient temperature of -7°C, the regulation temperature was almost reached at the end of the cycle.

With AU, the warm-up stage of the engine is highlighted as well as the different improvements. As seen in Figure IV-16 (a), at an ambient temperature of 20°C, the coolant temperature reaches 60°C with an advance 130s. Then, it reaches the regulation temperature around 566s of the driving cycle. Contrary to that, in the reference case, the engine stayed in transient conditions during all the driving cycle. The lubricant temperature showed a faster warm-up profile, 60°C is reached in an advance of 84s and 80°C is reached in advance of 426s. The friction losses were reduced by 7.7% and the fuel consumption benefits rises to 2.5% at an ambient temperature of 20°C at the end of the driving cycle.

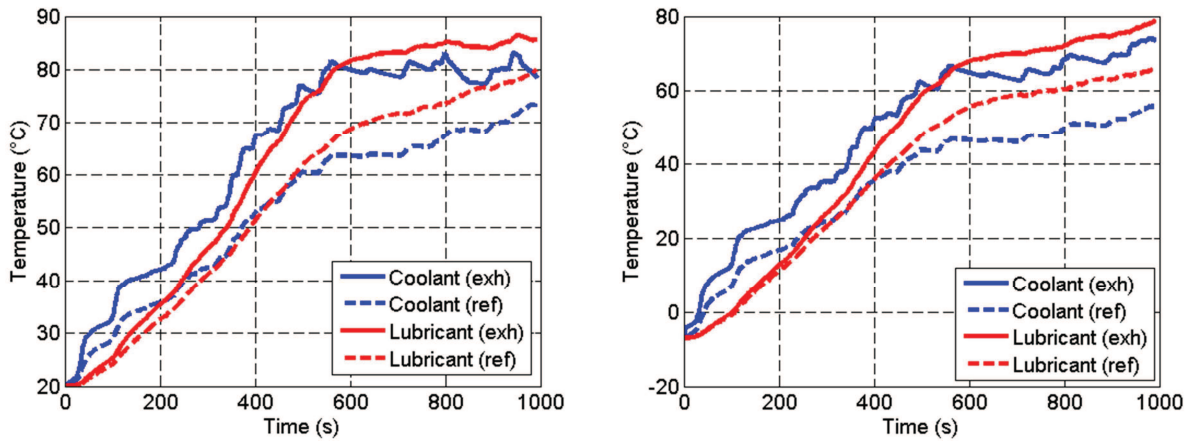

(a): Temperature profile at 20°C (b): Temperature profile at -7°C

Figure IV-16 Exhaust gas recovery temperature profiles over AU at both ambient temperatures

At an ambient temperature of -7°C (Figure IV-16 (b)), the coolant temperature reaches 60°C at 489s with the strategy applied. The reference case highest temperature at the end of the cycle was 55.5°C. The coolant temperature reaches 73.5°C at the end of the driving cycle marking a difference of 18°C with the reference case. The lubricant temperature reaches 60°C in an advance of 270s. However, 80°C was not reached by the lubricant at the end of the cycle for the two cases. The fuel consumption was reduced by 3.86% at an ambient temperature of -7°C.

With the strategy applied, the temperature of the lubricant stays lower than the coolant for a longer time than the reference case, leading to higher rate of heat loss from the coolant to the lubricant circuit.

IV.3.1.5. In-House developed Driving Cycle

The results issued from applying the exhaust heat recovery over HDC at two different ambient temperatures is illustrated in Figure IV-17.

Despite that the temperature profiles shows a very good improvement, the engine did not reach its regulation temperature at the end of the driving cycle at both ambient temperatures. At an ambient temperature of 20°C (Figure IV-17 (a)), the coolant reaches 60°C at 149s. However, this temperature was not reached with the reference case. At the end of HDC, the coolant reaches 71.3°C with the strategy applied, with a difference of 15.4°C with the reference case. The lubricant temperature exceeded 60°C with the new strategy at 205s, and ended the cycle with a temperature of 67°C higher by 12.2°C than the reference case.

The part (b) of Figure IV-17 depicts the temperature profiles at an ambient temperature of -7°C. The coolant and lubricant temperature did not reach 60°C with neither both strategies. At the end of the driving cycle, the coolant reaches 57°C, while the lubricant reaches 47°C with the strategy applied. The two fluids end with a temperature higher than the reference case. The difference is about 19°C for the coolant and 10°C for the lubricant. During both ambient temperatures, the lubricant temperature stayed lower than the coolant's. Heat transfer always occurred from the coolant to the lubricant, thus an indirect heating of the lubricant from the exhaust gases by the medium of the coolant.

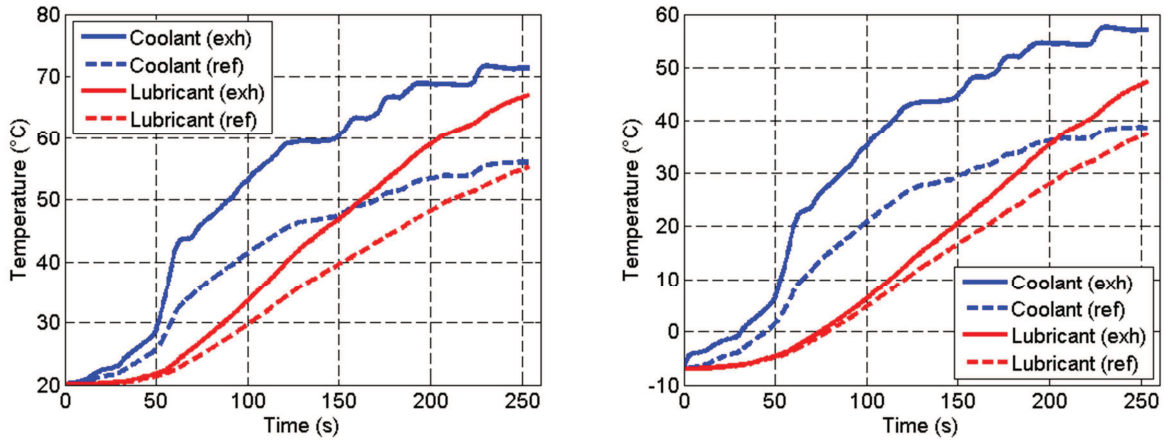

(a): Temperature profile at 20°C (b): Temperature profile at -7°C

Figure IV-17 Exhaust gas recovery temperature profiles over HDC at both ambient temperatures

Fuel consumption evaluation at an ambient temperature of 20°C gives benefits of 1.76%. At an ambient temperature of -7°C, the benefit rises to 1.89%.

Table IV-2 summarizes the different fuel consumption savings by applying the exhaust gas heat recovery. The biggest benefits are within Artemis Urban, the only cycle with the hugest modification. By applying the exhaust gas heat recovery, the engine during the Artemis urban reached the regulation temperature while it was under transient state in the reference case.

Table IV-2 Fuel consumption savings by applying the exhaust gas recovery strategy

Driving cycle	20°C	-7°C
NEDC	1.39%	2.31%
WLTC	1.69%	3.34%
AH cycle	1.02%	0.76%
AU cycle	2.46%	3.86%
HDC	1.76%	1.89%

Table IV-3 represents the different warm-up time savings for the different driving cycles at different ambient temperatures. $\Delta t_{coolant,T_i}$ displays the advance in time to reach the "$coolant$" temperature T_i, or the regulation temperature opt, obtained by applying the thermal management strategy. $\Delta t_{lubricant,T_i}$ is the advance in time obtained to attend the "$lubricant$" temperature T_i. The "-" in the table means that the temperature in demand is not reached in one of the two cases either the reference or with the strategy applied.

Table IV-3 Warm-up time savings (in seconds) for different cycles and ambient temperatures

Ambient temperature		NEDC	WLTC	AH	AU	HDC
20°C	$\Delta t_{coolant,60}$	161	254	48	130	-
	$\Delta t_{coolant,opt}$	212	176	82	-	-
-7°C	$\Delta t_{coolant,60}$	240	172	78	-	-
	$\Delta t_{coolant,opt}$	71	348	96	-	-
20°C	$\Delta t_{lubricant,60}$	101	92	37	84	-
	$\Delta t_{lubricant,80}$	166	145	28	426	-
-7°C	$\Delta t_{lubricant,60}$	172	208	43	270	-
	$\Delta t_{lubricant,80}$	135	181	43	-	-

During this case, the engine's lubricant was heated indirectly from the exhaust gases by the medium of the coolant. Some of the heat was lost to the coolant circuit and the engine masses. The next step is to test a direct warm-up of the oil by a direct exchange with the exhaust gases.

IV.4. Exhaust/oil heat exchanger

The one of the main losses of the engine is within friction losses that are high at low functioning temperature. With the cold start imposed on the homologated driving cycle, reducing the friction losses is necessary in order to answer the different emission and greenhouse laws.

Exhaust gas heat recovery with a lubricant heat exchanger is tested in this part with two different configurations. In the simulation code, the heat exchanger modeled before is used for this application. The different characteristics inside the heat exchanger stayed the same as it was underlined that these measurements were taken with a water experiment application. Thus, the heat exchanger efficiencies were conserved but the convection coefficients related to the lubricant were changed.

IV.4.1 Application - Configuration A

In configuration A, the exhaust/oil heat exchanger is placed always downstream the catalyst on the exhaust line, to not influence the catalyst take-off time. On the lubricant side, the heat exchanger was placed downstream the oil/coolant cooler and upstream the engine. This placement is chosen to have the better influence of the heat recovery on the friction losses, before losing some energy to the coolant side at the oil cooler.

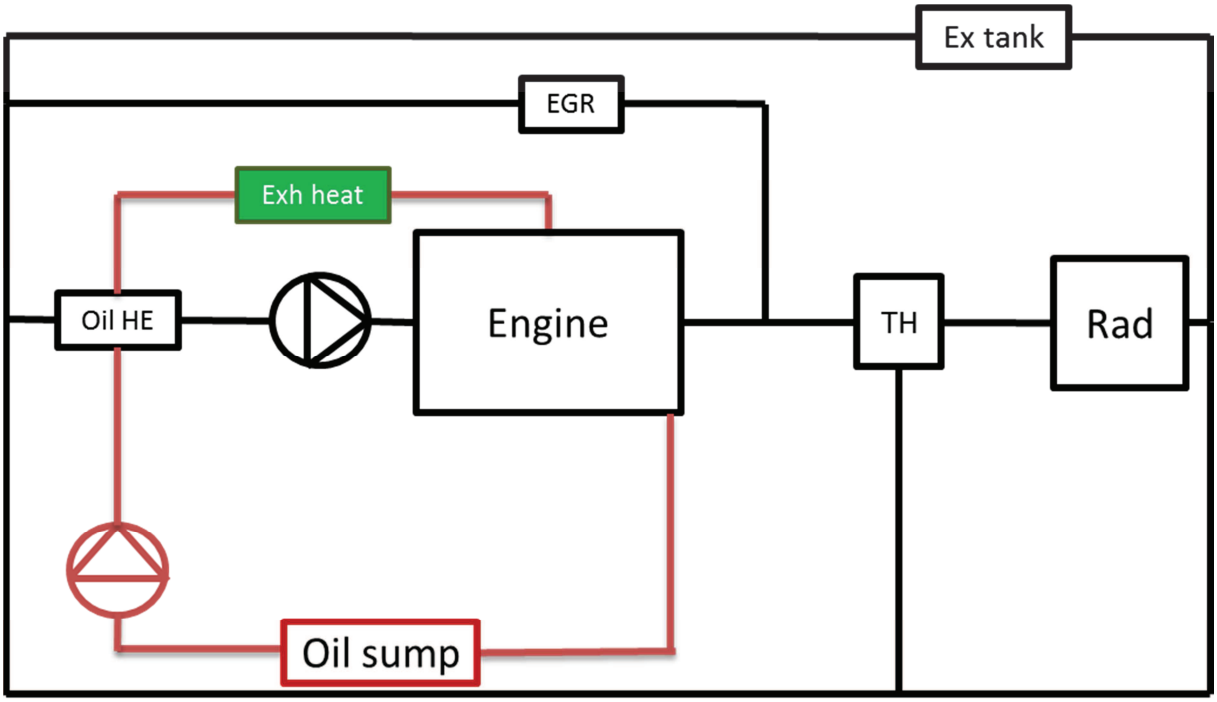

Figure IV-18 A schematic presentation of the exhaust gas heat recovery strategy applied on the oil circuit (Exh heat: Exhaust heat exchanger; TH: Thermostat; Oil HE: Oil heat exchanger; Ex tank: Expansion tank; Rad: Radiator)

The exhaust/oil heat exchanger is not controlled in the study and the heat transfer rate starts with the driving cycle. However, a bypass on the exhaust line can be proposed to prevent an overheating of the engine's lubricant. To have the maximum benefits of the strategy, no control over the lubricant's temperature was done.

The strategy will be applied over the different five driving cycles and at both ambient temperature of 20°C and -7°C.

IV.4.1.1. NEDC

The main results of the simulation over NEDC at different ambient temperatures are presented in Figure IV-20. The reference line in the different plots represents the engine basic configuration without any modification on the coolant or the lubricant circuits. The lubricant temperature profile is remarkably improved by using this strategy.

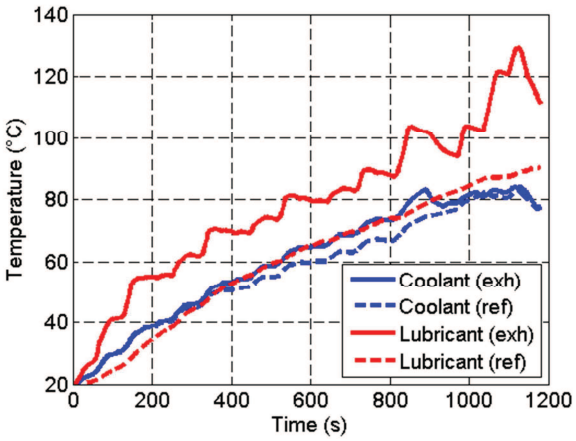

(a): Temperature profile at 20°C

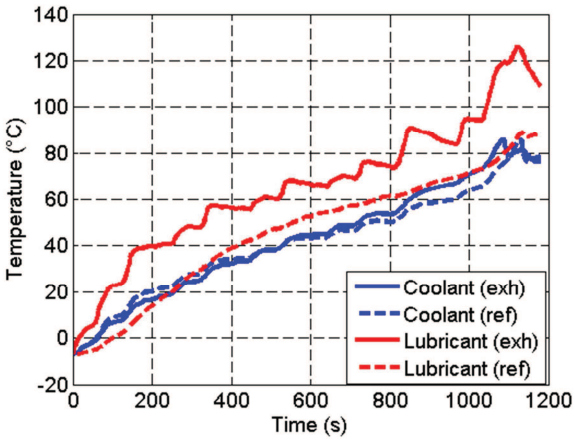

(b): Temperature profile at -7°C

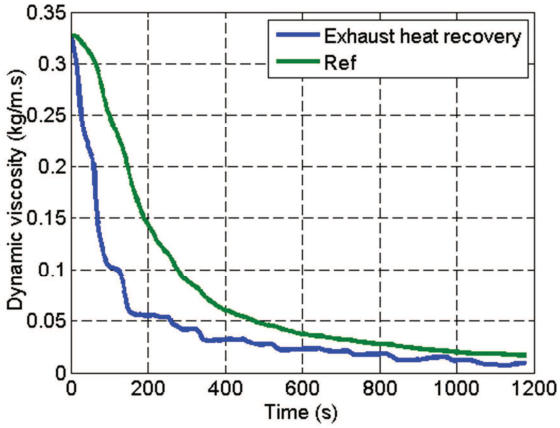

(c): Viscosity profile at 20°C

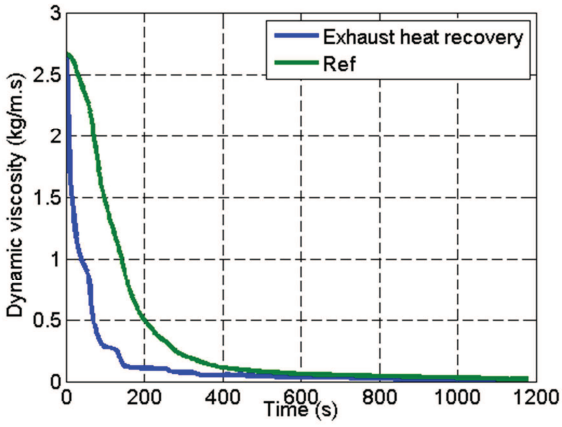

(d): Viscosity profile at -7°C

Figure IV-19 Exhaust gas recovery results over NEDC at both ambient temperatures

At an ambient temperature of 20°C (Figure IV-19 (a)), the coolant temperature profile showed an improvement during NEDC. The improvements are insignificant compared to that of the lubricant profile. The lubricant temperature rises sharply with the start of the driving cycle. It stays higher than the reference case during the whole driving cycle. It can be seen at the end of NEDC, that the lubricant temperature highlights the extra-urban driving conditions where its temperature increases sharply around 1000s. The lubricant temperature peak is 129°C and

is reached at 1120th second of the cycle. The lubricant took the lead over the coolant with the strategy during the driving cycle. Within this application, the oil cooler is a source of heat to the coolant circuit during NEDC. The lubricant temperature reaches 60°C with an advance of 252s and then reaches 80°C with an advance of 376s. The coolant is within this study heated in indirect way by the mean of the lubricant at the oil cooler. The coolant temperature improved remarkably starting 250s. However, a slight difference exists from the first seconds of the driving cycle. The coolant temperature reaches 60°C with an advance of 82s and the regulation temperature with an advance of 155s. Coolant temperature improvement means an improvement in the engine's temperature and thus less wall heat losses in the combustion chamber. Higher engine's lubricant temperature means lower friction losses of the engine. Less wall heat losses will lead to slightly increase the exhaust gas temperature. Higher exhaust gases temperature will lead to higher heat recovery at the heat exchanger and more improvements in the engine friction. Engine friction power reduction is related directly to engine efficiency improvements and thus its fuel consumption. Improving the engine's lubricant temperature is reflected in its viscosity profile (Figure IV-19 (c)). It can be seen even at 20°C, the improvement in the viscosity profile is well present. With the strategy applied, the lubricant viscosity drops enormously with the start of the driving cycle to the point where the viscosity starts converging to a certain value. At 84 s, the difference in viscosity profiles hits a peak with a difference of 0.153 kg/m/s equals to a decrease of 56.8% of its value. However, the highest decrease of the viscosity was at 150s with a reduction of 69.28%. The cumulative integral of the viscosity profile over the driving cycle leads to an improvement by 45.9%. Viscosity improvement will reduce the friction losses as it is shown in Figure IV-20 (a). The blue line representing the friction power with the exhaust heat recovery is almost lower than the red line representing the reference case during all the time in the driving cycle. Over the whole cycle, the friction power was reduced by 20.58%. The highest difference peak was around 150s of the driving cycle with a reduction that reached 33.45%. The fuel consumption benefits at the end of the driving cycle reached 5.53%.

At an ambient temperature of -7°C (Figure IV-19 (b)), the lubricant temperature reaches 60°C with an advance of 295s and 80°C faster in 258s. The coolant temperature reaches 60°C and the regulation temperature with an advance of 109s and 36s respectively. The high lubricant temperature has an effect on the different engine masses and will affect the wall heat losses. Wall heat losses to the coolant circuit are reduced within the strategy applied (Figure IV-21) in a manner that the heat recovered by the coolant at the oil cooler cannot cover its difference. And at an ambient temperature of -7°C, the heat losses to the ambient will be greater than that of 20°C, the coolant temperature profile with less heat input will lead to slightly reduced curve at the beginning of the driving cycle. The improvement in the lubricant temperature is reflected on a decrease in the viscosity profile (Figure IV-19 (d)). The viscosity resulting from applying the exhaust gas heat recovery decreases in a rapid manner to reach a converged value at the end of the driving cycle. The reduction of the viscosity at an ambient temperature of -7°C is much more significant than at 20°C. The cumulative value of the dynamic viscosity is reduced by 63.6%. The hugest reduction in percentage was around 85.8% at 150s of the driving cycle.

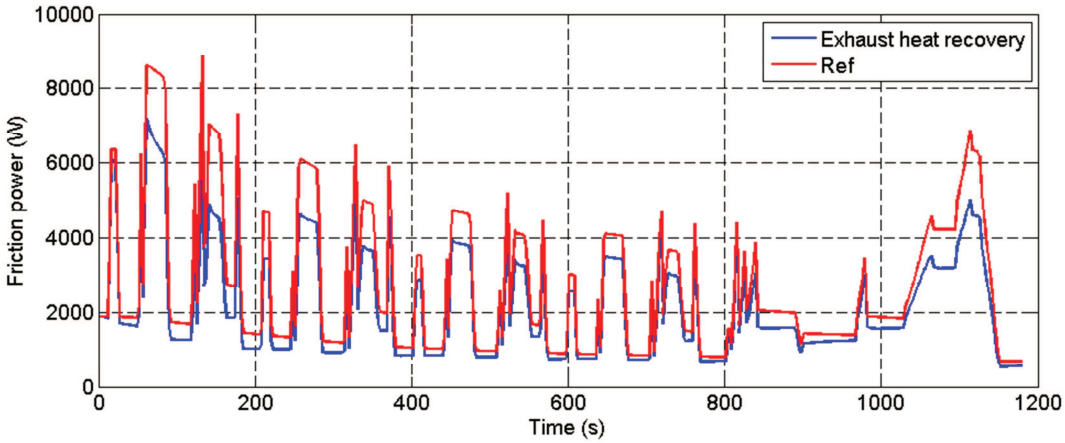

(a): Friction power at 20°C

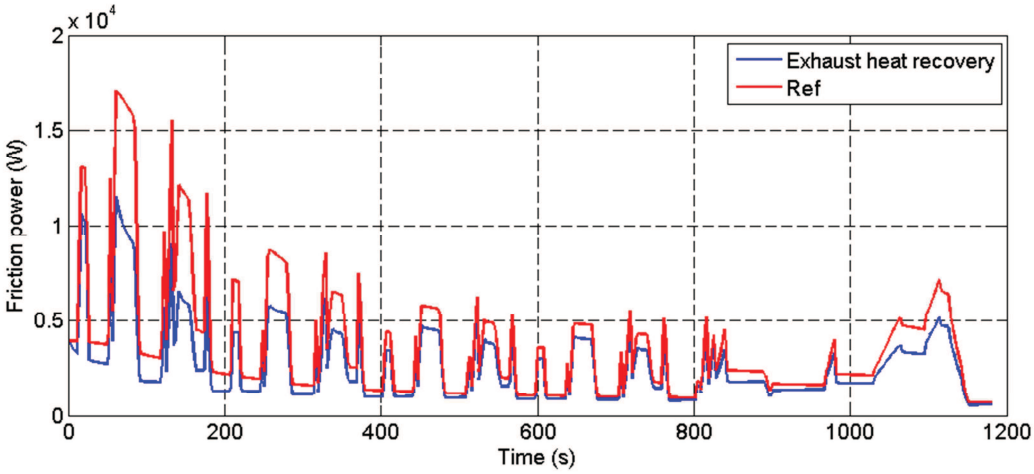

(b): Friction power at -7°C

Figure IV-20 Friction power over NEDC at both ambient temperatures

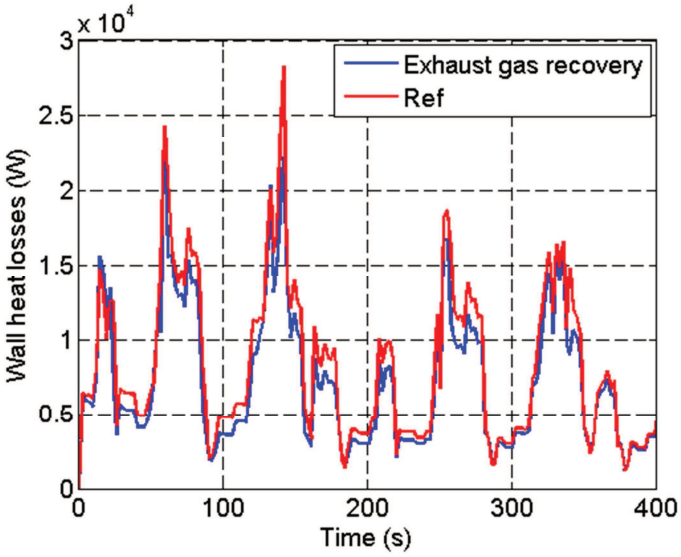

Figure IV-21 Wall heat losses over NEDC at -7°C zoomed on the first 400s

The friction power at an ambient temperature of -7°C depicted in Figure IV-20 (b) shows the reduction of the losses during the cycle. The total reduction of the cumulative friction power is 28.6%. This friction power reduction leads to fuel consumption benefits of 16.23% over the whole driving cycle.

The heat rate at the heat exchanger in this case is given in Figure IV-22. The peak of the heat rate is reduced to 20 kW compared to the exhaust/coolant heat exchanger (25 kW). The heat rate during the driving cycle ranged between 0.6 kW and 20 kW. Because of the low heat capacity of the oil compared to that of the coolant, even with less heat transferred to the former it raises quickly within the strategy.

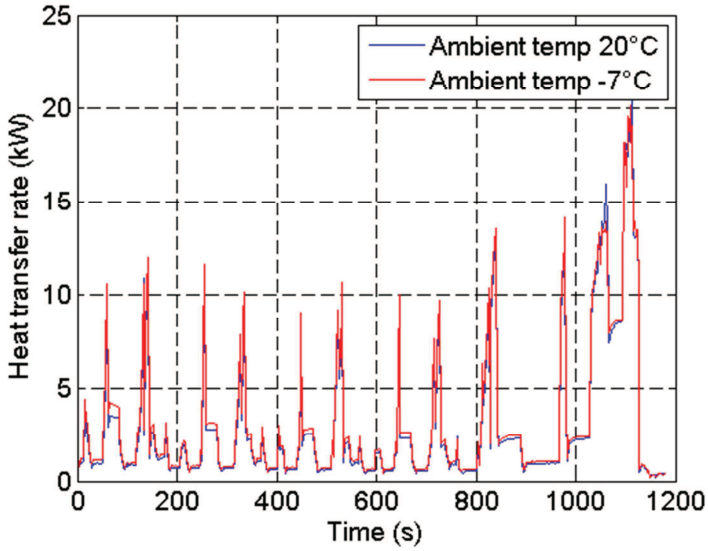

Figure IV-22 Heat transfer rate at the heat exchanger over NEDC at both ambient temperatures

IV.4.1.2. WLTC

Running the strategy over WLTC give the results depicted in Figure IV-23. The important changes in the temperature profile are remarkable with this driving cycle as the one before.

At an ambient temperature of 20°C (Figure IV-23 (a)), the lubricant temperature showed a significant improvement in the warm-up phase. However, the lubricant temperature did not rise softly like the reference case. The lubricant temperature within the strategy applied shows big variation once the regulation temperature of the engine is reached. These variations are in function of the engine operating points. Either the heat transfer rate at the exhaust/lubricant exchanger is high or either it is low depending on the exhaust gas flow rate and their temperature. Furthermore, during the steady state stage of the engine, the radiator branch of the coolant is opened, and heat is evacuated to the ambient. The lubricant seeds a portion of its heat to the coolant circuit at the oil cooler. Thus, depending on the intensity of the heat transferred to the lubricant at the exhaust exchanger and that transferred to the coolant, and the performance of the radiator the lubricant temperature will be varied during the steady state stage. The lubricant temperature reaches 60°C faster in 205s and then 80°C in advance of 347s. The coolant temperature profile shows an improvement with reaching the 60°C in advance of 145s and the regulation temperature was reached 93s before the reference case.

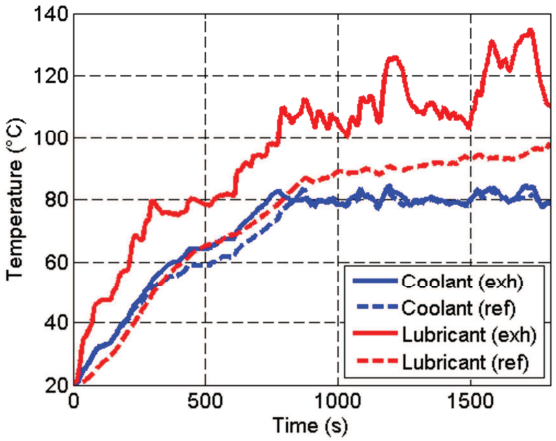

(a): Temperature profile at 20°C

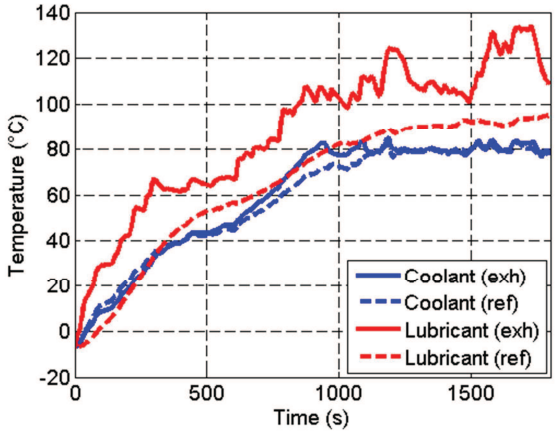

(b): Temperature profile at -7°C

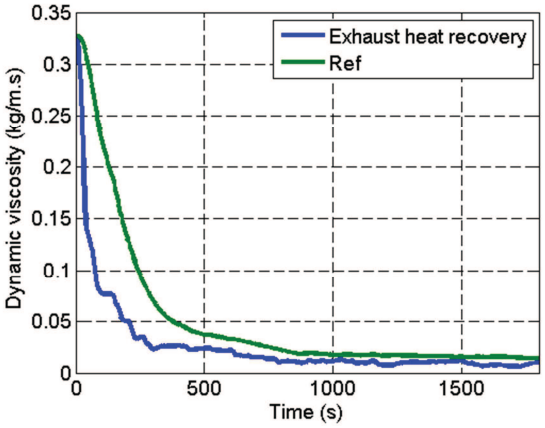

(c): Viscosity profile at 20°C

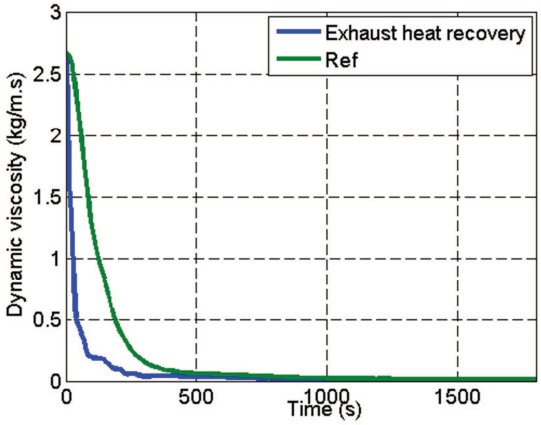

(d): Viscosity profile at -7°C

Figure IV-23 Exhaust gas recovery results over WLTC at both ambient temperatures

Furthermore, the viscosity profile in part (c) of Figure IV-23 reflects the improvement of the lubricant temperature. A drop of the viscosity is observed at the beginning of the cycle as the lubricant temperature increases quickly than the reference case. The lubricant temperature variation at high level did not influence largely the viscosity profile as the latter variations are insignificant at high lubricant temperature. At the end of the cycle, the cumulative viscosity was reduced by 49.6%. The huge difference of the lubricant temperature even at their highest temperature leads to significant difference in the viscosity profile at the end of the cycle (Figure IV-24). Friction losses hugest differences were shown at the start of the driving cycle where the viscosity difference was greater. However, the difference between the two cases (the strategy applied and the reference case) is remarkable throughout the whole driving cycle. At the end of the cycle, the friction losses were reduced by 20.9%. Fuel consumption benefits were 7.12% over WLTC at an ambient temperature of 20°C.

At -7°C as an ambient temperature (Figure IV-23 (b)), on one hand, the lubricant temperature showed an advance of 403s and 290s in reaching 60°C and 80°C respectively. On the other hand, the coolant rises up to 60°C before 47s than the reference case and reaches the regulation temperature with an advance of 243s. Similar to NEDC, the coolant profile at the

early stages of the driving cycle were higher with the reference case. The viscosity profile shows a great improvement in the early stages of the driving cycle, by preventing the engine to work in the high viscosity zone. Hence, friction losses are reduced remarkably in the first 400s as shown in Figure IV-24 (b). However, the viscosity plot shows that the viscosity of the lubricant converges after around 500s. This is not true. The scale of the viscosity changing at -7°C is bigger than at 20°C. Moreover, the difference in the viscosity level at the end of the cycle is insignificant compared to the changing at the first of the driving cycle. The latter is as important as the difference during the steady state stage at the ambient temperature of 20°C shown in Figure IV-23 (c). The difference of the friction power between the reference line and the strategy during the steady state stage is a proof (Figure IV-24 (b)). The friction power evaluation over the driving cycle gives a reduction of 29.4%. And the fuel consumption savings are 11.4% at the end of the driving cycle.

At both ambient temperatures, the lubricant temperature with the strategy applied takes the lead over the coolant temperature, and thus define the oil cooler as a heat source for the coolant circuit. The peak in the heat transfer rate at the heat exchanger during WLTC reaches 22 kW.

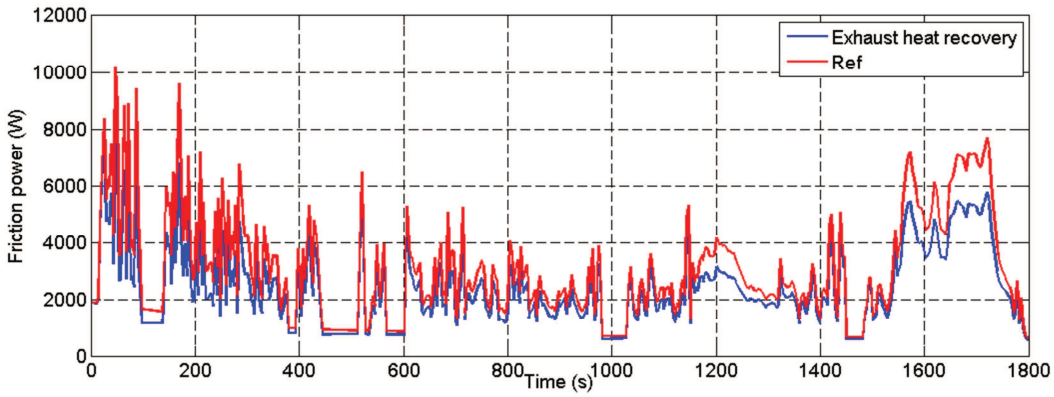

(a): Friction power at 20°C

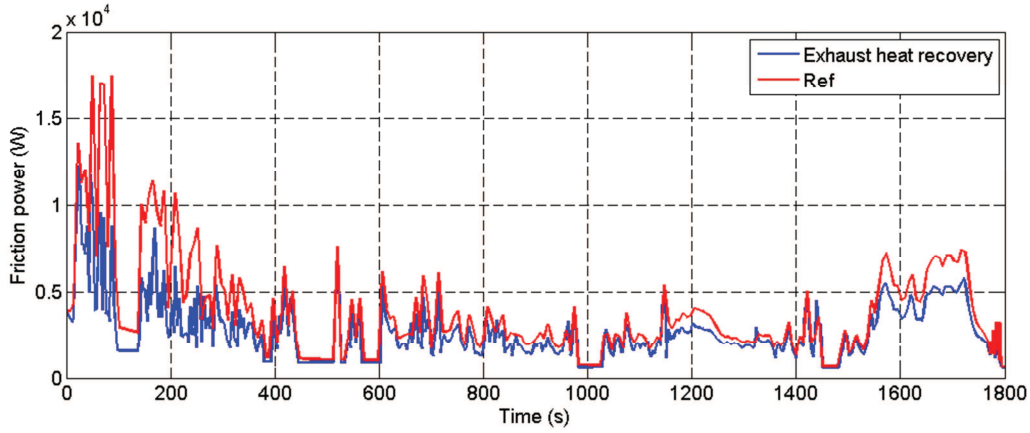

(b): Friction power at -7°C

Figure IV-24 Friction power over WLTC at both ambient temperatures

IV.4.1.3. Artemis Highway

Artemis highway simulations were ran at both ambient temperatures. Results concerning the coolant and the lubricant temperature as well as the friction power are illustrated in Figure IV-25.

The lubricant temperature is very noticeable with this driving cycle. It rises sharply in the first 200s of the driving cycle to reach a certain regulation phase temperature that is averaged around 130°C. However, for the reference case, the highest temperature of the lubricant at the end of the driving cycle reaches 103°C leading to a difference of 40°C at some point. This is due to the high operating points of the driving cycle. With AH, the heat transfer rate at the heat exchanger is the highest between the different driving cycles, similar to the previous configuration. The heat transfer rate reaches a maximum of 35 kW at the 254th second of the driving cycle. While the oil cooler during the warm-up was a heat source to the oil circuit with the reference case, it is considered as a heat source to the coolant circuit with the thermal management strategy applied.

At an ambient temperature of 20°C (Figure IV-25 (a)), the lubricant temperature reaches 60°C with an advance of 121s and reaches 80°C in 143s faster than the reference case. The lubricant temperature with the strategy applied rises up to 120°C in 241s, and enters a regulation phase starting 250s. However, the lubricant temperature reaches a maximum value of 137°C. The highest value of the lubricant temperature underlines the necessity of the control of the thermal management strategy to prevent the overheating of the lubricant and the breaking of the oil film. The coolant temperature compared to the reference case has an advance of 15s in reaching 60°C and 35s in reaching the regulation temperature. Similar to the previous driving cycle, an increase in the lubricant temperature lead to a decrease in the lubricant viscosity. The friction power in Figure IV-25 (c) highlights the big improvement by applying a direct heating of the engine's lubricant. Friction losses were reduced by 28.8% at the end of the driving cycle. The highest instant reduction in the friction losses is evaluated by 52.8% at around the 152th second of the cycle corresponding to 88.9% decrease in the viscosity value and 60°C difference in the lubricant temperature. Savings in the fuel consumption were valued to be 5.97% at the end of Artemis Highway.

At an ambient temperature of -7°C (Figure IV-25 (b)), the lubricant temperature rises to 60°C in 122s with an advance of 134s compared to the reference case. Then, it reaches 80°C ahead in 153s at the 149s of the driving cycle. In around 28 seconds, the lubricant temperature is increased by 20°C. The coolant temperature profile shows a slightly lower temperature than the reference case than rises to attend 60°C with an advance of 16s, and increases the difference to 30s when reaching the regulation temperature. Examining the friction power depicted in Figure IV-25 (d), the big difference at the early stages of the driving cycle is noticeable. The difference between the two plots decreases up along the driving cycle to have almost the same friction power at the end of the driving cycle. Exhaust gas heat recovery leads the engine to reduce its fuel consumption during every second of the driving cycle. This is due to the fact that the friction losses reduction leads to lower the fuel flow rate necessary to be injected in the combustion chamber to propel the vehicle. Friction losses reduction at the end of the driving cycle is assessed to be 36.41%. Fuel consumption benefits rises to 7.74%.

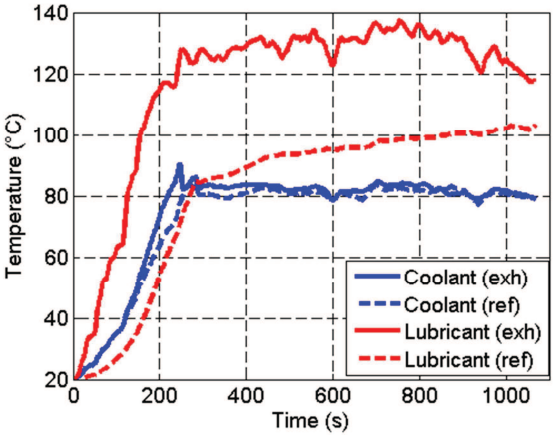

(a): Temperature profile at 20°C

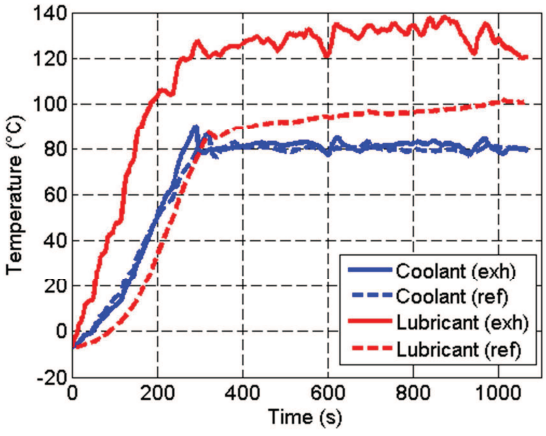

(b): Temperature profile at -7°C

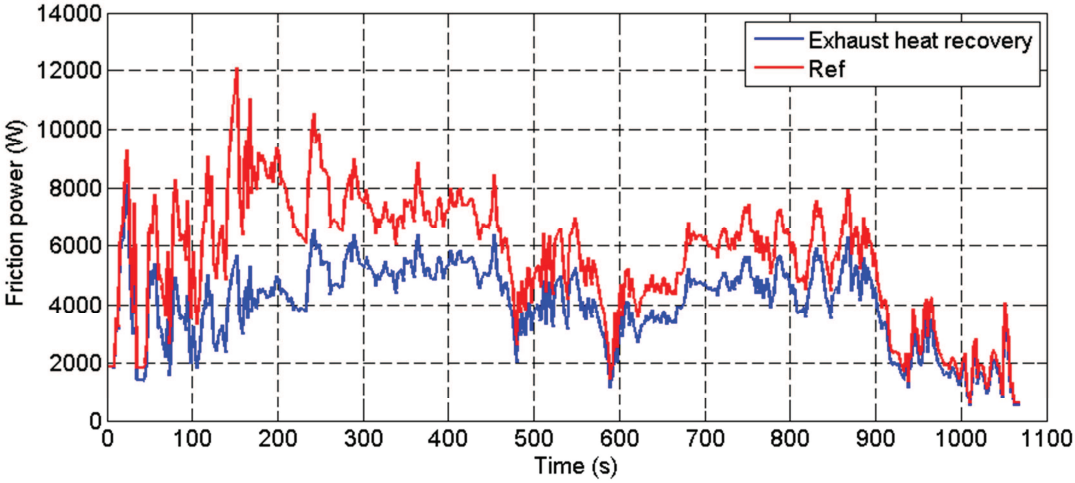

(c): Friction power at 20°C

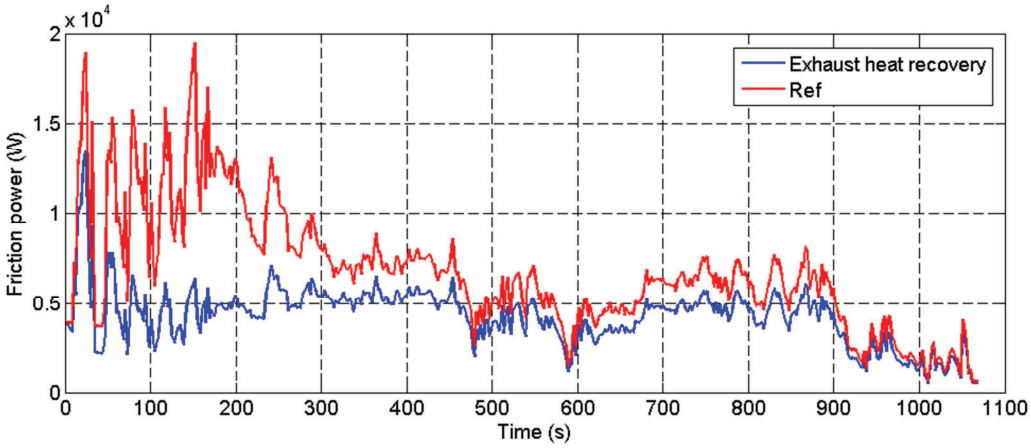

(d): Friction power at -7°C

Figure IV-25 Exhaust gas recovery results over AH at both ambient temperatures

IV.4.1.4. Artemis Urban

The temperature profiles of the coolant and the lubricant are depicted in Figure IV-26. The lubricant temperature profile similar to the previous driving cycles is noticeably improved by applying a direct heat transfer from the exhaust gases.

At an ambient temperature of 20°C (Figure IV-26 (a)), since the start of the cycle, the lubricant rises sharply marking a huge difference with the reference case. Comparing to the latter, the lubricant reaches 60°C in advance of 239s at the 244th second of the cycle and then reaches 80°C ahead of 624s. The highest temperature reached by the lubricant is 101°C around the end of AU. The coolant reaches 60°C with an advance of 68s, and then reaches its regulation temperature at 946s. For the reference case, the highest temperature of the coolant reached is around 73°C. The friction losses over the driving cycle give a reduction of 25.45% while the cumulative viscosity reached 55.4% at the end of the cycle. The assessment of the fuel consumption at the end of the cycle gives a benefit of 7.85%.

With a colder starting temperature of -7°C (Figure IV-26 (b)), the lubricant temperature attend 60°C sooner than the reference case by 429s. For the reference case, the lubricant does not reach the temperature of 80°C and ends up with a temperature of 63.7°C. However, with the strategy applied the lubricant reaches 80°C at the 546th of the cycle. The coolant during the reference case did not reach 60°C. Yet, with applying the strategy, the coolant starts with a temperature profile lower than the reference case but rises to attend 63.7°C at the end of the driving cycle. Friction losses were reduced by 35.3% and the fuel consumption savings at the end of the driving cycle were 17%.

Artemis Highway is known for its softness, as it is a representative of a city travel. The engine runs mostly at low operating points, thus in low efficiencies zone. Any improvement in the engine efficiency will be largely noticeable in terms of fuel consumption. The heat transfer rate reached a peak of 22 kW but its average over the driving cycle at an ambient temperature of 20°C is around 2.36 kW.

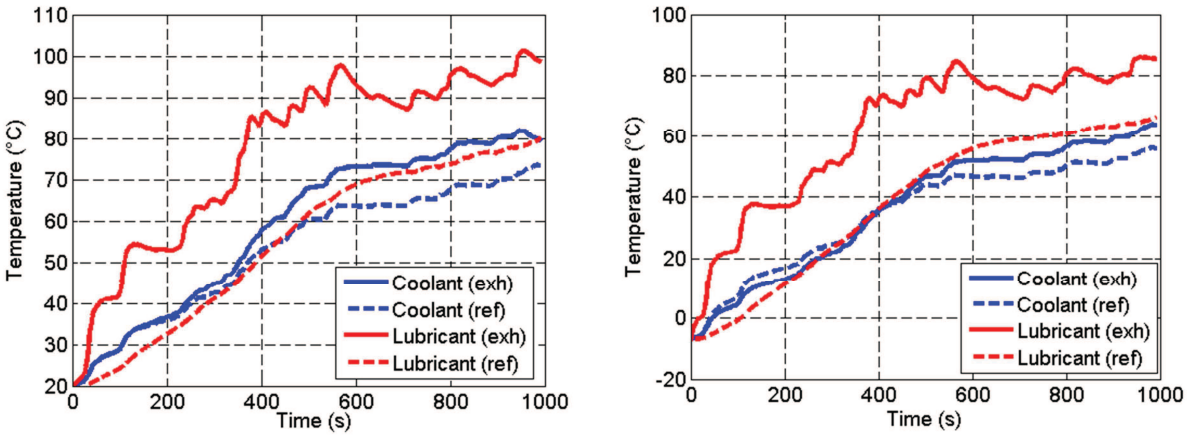

(a): Temperature profile at 20°C (b): Temperature profile at -7°C

Figure IV-26 Exhaust gas recovery temperature profiles over AU at both ambient temperatures

IV.4.1.5. In-House developed Driving Cycle

Figure IV-27 represents the coolant and lubricant temperature profiles over HDC at both ambient temperatures for applying the exhaust gas heat recovery strategy and the reference case in which the engine has the basic configuration of the coolant circuit.

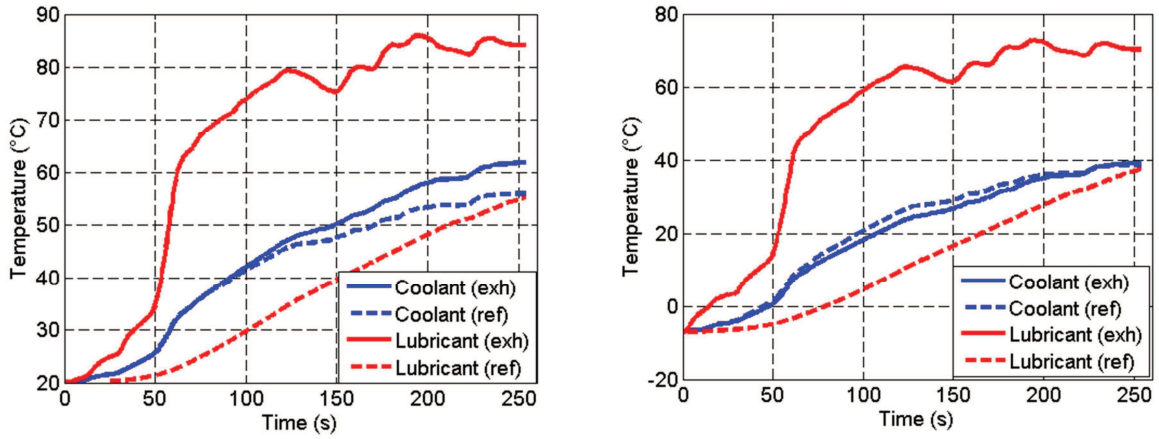

(a): Temperature profile at 20°C (b): Temperature profile at -7°C

Figure IV-27 Exhaust gas recovery temperature profiles over HDC at both ambient temperatures

At an ambient temperature of 20°C (Figure IV-27 (a)), the lubricant temperature profile exceeds 80°C and hits a peak of 86°C, while the reference case rises to 55.2°C at the end of the cycle. The lubricant reaches 60°C in 62s and 80°C in 162s. The coolant temperature showed an improvement after 100s of the cycle where it exceeds 60°C after 225s but does not reach the regulation temperature. Friction losses and fuel consumption were reduced by 36.8% and 13.65% respectively.

Lowering the ambient temperature to -7°C, allows the lubricant to reach only 70.3°C at the end of the driving cycle with a difference more than 30°C with the reference case. The lubricant reaches 60°C after 102s. The coolant profile is lower than the reference case but it ends up with a temperature of 39°C higher in 1°C. Friction losses were reduced by 52.2% and fuel consumption by 28.6%.

Heat transfer rate hits a peak of 33 kW during the cycle. The high increase in the lubricant temperature after 50s corresponds to the moment of the driving cycle with the acceleration to reach 90 km/h. Engine operating at high operating points will lead to high flow rate of exhaust gases in the heat exchanger and higher temperatures too, thus high heat transfer.

Table IV-4 summarizes the different results in terms of fuel consumption and friction power benefits over the different driving cycles and at both ambient temperatures for an exhaust gas heat recovery heating up the lubricant directly. Table IV-5 summarizes the warm-up time savings during the configuration A. the "-" in the table means the indicated temperature is not reached either by one of the two cases: the thermal management or the reference case.

The fuel consumption benefits depend largely during this strategy on the operating points of the engine and the length of the driving cycle. High operating points will lead to higher heat transfer at the exhaust line consequently to higher exhaust gases flow rate and temperature.

However, during the analysis, high operating temperatures of the lubricant were detected and a control over it was necessary to prevent the breaking of the oil film.

Control over the lubricant temperature can be done by by-passing the heat exchanger at the exhaust line and thus stops the heat transfer to the lubricant. One of the advantages of this bypass is lowering the back-up pressure once the lubricant or the engine reaches some level of temperature. By-passing the exhaust gas heat exchanger can be done at very high operating points to prevent a drop in the engine performance resulting from the back-up pressure at the exhaust line or in function of the temperature of the lubricant. Other solutions are to have a bigger radiator that helps evacuating the exceeding temperature, but will be a loss of time and money to evacuate heat which has been recovered at the exhaust line.

Configuration B was proposed to test the influence of the position of the exhaust heat exchanger on the lubricant temperature.

Table IV-4 Exhaust gas heat recovery with lubricant heat exchanger results at different ambient temperatures (Configuration A)

	Fuel consumption		Friction power	
Driving cycle	**20°C**	**-7°C**	**20°C**	**-7°C**
NEDC	5.52%	16.23%	20.58%	28.6%
WLTC	7.12%	11.4%	20.9%	29.4%
AH cycle	5.97%	7.74%	28.8%	36.41%
AU cycle	7.85%	17.02%	25.45%	35.3%
HDC cycle	13.64%	28.62%	36.8%	52.2%

Table IV-5 Warm-up time savings (in seconds) for different cycles and ambient temperatures (Configuration A)

Ambient temperature		**NEDC**	**WLTC**	**AH**	**AU**	**HDC**
20°C	$\Delta t_{coolant,60}$	82	145	15	68	-
	$\Delta t_{coolant,opt}$	155	93	35	-	-
-7°C	$\Delta t_{coolant,60}$	109	47	16	-	-
	$\Delta t_{coolant,opt}$	36	243	30	-	-
20°C	$\Delta t_{lubricant,60}$	252	205	121	239	-
	$\Delta t_{lubricant,80}$	376	347	143	624	-
-7°C	$\Delta t_{lubricant,60}$	295	403	134	429	-
	$\Delta t_{lubricant,80}$	258	290	153	-	-

IV.4.1 Application - Configuration B

In configuration B, the exhaust/oil heat exchanger placement on the exhaust line downstream the catalyst was not modified. On the lubricant side, the heat exchanger was placed downstream the engine and upstream the oil sump to prevent the lubricant reaching high temperatures by losing some heat in the oil sump as well as transfer other to the coolant circuit at the oil heat exchanger.

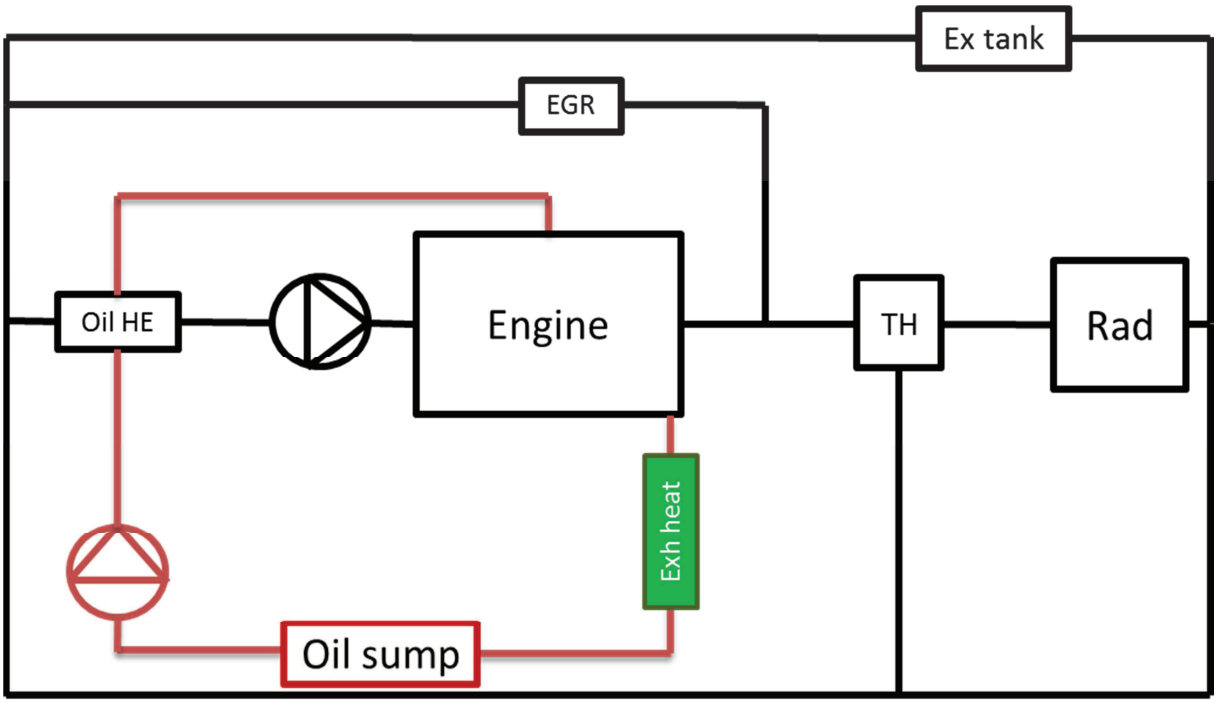

Figure IV-28 A schematic presentation of the exhaust gas heat recovery strategy applied on the oil circuit (Exh heat: Exhaust heat exchanger; TH: Thermostat; Oil HE: Oil heat exchanger; Ex tank: Expansion tank; Rad: Radiator)

IV.4.1.1. Results

Configuration B was tested over the five driving cycles and both ambient temperatures to assess the fuel consumption. The latter savings are assumed to get lower with this configuration as less heat will be available for the lubricant, thus less reduction in friction losses. However, this configuration aims to reduce the lubricant's high temperature and have a fuel consumption benefit.

Figure IV-29 represents the different temperature profiles of the coolant and the lubricant at an ambient temperature of 20°C. The dashed line represents the results of the Configuration A obtained in the previous section (section IV.4.1). The improvement in the lubricant temperature is always noticeable with the changing of the heat exchanger location on the lubricant circuit. However, the maximum temperature of the different driving cycles has changed with the new configuration. No exceeding of 120°C is observed. The highest lubricant temperature was registered within AH (Figure IV-29 (c)) that reaches 120.8°C at 761s and dropped after that.

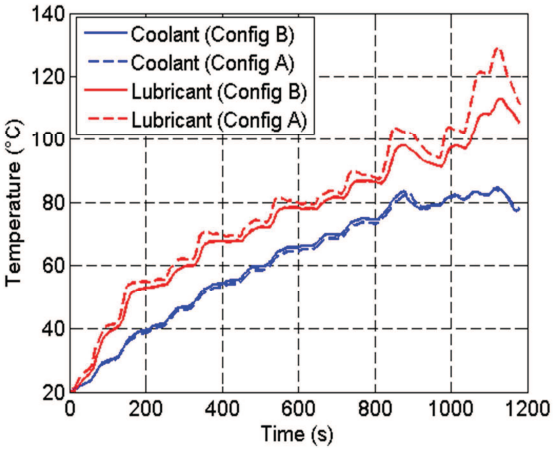

(a): NEDC

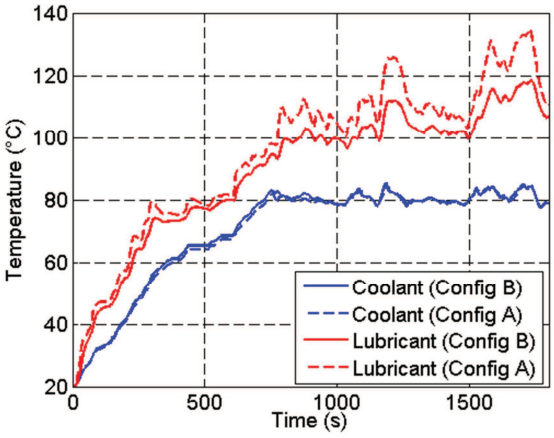

(b): WLTC

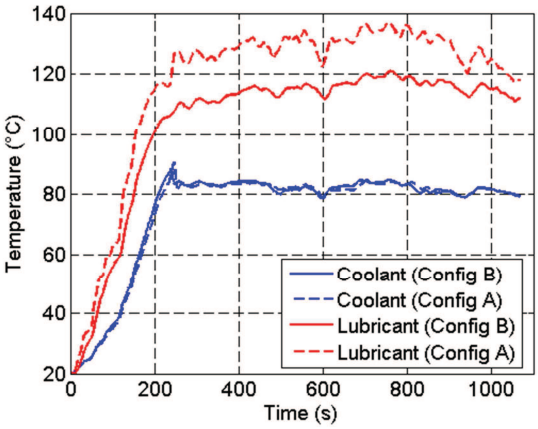

(c): Artemis Highway

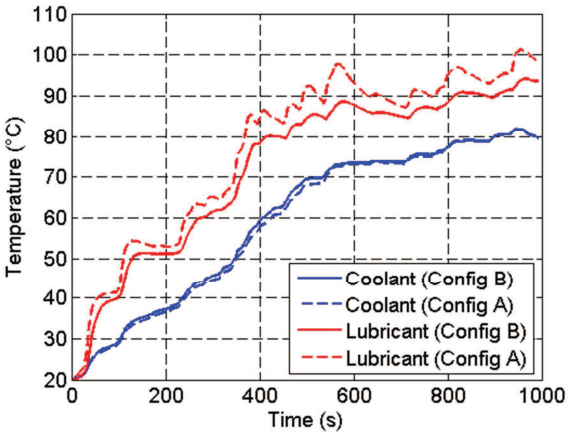

(d): Artemis Urban

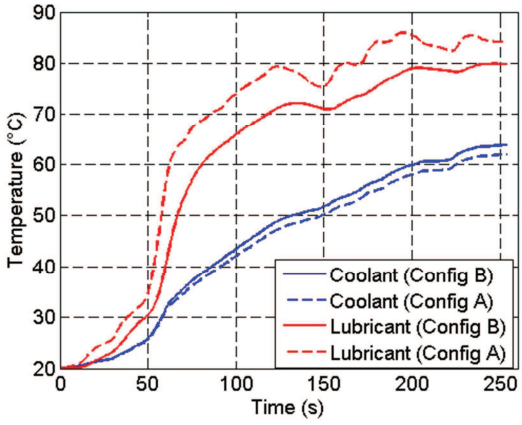

(e): In-House developed Driving Cycle

Figure IV-29 Coolant and lubricant temperature profiles of the configuration B at an ambient temperature of 20°C

NEDC (Figure IV-29 (a)): the highest temperature registered for the lubricant during Configuration B is 113°C, dropping 16°C from the Configuration A. However, the coolant reaches its regulation temperature 16s in advance compared to the configuration A.

WLTC (Figure IV-29 (b)): the lubricant reaches the highest temperature of 118°C while the highest temperature with Configuration A was 135°C. A drop of 17°C is registered with the new configuration. With Configuration B, coolant temperature reaches its regulation temperature in advance of 25s compared to Configuration A.

AH (Figure IV-29 (c)): the biggest difference in the highest temperature reached with this configuration is registered within this driving cycle, where an average of difference is maintained during the steady state stage of the engine. The highest temperature reached by the lubricant in this driving cycle is 121°C while during Configuration A, it hits a peak of 137°C. The coolant reaches its regulation temperature 8s earlier with Configuration B compared to Configuration A.

AU (Figure IV-29 (d)): the lubricant highest temperature reached during Configuration B is around 94°C, lower by 7°C than Configuration A. The coolant reaches the regulation temperature at the same time in the two configurations.

HDC (Figure IV-29 (e)): the highest temperature of the lubricant during Configuration B is 80°C while for Configuration A it was 86°C. The coolant temperature profile showed an improvement. At the end of the cycle the coolant reaches 63.7°C, higher by 2°C than Configuration A.

Temperature profiles at -7°C as ambient temperature were not shown because if preventing the overheating of the oil can be done with a higher ambient temperature, it surely can be controlled at lower ambient temperatures.

Fuel consumption benefits and friction power reduction are summed up in Table IV-6 for all the driving cycles and the two ambient temperatures. All the values of the benefits were reduced as supposed before the simulation. However, no overheating of the lubricant happened by changing the exhaust gas heat exchanger position on the lubricant circuit and yet it still promise good results in terms of fuel consumption.

Table IV-6 Exhaust gas heat recovery with lubricant heat exchanger results at different ambient temperatures (Configuration B)

	Fuel consumption		**Friction power**	
Driving cycle	**20°C**	**-7°C**	**20°C**	**-7°C**
NEDC	4.29%	13.95%	16.65%	24.65%
WLTC	4.95%	10.09%	15.94%	22.55%
AH cycle	4.13%	5.58%	21.22%	28.66%
AU cycle	4.95%	15.87%	21.21%	31.05%
HDC cycle	11.87%	26.19%	30.95%	47.57%

IV.5. Direct heating of coolant and lubricant

One last configuration is tested within this strategy. Two heat exchangers back to back were installed on the exhaust line: the first one to heat up the lubricant while the second is connected to the coolant. The two exchangers are placed downstream the catalyst to not affect its light-off time. On the coolant side the exchanger is placed as in section IV.3. On the lubricant side, the configuration A is used to have the best benefit of the new strategy (Figure IV-30).

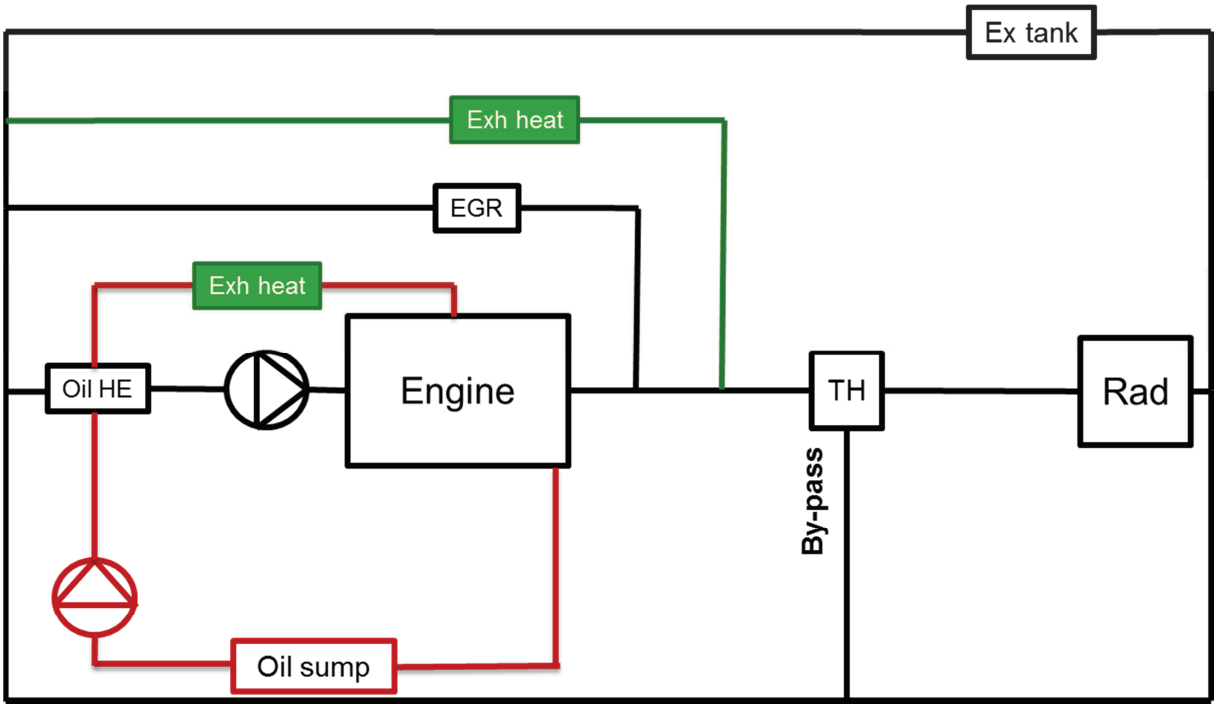

Figure IV-30 A schematic presentation of the exhaust gas heat recovery strategy applied on the oil circuit and the coolant circuit (Exh heat: Exhaust heat exchanger; TH: Thermostat; Oil HE: Oil heat exchanger; Ex tank: Expansion tank; Rad: Radiator)

The different plots, for the different driving cycles, are represented in Figure IV-31. The reference line represents the engine in its basic configuration. The temperature profiles prove that the first heat exchanger is efficient. The lubricant temperature within this strategy gets high as the one in Configuration A (section IV.4.1). However, the coolant temperature was not expected to get as high as the indirect lubricant heat-up configuration. In this part, the exhaust gases entering the second heat exchanger that exchange heat with the coolant are not at high temperatures as in the previous studies. Exhaust gases temperature drops remarkably after the first exchanger as depicted in Figure IV-32. The highest exhaust temperature entering the first heat exchanger is almost 500°C and it drops to around 220°C for the second heat exchanger. However, the coolant temperature profile during the different driving cycles is brought closer or better than the coolant temperature profile of configuration B, thus better than A. Despite that, fuel consumption assessments at the end of the different driving cycles are less as summarized in Table IV-7. The reason might be with the high back pressure level at the exhaust line. For high exhaust gases mass flow rates, the pressure drop over one heat exchanger can reach 430 mbar and even higher. Consequently for two heat exchangers, the

pressure drop can reach 1 bar in some cases. Higher back pressure can lead to lower engine performance, thus higher fuel consumption.

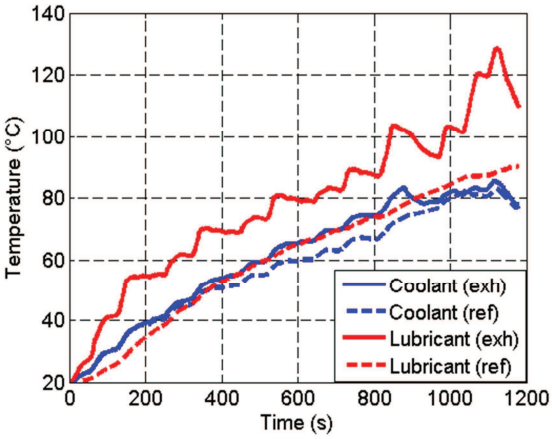

(a): NEDC

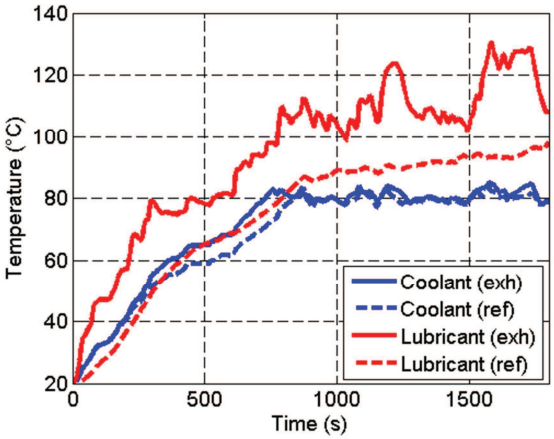

(b): WLTC

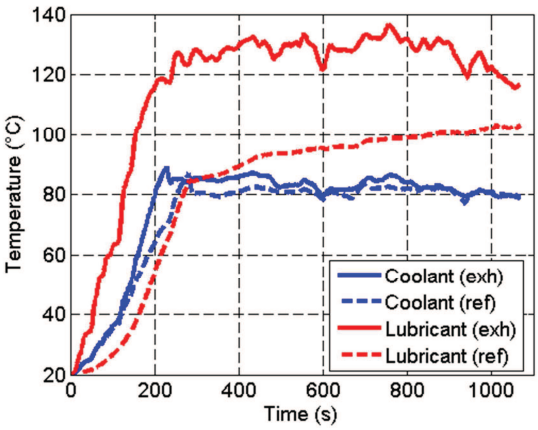

(c): Artemis Highway

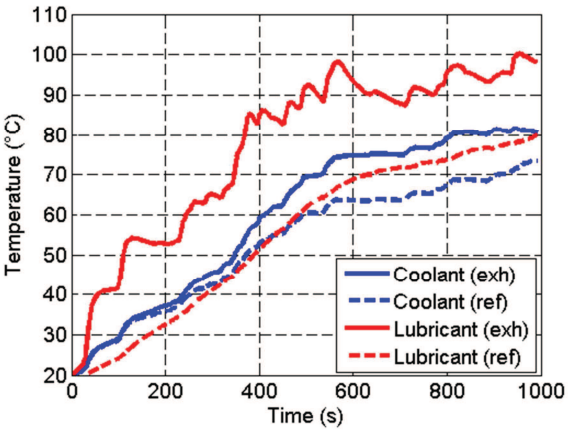

(d): Artemis Urban

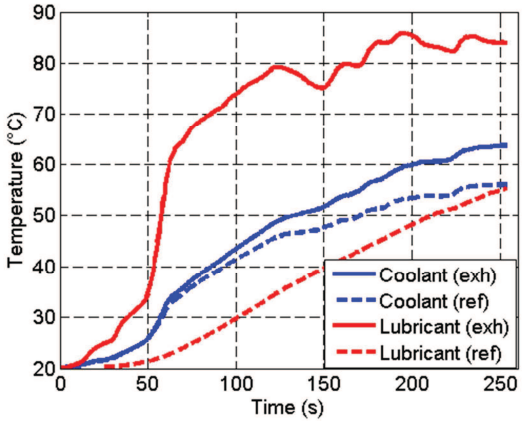

(e): In-House developed Driving Cycle

Figure IV-31 Coolant and lubricant tempreature profiles for two heat exchangers on the exhaust line

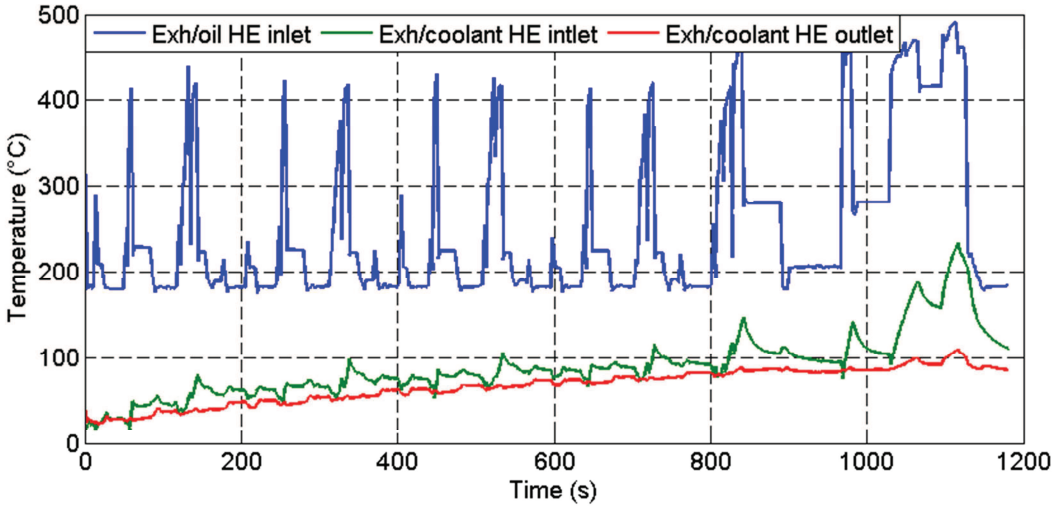

Figure IV-32 Exhaust temperatures over NEDC at 20°C as ambient temperature

Table IV-7 Fuel consumption savings with two heat exchangers

	Fuel consumption	
Driving cycle	**20°C**	**-7°C**
NEDC	4.85%	14.95%
WLTC	5.96%	12.02%
AH cycle	5.13%	6.95%
AU cycle	7.14%	17.27%
HDC cycle	13.57%	28.32%

Figure IV-33 summarizes the different results for the exhaust gas heat recovery done in this chapter. Direct heating of the lubricant is the best configuration as it allows the best fuel consumption savings. However, two configurations were proposed one allowing the lubricant to reach high level temperature, threatening breaking the oil film in the engine and thus high level of engine wear. The other configuration proposes to change the heat exchanger position and succeeded in limiting the lubricant temperature. The best gain of the strategy is obtained within HDC as it is a short driving cycle and highlights the importance of the transient phase, thus friction power reduction. The latter are at their highest level at the start of the driving cycle and their remarkable improvement is not mitigated by the length of the driving cycle.

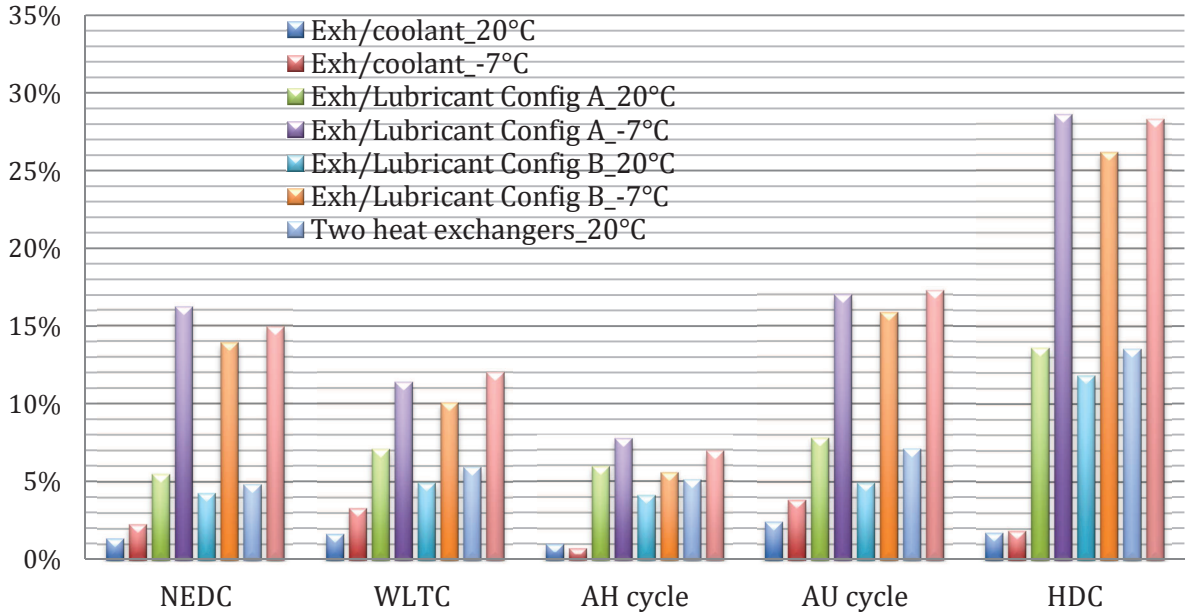

Figure IV-33 Fuel consumption savings for exhaust gas heat recovery for: different configurations, driving cycles and ambient temperatures.

A heat exchanger was installed on a test bench to characterize its heat exchange rate between hot air and water. Tests were held at Ecole Centrale de Nantes. 94 points were registered. Water flow rate, air temperature and air flow rate were varied during the tests. Water inlet temperature was set around 16°C. Heat rate between the two fluids as well as the pressure drops on both side were issued from the tests. The tests were used to calibrate the heat exchanger on GT-Suite. Calibration was made to have the minimum error on the coolant side, because it reflects the thermal state of the engine and thus the topic in concern in this study. Over 94 points, an average error of the coolant outlet temperature was 3.58%, while the error of the outlet air temperature was 13.8%.

Exhaust gas heat recovery was then applied on the engine. The exchanger was located downstream the catalyst to not alter its light off time. The study was divided in two big parts: indirect and direct heating of the lubricant. Indirect heating consists of heat exchange between the exhaust gases and the coolant on the first term and then heat exchange at the oil cooler. On the coolant side, the heat exchanger was installed in a new branch parallel to the EGR cooler with no control over the heat exchange between the two fluids. Numerical simulations were run over different driving cycles and ambient temperatures. A remarkable improvement in the coolant temperature was observed in the different results. Fuel consumption benefits ranged between 1.02% and 3.86% depending on several conditions.

Direct heating of the lubricant consists of installing an exhaust/oil heat exchanger. Two configurations were proposed in function of the position of the heat exchanger on the lubricant side. The first one consists of the maximum benefits of the strategy by installing the exchanger directly upstream the engine, thus eliminating any heat losses. Lubricant's temperature rises remarkably during the different simulations over different driving cycles. Lubricant high temperature reached a maximum of 130°C and more in WLTC and AH. A maximum of 624s advance of attending 80°C is registered in AU at an ambient temperature of 20°C. Friction power reductions ranged between 21% and 52% while fuel consumption benefits ranged between 5.5% and 28.6%. The second configuration consists of placing the heat exchanger downstream the engine and upstream the oil sump and oil cooler. This position is used to have a control over the lubricant temperature without any by-pass on the exhaust line. The second configuration succeeded in minimizing the high lubricant temperature. Maximum temperatures were dropped by around 17°C in both AH and WLTC. However, fuel consumption savings were reduced and ranged between 4.1% and 26.2%.

At the end, two heat exchangers back to back were proposed. The first one was to heat the lubricant and the second one was for the coolant. However, the high efficiency of the first heat exchanger did not allow the coolant to attend high heat transfer rate at the second exchanger. Despite that, the coolant temperature profile showed an improvement compared to the first configuration of lubricant direct heating. The back-pressure imposed by the two exchangers surpassed the improvement of the two exchangers and therefore the fuel consumption benefits were lower than the lubricant direct heating.

V. Other thermal management strategies

This final chapter of the thesis covers the valorization of different minor strategies.

It studies the influence of the oil's grade over the engine. The oil type is changed to 0W20 instead of 15W40.This strategy was tested over different driving cycles and at two ambient temperatures.

The next strategy is the engine insulation. The latter took some attention during the previous years and patents were done in the field of underhood management. But, the study will concern only the engine environment. Therefore, the insulation will be tested by reducing the exterior convection coefficient by 71% and then 100%. Simulations were run over different driving cycles at 20°C.

Following, the influence of by-passing the charge air cooler and the EGR cooler on the engine was studied.

Finally, the influence of rising the operating temperature of the engine by 20°C was valorized over two driving cycles at an ambient temperature of 20°C.

V.1. Oil's grade

To reduce the engine friction power, automotive industries tend to change the old lubricant used in the engine to a new one with low viscosity at low temperature. This part will valorize the using of that lubricant's type from a thermal point of view and assess the fuel consumption benefits within it.

During the study of the heat storage, the oil's grade influence on the strategy was studied. Savings were reduced compared to the oil's grade but still exist with the new lubricant. However, this part will cover the influence of the oil's grade on the basic engine configuration without any thermal management strategy applied.

The basic oil of type 15W40 will be replaced by 0W20. The kinematic viscosity of the two oil's grade is represented in Figure III-25.

V.1.1 Application on different driving cycles

Oil's grade 0W20 will be tested over the different five driving cycles chosen in this work and at two ambient temperatures: 20°C and -7°C.

V.1.1.1. NEDC

The main results of NEDC at the two ambient temperatures are represented in Figure V-1. Contrary to all the different numerical simulations done before, the coolant and lubricant temperature profile with the new oil's grade are lower than the reference case during all the driving cycle. The reference case is the engine basic configuration with neither modification in the hydraulic circuits nor in fluids' types.

At an ambient temperature of 20°C (Figure V-1 (a)), the coolant stays lower than the reference case during the driving cycle. However, it reaches the regulation temperature before the end of the cycle but in a delay of 30s compared to the reference case. At 60°C, the delay is more remarkable. It is for 120s. The delay is shortened by advancing because during the last stage of the NEDC, the engine works under higher operating points, leading to higher heat at the combustion chamber and thus higher loss to the coolant. The lubricant temperature reaches 60°C and 80°C in delay of 111s and 116s respectively. To explain the lowest temperature profile, friction power profile is depicted in Figure V-1 (c). The latter shows a significant reduction in the friction power with the new oil used in the engine. The improvement with the new oil's does not cover only one part of the driving cycle but exists throughout the whole cycle. The lower viscosity provided with 0W20 led to reduce the friction power of the engine. Consequently, the heat source level of the lubricant as well as the coolant decreased. Hence, the temperature profiles of the two fluids are lower than the reference case. The friction power was reduced by 24.2% with the new oil. And despite the lower temperature profiles, the fuel consumption savings were 6.28%. Moreover, almost the two profiles behave in the same manner as the reference line. The coolant temperature takes the lead in both cases, and then around 400s the lubricant rises higher.

At an ambient temperature of -7°C, the same behavior is observed (Figure V-1(b)). Because of lower friction power (Figure V-1(d)), fluids temperature profiles are lower than the reference case. Contrary to the reference case, the engine did not reach its regulation temperature at the end of the driving cycle. The coolant reaches 60°C in a delay of 88s.

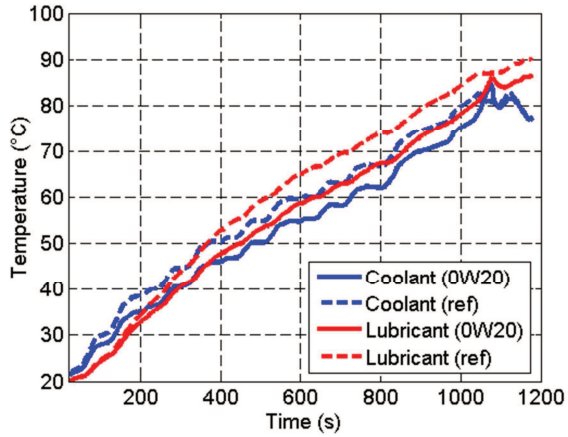

(a): Temperature profile at 20°C

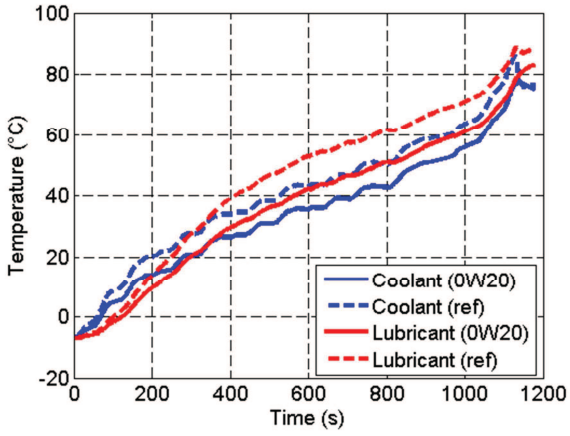

(b): Temperature profile at -7°C

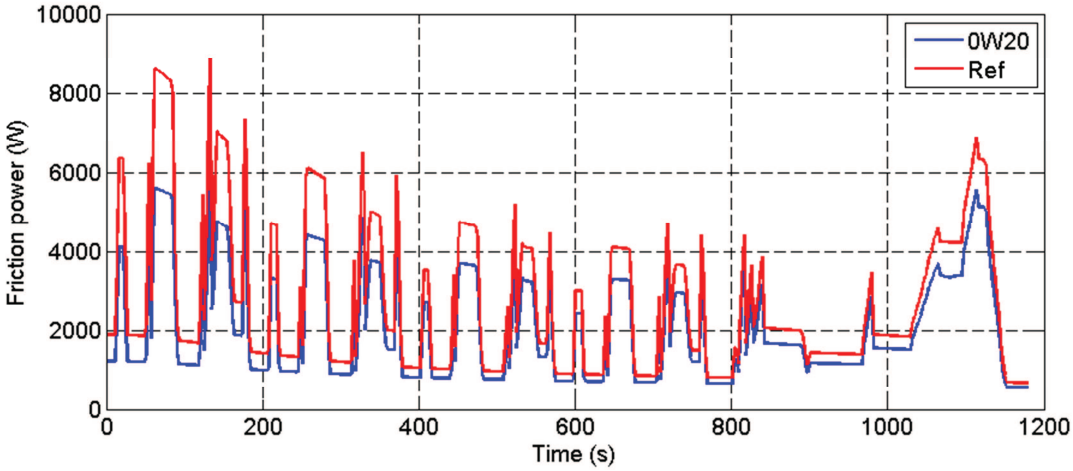

(c): Friction power at 20°C

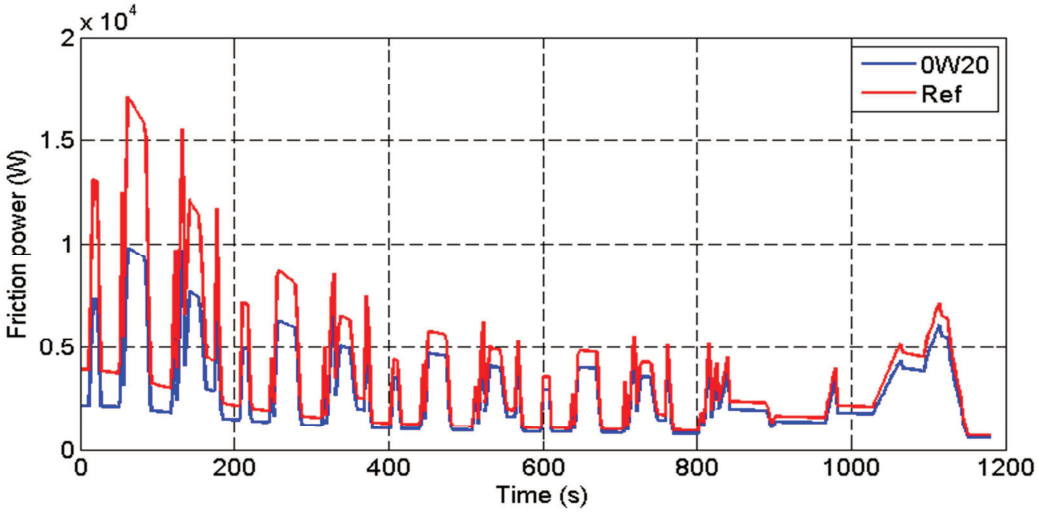

(d): Friction power at -7°C

Figure V-1 Main results of 0W20 over NEDC

The lubricant profile shows a delay of 216s and 51s in reaching 60°C and 80°C respectively. The friction power reductions rise to 26% at an ambient temperature of -7°C. Fuel consumption is reduced by 15.47%.

V.1.1.2. Other driving cycles

Similar to NEDC, the temperature profile for the different driving cycles behave in the same way as illustrated in Figure V-2. The temperature profiles with 0W20 were lower than the reference case.

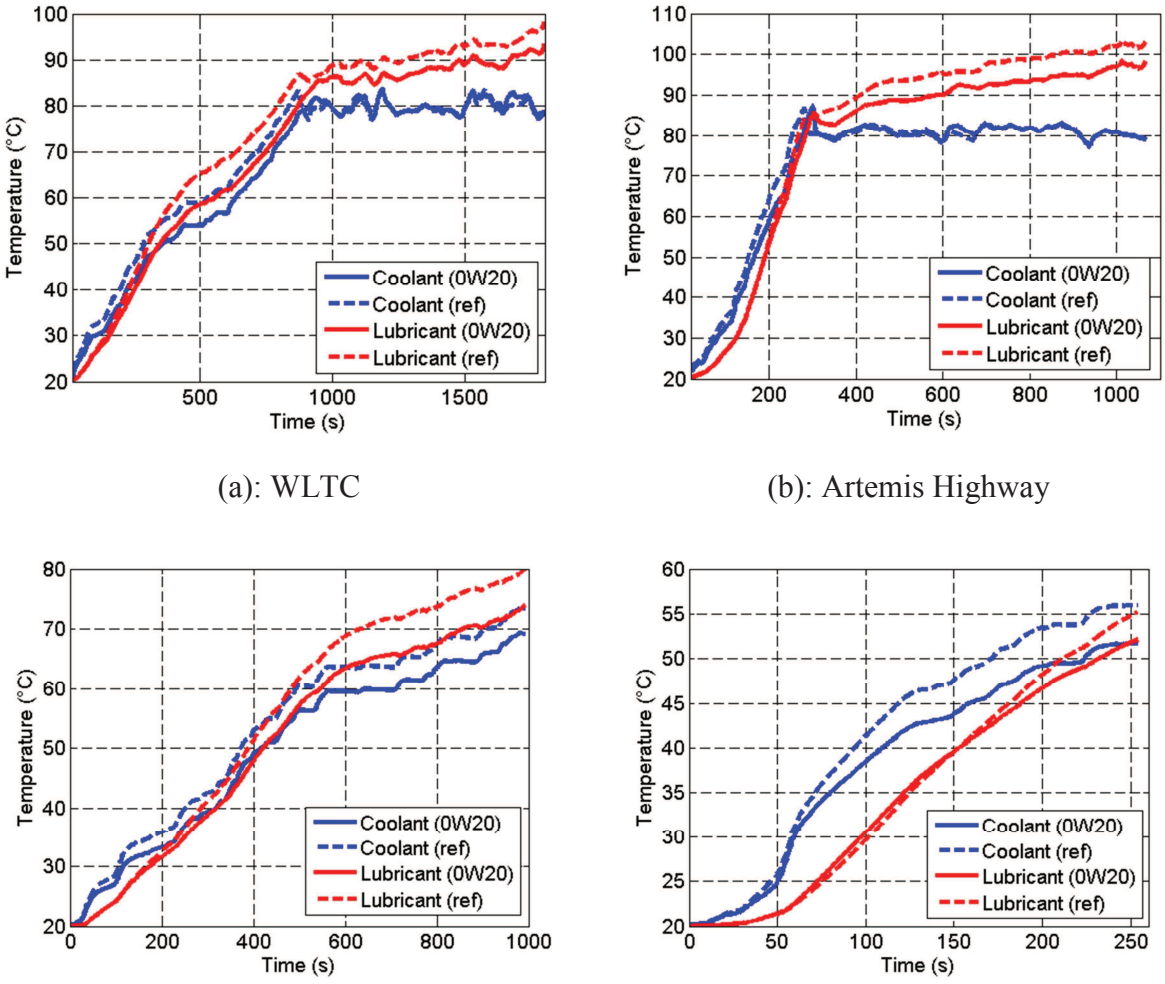

(a): WLTC (b): Artemis Highway

(c) : Artemis Urban (d): HDC

Figure V-2 Coolant and lubricant temperature profiles over different driving cycles at 20°C as an ambient temperature

For WLTC (Figure V-2 (a)), the coolant shows a delay of 96 seconds and 68 seconds to reach 60°C and the regulation temperature respectively. However, these differences are minimal during Artemis Highway driving cycle (Figure V-2 (b)). The lubricant temperature did not have a remarkable difference during the warm-up stage as a result of the high operating points of the engine. The lubricant reached 60°C and 80°C later by 8s and 16s compared to the reference line. The coolant showed a delay of 19s to reach 60°C and the regulation temperature. Even, once the regulation temperature is reached, the lubricant temperature with the new oil's grade is always lower than the reference case. AU temperature profiles as shown

in Figure V-2 (c) showed that the engine stayed in the warm-up phase with both types of lubricant. With 15W40, the lubricant reaches at the end of the cycle 80°C, but with 0W20 the highest temperature reached was 74°C. The coolant shows a delay of 220s in reaching 60°C. The biggest difference is due to the fact that with the delay in the coolant temperature around 60°C the engine entered the longest phase of the engine's stop during the driving cycle. HDC temperature profiles depicted in Figure V-2 (d) shows a close lubricant temperature during most of the driving cycle, and a slightly better profile between the 50^{th} and 150^{th} second of the cycle.

Figure V-3 represents the friction power of the different driving cycles at an ambient temperature of -7°C. The lowest ambient temperature was chosen to represent the friction power results because it highlights the difference between the two profiles. As mentioned before, a slightly changing in low temperature leads to a remarkable change in oil's viscosity, thus the friction power. Furthermore, AH (Figure V-3 (b)) and HDC (Figure V-3 (d)) friction power profiles show high difference between the two cases. Friction power is dependent also on the rotational engine speed. In these two driving cycles, the engine reaches high speed level in a very short time when the lubricant temperature is always at least, thus viscosity at highest. AU in Figure V-3 (c), shows that at the end of the driving cycle, the two friction power profiles are almost brought together. WLTC led to a reduction of 23.9% of friction power at -7°C, AH led to 24.1%, AU led to 28.9% and HDC led to 38.3%. The results confirm the previous analysis. Comparing AH and WLTC, because both driving cycles reaches their regulation temperature and high lubricant temperatures, AH reaches higher reduction level because it have high operating points during the cycle. Similar to that, comparing AU and HDC and despite that HDC is a shorter one, it underlines the friction difference due to the high engine speed after around only 50s of the cycle.

Table V-1 represents the fuel consumption benefits and friction power reduction for using a lubricant of type 0W20 over 15W40 over different driving cycles and at two ambient temperatures of 20°C and -7°C. Fuel savings varied between 3.7% and 25.22% depending on the conditions.

Table V-1 Fuel consumption savings and friction power reduction for 0W20

	Fuel consumption		Friction power	
Driving cycle	**20°C**	**-7°C**	**20°C**	**-7°C**
NEDC	6.28%	15.47%	24.2%	26%
WLTC	6.75%	9.25%	15.94%	23.9%
AH cycle	3.69%	5.74%	21.33%	24.1%
AU cycle	8.4%	15.82%	26.2%	28.9%
HDC cycle	11.62%	25.22%	30.95%	38.3%

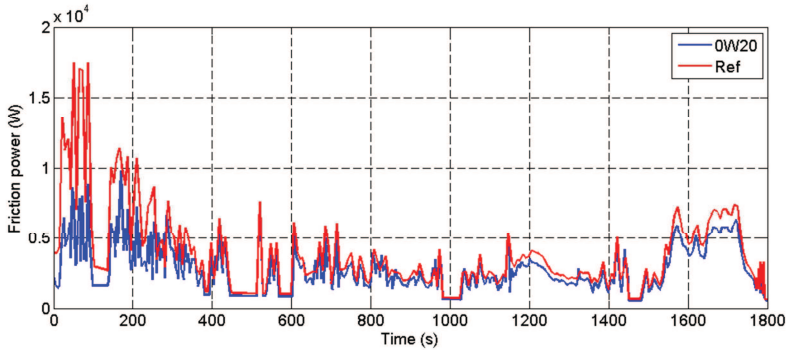

(a): WLTC

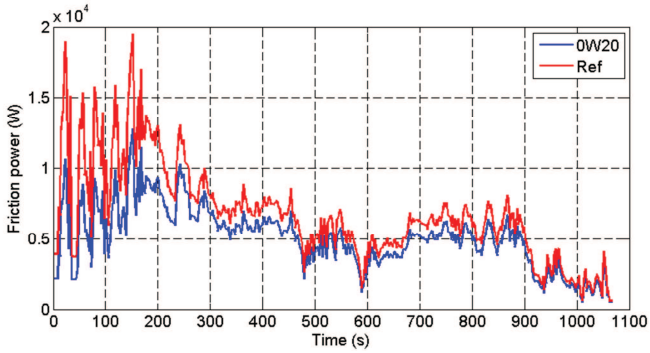

(b): Artemis Highway

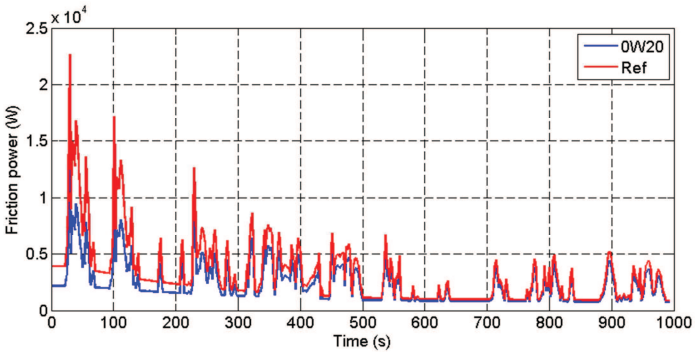

(c): Artemis Urban

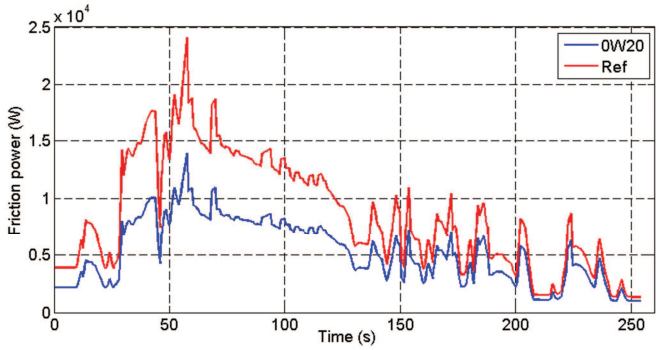

(d): HDC

Figure V-3 Friction power over different driving cycles at -7°C as an ambient temperature

V.2. Engine insulation

Engine insulation throughout the literature survey is mostly based on experimental setup. They tend to cover the different parts of the engine in order to reduce its radiation to the ambient as well as minimize its external convection coefficient. To valorize this strategy over numerical simulations, the engine exterior convection coefficient was reduced by 71% (from 70 to 20 W/m²/K) for the first case. The second case considers no heat exchange with the ambient with an exterior convection coefficient set to zero and thus a reduction of 100%. The latter is more a theoretical idea but it gives an insight over the maximal potential of this strategy.

Numerical simulations were run over the five different driving cycles at 20°C as an ambient temperature.

V.2.1 NEDC

Engine insulation temperature profiles for the numerical simulations over NEDC are illustrated in Figure V-4. The coolant temperature profile depicted in Figure V-4 (a) showed a remarkable improvement as well as the lubricant temperature profile (Figure V-4 (b)). Improvements were remarkable starting 180s on the plots but the difference started from 80s. Insulating the engine led to improve the engine warm-up phase, by limiting the engine heat loss to the ambient. The latter will lead to a faster engine mass warm-up, and thus the heat transmitted from the combustion chamber and the friction to both the fluids will be higher. Examining the coolant temperature profile, the regulation temperature was reached in advance of 186s and 263s for an insulation of 71% and 100% respectively. The improvement in the lubricant profile led to a reduction of the friction power by 2.5% for an insulation of 71%. For a total insulation of the engine, friction power was reduced by 3.7%. Fuel consumption benefits were 0.59% and 1.24% for an insulation of 71% and 100% respectively.

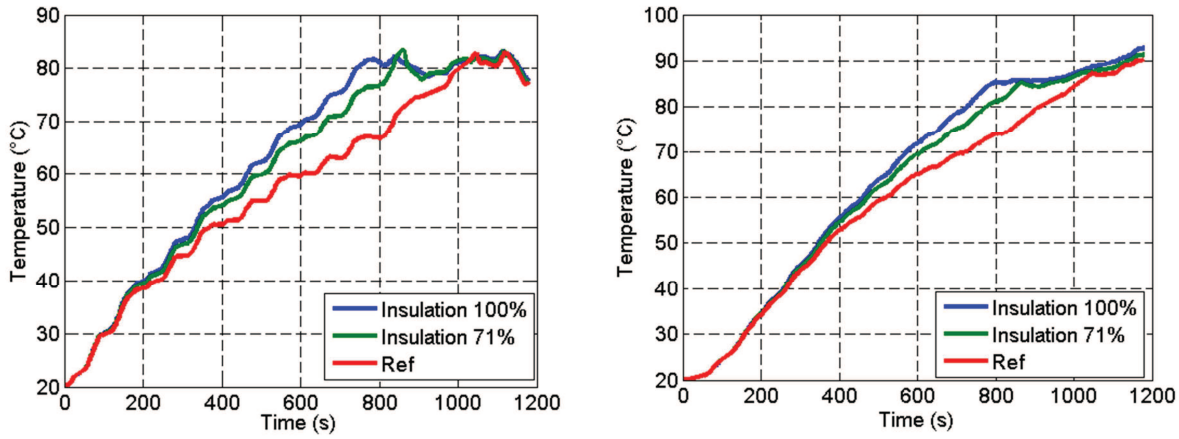

(a): Coolant (b): Lubricant

Figure V-4 Temperarature profiles for engine insulation over NEDC

The cool-down of the engine with the insulation was not tested in this study, thus no assessment of the heat retention during the soak period was done. However, such studies may give an insight of the initial temperature at the next start-up. It could be higher than the ambient and lead to more fuel consumption savings.

V.2.2 Other driving cycles

Coolant temperature profiles for the different driving cycles with a reduction of the exterior convection coefficient by 71% and 100% are depicted in Figure V-5 over the reference case which represents the engine basic configuration.

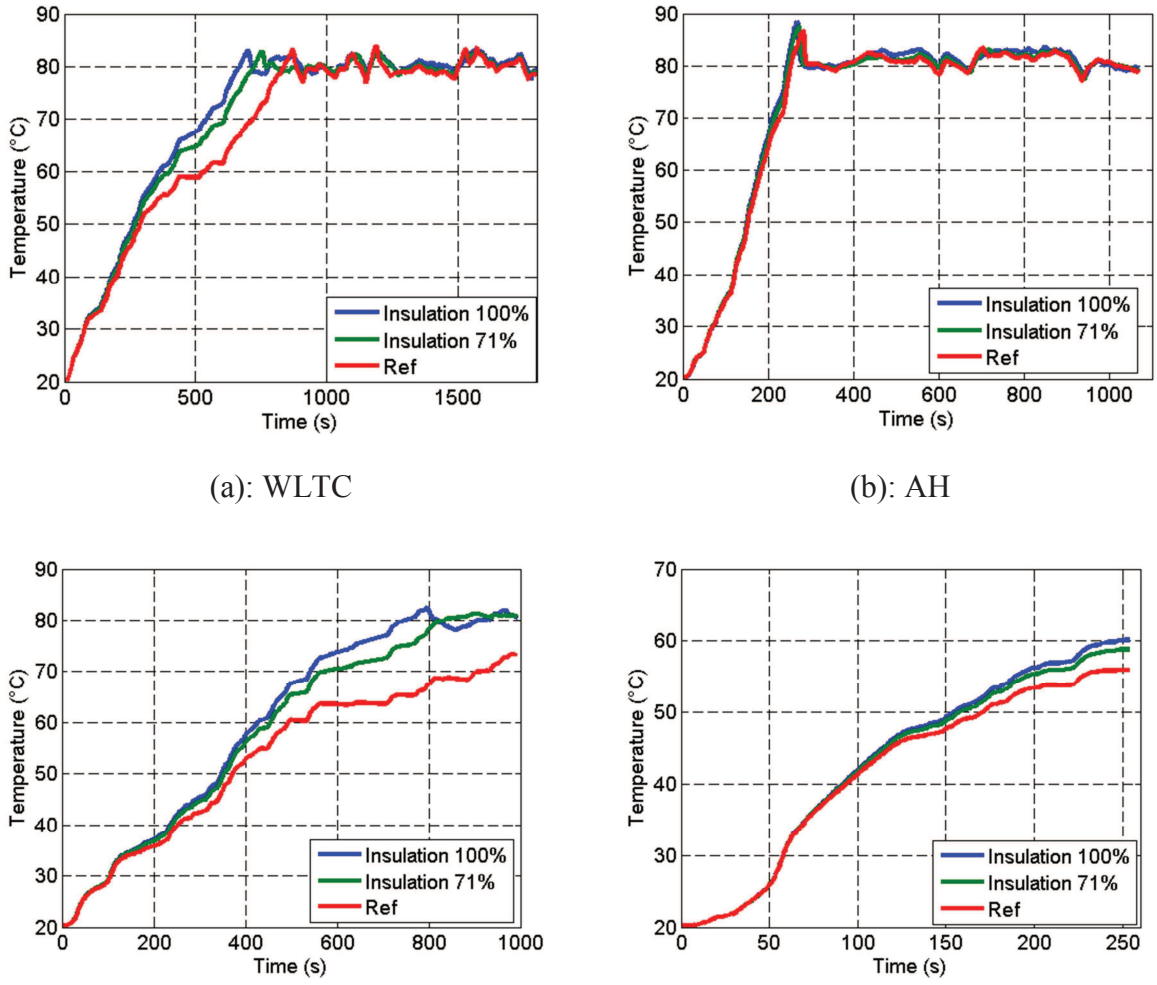

(a): WLTC (b): AH

(c) : AU (d): HDC

Figure V-5 Coolant temperature profiles for engine insulation over different driving cycles at an ambient temperature of 20°C

Examining the coolant profile for the different driving cycles demonstrates that the greatest improvements are within WLTC (Figure V-5 (a)) and AU (Figure V-5 (c)). On one hand, the strategy applied on WLTC led to a coolant reaching its regulation temperature by an advance of 118s and 172s for an insulation of 71% and 100%. On the other hand, numerical simulations over AU with insulation of 71% and 100% led to an engine running at an

regulation temperature at the end of the cycle while during the reference case it did not reach that temperature. AH (Figure V-5 (b)) warm-up stage is limited to its first 250s. Therefore no remarkable improvement in the coolant profile was obtained over this driving cycle. Furthermore, the insignificant improvement obtained during the warm-up phase will be lost at the end of the driving cycle. Similar to that, HDC (Figure V-5 (d)) did not show the remarkable improvement found in the previous driving cycles. HDC is a short cycle and for the insulation to have an effect on the fluid temperature, almost half of the driving cycle is over. Fuel consumption savings for the different driving cycles and for the different level of insulation are given in Table V-2.

Table V-2 Fuel consumpton benefits with inuslation of 71% and 100% over different driving cycles

	Fuel consumption	
Driving cycle	**71%**	**100%**
NEDC	0.59%	1.24%
WLTC	0.91%	1.29%
AH cycle	-	-
AU cycle	1.85%	1.97%
HDC cycle	0.08%	0.11%

The engine insulation study did not show remarkable improvements in terms of fuel consumption. Once the engine reaches its steady state stage, it will need to evacuate more heat to the ambient. Insulating the engine traps more heat into the engine which will be transferred to the coolant circuit. Then, the coolant circuit tries to evacuate this extra heat to the ambient at the radiator. The latter are customized to have a specific efficiency. To evacuate the extra heat, heat exchangers need to be maximized. Despite that the underhood space management causes some problems, maximizing the heat exchangers costs will exceed the savings done by the fuel consumption. Furthermore, water pumps should be modified to fit the new coolant circuit and the bigger pressure drop of the radiator. Finally, engine insulation fuel consumption savings were less than 2% even for the coldest winter days. Consequently, other strategies will be prior to apply on the internal combustion engine.

V.3. Charge air cooler by-pass

One of the main losses is the heat transferred to the coolant and the combustion chamber at the start of the driving cycle, thus the low combustion efficiency at low ambient temperatures. By-passing the charge air cooler was proposed to help boost the combustion chamber wall temperature and thus have a better engine efficiency. The by-pass was temperature controlled. If the engine temperature did not reach 80°C, the by-pass branch is opened. However, the charge air cooler branch was never closed. Figure V-6 represents the air mass flow rate evolution through the bypass and the charge air cooler. It reflects that most of the air mass flow is flowing in the by-pass till the 1000th second of the cycle when the engine reaches its

regulation temperature. Therefore, as shown in Figure V-7, the outlet temperature of the charge air cooler is higher than the reference case (the engine without a charge air cooler bypass). An average of 12°C is almost obtained with by-passing the charge air cooler. Some instant temperature recorded higher difference. Consequently at 1000 s, because the by-pass is shut down, the outlet temperature drops to the reference case temperature. Despite the improvement at the outlet of the Charge Air Cooler, when the air has been mixed with EGR, its temperature did not show any remarkable improvement at the inlet of the different cylinders as shown in Figure V-8. Consequently, no remarkable variations were brought to the system, numerical simulations were run over the different driving cycles and the fuel consumption benefits comparison gave an overconsumption. The latter may be resulting from the filling efficiency of the engine. The intake line was modeled to have the closest pressure wave behavior in the intake line to have the best filling efficiency.

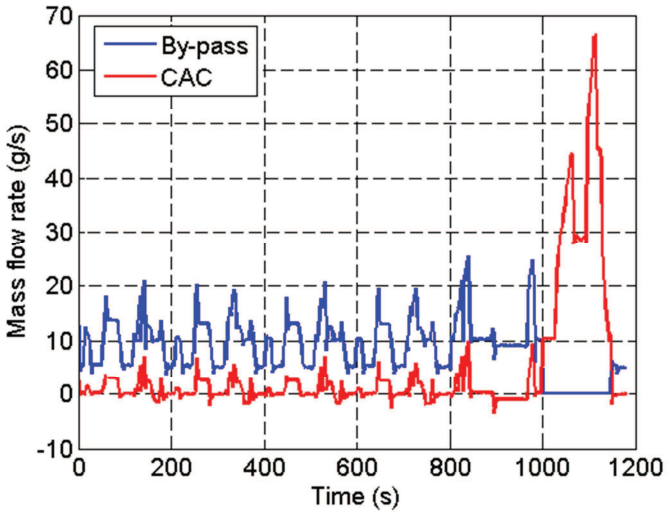

Figure V-6 Air mass flow rate during NEDC

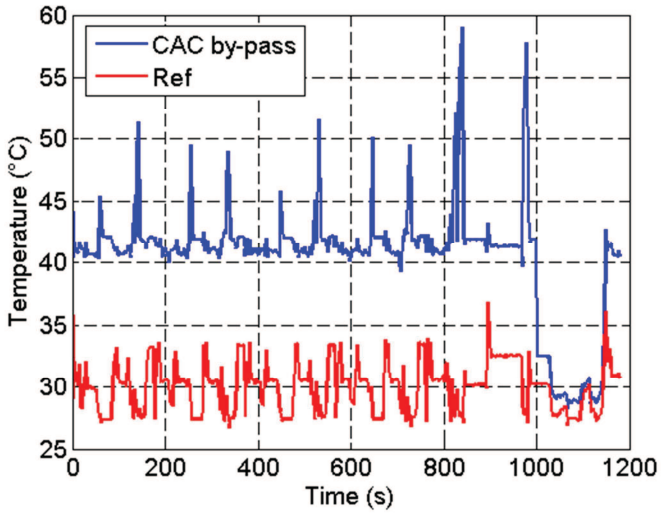

Figure V-7 Charge air cooler outlet temperature during NEDC

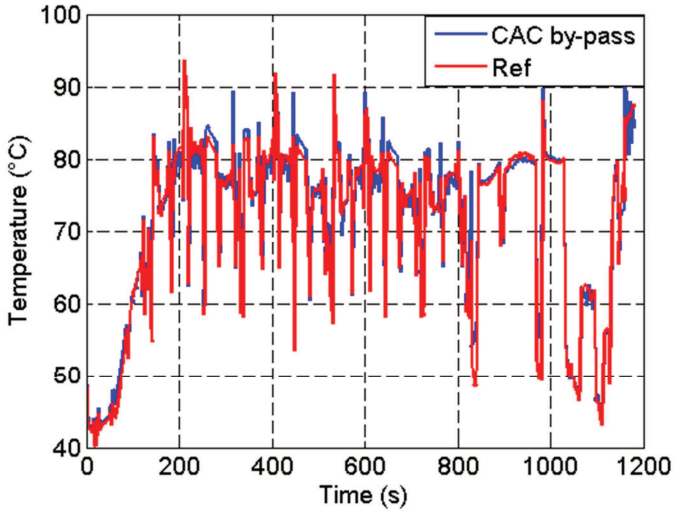

Figure V-8 Engine air inlet temperature during NEDC

V.4. EGR cooler by-pass

By-pass EGR cooler study is proposed to have a hotter combustion chamber, thus cylinder. Therefore, the wall heat losses should be reduced. Similar to the previous section, EGR by-pass was temperature controlled. The by-pass branch opens while the engine temperature is lower than 80°C. However, for this strategy, two valves control the EGR cooler, once the by-pass is opened, the access to the EGR cooler is blocked by another one. Generally, it is similar to the behavior of the thermostat by blocking the radiator branch while the engine did not reach the steady state stage. Air mass flow rate in the by-pass branch and the EGR cooler are depicted in Figure V-9. It is shown that the EGR flows into the by-pass branch from the start of the cycle until around 1030th second of the cycle. Comparing to the previous section, by-passing the EGR led to a longer warm-up state of the engine. This is due to the lower heat source of the coolant circuit. By-passing EGR cooler, did not lead to a remarkable improvement in the inlet air temperature at the cylinders as shown in Figure V-10. The inlet temperature is remarkably improved at the first 100s of the driving cycle. However, engine mass inertia did not lead to an influence of the engine warm-up temperature as it is shown in Figure V-11. Moreover, with the same fuel injection conditions as injection time, hotter air may lead to a modification in the combustion process in function of the crank angle in a way that does not suit perfectly the engine. Furthermore, higher temperature in the combustion chamber may lead to higher NOx emissions. For this reason, fuel consumption for the different driving cycles were not evaluated expecting to have an overconsumption with that strategy from a thermal management point of view. The delay in reaching the regulation temperature was obtained at the different driving cycles and different ambient temperatures. Finally, to evaluate the benefits of this strategy in term of catalyst light off, a comparison of the exhaust gas temperature did not show any improvements of the latter temperature especially in high levels over 300°C (necessary for the good functioning of the after treatment setups).

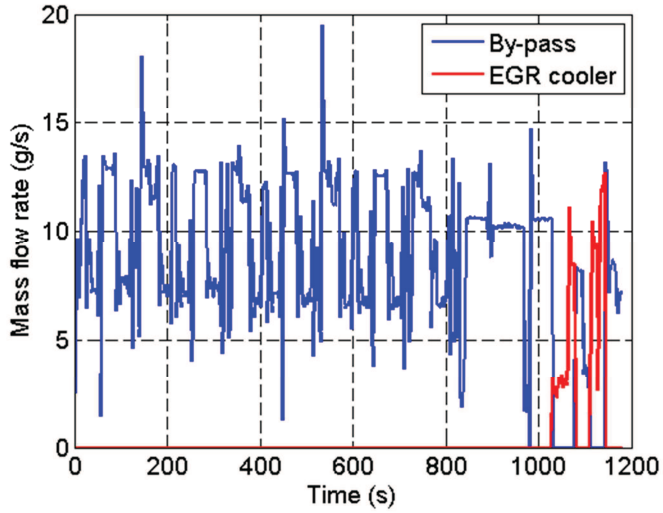

Figure V-9 EGR flow rate over NEDC

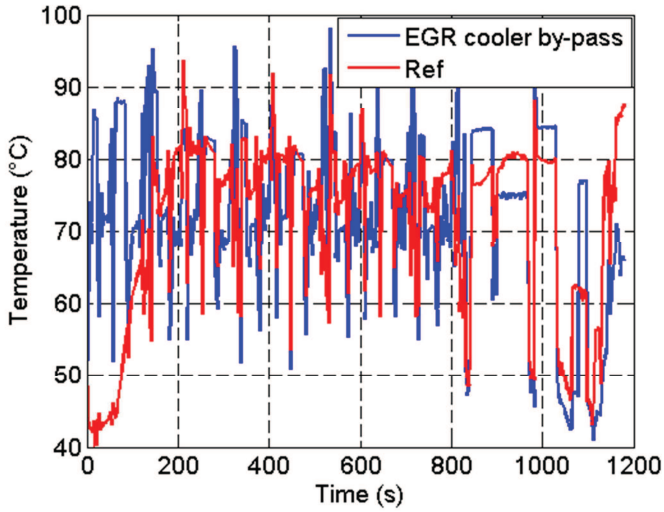

Figure V-10 Engine inlet temperature during NEDC

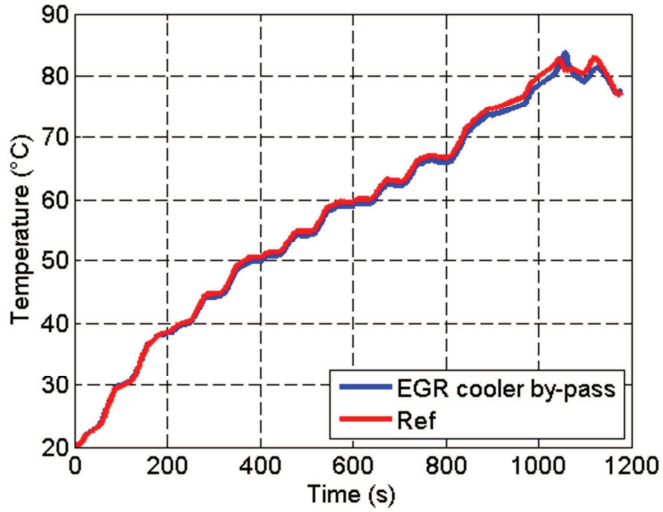

Figure V-11 Coolant temperature profile over NEDC

V.5. High temperature set point

Rising the regulation temperature of the engine will lead to lower heat losses during the steady state stage of the engine. Despite that the engine will stay in transient stage longer, but it will not affect his efficiency because it is happening at high temperatures. The increase in the operating temperature will raise the engine oil temperature, then lowering frictional losses in the engine, subsequently improving the fuel efficiency of the engine.

The operating point of the engine is increased by 20°C, and set to 103°C. The modification is done on the thermostat block where its opening and closing temperatures were increased by 20°C. Numerical simulations were run for the three first driving cycles: NEDC, WLTC and AH. It is only during these three driving cycles the engine goes into the steady state stage. The ambient temperature was set to 20°C. NEDC cycle reaches the regulation temperature late during the cycle and thus the strategy led to 0.03% improvement in the fuel consumption. Plots regarding NEDC will not be presented within the results.

A comparison between the two operating temperatures over WLTC and AH is illustrated in Figure V-12. For both driving cycles, as predicted, the warm-up stage is common between the two cases. The reference case represents the engine with an operating temperature of 83°C. However, the warm-up is extended with the new strategy to reach higher operating temperature. The difference between the two cases can be seen starting from the instance when the reference case enters into the steady state stage. Then, the latter has been modified within the new strategy. During WLTC (Figure V-12 (a)), the lubricant temperature exceeds the coolant at the same moment of the reference case. However for AH (Figure III-11 (b)), the lubricant behaves similar to the reference case and will not exceed the coolant unless the engine reaches its steady state stage.

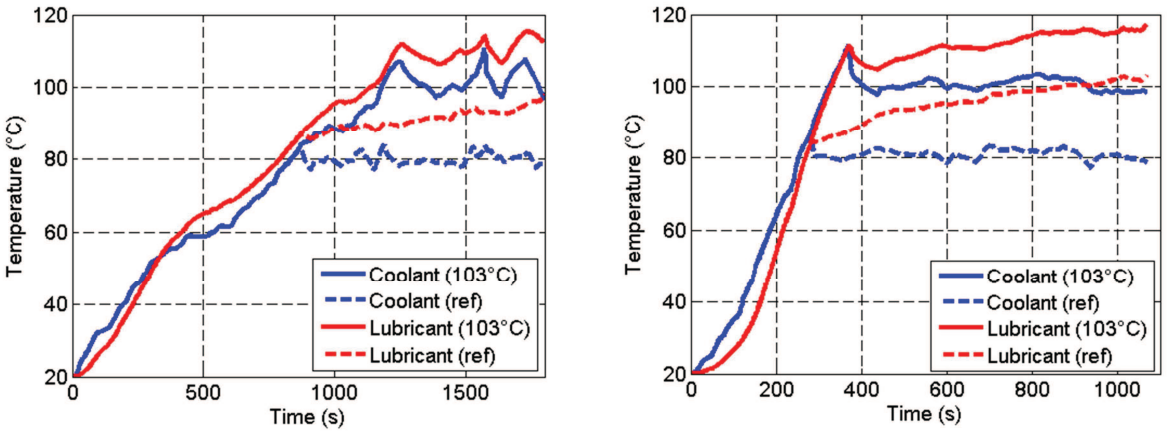

(a): WLTC (b): AH

Figure V-12 Coolant and lubricant temperature prfoiles with an operating temperature of 103°C over different driving cycles at 20°C

During WLTC, the engine reaches its new operating point at 1246s. The lubricant rises to around 115°C as a maximum temperature while the reference engine's lubricant reaches a maximum temperature of 98°C. The temperature difference during the steady state stage will

lead to minor difference in the lubricant viscosity. However, the friction power was reduced by 6.24% leading to 2.12% saving in fuel consumption.

For AH, the increase in the fluids temperatures continue sharply to reach the regulation temperature of the engine around 369s of the cycle. The lubricant temperature difference between the two cases was almost constant during the steady stage of the engine. The lubricant reaches a temperature of 117°C at the end of the cycle with the strategy while it was 103°C with the reference case. Similar to WLTC, increasing the coolant temperature by an average of 20°C will not lead to the same increase of the lubricant. Friction losses for AH was decreased by 7.75% leading to a reduction in fuel consumption of 1.22%.

Oil's grade was valorized by changing the oil type from 15W40 to 0W20. Lubricant viscosity was reduced at low temperature by using the new oil's grade. The strategy was tested over different driving cycles at 20°C and -7°C as an ambient temperature. Fluid's temperature profiles showed a delay in reaching regulation temperatures and were lower than the reference case. It is due to the friction power reduction with the new oil type, thus the total heat source to the hydraulic circuits. Friction power reduction ranged between 16% and 38% while fuel savings varied between 3.7% and 25.2%.

Engine insulation consists of reducing the external convection coefficient by 71% and 100%. The latter is considered as an engine fully insulated. Engine insulation was tested over different driving cycles to assess the fuel consumption reduction at an ambient temperature of 20°C. However, improvement during the soak period was not studied. Yet, if the latter was taken into consideration, fuel consumption can be improved because of an initial higher temperature of the engine during the cold start. Engine insulation had a better impact on NEDC, WLTC and AU. AH represents severe driving style, leading to an regulation temperature early in the cycle, thus, not highlighting the importance of the engine insulation. Moreover, HDC is a short cycle not giving the time for the insulation to have an influence on the engine. Fuel consumption benefits ranged from 0.08% to 2% depending on the driving conditions.

By-passing the charge air cooler and the EGR to improve the cylinder temperature during the early stages of the driving cycle did not show any remarkable improvements. The high air temperature resulting from by-passing the charge air cooler was neglected by the EGR temperature. By-passing the EGR led to a higher intake mixture at the cylinder but not influencing the thermal state of the engine. Furthermore, higher intake mixture will lead to a lower filling efficiency and changing the combustion process time calibrated to the good operating of the engine. Exhaust temperature were monitored to notify if any improvements to the catalyst light off time exist.

High temperature set point was the last strategy to be tested. Thermostat opening temperature was increased by 20°C, and thus the engine operating temperature. Contrary to the previous strategies, high temperature set point influences the steady state stage of the engine and not the warm-up stage. However, the latter was extended within the new strategy. This strategy had only an influence on NEDC, WLTC and AH because they are the only driving cycles to reach the steady state stage. NEDC reaches its regulation temperature at the end of cycle leading to an insignificant fuel savings with the new strategy of 0.03%. High operating temperature will lead to higher lubricant temperatures too. However, increasing the coolant temperature by 20°C will not lead to the same increase in the lubricant temperature. Fuel savings were 2.12% and 1.22% for WLTC and AH respectively.

Conclusion

Thermal management proved to be effective in reducing the fuel consumption. Thermal management's target is to let the engine run at its regulation temperature as quickly as possible. Moreover, it can let the engine work at high temperature level during its steady state stage but always with respect to its thermal stresses. The target of this thesis was to valorize the best thermal management strategies that fit on a 4-cylinder turbocharged Diesel Engine using numerical simulations.

For that purpose, engine model was built upon different engine tests done in Ecole Centrale de Nantes. Engine model covers the air path as well as the coolant and the lubricant paths. To identify the best thermal management strategies suitable to the engine (and can get the best engine fuel savings to answer the different emissions regulations), an energy balance was applied on the engine. During this thesis, the energy balance did not cover a specific operating point but a complete driving cycle. Driving cycles were chosen in a way to cover a variety of driving styles going from the homologated ones to highway, city and suburban driving styles. The main outcomes of the energy balance highlighted the importance of the friction power losses, heat within the exhaust gases and transferred to the coolant circuit. Moreover, it was noticed that during the steady state stage, when the engine reaches its thermal equilibrium, the heat transferred to the coolant as well to the lubricant were totally lost to the ambient air. Based on that, aiming to reduce the friction losses at the first stage of the cycle as well as the wall heat losses were primordial. Furthermore, reducing the latter by using the main heat losses of the engine (heat transferred to the ambient and the exhaust gases) was the most logical.

Heat storage was the first thermal management strategy to be tested during this work (Chapter 3). A first application on the coolant was studied. Hot coolant storage tank of 3L was added to the coolant circuit and was controlled by different valves depending on the temperature. Different configurations were proposed to study the influence of the strategy on the coolant, the lubricant and the system. Coolant temperature profiles showed an improvement by increasing the initial starting temperature of the cycle. However, all along the cycle the coolant temperature with the new strategy converged later to the reference case because of the lower heat source available within the new strategy. No remarkable advance in the regulation temperature was registered using this strategy. Furthermore, one configuration aimed to use the hot coolant directly to heat up the oil via the oil cooler. However, a part of the heat transferred to the lubricant circuit was lost in the oil cooler thermal inertia. Therefore, fuel consumption savings were lower within that configuration. Furthermore, no valve configuration was tested. It brought good fuel benefits to the system, but running the engine over the different driving cycles with the storage tank at the ambient temperature had major drawback: a remarkable fuel overconsumption. Hot coolant storage strategy proved its importance in reducing the fuel consumption of the engine over the different driving cycles at warm days as well as at the coldest. The best outcome was with the first configuration: placing the storage tank in the radiator branch, downstream the thermostat and upstream the radiator. Hence, the added volume will not influence the warm-up stage of the engine during the cold start and will be charged once the regulation temperature was reached and the engine running in its steady state stage.

A second application of the heat storage was on the lubricant (Chapter 3). Similar to the first, hot oil storage tank of 1L was added to the lubricant circuit and was controlled by a valve in function of the temperature. The storage tank was isolated from the engine during the warm-up stage. It was charged during the steady state stage. During the next cold start, the hot lubricant is circulated in the engine, leading to lower the oil's viscosity at low temperature, the major factor behind the high friction power. Similar to the coolant strategy, the lubricant within the hot oil storage thermal management strategy started with a higher temperature than converges to the reference case due to the low heat source for the hydraulic circuits. Contrary to the first strategy, reducing the friction power leads to a direct fuel consumption improvement. The former will lead to lower the wall heat losses. Reducing wall heat losses will have two influences: improving the combustion efficiency, thus the fuel consumption and at the same time will lead to increase the exhaust gases temperature and thus their energy losses. Then, other configurations were proposed to improve the hot oil storage strategy. Integrating the storage in the oil sump consists of isolating a part of it. Hence, this configuration combines the heat storage and reducing the oil mass inertia of the system. The control of the isolating part is done with a valve in function of the temperature at first place and then adding the criterion of the rotational engine speed. A third configuration was evaluating the storage strategy with no valves. The first proposition brought higher benefits in terms of fuel consumption. However, the engine speed criterion had a drawback on some driving cycle, improvements on some and insignificant influence on the others. Hot oil storage strategy proved its importance in reducing the high friction power levels at the first stages of an engine cold start. Long driving cycles led to recharge the storage tank in the warm days and some cycles succeeded during the cold days. However, the short cycles stayed in warm-up stage until the end of the driving cycle. These cycles were imagined used back to a long one.

Exhaust gas heat recovery was the second thermal management strategy to apply in order to improve the fuel consumption (Chapter 4). During chapter 2, it was proved that exhaust gas losses are important for the different driving cycles and get higher through the cycle. To recover this energy, a heat exchanger was installed on the exhaust line downstream the catalyst to not alter its light-off time. An original EGR cooler was chosen and characterized on an experimental test bench to add it to the engine model. Experimental tests were done at Ecole Centrale de Nantes. Data points covered different water mass flow rates, different air mass flow rates and temperatures. Once the heat exchanger model showed a good agreement with the experimental setup, it was implemented in the engine model. Two major propositions were tested: indirect and direct heating of the lubricant. The first one used the coolant as a medium fluid between the exhaust gases and the lubricant. The results showed a remarkable improvement in the coolant temperature profile. Important advances in reaching the regulation temperature were registered during the study. Lubricant temperature showed good improvements too. However with the direct heating of the lubricant, the latter reached high temperature level faster than before. Improving the lubricant temperature will lead to reduce its viscosity and thus the friction power losses. The drawback of the direct heating of the oil was the high level of lubricant temperature reached during some driving cycles that may lead to an oil film break-down and further complications in the engine. The solution was to move the heat exchanger from downstream the oil cooler to downstream the engine. It allows the

lubricant to exchange some heat at the oil sump as well as at the oil cooler before entering the engine. Despite that the second configuration led to lower the high level of the lubricant in the driving cycles, it reduced the fuel consumption savings. A by-pass on the exhaust line can be another solution for this drawback. A final study was to install two heat exchangers back to back: the first is to heat the lubricant and the second is for the coolant. However, the improvement brought to the coolant temperature profile compared to the direct heating of the lubricant did not cover the drawback of the back pressure imposed by the two heat exchangers on the exhaust line.

The study was also done on with different minor strategies. The last chapter, chapter 5, includes five different strategies: influence of oil's grade, engine insulation, charge air cooler by-pass, EGR by-pass and high temperature set point. Changing the oil type to 0W20 (less dependent on the temperature) led to fuel benefits. It has a low viscosity at low temperature leading to low friction power at the start of the driving cycle. Furthermore, the influence of the oil's grade was tested on the heat storage strategy during chapter 3. Engine insulation was tested by reducing the external convection coefficient of the engine by 71% and then by 100%. The latter meant to have no heat losses to the ambient. By-passing the charge air cooler and the EGR cooler had a purpose to increase the cylinder temperature by increasing the intake air mixture to improve the combustion efficiency. However, increasing the air mixture temperature will lead to lower the filling efficiency. By-passing the EGR cooler, a heat source of the coolant led to longer warm-up stage of the engine. High temperature set point was tested by increasing the functioning temperature of the engine by 20°C. This is the only strategy that brings improvements during the steady state stage. Hence, three driving cycles did not show any improvements regarding this strategy. Increasing the temperature of the engine will lower the wall heat losses as well as the friction power. Therefore, fuel savings were registered for the other driving cycles.

Numerical simulations for almost all the strategies were run over five different driving cycles: NEDC, WLTC, AH, AU and HDC. The latter is an in-house developed driving cycle representing a high speed driving for a short time. The strategies were tested at two ambient temperatures: 20°C and -7°C. Most of the thermal management strategies tested in this work influence the transient stage, the warm-up stage of the engine. On one hand, driving cycles with a short transient stage were the one showing the less improvement with the different strategies. On the other hand, AH and HDC were two driving cycles with an engine running always in a thermal transient state. Strategies had the highest influences on these driving cycles. Moreover, the highest improvements were obtained at the lowest ambient temperature: -7°C. At low temperature, the lubricant viscosity variation is much more important. Friction power improvements are directly linked to fuel consumption savings.

The work in this thesis extends to many perspectives:

- Valorizing other thermal management strategies: Latent heat storage using Phase Change Materials (PCM). This strategy needs to build an experimental setup to characterize the behavior of the materials during the solidification and liquefaction stages. Moreover, a study over the PCM existing on the market is needed to find the optimal one for the thermal behavior of the engine.

- Valorizing the influence of the oil's grade on the exhaust gases heat recovery. Changing the type of the lubricant lowered the fuel benefits with the heat storage. It will be interesting to valorize its influence on the direct heating of the lubricant with the exhaust gases, because the latter's benefits are based on the improvement of the viscosity at low temperature.
- Extending the study of the engine insulation to the soak period. Assessing the temperature drop over the night and have a new initial temperature of the different fluids during the next cold start.
- Having a more developed thermal model. Introduce a nodal model of the different thermal masses of the engine replacing the existing 5-Masses simple model used in this simulation. The nodal model will have a more realistic behavior over the temperature distribution in the engine and lead to a more developed lubricant circuit too. Moreover, introducing the different masses will increase the degree of freedom in the system and allows the application of new strategies as well as the study of its influence on the different engine parts.
- This study was based on neglecting the cabin heater. Different thermal strategies will be interested for a cabin heat application and the human body comfort in the vehicle. During the cold days, the warm-up is largely influenced by the different facilities of the cabin comfort: its thermal comfort as well as the defogging and defrosting.
- Every thermal management was always studied and valorized alone. What about combining different thermal management strategies and analyzing the effect of the cumulative benefits.
- Different studies done during this thesis were on a Diesel engine. Shifting to Gasoline engine will bring more insight about the influence of the thermal management strategies on different engine types.
- Introducing the hybrid vehicle. Coupling the internal combustion engine model with an electrical one will lead to manage the different thermal behavior of the two engine types, as well as the battery and the thermal comfort of the cabin.

Publications

Articles in international journals

- **H. SARA**, D. CHALET, M. CORMERAIS and J-F. HETET, "Oil Strategies Benefits over Different Driving Cycles using Numerical Simulation", Journal of Thermal Science. **Submitted, accepted and currently in press.**
- **H. SARA**, D. CHALET, M. CORMERAIS and J-F. HETET, "Evaluation of hot water storage strategy in internal combustion engine on different driving cycles using numerical simulations", IMechE Part D: Journal of Automobile Engineering. **Submitted, accepted and currently in press.**

International conferences with technical papers

- **H. SARA**, D. CHALET, M. CORMERAIS and J-F. HETET, "A Detailed study of an energy balance using numerical simulation on a Diesel engine during transient and permanent phase", **FISITA 2016**, World automotive congress, Busan, South Korea, 26-30 September 2016.
- **H. SARA**, D. CHALET, M. CORMERAIS, T. MARIMBORDES and J-F. HETET, "Fuel consumption assessments of using a hot water storage strategy on a Diesel engine at different ambient temperatures", **VTMS 13**, Vehicle thermal managements systems conference, ILEC Conference Center, London, UK, 17-18 May 2017.

Seminar

- 14-17 June 2016 - **CRIEC 2016** (22ème édition du Colloque de Recherche Inter Ecoles Centrales et Centrale Supelec) | Campus de Centrale Supelec (Châtenay-Malabry et Gif-sur-Yvette).
    - **Poster** : **H. SARA**, D. CHALET, M. CORMERAIS, J-F. HETET and T. MARIMBORDES, "Hot Water Storage Strategy On An Internal Combustion Engine To Reduce CO_2 Emissions"

Résumé en français

1. Introduction

L'augmentation de la concentration des gaz à effet de serre dans l'atmosphère abouti au réchauffement climatique. Le dioxyde de carbone ($CO_{2)}$ est l'un des gaz à effet de serre émit par des activités humaines. En 2011, la part de l'Europe dans l'émission globale de CO2 était de 10% [1]. Cependant en 2010, une étude statistique a montré que le secteur automobile est classé premier en terme de consommation d'énergie avec un pourcentage de 33.2% [3]. De plus, une projection en 2030 estime que l'utilisation du moteur à combustion interne pour le transport est de 67% [7]. Avec ces problèmes, les normes de dépollution deviennent de plus en plus sévères et les constructeurs automobiles cherchent à réduire la consommation en carburant des véhicules. La quantité de CO_2 permise en 2020/21 sera de 95g/km [10]. A partir de 2019, tout gramme dépassant le seuil sera taxé par 95€ par véhicule vendue [13]. Pour valoriser les émissions d'un véhicule, des cycles d'homologation sont utilisés. Le cycle NEDC était celui homologué jusqu'à Euro 5 et il va être remplacé par le cycle WLTC pour Euro 6. Ces cycles imposent un démarrage à froid du véhicule.

En outre, des études statistiques faites par la commission européenne déclare que le trajet moyen en véhicule en Europe est de 10 km et pour une période de temps courte [16]. Ces conditions aboutissent à un moteur fonctionnant en mode transitoire.

Dans un premier temps, afin d'améliorer le rendement du moteur, les experts ont cherché à améliorer le rendement de combustion, le rendement de remplissage, à modifier le temps d'ouverture et de la fermeture des soupapes … Cependant, ces stratégies n'améliorent pas la montée en température du moteur. Pour cela, la bonne gestion thermique est l'un des moyens les plus efficaces pour réduire la consommation du moteur. La gestion thermique du moteur est l'étude des flux de chaleur et les pertes énergétiques de ce dernier. L'énergie introduite dans le moteur avec le carburant injectée n'est pas utilisée en totalité pour faire avancer le véhicule mais une partie importante est perdue sous forme de chaleur soit avec les gaz d'échappement, soit en cédant de la chaleur au circuit de refroidissement ou soit sous forme de frottements. L'objectif de la gestion thermique est d'améliorer la phase de montée en température du moteur, ainsi qu'augmenter la température de régulation. Cette dernière doit toujours prendre en compte les contraintes thermiques des différentes parties du moteur. Une application de la gestion thermique sur le moteur consiste à déterminer un nouveau produit qui permet aux différents composants du moteur d'atteindre leurs températures de fonctionnement le plus rapidement possible. En effet, pour valoriser ces stratégies et les concepts développés, les constructeurs ont tendance à utiliser la simulation numérique plutôt que de concevoir des prototypes et de les tester sur différents bancs d'essais.

L'objectif de la thèse est de valoriser et analyser les nouveaux systèmes de gestion thermique par simulation numérique. Pour cela, un modèle a été développé avec le code de simulation GT-Suite, calibré avec des essais moteurs, puis les différentes stratégies thermiques ont été testées pour les différents cycles d'homologations et différentes températures ambiantes.

Le chapitre 1 présente une étude bibliographique sur le sujet. La modélisation des différents transferts thermiques dans le moteur, ainsi que les différentes sources de chaleur ont été présentées. Ensuite, les bilans d'énergie et d'exergie sont introduits. Enfin, les différentes

stratégies thermiques étudiées ont été définies et présentées en soulignant leurs potentiels pour améliorer le rendement du moteur.

Les travaux de la thèse commencent dans le chapitre 2. Ce chapitre commence par l'introduction des essais moteurs faits à l'Ecole Centrale de Nantes nécessaires pour le développement du modèle du moteur et de ses circuits de refroidissement et de lubrification en utilisant le logiciel GT-Suite. Une fois le modèle calibré, les différents cycles d'homologation sont définis. Puis un bilan d'énergie qui couvre non seulement le moteur mais ses circuits hydrauliques a aussi été effectué. Le but de ce bilan d'énergie est de déterminer les différentes pertes dans le moteur ainsi que les stratégies thermiques nécessaires permettant de récupérer cette énergie.

Le chapitre 3 étudie les solutions de stockage d'énergie. L'étude est divisée en deux parties. La première est le stockage d'énergie avec du liquide de refroidissement. L'étude consiste à définir le bon volume de stockage, la température initiale, les différentes pertes de chaleur pendant le temps d'arrêt du moteur, ainsi que l'influence de la masse ajoutée. La deuxième partie permet d'étudier les systèmes de stockage d'énergie avec de l'huile. Les deux stratégies sont valorisées avec cinq cycles différents de conduites ainsi que deux températures ambiantes 20°C et -7°C et sous forme de plusieurs configurations.

La récupération de chaleur au sein des gaz d'échappement est mise en œuvre dans le chapitre 4. Un échangeur thermique est caractérisé sur un banc d'essais puis modélisé. Le réchauffement indirect et direct d'huile, ainsi que les deux stratégies en série, ont été testés avec différentes conditions.

Puis différentes stratégies de fonctionnement au niveau du moteur ont été étudiées et valorisées dans le chapitre 5. Ces stratégies sont : le type d'huile, l'isolation du moteur, le by-pass du refroidisseur d'air suralimenté, le by-pass du refroidisseur d'EGR et une température de régulation du moteur élevée.

Finalement, une conclusion résume les différents résultats et présente les perspectives de ces travaux de thèse.

2. Chapitre 1 - Etude bibliographique

Modélisation

En modélisant les transferts thermiques dans le moteur, les conséquences des modifications des architectures moteur peuvent être facilement évaluées en réduisant ainsi le nombre de prototype et les essais au banc d'essais moteurs. Cela permet une conception et une évolution plus rapide des moteurs, plus économique et avec une gestion thermique améliorée. Malgré le fait que la simulation des moteurs soit plus rapide et moins chère que la construction des prototypes, les modèles ont besoin de nombreux paramètres d'entrée, et de moyens de calculs de plus en plus performant.

La source de chaleur du moteur est due à la combustion ainsi qu'aux frottements des différentes parties tournantes.

Deux types de transferts thermiques ont lieu dans la chambre de combustion : convection forcée et radiation. Il faut noter que le terme radiatif est négligeable dans les moteurs à allumage commandé, puisqu'il ne présente que 3 à 4% des transferts thermiques. Au contraire, les moteurs Diesel, qui, à cause des suies, du dioxyde de carbone et de la vapeur d'eau, ont un niveau d'échange radiatif de 7 à 23% [19].

La corrélation pour le coefficient d'échange global la plus utilisée est celle de Woschni [21]. Cependant cette corrélation a subi plusieurs modifications au fil des ans selon les différents essais expérimentaux [19], [20], [22]–[24].

La deuxième source de chaleur est associée aux frottements. Elle est proportionnelle à la viscosité d'huile, à la vitesse de rotation du moteur mais moins dépendante du couple. Différentes études ont été réalisées pour la détermination des pertes par frottements dont la plupart était faites dans des conditions statiques avec des corrections pour se rapprocher du comportement réel des frottements pendant la phase transitoire [26], [29], [30].

Les transferts thermiques avec l'eau, l'huile et l'environnement extérieur sont développés dans plusieurs travaux de recherche [22], [32]–[39].

La modélisation nodale est une des méthodes de modélisation existantes. Elle a fait ses preuves dans différentes applications, et est basée sur l'analogie thermique/électrique. Cette méthode consiste à découper les volumes physiques de différentes parties de moteurs, les masses métalliques, le circuit de refroidissement et le circuit de lubrification en un nombre de volume fini isotherme. Chaque petit volume présente un nœud avec un bilan énergétique qui prend en considération les interactions avec les nœuds voisins de type d'échange convectif, conductif et radiatif ainsi que les échanges avec les sources de chaleur. Dans le cas de régime transitoire, les paramètres thermo-physique du volume telle que la viscosité dynamique, la conductivité thermique … varient en fonction des variables intensives telle que la température, la pression … La modélisation nodale a été effectuée dans de nombreux travaux [41]–[49].

Bilan d'énergie

L'énergie est une grandeur physique qui caractérise l'état d'un système et qui est conservée au cours des transformations. L'énergie s'exprime en joules. Elle peut prendre plusieurs formes mécanique, électrique, magnétique, nucléaire, thermique, chimique …Les

fondamentaux de l'énergie ont été étudiés par Marty [53] et bien décrits par Winterborne [54]. L'entropie permet de quantifier la dégradation de l'énergie par les irréversibilités des transferts et des transformations énergétiques. La définition suivante de l'exergie est donnée par Lallemand [57]:

L'exergie d'une certaine quantité de matière contenue dans un système est une mesure du potentiel de production (ou de réception) d'un travail maximal (ou minimal) par le supersystème (constitué du système et de son milieu ambiant), qui permettra à cette quantité de matière d'être ramenée de son état initial à un état d'équilibre inerte avec le milieu ambiant.

La plupart des bilans énergétiques du moteur sont couplés à des bilans exergétiques. Le bilan exergétique montre que la totalité de l'énergie perdue en forme de transferts thermiques aux parois ou avec les gaz d'échappement ne peut pas être totalement récupérée en énergie ou converti en travail. Ainsi, une partie de l'énergie est perdue à cause des irréversibilités de la combustion [70]–[78]. Les bilans énergétiques sont différents suivant le type de moteur (à allumage commandé ou à allumage par compression), de véhicules (léger ou non), du nombre de cylindres, suivant que le moteur est refroidi ou isolé, etc… [55], [58], [62], [64], [67], [72], [75], [81]–[83]. Presque tous les bilans soulignent trois importantes pertes dans le moteur : transfert thermiques aux parois, les gaz d'échappement et les frottements. Cependant toutes les applications étaient pour des points de fonctionnement précis du moteur et rares sont les bilans énergétiques réalisés sur des cycles d'homologations.

Systèmes de gestion thermiques

Thermostat

Le thermostat traditionnel est un thermostat mécanique qui par expansion, à cause de l'élévation de la température, ouvre la branche du radiateur. Le thermostat classique a été remplacé par le 'smart' thermostat contrôlé électriquement. Le thermostat fonctionne en maintenant une température stable du liquide de refroidissement aboutissant ainsi à une fluctuation relativement importante de la température des masses métalliques. Au contraire, le thermostat électrique maintient une température stable des masses métalliques en faisant varier la température du liquide [42], [85]. 0.9% de réduction de consommation spécifique est obtenue en utilisant ce type de thermostat [86].

Audi/Volkswagen ont ajouté une résistance électrique afin de réchauffer le thermostat et ainsi augmenter la plage de fonctionnement du thermostat [87], [88].

Les thermostats à multivoies sont aujourd'hui répandus. Tous les constructeurs automobiles en développent. Il s'agit d'une vanne qui peut contrôler plusieurs branches en même temps : le radiateur, le chauffage d'habitacle, le refroidisseur d'EGR … Différentes stratégies peuvent être appliquées avec ces vannes comme : Split cooling, zero flow, régulation à haute température … Le gain en consommation ainsi que la montée en température peuvent varier en fonction du cas d'application [90]–[99].

Pompes

Dans un premier temps, les pompes ont été entrainées par le vilebrequin et ont été conçues pour le refroidissement du moteur dans les conditions les plus sévères aboutissant ainsi à un

refroidissement excessif du moteur dans les autres cas. Les pompes électriques ont la possibilité de contrôler le débit du liquide de refroidissement selon la demande. Lors du départ à froid, la pompe délivre le débit minimal (0-flow) et lorsque le moteur a atteint sa température de fonctionnement, les performances de la pompe augmentent afin de fournir le débit nécessaire pour le refroidissement du moteur. Une pompe électrique est souvent couplée à un thermostat électronique ainsi qu'à un ventilateur électrique. Le contrôle électrique donne une grande souplesse pour manipuler les différents systèmes selon les conditions. De plus, elle diminue les pertes auxiliaires du moteur. Selon les différentes applications, une réduction de la montée en température de 23.3% ainsi qu'un gain de consommation de 2.5% sont obtenus [49], [85], [89], [101], [102], [107].

Stratégies de gestion thermiques

Zero-flow

La stratégie 0-flow restreint le débit du liquide de refroidissement au moteur seul tant que ce dernier fonctionne à basse température. Cette stratégie est appliquée avec la pompe électrique. Elle aboutit à l'élévation de la température du liquide de refroidissement et de l'huile de lubrification donc à une diminution des frottements. Des gains de consommation de 1.5% ainsi qu'une réduction de la phase de montée en température de 45% sont obtenus selon les applications [17], [23], [104].

Split cooling

La technique propose deux circuits de refroidissement : un pour la culasse et l'autre pour le bloc cylindre permettant ainsi une flexibilité pour la régulation des températures dans chaque compartiment du moteur. Les conditions désirées consistent à avoir une culasse qui fonctionne à une température plus basse améliorant ainsi le rendement volumétrique. Une température plus élevée du bloc engendre une diminution des frottements. Cette stratégie peut être appliquée avec des vannes multivoies [95]. Selon Pang *et al.* [108] cette stratégie peut aboutir à un gain de consommation de 4-6%. L'influence de split lubrification a également été testée par Zhao *et al.* [111]. Le débit de l'huile dans le bloc moteur et dans la culasse influence d'une façon importante le flux de chaleur transmis au circuit de lubrification.

Température de régulation élevée

Une augmentation de la température de fonctionnement du moteur est obtenue en permettant l'accès au radiateur avec une température plus élevée. Cette stratégie augmente la température et diminue donc les frottements du moteur. De plus, une température plus élevée diminue les pertes aux parois et améliore ainsi le rendement de la combustion. Selon les applications, les gains de consommation varient entre 1.6% et 5% [83], [95], [102], [112]–[115].

Isolation du moteur

Afin de limiter les pertes par radiation et convection vers l'environnement extérieur, l'isolation du moteur peut être effectuée. Pour cela, des couches d'isolants peuvent être appliquées sur une partie spécifique du moteur ou sur tout le moteur [17], [100], [116]–[118]. Selon les études, les gains sont valorisés soit en termes de gain de consommation soit en termes de réduction de pertes de température pendant le temps d'arrêt du moteur. Une autre possibilité de gérer la thermique sous-capot véhicule consiste à utiliser des volets obturateurs.

Une étude faite par Makam *et al.* [119] abouti à l'augmentation de la température du fluide de lubrification de 20°C.

Carter d'huile

Le carter d'huile à volume variable a pour objectif de réduire la masse totale d'huile de lubrification mise en circulation pendant le départ à froid du moteur. Cette stratégie fut le centre d'études de plusieurs chercheurs scientifiques qui aboutissent à des résultats prometteurs en terme de température ainsi qu'en terme de consommation en carburant. Les résultats en consommation ont variés entre un gain de 0.8% à 10% selon les différentes conditions de mesures et d'études [100], [122]–[124].

Le type d'huile a une grande influence sur la consommation d'un moteur. Pour les basses températures et en changeant le type d'huile, la viscosité d'huile baisse, aboutissant à une réduction des frottements. Des réductions de 4.7% sont obtenues dans les études de Nouvel *et al.* [125] .

Récupération de chaleur

La récupération de chaleur au sein des gaz d'échappement a été étudiée par plusieurs chercheurs. Dans un premier temps, le cycle de Rankine a été étudié [79], [127], [128]. De nos jours, les échangeurs thermiques sur la ligne d'échappement sont le centre d'attention de plusieurs études [86], [130], [132]. Cependant, l'installation des échangeurs sur la ligne d'échappement doit prendre place en aval des catalyseurs pour ne pas retarder leur activation. L'application de cette stratégie selon les différentes conditions aboutissent à des gains remarquables variant de 0.6% jusqu'à 15% [31], [99], [131], [133], [135], [136].

Stockage d'énergie

Le stockage d'énergie consiste à stocker de l'énergie pendant la phase de régulation du moteur afin de l'utiliser durant le prochain démarrage à froid. Deux méthodes de stockages existent : soit sous la forme de chaleur sensible soit sous la forme de chaleur latente. La deuxième forme nécessite l'ajout d'un échangeur (elle a besoin de plus de temps pour le processus d'échange thermique).

Le stockage d'énergie dans de l'eau chaude a été testé par Kuze *et al.* [137] et permettant d'obtenir un gain de 3% en consommation après 20 min pour une température ambiante de 5°C. La même stratégie a de nouveau été testée par Reverault *et al.* [122] en l'appliquant sur plusieurs cycles d'homologation et par Bent *et al.* [116] en introduisant le split cooling.

Le stockage sous forme de chaleur latente est fait en utilisant des matériaux à changement de phases (MCP). La difficulté est de choisir le MCP qui est le plus adaptable à l'application. Plusieurs types ont été comparés par Kim *et al.* [139]. Les études concernant cette stratégie diffèrent par le ballon de stockage, sa forme, son isolation ainsi que le PCM utilisé [122], [140]–[142].

Les matériaux à changement de phases ont également été utilisés pour la gestion thermique des batteries dans les véhicules hybrides [151]–[153].

3. Chapitre 2 – Préparation des travaux de la thèse

Modèle du moteur

Les études sont faites sur un moteur Diesel, 4 cylindres, turbocompressé. Les caractéristiques du moteur sont présentées dans le tableau suivant.

Tableau 1- Caractéristiques du moteur

Type de moteur	Allumage par compression
Rapport de compression	15.3
Nombre de cylindres	4 cylindres en ligne
Nombre de soupapes par cylindre	4
Diamètre	76 mm
Course	80.5 mm
Puissance maximale	75.4 kW at 4000 tr/min
Couple maximal	227 N.m at 2750 tr/min

Les essais moteurs ont été faits aux bancs d'essais de l'Ecole Centrale de Nantes. Des modifications ont été faites au moteur avant son installation sur le banc. Des essais transitoires et statiques ont été enregistrés afin de calibrer le modèle du moteur et ses circuits de refroidissement et de lubrification. Pour les essais stabilisés une cartographie a été réalisée. Le couple du moteur a varié de 20 N.m à 200 N.m avec un incrément de 20 N.m tandis que la vitesse de rotation du moteur a varié de 1000 tr/min à 4200 tr/min avec un incrément de 100 tr/min. De plus, des tests avec un démarrage à froid ont été faits.

A partir de ces essais, un modèle de moteur a été développé dans l'environnement GT-Suite. Le modèle est divisé en deux parties : le modèle 'haute fréquence' qui comporte la partie combustion ainsi que les tubulures d'admission et d'échappement. Le pas de temps du modèle HF est 1° d'angle de vilebrequin. La deuxième partie concerne les circuits hydrauliques : refroidissement et lubrification. Le modèle thermique contient les différents compartiments des circuits hydrauliques : la pompe à eau, la pompe à huile, le radiateur, le carter d'huile, le thermostat, la vase d'expansion, le refroidisseur d'EGR et le refroidisseur d'huile. Le chauffage de l'habitacle n'est pas pris en compte dans cette étude mais modélisé sous forme de pertes de charges dans la branche de l'échangeur avec l'EGR. Le pas de temps du modèle thermique est de 1s. Ces deux modèles sont dépendants l'un de l'autre. Le modèle HF fournit les flux de chaleur nécessaires pour l'échauffement des fluides, tandis que le modèle thermique renseigne les températures nécessaires pour le bon fonctionnement de la combustion. De plus, la température du lubrifiant est utilisée pour la correction des forces de frottements introduisant ainsi la dépendance de ces derniers à la viscosité d'huile.

Les cycles d'homologation

Les différentes stratégies de gestion thermique seront testées sur différents cycles routiers.

NEDC

Le cycle NEDC est le premier cycle choisi car il est le cycle homologué officiel utilisé pour valoriser les émissions des véhicules pour répondre aux normes de dépollution. Le cycle NEDC est composé d'une répétition d'un ancien cycle ECE-15 à domination urbaine, auquel s'ajoute un cycle extra-urbain. Avec euro 7, le cycle NEDC est prévu d'être remplacé par le cycle WLTC.

WLTC

Le cycle WLTC a trois cycles appliqués en fonction de la puissance massique du véhicule. La majorité des véhicules légers appartient au WLTC classe 3. Ce dernier est divisé en quartier parties : basse, moyenne, haute et très haute vitesse. Le cycle WLTC est le cycle harmonisé au niveau mondial.

Artemis Highway

Les cycles d'Artémis sont des cycles basés sur des études statistiques en Europe. Ce ne sont pas des cycles légalisés pour la mesure des émissions. Cependant, ces cycles sont représentatifs et proche du mode de conduite des européens. L'Artémis Highway est un cycle sévère où le véhicule atteint des vitesses élevées dans un temps de conduite très court. Le cycle dure 1068s pendant lequel le véhicule parcourt une distance de 28.7 km.

Artemis Urban

Ce cycle est représentatif d'un cycle de conduite en ville. La durée du cycle est de 993s et la voiture parcoure seulement 4.8 km avec une moyenne de vitesse de 17.7 km/h. Durant ce cycle, le moteur est sous faibles charges la plupart du temps et presque toujours en phase transitoire.

HDC

Un nouveau cycle de conduite est proposé comme présenté sur la figure 1. Il a été choisi comme un compromis entre les deux cycles Artémis choisis pour cette étude. La voiture atteint une vitesse élevée de 90 km/h après 50s. De plus, le véhicule parcoure une distance de 2 km. Il dure 254s et est représentatif d'un cycle de conduite pour un déplacement très court domicile-travail.

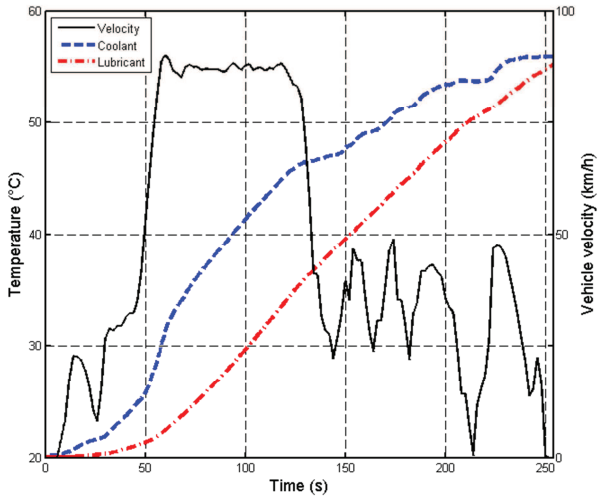

Figure 1 – HDC

Bilan d'énergie

Un bilan d'énergie a été réalisé au niveau du moteur et de ses circuits de refroidissement et de lubrification afin de souligner les pertes de chaleur dans le système. Le bilan d'énergie est appliqué aux différents cycles d'homologations cités précédemment. Le cycle NEDC sera développé dans ce résumé.

NEDC

La température optimale du moteur est atteinte autour de la seconde 1016 du cycle. Le bilan d'énergie est appliqué à quatre moments différents du cycle. Trois qui couvrent la phase transitoire : le début (phase A : 100-200 s), le milieu (phase B : 400-600 s) et la fin (phase C : 800-900 s). Un quatrième pendant la phase permanente du moteur (phase D : 1050-1150 s).

Au début du cycle, et parce que le moteur est toujours froid, la chaleur émise par la combustion ainsi que par les frottements est globalement transmise à la masse métallique tandis que seulement 1.7% est transmise au circuit de lubrification et 10.2% au circuit de refroidissement (Figure 2 - (a)). Ces pertes peuvent être réduites par une diminution de la masse métallique du moteur ou de l'isolation de ce dernier. Cependant, l'isolation du moteur peut aboutir à l'augmentation de la dimension du radiateur pour maintenir la température de fonctionnement du moteur. La figure 2 – (b) montre que la source de chaleur du circuit de lubrification pendant la phase A du cycle n'est pas seulement la combustion et les frottements mais une part importante (environ 52.6%) est fournie par l'échangeur huile/eau. Pendant la phase A du cycle, la température de l'eau est plus élevée que celle de l'huile aboutissant à un transfert de chaleur du premier au second. Cependant, pendant les différentes phases du cycle, la température d'huile s'élève plus haut que celle de l'eau et sa source de chaleur sera limitée à la combustion et aux frottements. Les 52.6% de chaleur gagnée par l'huile n'est qu'une perte pour le circuit de refroidissement et elle correspond à environ 22.3% de la totalité du bilan d'énergie du circuit de refroidissement (Figure 2 – (e)). La partie restante (autour de 77%) est utilisée pour la montée en température du liquide de refroidissement. Pendant la phase B du cycle, la température d'huile s'élève au-delà de celle de l'eau. Malgré le fait que pendant la phase A toute la chaleur transmise à l'huile est utilisée pour sa montée en

température, pendant la phase B, cette valeur est abaissée jusqu'à 55.4%. 39.3% sont transmises au circuit de refroidissement au niveau de l'échangeur huile/eau (Figure 2 – (c)).

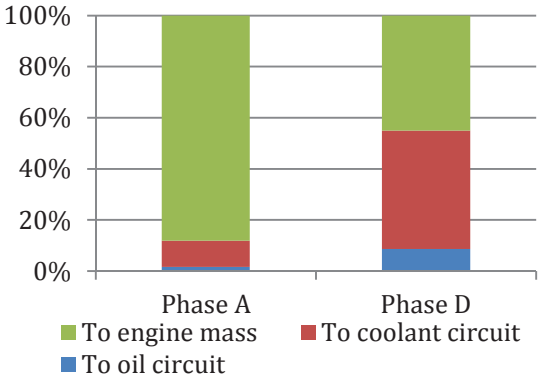

(a) : Engine thermal power source destiny

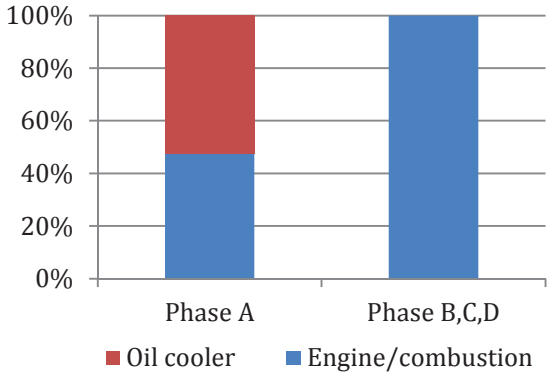

(b) : Oil thermal power source

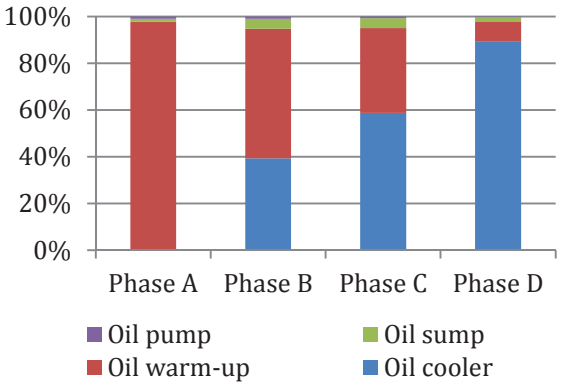

(c) : Oil circuit energy balance

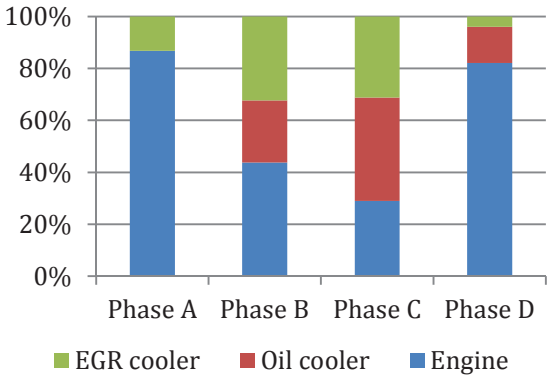

(d) : Coolant thermal power source

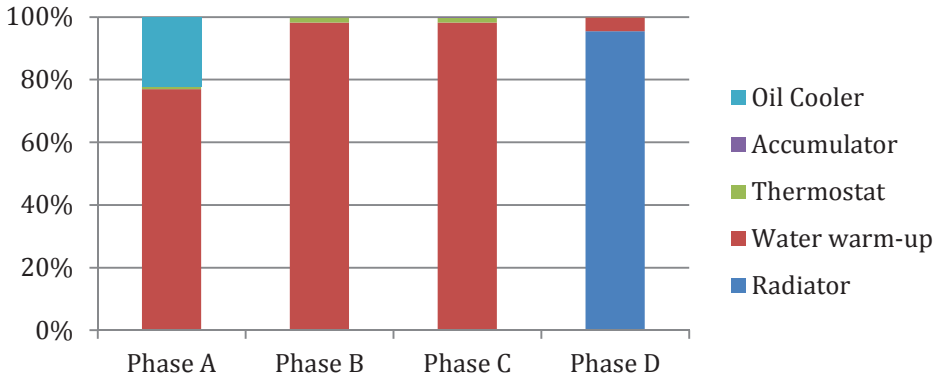

(e): Coolant circuit energy balance

Figure 2 – Bilan d'énergie des circuits de refroidissement et de lubrification

A partir de cette phase, le circuit de lubrification est considéré comme une source de chaleur pour le circuit de refroidissement (Figure 2 – (d)). La source de chaleur du circuit de lubrification pour l'eau atteint son maximum dans la phase C à cause du plus grand gradient de température entre les deux fluides. De plus, à la fin de la phase transitoire avec la

température de l'eau qui augmente et l'accès au radiateur toujours fermé, les pertes aux parois de la chambre de combustion diminue en pourcentage. Lorsque la température de régulation est atteinte, la chaleur est évacuée au sein du radiateur. Pour cela, pendant la phase D, la part de la chaleur du moteur cédée au liquide de refroidissement s'élève jusqu'à 46.4%. De plus, 89% de la chaleur du circuit de lubrification est transmise au circuit de refroidissement. Ce pourcentage ne constitue que 13.8% de la totalité de la chaleur transmise au circuit de refroidissement. Le bilan d'énergie du circuit de refroidissement pendant la phase D indique que presque la totalité de la chaleur du circuit de refroidissement (moteur, circuit de lubrification et EGR) est évacuée à l'air ambiant via le radiateur.

Le bilan d'énergie du moteur présenté dans la figure 3 montre l'évolution des différentes pertes du moteur au fur et à mesure du cycle. Les frottements diminuent en avançant dans le cycle car ils sont proportionnels à la viscosité de l'huile, et le dernier est inversement proportionnel à la température d'huile. Le niveau de frottements diminue de 19% durant la phase A à 6.6% durant la phase D. Les pertes avec les gaz d'échappement augmentent avec la diminution des pertes aux parois. Cette dernière diminution provient de la réduction du gradient de température entre les gaz de combustion et les parois de la chambre. A la fin du cycle, la température du liquide de refroidissement est élevée aboutissant à une diminution des pertes aux parois donc une augmentation de la température des gaz d'échappement. Les pertes au sein des gaz d'échappement augmentent de 16% (phase A) à 27% (phase D).

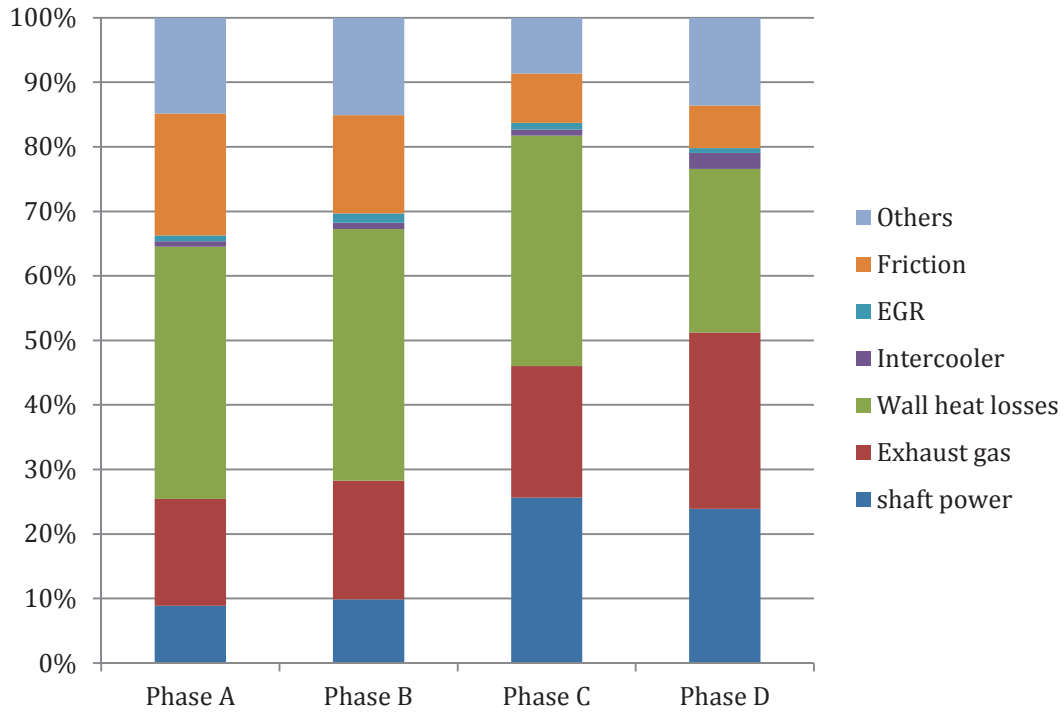

Figure 3 - Bilan d'énergie du moteur pour NEDC

Le bilan d'énergie était ensuite appliqué aux différents cycles d'homologation, le raisonnement est basé sur le même principe que pour le cycle NEDC et les conclusions des bilans sont les suivantes :

- La réduction des frottements est primordiale lorsque le moteur est froid. De plus, les bilans d'énergie montrent que pendant les phases de régulation, une partie importante de la chaleur du circuit de lubrification est transmise à l'eau qui l'évacue à l'air au sein du radiateur. Le stockage d'huile chaude pendant la phase de régulation afin de l'utiliser pendant le prochain démarrage à froid peut aboutir à la réduction des frottements au début du cycle.
- Une des pertes les plus importantes sont les pertes aux parois. Ces pertes ne peuvent pas être éliminées car elles assurent le bon fonctionnement du moteur. Une réduction de la masse du moteur ainsi que son isolation peuvent aboutir à une montée en température plus rapide. L'énergie perdue pendant la phase transitoire est utilisée pour réchauffer les différentes parties du moteur. Pendant la phase de régulation, la totalité de la chaleur est transmise à l'air ambiant et ainsi perdue. Donc, un stockage d'énergie avec le liquide de refroidissement pendant la phase de régulation permet d'utiliser cette chaleur pour améliorer l'efficacité du moteur au démarrage à froid.
- Les gaz d'échappement portent une énergie qui est complètement perdue une fois que ces gaz sont évacués à l'air ambiant. Une récupération de l'énergie au sein des gaz d'échappement en installant des échangeurs thermiques avec les fluides du moteur permettrait à d'améliorer la montée en température de ces derniers. Une diminution des frottements et des pertes aux parois sera obtenue donc une amélioration du rendement moteur.

4. Chapitre 3 - Stockage d'énergie

Stockage d'énergie avec le liquide de refroidissement

Le principe de la stratégie consiste à conserver de l'eau chaude lorsque le moteur est en phase de régulation pour la faire circuler lors du démarrage à froid. Un réservoir d'eau chaude est placé en aval du thermostat et en amont du radiateur dans le but de ne pas influencer la phase transitoire du moteur. Le volume de stockage est contrôlé par plusieurs vannes qui s'ouvrent en fonction de la température. Une fois la température de régulation du moteur atteinte, le thermostat ouvre la circulation vers le radiateur et ainsi le stockage de l'eau chaude prend place. Lors du démarrage à froid, tant que la température du volume de stockage est plus élevée que celle du moteur et tant que le thermostat est fermé, les vannes qui contrôlent la circulation de l'eau chaude vers le moteur s'ouvrent. Lorsqu'une de ces conditions n'est pas vérifiée, ces deux vannes se ferment et le moteur retourne à son état de base.

Les études commencent par la détermination du volume du stockage convenable pour le bon fonctionnement de la stratégie. Des simulations numériques sur le cycle NEDC à une température de 20°C ont été faites en faisant varier le volume du stockage entre 1L, 2L, 3L, 4L et 5L. La température de stockage était égale à celle de la température ambiante. Les résultats donnent une température finale du stockage de 80° pour les volumes d'1L et 2L, tandis que le 3L atteint 76°C, le 4L atteint 71°C et le 5L monte jusqu'à 65°C. D'une part, les premières études montrent que les volumes 1L et 2L n'aboutissent pas à une amélioration importante dans le comportement du moteur. D'autre part, les volumes 4L et 5L sont considérés comme des volumes élevés surtout pour l'encombrement sous-capot. De plus, en tenant compte des pertes thermiques lors de l'arrêt du moteur, ces volumes vont baisser en température pour le prochain démarrage à froid. Afin de déterminer la température initiale de stockage d'eau chaude pour le démarrage à froid, des simulations numériques ont été réalisées en fonction de cette température avec un volume de 3L. La température initiale est comprise entre 30°C et 80°C avec un pas de 10°C. Une température de 60°C a été prise comme une valeur convenable. Ceci a été possible en étudiant l'isolation de ce volume, en choisissant un plastique dont les caractéristiques étaient fournies par MANN+HUMMEL. Pour une période de 15 heures, le volume de 3L perd 15°C.

L'influence de la température ambiante a aussi été étudiée. La température ambiante a été modifiée à partir des 4 valeurs suivantes : 20°C, 10°C, 0°C et -7°C. En diminuant la température ambiante, le moteur met plus de temps pour atteindre sa température de régulation. De plus, avec une température plus basse, les forces de frottements sont plus élevées. Dans ces conditions, la consommation en carburant du moteur pour tous les cycles d'homologation augmente. Cependant, l'augmentation diffère d'un cycle à un autre, dépendant de son style de conduite, donc le temps pour lequel le moteur est en phase transitoire. Par exemple, pour AH le moteur atteint sa température de régulation après environ 300s et ainsi la surconsommation est de 3.8% entre les deux extrêmes températures ambiantes. Pour HDC, cette valeur augmente jusqu'à 40.3% car le moteur est toujours en phase transitoire et ce cycle met en valeur les frottements du moteur car la température n'a pas le temps de monter assez haut après seulement 254s.

Cette stratégie est ensuite appliquée sur les différents cycles avec un volume de stockage de 3L, une température initiale de 60°C et pour deux températures ambiantes : 20°C et -7°C.

NEDC

Les profils de température pour le cycle NEDC sont illustrés dans la figure 5. La courbe en pointillés (ref) présente le moteur dans sa configuration basique sans volume de stockage. Pour une température ambiante de 20°C (Figure 5 – (a)), le liquide de refroidissement présente une avance au début du cycle pour converger ensuite vers la température de référence et atteint la température de régulation au même instant. Cette avance est due à la circulation de l'eau chaude dans le moteur réduisant ainsi les pertes aux parois. Cependant, cette avance diminue au fur et à mesure car avec une température d'eau plus élevée, les pertes aux parois diminuent et donc la source de chaleur du circuit de refroidissement diminue. De plus, avec une température plus élevée, le gradient de température entre les deux fluides augmente au début du cycle améliorant ainsi l'échange entre eux. Pour cela, le profil de température de refroidissement avec la stratégie ne reste pas parallèle à celui de la référence. Le liquide de refroidissement atteint 60°C en avance de 64s. L'huile de lubrification atteint 60°C avec une avance de 34s. Cette stratégie réduit la consommation du carburant de 0.26%.

Pour une température ambiante de -7°C (Figure 5 – (b)), le liquide de refroidissement commence avec une température plus élevée que 0°C, et le liquide atteint 20°C avec une avance de 61s tandis que le lubrifiant atteint 50°C avec une avance de 17s. Le gain de consommation est de 1.17%.

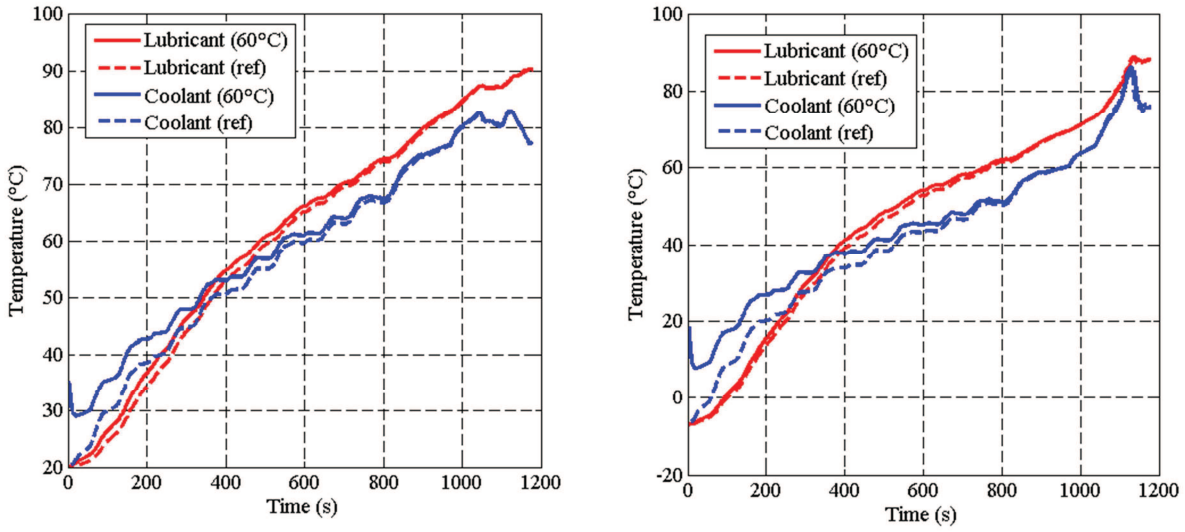

(a) : ambient temperature 20°C (b) : ambient temperature -7°C

Figure 5 – Profil des températures pour deux températures ambiantes pour NEDC

A la fin du cycle NEDC, le volume de stockage atteint de nouveau un niveau de température élevée, suffisant pour la réutilisation du stockage pour un prochain démarrage à froid.

A la fin de cette étude, il a été décidé d'étudier l'impact d'un ajout de masse associée à ce système sur le fonctionnement global. Une masse de 4 kg a été ajoutée mais le profil de

température du liquide de refroidissement ne montre aucune modification. C'est pour cette raison que la faible masse ajoutée au système n'a pas été étudiée par la suite.

Suite à cela, une application sur les différents cycles a été faite, et les résultats obtenus en terme de consommation en carburant sont donnés dans le tableau 2. Les gains en consommation sont plus importants à -7°C.

Tableau 2 - Gain en consommation suite à l'application du stockage d'eau chaude

Cycle	20°C	-7°C
NEDC	0.26%	1.17%
NEDC (à la fin de la phase transitoire)	0.37%	1.17%
WLTC	1.2%	1.83%
WLTC (à la fin de la phase transitoire)	2.36%	3.43%
AH cycle (à la fin de la phase transitoire)	1.09%	1.13%
AU cycle	0.97%	3.04%
HDC	1.24%	1.4%

Deux autres architectures ont également été proposées. L'architecture beta consiste à changer la sortie du volume de stockage et de la mettre en aval de l'échangeur huile/eau pour avoir une influence sur l'huile. Le contrôle des trois vannes n'a pas changé. Les résultats montrent une réduction des gains avec la deuxième configuration. Le profil de température du liquide de refroidissement est inférieur avec cette architecture indiquant un transfert de chaleur au sein de l'échangeur. Malgré cela, le profil de température de l'huile de lubrification ne montre aucune amélioration à cause de l'inertie de l'échangeur.

L'architecture gamma consiste à placer le volume de stockage en amont du thermostat sans aucun contrôle. Ainsi le volume total du moteur pendant la phase transitoire est augmentée de 3L. Lorsque le volume ajouté est à une température ambiante le moteur surconsomme plus que les améliorations notées lors de la simulation avec un volume de stockage à une température élevée. La figure 6 résume l'ensemble des gains obtenus pour les trois architectures.

L'étude du stockage d'eau se clôture avec l'étude de l'influence du type d'huile. L'huile utilisée pendant la simulation a été modifiée. La 15W40 a été remplacée par la 0W20. Les gains de consommation ont été abaissés mais sont toujours existants.

Stockage d'huile chaude

Le principe de cette stratégie est proche de la précédente. Pendant la phase de régulation, de l'huile chaude est stockée dans un volume isolé placé dans une branche parallèle au carter d'huile. Une vanne contrôle cette branche, elle s'ouvre en fonction de la température. Si la température du volume de stockage est plus élevée de celle de l'huile du moteur ou si la température de l'huile du moteur dépasse 90°C, la vanne ouvre l'accès au volume du stockage. Pendant la phase transitoire, le volume de stockage est isolé du moteur et n'influence pas sa montée en température. Le volume est de 1L et sa température initiale est

de 70°C. Cette stratégie est ensuite appliquée sur les différents cycles pour deux températures ambiantes : 20°C et -7°C.

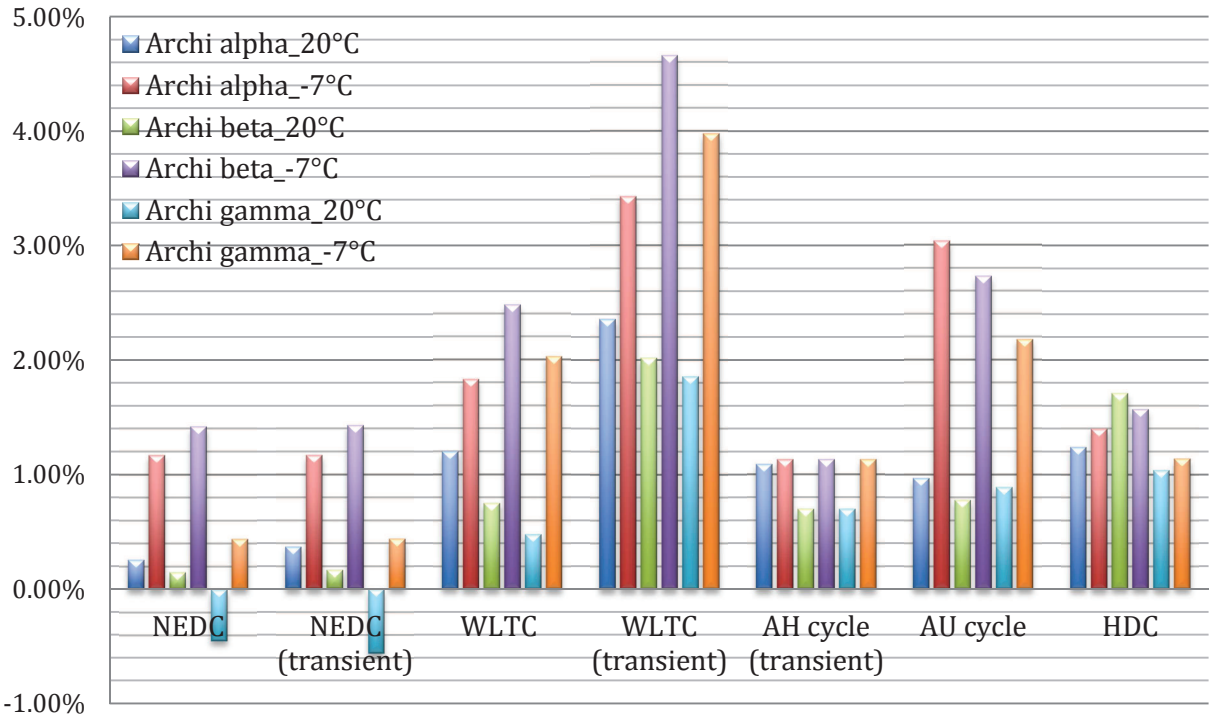

Figure 6 – Gain en consommation des différentes configurations de stockage d'eau

NEDC

Le profil de température ainsi que le profil de la viscosité de l'huile sont présentés dans la figure 7. La stratégie n'avait pas une influence remarquable sur le profil de la température du fluide de refroidissement. Au contraire, l'huile de lubrification montre une amélioration au début du cycle avec une température de plus de 12°C par rapport à la température de base (Figure 7 – (a)). La température d'huile tend à diminuer avec l'utilisation du volume de stockage. Une fois que la température du stockage est égale à celle de l'huile du moteur, la vanne ferme la branche du volume et le moteur reprend sa configuration de base. L'amélioration de la température d'huile au début du cycle aboutit à une chute importante de la viscosité comme illustré dans la figure 7 – (b). La chute atteint un maximum de réduction de 51.3% à la 16ème seconde du cycle. Les forces de frottements sont ainsi réduites de 1.6% et les gains en consommation sont de 0.03%. Pour une température ambiante de -7°C, les profils de température montrent la même tendance que celles présentées à la figure 7. Le lubrifiant avait une avance de 20°C au début du cycle. Le profil de la viscosité atteint une différence maximale de 81.3% à 20s. La réduction de la viscosité du lubrifiant est plus importante à basse température. Cette importante réduction se traduit par une diminution des forces de frottements qui sont réduites de 4.9% et le gain en consommation atteint 6.63%. A la fin du cycle NEDC, la recharge du volume de stockage avec de l'huile chaude n'a pas eu lieu. Une

des solutions est d'abaisser la température d'ouverture de la vanne du volume de stockage de 90° à 80°C.

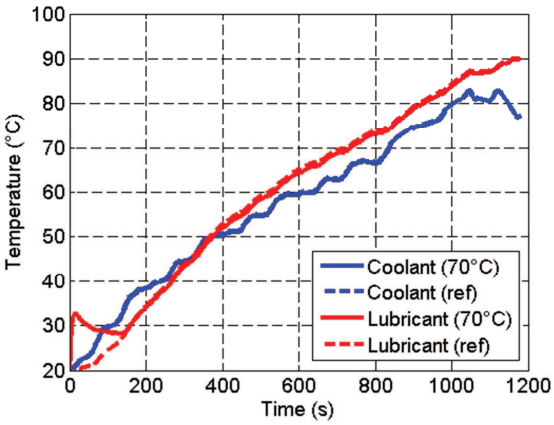

(a): Temperature profile at 20°C

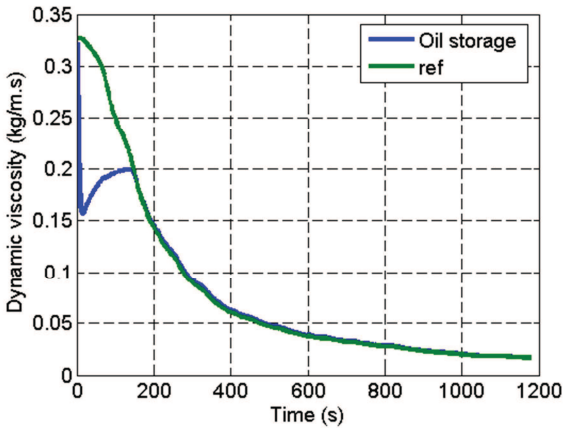

(b): Viscosity profile at 20°C

Figure 7 – Les résultats du stockage d'huile chaude pour NEDC à 20°C

Suite à cela une application sur les différents cycles a été faite, et les résultats en terme de consommation du carburant sont présentés dans le tableau 3.

Tableau 3 - Gain en consommation et de frottements suite à l'application du stockage d'huile chaude

	Consommation		Puissance de frottement	
Cycle	**20°C**	**-7°C**	**20°C**	**-7°C**
NEDC	0.03%	6.63%	1.66%	4.9%
WLTC	1.1%	5%	0.9%	5.84%
AH cycle	-0.12%	0.12%	0.76%	3.5%
AH cycle (à la fin de la phase transitoire)	0.6%	2.24%	3.67%	8.24%
AU cycle	1.2%	5.37%	2.49%	6.31%
HDC cycle	2.47%	8.5%	6.67%	16.7%

La première configuration consiste à ajouter un volume d'1L au circuit de lubrification. Pour améliorer la stratégie du stockage d'huile chaude. Une architecture d'un carter d'huile multifonctionnel a été proposée. Elle consiste à intégrer le volume du stockage dans le carter, donc à isoler thermiquement un litre déjà existant dans le carter. Cette architecture unit la stratégie du stockage d'huile avec celle de la réduction de la masse d'huile du système. L'architecture a été proposée sous formes de 3 configurations. Le volume du stockage est contrôlé pour la configuration A en fonction de la température comme la première architecture étudiée. La configuration B introduit le contrôle en fonction de la vitesse de rotation du moteur avec la température tandis que la troisième configuration, Configuration C, consiste à ne pas contrôler le volume isolé du carter. Les configurations A et B ont montré le

même profil de température sauf pour quelques instants où le moteur dépasse 2500 tr.min^{-1} (ce n'est pas le cas pour les cycles AU et HDC). Avec la configuration C, la montée en température du lubrifiant était plus uniforme que les autres configurations. En effet, la Configuration A présente les meilleures améliorations en terme de consommation et la configuration C montre des améliorations même en supprimant toute forme de contrôle. Les résultats sont illustrés dans la figure 8.

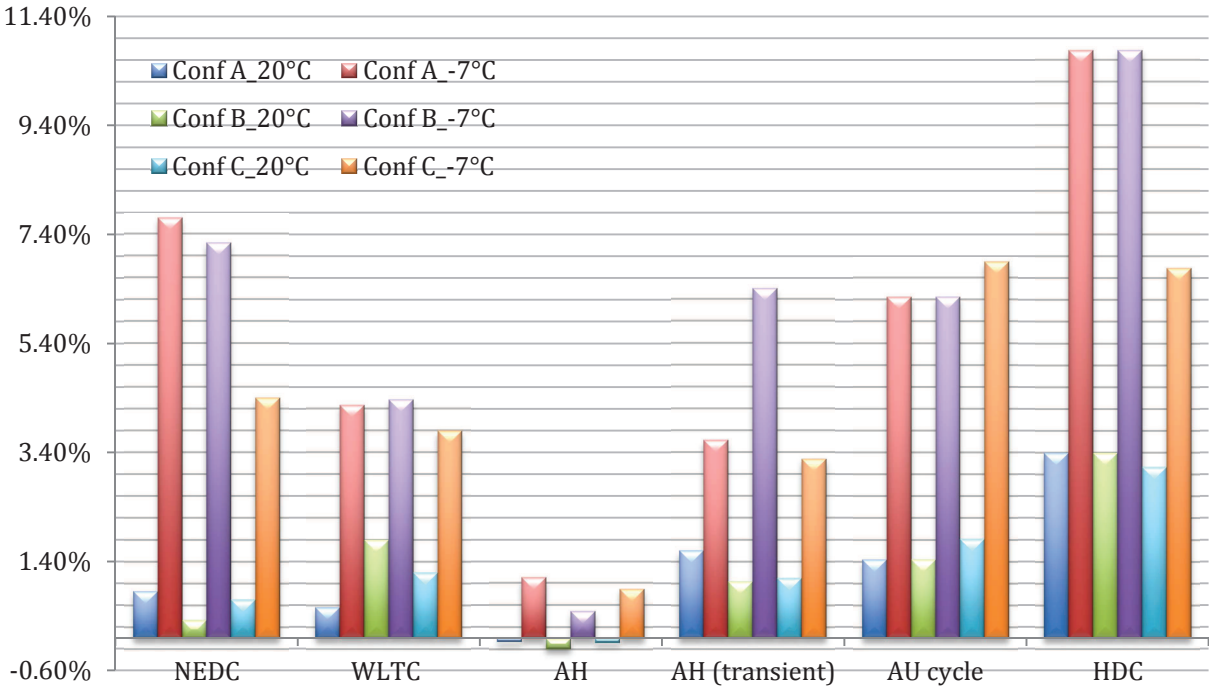

Figure 8 – Gain en consommation des différentes configurations de stockage d'huile

5. Chapitre 4 - Récupération de chaleur

Caractérisation de l'échangeur

Un échangeur d'EGR utilisé sur une Peugeot Boxer 3 a été installé sur un banc d'essais pour être caractérisé. Le banc permet de mesurer les températures d'entrée et sortie de l'air et de l'eau ainsi que les pressions. La température de l'eau à l'entrée était autour de 16°C. Le débit de l'eau a varié entre 4 valeurs : 6, 10, 16 et 23.3 $l.min^{-1}$. Pour chaque débit d'eau, la température d'entrée de l'air a été ajustée à 300, 400 et 500°C. Et pour chaque température le débit d'air a varié entre les valeurs suivantes : 30, 60, 100, 130, 200, 270, 350 et 440 $kg.h^{-1}$. Ainsi 94 points ont été enregistrés. A partir de ces mesures, l'échange thermique entre les deux fluides a été caractérisé ainsi que les pertes de pression au niveau des deux fluides. L'efficacité de l'échangeur variait entre 0.75 et 1. Trois points présentent une efficacité faible de 0.5 pour le débit d'eau de 6 $l.min^{-1}$.

Puis, l'échangeur a été modélisé avec GT-Suite. La notion 'Maître-Esclave' a été utilisée. Les différentes caractéristiques géométriques ont été prises en compte ainsi que les valeurs d'échanges thermiques, ainsi que les pertes de charge. La calibration de l'échangeur a été faite et l'erreur moyenne pour la température de sortie de l'eau est de 3.5%. Dans la suite, l'échangeur a été ajouté au modèle du moteur. Il était installé sur la ligne d'échappement en aval du catalyseur. Plusieurs configurations ont été testées.

Réchauffement indirect de l'huile

La première stratégie consiste à réchauffer indirectement l'huile du moteur en utilisant le liquide de refroidissement pour récupérer la chaleur des gaz d'échappement. Pour cette configuration, l'échangeur côté circuit de refroidissement a été installé dans une branche parallèle à celle du refroidissement d'EGR. L'échange eau/gaz d'échappement n'était pas contrôlé lors des simulations. L'étude a été faite sur les cinq cycles ainsi que pour les deux températures ambiantes : 20 et -7°C.

NEDC

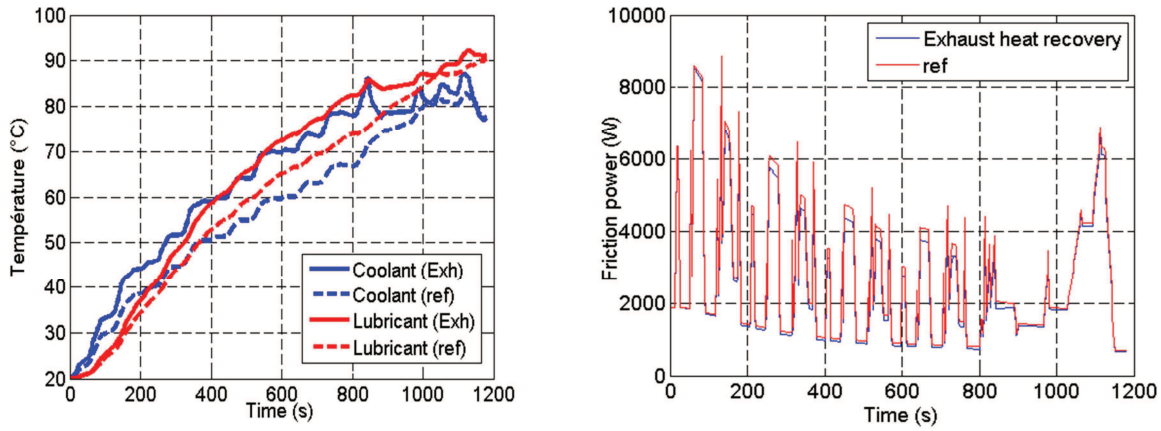

(a): Temperature profile at 20°C (b): Friction power at 20°C

Figure 9 – Les résultats de la récupération de chaleur pour un réchauffement indirect de l'huile pour NEDC à 20°C

Les résultats pour la simulation du NEDC à une température de 20°C sont illustrés dans la figure 9. La ligne pointillée en bleu représente le moteur en configuration de base sans aucune stratégie de gestion thermique. La figure 9 – (a) montre l'amélioration remarquable des profils de température des deux fluides. Dès le début du cycle, un échange a lieu. Le profil de température du liquide de refroidissement est plus élevé pendant toute la phase transitoire. Il atteint 60°C avec une avance de 161s et la température optimale est atteinte pour la première fois à 833s. Le chauffage indirect de l'huile se fait au sein de l'échangeur eau/huile. Le gradient de température entre les deux fluides augmente au début du cycle aboutissant à l'amélioration de l'échange. Le lubrifiant atteint une température de 60°C avec une avance de 101 secondes et 80°C avec une avance de 166s. Une fois que la température de régulation est atteinte et que l'eau circule dans le radiateur, l'huile commence à converger vers le profil de la température de référence. L'amélioration de la montée en température de l'huile se traduit par une réduction des forces de frottements comme montré dans la figure 9 – (b). Ainsi une réduction des forces de frottements de 4.9% a été obtenue et le gain en consommation était de 1.39%. Ces réductions augmentent avec une température ambiante de -7°C jusqu'à 5.9% et 2.31% respectivement. Les transferts thermiques dans l'échangeur atteignent un maximum de 25 kW pendant la partie extra-urbaine du cycle, où le moteur est à des vitesses de rotation plus élevées donc des débits plus élevées dans l'échangeur.

La contre pression imposée par l'échangeur sur la ligne d'échappement a sûrement une influence sur le fonctionnement du moteur. Pour cela, deux tests ont été effectués pour le cycle NEDC avec une diminution des pertes de charge côté air de 50% et de 100%. Les gains en consommation étaient de 1.4 et 1.48% respectivement.

Cette configuration a ensuite été testée sur les autres cycles d'homologation et les résultats sont résumés dans le tableau suivant.

Tableau 4 - Gain de consommation suite à l'application de la récupération de chaleur pour un réchauffement indirect d'huile

Cycle	20°C	-7°C
NEDC	1.39%	2.31%
WLTC	1.69%	3.34%
AH cycle	1.02%	0.76%
AU cycle	2.46%	3.86%
HDC	1.76%	1.89%

Réchauffement direct de l'huile

La deuxième stratégie consiste à réchauffer directement de l'huile du moteur. Pour cela, l'huile a été mise en échange direct avec les gaz d'échappement. L'échangeur a été installé dans le circuit de lubrification en aval de l'échangeur huile/eau et en amont du moteur. De même, le contrôle d'échange entre les deux fluides n'a pas eu lieu dans cette configuration. La

configuration a été testée pour les différents cycles d'homologation et pour les deux températures ambiantes : 20 et -7°C.

NEDC

Les résultats concernant la température ambiante de 20°C pour le cycle NEDC sont représentés dans la figure 10.

Le profil de température du liquide de refroidissement montre une amélioration durant la stratégie, mais cette amélioration est négligeable par rapport à celle obtenue avec l'huile de lubrification. Le dernier monte rapidement dès le début du cycle. De plus, vers la fin du cycle, la température de l'huile montre l'intensité de la partie extra-urbaine du cycle avec une hausse importante de la température vers la 1000ème seconde du cycle. L'huile atteint une température maximale de 129°C vers la seconde 1120 du cycle. Au contraire des stratégies précédentes, la température de l'huile est plus élevée que celle du liquide de refroidissement tout au long du cycle et ainsi l'échangeur huile/eau est considérée comme source de chaleur pour l'eau.

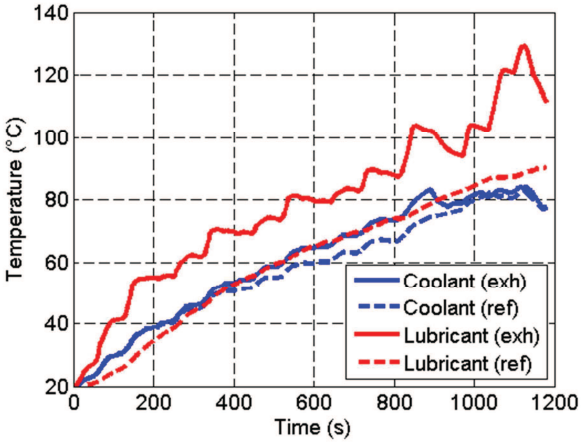

(a): Temperature profile at 20°C

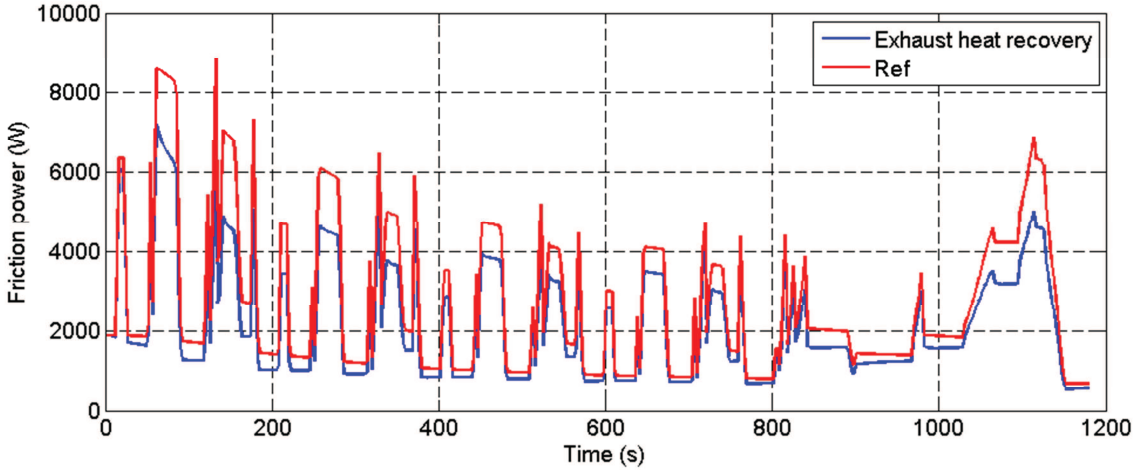

(b): Friction power at 20°C

Figure 10 – Les résultats de la récupération de chaleur pour un réchauffement direct de l'huile pour NEDC à 20°C

Selon la figure 10 – (a), l'huile avec cette stratégie atteint la température 60°C avec une avance de 252s et puis 80°C avec une avance de 376s. Le liquide de refroidissement présente une amélioration autour de 400s et atteint 60°C avec une avance de 82s et la température de régulation avec une avance de 155s. L'amélioration apportée à la température de l'huile se reflète sur le profil des forces de frottements comme présenté dans la figure 10 – (b). Une différence entre les deux courbes est présente pendant tout le cycle. Les frottements sont réduits de 20.58% à la fin du cycle aboutissant à un gain en consommation de 5.53%.

Pour une température ambiante de -7°C, ces réductions augmentent jusqu'à 28.6% et 16.23% pour les frottements et la consommation du carburant respectivement. Le tableau 5 résume les différents gains pour les différents cycles.

Tableau 5 - Gain en consommation suite à l'application de la récupération de chaleur pour un réchauffement direct d'huile

	Consommation		Puissance de frottement	
Cycle	**20°C**	**-7°C**	**20°C**	**-7°C**
NEDC	5.52%	16.23%	20.58%	28.6%
WLTC	7.12%	11.4%	20.9%	29.4%
AH cycle	5.97%	7.74%	28.8%	36.41%
AU cycle	7.85%	17.02%	25.45%	35.3%
HDC cycle	13.64%	28.62%	36.8%	52.2%

Un des inconvénients de cette configuration est associé au fait que les niveaux de températures d'huile sont élevés. Pour le cycle NEDC, l'huile atteint une température maximale de 129°C, cette température s'élève jusqu'à 135°C et 137°C pendant les cycles WLTC et AH respectivement. Pour faire face à ce problème et pour éviter la rupture du film d'huile, une modification de la configuration a été proposée. Elle consiste à placer l'échangeur dans le circuit de lubrification en aval du moteur et en amont du carter d'huile. L'huile sortant de l'échangeur avec les gaz d'échappement peut échanger de la chaleur dans le carter d'huile ainsi qu'avec le liquide de refroidissement au sein de l'échangeur huile/eau avant d'arriver au moteur. Comme résultat, les températures maximales de l'huile ont été abaissées : pour le cycle NEDC, l'huile atteint une température maximale de 113°C, pour le cycle WLTC 118°C et pour le cycle AH 121°C. Cependant avec la configuration B, les gains en consommation ainsi que les réductions de frottements sont de niveau plus bas que la configuration initiale.

Une dernière stratégie consiste à faire un réchauffement direct de l'huile et de l'eau en installant deux échangeurs en série. Le premier réchauffe l'huile dans sa configuration initiale et le deuxième réchauffe l'eau. Les températures d'huile augmentent presque comme la configuration du réchauffement direct. Le profil de température du liquide de refroidissement s'améliore par rapport à la configuration de réchauffement direct de l'huile mais reste plus bas que celui de la première stratégie. Les gains en consommation étaient moins biens que le réchauffement direct à cause de la contre pression appliquée par les deux échangeurs en série.

6. Chapitre 5 - Différentes stratégies de gestion thermique

Le type d'huile

Le type d'huile a été changé du 15W40 à 0W20. Le nouveau type d'huile fournit un niveau de viscosité plus bas pour les températures basses de l'huile. La stratégie a été testée pour les différents cycles d'homologation et pour deux températures ambiantes 20°C et -7°C. Les profils de température ont montré un retard pour atteindre la température de régulation du moteur et ils ont été plus bas que les profils de référence (le moteur sans aucune stratégie thermique et avec une huile de type 15W40). Cela est dû à la réduction des forces de frottements et donc la réduction de l'énergie fournie aux circuits de refroidissement et de lubrification du moteur. Une réduction des frottements entre 16% et 38% a été obtenue tandis que les gains en consommation ont varié entre 3.7% et 25.2% selon les cycles et la température ambiante.

L'isolation du moteur

La stratégie de l'isolation du moteur a été testée en réduisant le coefficient de convection extérieure de 71% (de 70 W/m²/k à 20 W/m²/k) puis de 100%. Une réduction de 100% signifie que le moteur est complétement isolé thermiquement. L'isolation du moteur a été testée pour les différents cycles et pour une température ambiante de 20°C. Cependant, la chute de température pendant l'arrêt du moteur n'était pas étudiée. Une telle étude peut amener à démarrer le moteur à des températures plus élevées que la température ambiante et aboutir ainsi à une amélioration de l'efficacité du moteur. L'isolation du moteur a une influence plus importante sur les cycles NEDC, WLTC et AU. Le cycle AH représente un cycle plus sévère que les autres, pendant lequel le moteur fonctionne souvent à charge élevée durant la phase transitoire. Ce comportement abouti à atteindre la température de régulation rapidement, ne permettant pas de mettre en valeur la stratégie d'isolation du moteur. De plus, le cycle HDC est considéré comme un cycle court ne permettant pas à cette stratégie d'avoir une influence importante sur le moteur. Les gains en consommation ont varié entre 0.08% et 2% selon les conditions.

By-pass CAC et EGR

La stratégie consiste à ne pas refroidir l'air de suralimentation, ni la recirculation des gaz d'échappement, afin d'augmenter la température des cylindres durant les premiers phases des cycles. L'élévation de la température de l'air de suralimentation a été négligée par rapport à la température d'EGR. Le by-pass du refroidisseur d'EGR aboutit à une température de l'air plus élevée à l'entrée des cylindres sans influencer l'état thermique du moteur. En outre, une température d'air plus élevée aboutit à la réduction du rendement de remplissage du moteur ainsi qu'à la variation du temps de l'inflammation du mélange dans le cylindre. Les températures des gaz d'échappement ont été surveillées pour signaler si le catalyseur atteint la température d'amorçage en avance.

La température de régulation

La dernière stratégie à tester est la température de régulation du moteur. La température de l'ouverture du thermostat a été augmentée de 20°C. Au contraire des stratégies précédentes, la température de régulation influence la phase de régulation du moteur et non pas sa montée en

température. Cependant, cette dernière a été prolongée avec la nouvelle stratégie. Une température de régulation élevée a eu une influence seulement sur les cycles NEDC, WLTC et AH car les cycles AU et HDC n'atteignent pas la température de régulation. Le cycle NEDC atteint la température de régulation vers la fin du cycle, et le gain en consommation a été négligeable. Une température de fonctionnement élevée entraînera une élévation de la température d'huile mais pas de la même façon. Les économies de carburant ont été de 2.12% et 1.22% pour les cycles WLTC et AH respectivement.

7. Conclusions et perspectives

La gestion thermique est un des moyens de réduction de la consommation spécifique d'un véhicule. Avec le réchauffement climatique, les normes de dépollution deviennent de plus en plus sévères et les constructeurs automobiles cherchent à améliorer le rendement des véhicules. Le but de ces travaux de recherche est de valoriser, par simulation numérique, les nouveaux systèmes de gestion thermique en fonction du cycle d'homologation et de la température ambiante.

Un modèle de simulation 1-D du moteur et de ses circuits de refroidissement et de lubrification ont été développés en utilisant le logiciel GT-Suite. Quatre cycles d'homologation ont été choisis : NEDC, WLTC, AH et AU. De plus, un nouveau cycle a été proposé durant cette étude. Le bilan d'énergie effectué pendant les différentes phases des cycles souligne l'importance du stockage et de la récupération d'énergie.

Le stockage d'énergie dans un volume eau et/ou d'huile abouti à l'amélioration de la montée en température des deux fluides. Plusieurs configurations ont été proposées comme, par exemple, un carter d'huile multifonctionnel. Ainsi, une réduction importante de la consommation en carburant est obtenue.

La récupération de chaleur au sein des gaz d'échappement est ensuite mise en œuvre. L'échangeur est caractérisé sur un banc d'essais puis modélisé. Le réchauffement indirect et direct d'huile abouti à une réduction importante des frottements et de la consommation. Une configuration est proposée afin de contrôler la température maximale de l'huile.

Finalement, différentes stratégies comme : le type d'huile, l'isolation du moteur, une température de régulation plus élevée etc… ont été étudiées et valorisées.

Les travaux de recherche de cette thèse s'étendent à de nombreuses perspectives :

- Valorisation de nouvelles stratégies : stockage de la chaleur latente en utilisant des matériaux à changement de phase. L'étude consiste à faire des essais pour caractériser le comportement de ces matériaux suivant les différents niveaux de températures.
- Etude de l'influence du type d'huile sur la stratégie de la récupération des gaz d'échappement. Ce dernier se base sur les forces de frottements et l'amélioration de la viscosité d'huile à basse température, ainsi un changement du type d'huile aura une plus grande influence.
- Développement du modèle thermique : remplacer le modèle 5 masses proposées par GT-Suite avec un modèle nodal plus développé. Ce type d'amélioration permettra d'être plus représentatif de la physique ce qui permettra d'améliorer les résultats. Il permet également d'avoir plus de degrés de liberté pour appliquer d'autres stratégies et contrôler plus d'éléments.
- Introduction du chauffage d'habitacle dans l'étude et valorisation de l'amélioration qui peut être apportée avec les différentes stratégies.
- Combinaison de plusieurs stratégies et étude du cumul des effets.
- Changement du type de moteur : application sur des moteurs à allumage commandé.
- Introduction du véhicule hybride : le couplage entre un modèle d'un moteur à combustion interne avec un circuit de moteur électrique et gérant ainsi les différentes

températures de fonctionnement du moteur à combustion interne, du moteur électrique, de la batterie, du chauffage de l'habitacle.

References

[1] T. A. Boden, R. J. Andres, and G. Marland, “Global, Regional, and National Fossil-Fuel CO2 Emissions,” Jan. 2015.

[2] World bank, *World development report 2010 - Development and climate change*, vol. 1942, no. 2003. Washingnton, DC: World Bank, 2010.

[3] “Consumption of energy - Statistics Explained.” [Online]. Available: http://ec.europa.eu/eurostat/statistics-explained/index.php/Consumption_of_energy. [Accessed: 12-Apr-2017].

[4] B. Bohr, “Bosch sees future requiring multiple powertrain technologies; the larger the vehicle, the more the electrification.” [Online]. Available: http://www.greencarcongress.com/2013/06/bosch-20130618.html. [Accessed: 12-Apr-2017].

[5] E. Uherek *et al.*, “Transport impacts on atmosphere and climate: Metrics,” *Atmos. Environ.*, vol. 44, no. 37, pp. 4648–4677, 2010.

[6] European Commission, “A European strategy for low-emission mobility,” 2016.

[7] European Commission, *EU Reference Scenario 2016 - Energy, Transport and GHG emissions trends to 2050*. European Commission, 2016.

[8] International Energy Agency, “CO2 emissions from fuel combustion Highlights,” Paris, 2016.

[9] S. Díaz, U. Tietge, and P. Mock, “CO 2 emissions from new passenger cars in the EU : Car manufacturers ’ performance in 2014,” *Int. Counc. Clean Transp.*, no. July, 2015.

[10] European Parliament and Council of the European Union, “Regulation (EU) No 333/2014,” *Off. J. Eur. Union*, vol. 103, no. 333, pp. 15–21, 2014.

[11] European Parliament and Council of the European Union, “Regulation (EC) no. 443/2009,” *Off. J. Eur. Union*, vol. 140, no. 1, pp. 1–15, 2009.

[12] “Carbon (CO2) Emissions Comparison for Different forms of transport.” [Online]. Available: http://www.beagleybrown.com/planes-trains-or-automobiles-carbon-emissions-compared-for-different-forms-of-transport/. [Accessed: 12-Apr-2017].

[13] European Commission., “2012/100/EU: Commission Decision of 17 February 2012 on a method for the collection of premiums for excess CO 2 emissions from new passenger cars pursuant to Regulation (EC) No 443/2009 of the European Parliament and of the Council Text with EEA relevance,” *OJ L*, vol. 47, pp. 71–72, 2012.

[14] Delphi, “Worldwide Emissions Standards,” *Quality*, pp. 0–103, 2013.

[15] G. Patel, L. P. Goswami, C. Khadia, P. K. Sen, and S. K. Bohidar, “A Study on Problem, Causes and Aids of Cold Start Performance on Internal Combustion Engine,” *Int. J. Res.*, vol. 1, no. 10, pp. 1019–1023, 2014.

[16] European Commission, “Analysis of National Travel Statistics in Europe,” Seville, 2013.

[17] C. Rouaud, D. Gerard, D. Issartel, B. Pfeffer, S. Grolet, and R. D. Dtaa, “Thermal management solutions for Diesel engine,” *SIA Publ.*, pp. 1–9.

[18] B. J. Luptowski, D. Adekeye, and T. Straten, “Coupled Engine / Cooling System Simulation and its Application to Engine Warm-up,” *SAE Tech. Pap.*, vol. 2005-01–20, 2005.

[19] A. Alexandre and L. Tomaselli, “Analyse des transferts énergétiques dans les moteurs

automobiles," *Tech. l'ingénieur*, vol. 33, no. BM2900, pp. 1–16, 2004.

[20] L. Jarrier and D. Gentile, "Simulation du comportement thermique transitoire d'un moteur à combustion interne et à allumage commandé," *Rev. Générale Therm.*, vol. 36, pp. 520–533, 1997.

[21] G. Woschni, "A Universally Applicable Equation for the Instantaneous Heat Transfer Coefficient in the Internal Combustion Engine," *SAE Int.*, vol. 670931, 1967.

[22] P. Douxchamps, "Diesel Thermal Management Optimization for effective efficiency improvement," Université Libre de Bruxelles, 2010.

[23] R. Cipollone and C. Villante, "A Fully Transient Model For Advanced Engine Thermal Management," *SAE Tech. Pap.*, vol. 2005-01–20, no. 724, 2005.

[24] F. W. Koch and F. G. Haubner, "Cooling System Development and Optimization for DI Engines," *SAE Tech. Pap.*, vol. 2000-01–02, 2000.

[25] J. B. Heywood, *Internal combustion engine fundamentals*. 1988.

[26] L. Jarrier, J. C. Champoussin, E. C. De Lyon, R. Yu, and D. R. Renault, "Warm-Up of a D . I . Diesel Engine : Experiment and Modeling," *SAE Tech. Pap.*, vol. 2000-01–02, 2000.

[27] M. Benhassaine, "Etude expérimentale et modélisation des frottements locaux et instantanés piston-chemise en moteur Diesel," Ecole Centrale de Lyon, 1992.

[28] B. W. Millington and E. R. Hartles, "Fricitional losses in Diesel engines," in *SAE Technical Paper*, 1968, no. 680590.

[29] P. J. Shayler, S. J. Christian, and T. Ma, "A Model for the Investigation of Temperature , Heat Flow and Friction Characteristics During Engine Warm-Up," *SAE Tech. Pap.*, vol. 931153, 1993.

[30] D. Chalet, M. Lesage, M. Cormerais, and T. Marimbordes, "Nodal modelling for advanced thermal-management of internal combustion engine," *Appl. Energy*, vol. 190, pp. 99–113, 2017.

[31] J. P. Zammit, "Managing engine thermal state to reduce friction losses during warm-up," The University of Nottingham, 2012.

[32] M. M. Umekar and D. Govindaraj, "Heat Transfer Calculations for Cooling System Performance Prediction and Experimental Validation," *SAE Tech. Pap.*, vol. 2011-26–0, 2011.

[33] F. Pirotais, "Contribution à la modélisation du flux thermique disponible pour le chauffage d'un habitacle d'automobile après un démarrage à froid."

[34] Y. Danno, H. Kamada, and T. Kitada, "Efficacy and feasibility of cylinder block oil-cooling for passenger car engines," *JSAE Rev.*, vol. 10, no. 4, pp. 36–43, 1989.

[35] J. R. Welty, C. E. Wicks, R. E. Wilson, and G. L. Rorrer, *Fundamentals of Momentum, Heat, and Mass Transfer*, Fifth edit. John Wiley & Sons, 2008.

[36] F. P. Incropera, T. L. Bergman, A. S. Lavine, and D. P. DeWitt, *Fundamentals of Heat and Mass Transfer*, 7th editio. John Wiley & Sons, 2011.

[37] T. Fujita and T. Ueda, "Heat transfer to falling liquid films and film breakdown-I. Subcooled liquid films," *Int. J. Heat Mass Transf.*, vol. 21, no. 2, pp. 97–108, 1978.

[38] W. J. Seale and D. H. C. Taylor, "Spatial Variation of Heat Transfer to Pistons and Liners of Some Medium Speed Diesel Engines," *Proc. Inst. Mech. Eng.*, vol. 185, no.

1, pp. 203–218, 1970.

[39] S. Bohac, D. Baker, and D. Assanis, “A global model for steady state and transient SI engine heat transfer studies,” *SAE Tech. Pap.*, vol. 960073, 1996.

[40] A. Bontemps and J.-F. Fourmigué, “Échangeurs de chaleur Dimensionnement thermique,” *Tech. l’ingénieur*, vol. 33, no. B 2 342, 1994.

[41] A. Alexandre and L. Tomaselli, “Modélisation thermique des moteurs: Outils numériques généraux,” *Tech. l’ingénieur. Génie mécanique*, vol. 33, no. BM 2 901, pp. 0–12, 2006.

[42] J. R. Wagner, M. C. Ghone, D. W. Dawson, and E. E. Marotta, “Coolant Flow Control Strategies for Automotive Thermal Management Systems,” *SAE Tech. Pap.*, vol. 2002-01–07, 2002.

[43] J. R. Wagner, V. Srinivasan, D. M. Dawson, and E. E. Marotta, “Smart Thermostat and Coolant Pump Control for Engine Thermal Management Systems,” *SAE Tech. Pap.*, vol. 2003-01–02, 2003.

[44] C. Charmantray, R. Yu, and J. C. Champoussin, “Modélisation de la montée en température des moteurs Sensibilités et axes de progrès,” pp. 1–8, 2010.

[45] S. Salbrechter, M. Krenn, G. Pirker, A. Wimmer, and M. Nöst, “Engine Operating Parameter-based Heat Transfer Simulation to Predict Engine Warm-up,” *SAE Tech. Pap.*, vol. 2014-01–11, 2014.

[46] A. K. da Silva, M. Lebrun, and S. Samuel, “Modeling and Simulation of a Cooling System Using Multiport Approach,” *SAE Tech. Pap.*, vol. 2000-01–02, no. 724, 2000.

[47] N. R. Agarwal, “Modeling, Validation and Analysis of an Advanced Thermal Management System for Conventional Automotive Powertrains,” The OhioState University, 2012.

[48] J. Lahuerta and S. Samuel, “Numerical simulation of warm-Up characteristics and thermal management of a GDI engine,” *SAE Tech. Pap.*, vol. 2013-01–08, 2013.

[49] D. Jung, J. Yong, H. Choi, H. Song, and K. Min, “Analysis of engine temperature and energy flow in diesel engine using engine thermal management,” *J. Mech. Sci. Technol.*, vol. 27, no. 2, pp. 583–592, 2013.

[50] A. Alexandre and L. Tomaselli, “Modélisation thermique des moteurs - modélisation de la combustion,” *Tech. l’ingénieur*, vol. BM 2 902, 2007.

[51] F. Pirotais, J. Bellettre, O. Le Corre, M. Tazerout, G. De Pelsemaeker, and G. Guyonvarch, “A Diesel Engine Thermal Transient Simulation : Coupling Between a Combustion Model and a Thermal Model,” *SAE Tech. Pap.*, vol. 2003-01–02, 2003.

[52] J. Galindo, H. Climent, B. Plá, and V. D. Jiménez, “Correlations for Wiebe function parameters for combustion simulation in two-stroke small engines,” *Appl. Therm. Eng.*, vol. 31, no. 6–7, pp. 1190–1199, 2011.

[53] P. Marty, “Ship energy efficiency study: development and application of an analysis method,” Ecole centrale de Nantes, 2014.

[54] D. E. Winterbone, *Advanced Thermodynamics for Engineers*. John Wiley & Sons, 1997.

[55] W. H. Lipkea and A. D. Dejoode, “A comparison of the Performance of Two Direct Injection Diesel Engines From a Second Law Perspective,” *SAE Tech. Pap.*, vol. 890824, 1989.

[56] R. Benelmir, A. Lallemand, and M. Feidt, “Analyse exergétique,” *Tech. l’ingénieur*, vol. BE 8015, 2002.

[57] A. Lallemand, “Energie , Exergie , Économie,” in *Journees internationales de Thermique*, 2007.

[58] C. Sayin, M. Hosoz, M. Canakci, and I. Kilicaslan, “Energy and exergy analyses of a gasoline engine,” *Int. J. Engine Res.*, vol. 31, no. 3, pp. 259–273, 2007.

[59] C. D. Rakopoulos and E. G. Giakoumis, “Second-law analyses applied to internal combustion engines operation,” *Prog. Energy Combust. Sci.*, vol. 32, no. 1, pp. 2–47, 2006.

[60] P. F. Flynn, K. L. Hoag, M. M. Kamel, and R. J. Primus, “A New Perspective on Diesel Engine Evaluation Based on Second Law Analysis,” *SAE Tech. Pap.*, vol. 840032, 1984.

[61] F. Bozza, R. Nocera, A. Senatore, and R. Tuccillo, “Second Law Analysis of Turbocharged Engine Operation,” *SAE Tech. Pap.*, vol. 910418, 1991.

[62] N. Al-Najem and J. Diab, “Energy-exergy analysis of a Diesel engine,” *Heat Recover. Syst. CHP*, vol. 12, no. 6, pp. 525–529, 1992.

[63] T. J. Kotas, *The Exergy Method of Thermal Plant Analysis*, 1995th ed. Krieger publishing company, 1995.

[64] G. Bourhis and P. Leduc, “Energy and Exergy Balances for Modern Diesel and Gasoline Engines,” *Oil Gas Sci. Technol. – Rev. l’Institut Français du Pétrole*, vol. 65, no. 1, pp. 39–46, 2010.

[65] R. J. Primus, K. L. Hoag, P. F. Flynn, and M. C. Brands, “An appraisal of advanced engine concepts using second law analysis techniques,” *SAE Tech. Pap.*, vol. 841287, 1984.

[66] A. V. Bueno, J. A. Velásquez, and L. F. Milanez, “Exergy Based Diagnosis of In-Cylinder Diesel Engine,” in *SAE Technical Paper*, 2004, vol. 2004-01–32.

[67] J. Agudelo, A. Agudelo, and J. Pérez, “Energy and Exergy analysis of a light duty diesel engine operating at different altitudes,” *Rev. Fac. Ing.*, no. 48, pp. 45–54, 2009.

[68] I. Sezer and A. Bilgin, “Effects of charge properties on exergy balance in spark ignition engines,” *Fuel*, vol. 112, pp. 523–530, 2013.

[69] I. Dincer and M. Rosen, “Thermodynamic Fundamentals,” in *Exergy, Energy, Environment and Sustainable Development*, Elsevier Ltd, 2007.

[70] J. A. Caton, “A Review of Investigations Using the Second Law of Thermodynamics to Study Internal- Combustion Engines,” *SAE Tech. Pap.*, vol. 2000-01–10, 2000.

[71] C. D. Rakopoulos and E. G. Giakoumis, “Simulation and exergy analysis of transient diesel-engine operation,” *Energy*, vol. 22, no. 9, pp. 875–885, 1997.

[72] J. Fu, J. Liu, R. Feng, Y. Yang, L. Wang, and Y. Wang, “Energy and exergy analysis on gasoline engine based on mapping characteristics experiment,” *Appl. Energy*, vol. 102, pp. 622–630, 2013.

[73] A. Abusoglu and M. Kanoglu, “First and second law analysis of diesel engine powered cogeneration systems,” *Energy Convers. Manag.*, vol. 49, no. 8, pp. 2026–2031, 2008.

[74] A. Abusoglu and M. Kanoglu, “Exergetic and thermoeconomic analyses of diesel engine powered cogeneration: Part 1 - Formulations,” *Appl. Therm. Eng.*, vol. 29, no.

2–3, pp. 234–241, 2009.

[75] A. C. Alkidas, “The Use of Availability and Energy Balances in Diesel Engines,” *SAE Tech. Pap.*, vol. 890822, 1989.

[76] J. Li, L. Zhou, K. Pan, D. Jiang, and J. Chae, “Evaluation of the thermodynamic process of indirect injection diesel engines by the first and second law,” *SAE Tech. Pap.*, vol. 952055, 1995.

[77] J. A. Velásquez and L. F. Milanez, “Analysis of the Irreversibilities in Diesel Engines,” *SAE Tech. Pap.*, vol. 940673, 1994.

[78] H. Li and R. S. Figliola, “Optimization of an automotive cooling system based on exergy analysis,” *SAE Tech. Pap.*, vol. 2004-01–35, 2004.

[79] P. Punov, T. Evtimov, R. Chiriac, A. Clenci, Q. Danel, and G. Descombes, “Progress in high performance, low emissions, and exergy recovery in internal combustion engines,” *nternational J. Energy Res.*, 2016.

[80] S. Lion, M. G. Momesso, I. Vlaskos, C. Rouaud, and R. Taccani, “Combined Engine-ORC Thermodynamic Analysis Based on a Second Law and Thermo-Economic Approach,” in *Vehicle Thermal Management Systems (Vtms 13)*, 2017, pp. 205–218.

[81] I. Taymaz, “An experimental study of energy balance in low heat rejection diesel engine,” *Energy*, vol. 31, no. 2–3, pp. 364–371, 2006.

[82] Sekmen Perihan; Yılbaşı Zeki, “Application of Energy and Exergy Analyses To a Ci Engine,” *Math. Comput. Appl.*, vol. 16, no. 4, pp. 797–808, 2011.

[83] F. Payri, P. Olmeda, J. Martín, and R. Carreño, “Experimental analysis of the global energy balance in a DI diesel engine,” *Appl. Therm. Eng.*, vol. 89, no. x, pp. 545–557, 2015.

[84] C. A. Romero, A. Torregrosa, P. Olmeda, and J. Martin, “Energy Balance During the Warm-Up of a Diesel Engine,” *SAE Tech. Pap.*, vol. 2014-01–06, pp. 2–11, 2014.

[85] J. F. Eberth, J. R. Wagner, B. a Afshar, and R. C. Foster, “Modeling and Validation of Automotive ‘Smart’ Thermal Management System Architectures,” *SAE Tech. Pap.*, vol. 2004-1–0, 2004.

[86] S. Klopstein, S. Lauer, and F. Maassen, “Interpretation tools and concepts for the heat management in the drive train of the future,” *SAE Tech. Pap.*, vol. 2011-01–06, 2011.

[87] Volkswagen AG, “Self-styudy programme 222: Electronically mapped cooling system,” Wolfsburg.

[88] Gustav Wahler GmbH u. Co. KG, “Thermostats.” [Online]. Available: https://www.yumpu.com/en/document/view/11680638/thermostats-gustav-wahler-gmbh-u-co-kg/3. [Accessed: 10-May-2017].

[89] T. Mitchell, M. Salah, J. Wagner, and D. Dawson, “Automotive thermostat valve configurations: enhanced warm-up performance,” *J. Dyn. Syst. Meas. Control*, vol. 131, no. 4, p. 44501, 2009.

[90] W. Krause and K. H. Spies, “Dynamic Control of the Coolant Temperature for a Reduction of Fuel Consumption and Hydrocarbon Emission,” *SAE Tech. Pap.*, vol. 960271, no. 412, 1996.

[91] E. S. Mohamed, “Development and analysis of a variable position thermostat for smart cooling system of a light duty diesel vehicles and engine emissions assessment during NEDC,” *Appl. Therm. Eng.*, vol. 99, pp. 358–372, 2016.

[92] The ITB group, “Automotive engine air and cooling systems - 2012,” 2012.

[93] N. Ap and M. Tarquis, “Innovative Engine Cooling Systems Comparison,” *SAE Tech. Pap.*, vol. 2005-01–13, no. 724, 2005.

[94] S. Saab, “Etude par simulation 0D des systèmes thermiques du groupe motopropulseur et de l’habitacle d’un véhicule automobile en vue de réduire sa consommation de carburant,” Ecole Centrale de Nantes, 2014.

[95] M. Cormerais, Y. Thevenoux, H. Mezher, T. Marimbordes, and D. Chalet, “Influence of Active Cooling Thermal management Valve on Fuel Consumption and Engine Warm-up : Simulation and Tests,” *SIA Publ.*, vol. R-2014-02-, pp. 1–8.

[96] M. Cormerais, T. Marimbordes, S. Warnery, D. Chalet, H. Mezher, and L. Roussel, “ACT Valve: Active Cooling Thermomanagement Valve,” *SAE Tech. Pap.*, vol. 2014-01–06, 2014.

[97] A. Morein and P. Schaefer, “Schaeffler Thermal Management Module,” in *SAE 2013 thermal management systems symposium*, 2013.

[98] A. Morein and S. Hurst, “The Schaeffler Thermal Management Module,” in *5th European Workshop: Mobile air conditioning and vehicle thermal systems*, 2013.

[99] E. Barrieu, N. Becker, and A. Rossi, “Engine Warm-up Optimization Using Innovative Components,” *SIA Publ.*, vol. R-2013-06-, pp. 1–10, 2013.

[100] A. Roberts, R. Brooks, and P. Shipway, “Internal combustion engine cold-start efficiency: A review of the problem, causes and potential solutions,” *Energy Convers. Manag.*, vol. 82, pp. 327–350, 2014.

[101] K. W. Choi, K. B. Kim, and K. H. Lee, “Investigation of emission characteristics affected by new cooling system in a diesel engine,” *J. Mech. Sci. Technol.*, vol. 23, no. 7, pp. 1866–1870, 2009.

[102] H. Couëtouse and D. Gentile, “Cooling System Control in Automotive Engines,” *SAE Tech. Pap.*, vol. 920788, 1992.

[103] W. Nessim and F. Zhang, “Powertrain Warm-up Improvement using Thermal Management Systems,” *Int. J. Sci. Technol. Res.*, vol. 1, no. 4, pp. 151–155, 2012.

[104] R. D. Chalgren, “Thermal Comfort and Engine Warm-Up Optimization of a Low-Flow Advanced Thermal Management System,” *SAE Tech. Pap.*, vol. 2004-1–0, 2004.

[105] R. D. J. Chalgren and D. J. Allen, “Light Duty Diesel Advanced Thermal Management,” *SAE Tech. Pap.*, vol. 2005-01–20, 2005.

[106] R. W. Jorach, F. Atschreiter, and A. Gößling, “Integrated Thermal Management : System Approach towards CO 2 Reduction,” in *25th Aachen Colloquium Automobile and Engine Technology 2016*, 2016, pp. 491–508.

[107] B. Zhou, X. Lan, X. Xu, and X. Liang, “Numerical model and control strategies for the advanced thermal management system of diesel engine,” *Appl. Therm. Eng.*, vol. 82, pp. 368–379, 2015.

[108] H. H. Pang and C. J. Brace, “Review of engine cooling technologies for modern engines,” *Proc. Inst. Mech. Eng. Part D J. Automob. Eng.*, vol. 218, pp. 1–7, 2004.

[109] C. Donn, W. Zulehner, D. Ghebru, U. Spicher, and M. Honzen, “Experimental Heat Flux Analysis of an Automotive Diesel Engine in Steady-State Operation and During Warm-Up,” *SAE Tech. Pap.*, vol. 2011-24–0, 2011.

[110] A. Osman, A. S. Sabrudin, M. A. Hussin, and Z. A. Bakri, “Desing and Simulations of an Enhanced and Cost Effective Engine Split Cooling Circuit,” *SAE Tech. Pap.*, vol. 2013-01–16, 2013.

[111] C. Zhao, P. Shayler, L. Cheng, and R. Gilchrist, “The influence on warm-up of split head and block circuits for oil and coolant, and the effect of main gallery location,” in *Vehicle Thermal Management Systems (Vtms 13)*, 2017, pp. 29–43.

[112] R. Burke and C. Brace, “The Effects of Engine Thermal Conditions on Performance, Emissions and Fuel Consumption,” *SAE Tech. Pap.*, vol. 2010-01–08, pp. 1–15, 2010.

[113] M. Yousry, J. H. Johnson, and S. M. Pandit, “A statistical Approach to Determining the Effects of Speed , Load , Oil and Coolant Temperature on Diesel Engine Specific Fuel Consumption,” *SAE Tech. Pap.*, vol. 780971, 1978.

[114] D. Di Battista and R. Cipollone, “Oil thermal management during engine transients from a cold state,” in *Vehicle Thermal Management Systems (Vtms 13)*, 2017, pp. 221–230.

[115] G. E. Andrews, J. R. Harris, and A. Ounzain, “SI Engine Warm Up: Water and lubricating Oil Temperature Influences,” *SAE Tech. Pap.*, vol. 892103, 1989.

[116] E. Bent, P. Shayler, A. La Rocca, and C. Rouaud, “The effectiveness of stop-start and thermal management measures to improve fuel economy,” *Vehicle Thermal Management Systems Conference and Exhibition (VTMS11)*. pp. 27–39, 2013.

[117] C. Bertolini, T. Courtois, and D. Caprioli, “Engine encapsulation solutions and methods to support NVH and Thermal design optimization,” *SIA Publ.*, vol. R-2015-07-, pp. 1–10, 2015.

[118] A. Roberts, R. Brooks, P. Shipway, R. Gilchrist, and I. Pegg, “Reducing Energy Losses from Automotive Engine Lubricants by Thermal Isolation of the Engine Mass,” *SAE Tech. Pap.*, vol. 2014-01–06, 2014.

[119] S. Makam, C. Dubbs, Y. Roosien, F. Lin, and W. Resh, “Analytical Study of Thermal Management: A Case Study of Underhood Configurations,” *SAE Tech. Pap.*, vol. 2015-01–03, 2015.

[120] L. Huber, “Actuated Grille Shutter systems for CO2 reduction,” *MMT Symp.*, 2011.

[121] K. Robinson, J. G. Hawley, N. a F. Campbell, and D. G. Tilley, “A Review of Precision Engine Cooling,” *SAE Tech. Pap.*, vol. 1999-01–05, 1999.

[122] P. Revereault, C. Rouaud, and A. Marchi, “Fuel Economy and Cabin Heating Improvements Thanks to Thermal Management Solutions Installed in a Diesel Hybrid Electric Vehicle,” *SAE Tech. Pap.*, vol. 2010-01–08, 2010.

[123] O. P. Taylor, R. Pearson, and R. Stone, “Reduction of CO 2 Emissions through Lubricant Thermal Management During the Warm Up of Passenger Car Engines,” *SAE Tech. Pap.*, vol. 2016-01–08, 2016.

[124] C. Zhao, P. Shayler, and R. Gilchrist, “Influence of Sump Design on Oil Warm-up and Cool-down Behaviour,” in *Vehicle Thermal Management Systems (Vtms 13)*, 2017, pp. 3–15.

[125] N. I. Nouvel, N. Obrecht, and S. Crane, “Towards 0W-16 engine oil viscosity grade in Europe – German OEM fuel economy tests,” in *SIA POWERTRAIN:The low CO2 spark ignition engine of the futureand its hybridization*, 2015, pp. 141–149.

[126] F. Altenschmidt, S. Binder, and S. Loll, “A Thermodynamic Comparison of SI-Engine

Combustion Systems," in *SIA POWERTRAIN:The low CO2 spark ignition engine of the futureand its hybridization*, 2015, pp. 15–22.

[127] L. Guillaume, A. Legros, R. Dickes, and V. Lemort, "Thermo-economic optimization during preliminary design phase of organic Rankine cycle systems for waster heat recovery from exhaust and recirculated gases of heavy duty trucks," in *Vehicle Thermal Management Systems (Vtms 13)*, 2017, pp. 109–125.

[128] R. Daccord, J. Mélis, A. Darmedru, A. Debaise, T. Kientz, and E. Davin, "A Piston Expander for Exhaust Heat Recovery on Heavy Commercial Vehicles," in *FISITA 2016 : World automotive congress*, 2016.

[129] A. F. Agudelo, R. Garcia-Contreras, J. R. Agudelo, and O. Armas, "Potential for exhaust gas energy recovery in a diesel passenger car under European driving cycle," *Appl. Energy*, vol. 174, pp. 201–212, 2016.

[130] P. E. Farrant, A. Robertson, J. Hartland, and S. Joyce, "The application of thermal modelling to an engine and transmission to improve fuel consumption following a cold start," *SAE Tech. Pap.*, vol. 2005-01–20, 2005.

[131] C. N. Grimaldi, C. Poggiani, A. Cimarello, M. De Cesare, and G. Osbat, "An Integrated Simulation Methodology of Thermal Management Systems for the CO 2 Reduction after Engine Cold Start," *SAE Tech. Pap.*, vol. 2015-01–03, 2015.

[132] W. Frank, "A novel exhaust heat recovery system to reduce fuel consumption," in *FISITA Proceedings - F2010-A073*, 2010.

[133] F. Will and A. Boretti, "A New Method to Warm Up Lubricating Oil to Improve the Fuel Efficiency During Cold Start," *SAE Int. J. Engines*, vol. 4, no. 1, pp. 175–187, 2011.

[134] F. Will, "Fuel conservation and emission reduction through novel waste heat recovery for internal combustion engines," *Fuel*, vol. 102, pp. 247–255, 2012.

[135] R. D. Burke, C. J. Brace, A. Lewis, A. Cox, and I. Pegg, "Analysis of energy flows in engine coolant, structure and lubricant during warm-up," *Veh. Therm. Manag. Syst. Conf. Exhib. (Vtms 10)*, pp. 167–176, 2011.

[136] V. Pandiyarajan, M. Chinna Pandian, E. Malan, R. Velraj, and R. V. Seeniraj, "Experimental investigation on heat recovery from diesel engine exhaust using finned shell and tube heat exchanger and thermal storage system," *Appl. Energy*, vol. 88, no. 1, pp. 77–87, 2011.

[137] Y. Kuze, H. Kobayashi, H. Ichinose, and T. Otsuka, "Development of New Generation Hybrid System (THS II)– Development of Toyota Coolant Heat Storage System –," *SAE Tech. Pap.*, vol. 2004-01–06, 2004.

[138] A. Sharma, V. V. Tyagi, C. R. Chen, and D. Buddhi, "Review on thermal energy storage with phase change materials and applications," *Renew. Sustain. Energy Rev.*, vol. 13, no. 2, pp. 318–345, 2009.

[139] K. Kim, K. Choi, Y. Kim, K. Lee, and K. Lee, "Feasibility study on a novel cooling technique using a phase change material in an automotive engine," *Energy*, vol. 35, no. 1, pp. 478–484, 2010.

[140] O. Schatz, "Cold Start Improvement by use of Latent Heat Stores," *SAE Tech. Pap.*, vol. 921605, 1992.

[141] M. Gumus, "Reducing cold-start emission from internal combustion engines by means of thermal energy storage system," *Appl. Therm. Eng.*, vol. 29, no. 4, pp. 652–660,

2009.

[142] J. Vetrovec, “Engine Cooling System with a Heat Load Averaging Capability,” *SAE Tech. Pap.*, vol. 2008, no. 724, pp. 1–1168, 2008.

[143] A. Nour Eddine, D. Chalet, L. Aixala, P. Chesse, X. Faure, and N. Hatat, “Experimental analyses of thermoelectric generator behavior using two types of thermoelectric modules for marine application,” *Int J Electr Comput Energ Electron Commun Eng*, vol. 2016, no. 10, 2016.

[144] J. K. Wolfahrt *et al.*, “Aspects of Cabin Fluid Dynamics, Heat Transfer, and Thermal Comfort in Vehicle Thermal Management Simulations,” *SAE Tech. Pap.*, vol. 2005-01–20, 2005.

[145] O. Kaynakli and M. Kilic, “An investigation of thermal comfort inside an automobile during the heating period,” *Appl. Ergon.*, vol. 36, no. 3, pp. 301–312, 2005.

[146] A. Alahmer, A. Mayyas, A. A. Mayyas, M. A. Omar, and D. Shan, “Vehicular thermal comfort models; A comprehensive review,” *Appl. Therm. Eng.*, vol. 31, no. 6–7, pp. 995–1002, 2011.

[147] E. Samadani, L. Gimenez, W. Scott, M. Fowler, and R. Fraser, “Thermal Behavior of Two Commercial Li-Ion Batteries for Plug-in Hybrid Electric Vehicles,” *SAE Tech. Pap.*, vol. 2014-01–18, 2014.

[148] H. S. Hamut, I. Dincer, and G. F. Naterer, “Analysis and optimization of hybrid electric vehicle thermal management systems,” *J. Power Sources*, vol. 247, pp. 643–654, 2014.

[149] A. Pesaran, A. Vlahinos, and T. Stuart, “Cooling and preheating of batteries in hybrid electric vehicles,” *6th ASME-JSME Therm. Eng. Jt. Conf.*, pp. 1–7, 2003.

[150] A. Vlahinos and A. a. Pesaran, “Energy Efficient Battery Heating in Cold Climates,” *SAE Tech. Pap.*, vol. 2002-01–19, 2002.

[151] R. Sabbah, R. Kizilel, J. R. Selman, and S. Al-Hallaj, “Active (air-cooled) vs. passive (phase change material) thermal management of high power lithium-ion packs: Limitation of temperature rise and uniformity of temperature distribution,” *J. Power Sources*, vol. 182, no. 2, pp. 630–638, 2008.

[152] R. Kizilel, A. Lateef, R. Sabbah, M. M. Farid, J. R. Selman, and S. Al-Hallaj, “Passive control of temperature excursion and uniformity in high-energy Li-ion battery packs at high current and ambient temperature,” *J. Power Sources*, vol. 183, no. 1, pp. 370–375, 2008.

[153] X. Zhang, X. Kong, G. Li, and J. Li, “Thermodynamic assessment of active cooling/heating methods for lithium-ion batteries of electric vehicles in extreme conditions,” *Energy*, vol. 64, pp. 1092–1101, 2014.

[154] K. Murashko, H. Wu, J. Pyrhönen, and L. Laurila, “Modelling of the Battery Pack Thermal Management System for Hybrid Electric Vehicles,” *16th Eur. Conf. Power Electron. Appl.*, pp. 1–10, 2014.

[155] C. Park and A. K. Jaura, “Thermal Analysis of Cooling System in Hybrid Electric Vehicles,” *SAE Tech. Pap.*, vol. 2002-01–07, 2002.

[156] M. Shams-Zahraei, A. Z. Kouzani, S. Kutter, and B. Bäker, “Integrated thermal and energy management of plug-in hybrid electric vehicles,” *J. Power Sources*, vol. 216, pp. 237–248, 2012.

[157] R. Johri and Z. Filipi, “Optimal Energy Management of a Series Hybrid Vehicle with

Combined Fuel Economy and Low-Emission Objectives," *Proc. Inst. Mech. Eng. Part D J. Automob. Eng.*, vol. 228, no. 12, pp. 1424–1439, 2014.

[158] P. Chambon, D. Deter, D. Irick, and D. Smith, "PHEV Cold Start Emissions Management," *SAE Int. J. Alt. Power.*, vol. 2, no. 2, pp. 252–260, 2013.

[159] A. Sciarretta, J. C. Dabadie, and G. Font, "Automatic Model-Based Generation of Optimal Energy Management Strategies for Hybrid Powertrains," in *SIA POWERTRAIN:The low CO2 spark ignition engine of the futureand its hybridization*, 2015, pp. 375–382.

[160] M. Stöcker, N. Rohleder, H. Möckel, U. Säger, and M. Hailer, "Thermal Management for Energy – Efficient Improvement of Automobile Cooling Systems Based on Navigation Data," *25th Aachen Colloq. Automob. Engine Technol. 2016*, pp. 437–454, 2016.

[161] S. Gmeiner, P. Rajan, J. Gissing, and D. Backes, "VOSS Innovative Valve Technology for Thermal Management," in *25th Aachen Colloquium Automobile and Engine Technology*, 2016, no. section 2, pp. 471–490.

[162] M. Hopp, C. Ebert, K.-H. Hassel, and H. Dismon, "Thermal Conditioning and Efficiency Increase of Electric Vehicles Using a Heat Pump," in *25th Aachen Colloquium Automobile and Engine Technology 2016*, 2016, pp. 455–470.

[163] F. Bozza, V. De Bellis, A. Gimelli, and M. Muccillo, "Strategies for improving fuel consumption at part-load in a downsized turbocharged SI engine: a comparative study," *SAE Int. J. Engines*, vol. 7, no. 1, pp. 60–71, 2014.

[164] A. Gimelli, M. Muccillo, and O. Pennacchia, "Study of a new mechanical variable valve actuation system: Part II--estimation of the actual fuel consumption improvement through one-dimensional fluid dynamic analysis and valve train friction estimation," *Int. J. Engine Res.*, vol. 16, no. 6, pp. 762–772, 2015.

[165] "The different driving cycles." [Online]. Available: http://www.car-engineer.com/the-different-driving-cycles/. [Accessed: 27-Feb-2017].

[166] T. Barlow, S. Latham, I. Mccrae, and P. Boulter, "A reference book of driving cycles for use in the measurement of road vehicle emissions," *TRL Publ. Proj. Rep.*, p. 280, 2009.

[167] P. Mock, J. German, A. Bandivadekar, and I. Riemersma, "Discrepancies between type- approval and ' real-world ' fuel- consumption and CO 2 values," *Int. Counc. Clean Transp.*, vol. 2012–2, pp. 1–12, 2012.

[168] P. Mock, J. Kühlwein, U. Tietge, V. Franco, A. Bandivadekar, and J. German, "The WLTP: How a new test procedure for cars will affect fuel consumption values in the EU," *Int. Counc. Clean Transp.*, vol. 2014–9, no. October 2014, 2014.

[169] "Emission Test Cycles: Common Artemis Driving Cycles (CADC)." [Online]. Available: https://www.dieselnet.com/standards/cycles/artemis.php. [Accessed: 27-Feb-2017].

UNIVERSITE BRETAGNE LOIRE

CENTRALE NANTES

Thèse de Doctorat

Hanna SARA

Etude et valorisation de nouveaux systèmes de gestion thermique d'un groupe motopropulseur automobile

Analysis and valorization of new thermal management systems for a vehicle powertrain application

Résumé

La gestion thermique est un des moyens de réduction de la consommation spécifique d'un véhicule. Avec le réchauffement climatique, les normes de dépollution deviennent de plus en plus sévères et les constructeurs automobiles cherchent à améliorer le rendement des véhicules. Le but de ces travaux de recherche est de valoriser, par simulation numérique, les nouveaux systèmes de gestion thermique en fonction du cycle d'homologation et de la température ambiante.
Un modèle de simulation 1-D du moteur et de ses circuits de refroidissement et de lubrification ont été développés en utilisant le logiciel GT-Suite. Quatre cycles d'homologation ont été choisis : NEDC, WLTC, AH et AU. De plus, un nouveau cycle a été proposé durant cette étude. Le bilan d'énergie effectué pendant les différentes phases des cycles souligne l'importance du stockage et de la récupération d'énergie.
Le stockage d'énergie dans un volume eau et/ou d'huile abouti à l'amélioration de la montée en température des deux fluides. Plusieurs configurations ont été proposées comme, par exemple, un carter d'huile multifonctionnel. Ainsi, une réduction importante de la consommation en carburant est obtenue.
La récupération de chaleur au sein des gaz d'échappement est ensuite mise en œuvre. L'échangeur est caractérisé sur un banc d'essais puis modélisé. Le réchauffement indirect et direct d'huile abouti à une réduction importante des frottements et de la consommation. Une configuration est proposée afin de contrôler la température maximale de l'huile.
Finalement, différentes stratégies comme : le type d'huile, l'isolation du moteur, une température de régulation plus élevée etc… ont été étudiées et valorisées.

Mots clés
Moteur à combustion interne, Moteur Diesel, Gestion thermique, Bilan d'énergie, Stockage d'énergie, Stockage d'eau chaude, Stockage d'huile chaud, Récupération d'énergie, Echangeur thermique, Température, Consommation de carburant.

Abstract

Thermal management proved itself in improving the fuel efficiency of the engine. Nowadays, automotive companies tend to apply different strategies to answer the greenhouse severe laws. The PhD aim is to valorize and analyze the different thermal management strategies with numerical simulations over different driving cycles and ambient conditions.
A 1-D simulation code of the engine and its hydraulic circuits were built using GT-Suite. Four known driving cycles were chosen: NEDC, WLTC, AH and AU. In addition, an in-house developed driving cycle was introduced. An energy balance made over the different stages of the driving cycles underlines the importance of the heat storage and the exhaust heat recovery strategies.
Heat recovery was applied over the coolant and the oil at ambient temperatures of -7°C and 20°C. Hot coolant storage and hot oil storage led to improve the coolant and lubricant initial temperatures respectively. Different configurations (total of 7) were proposed and studied. A multifunctional oil sump was introduced. Important fuel consumption savings were obtained.
Exhaust heat recovery was then valorized. Heat exchanger was characterized over experimental setup then added to the engine model. Indirect and direct heating of the lubricant as well as both strategies back to back were tested. Remarkable friction reduction and fuel savings were obtained. Special configuration was proposed to control the lubricant high temperature instead of the bypass on the exhaust line.
The study ended by valorizing minor strategies as the oil's grade influence, the engine insulation, high temperature set point …

Key Words
Internal combustion engine, Diesel engine, Thermal management, Energy balance, Heat storage, Hot coolant storage, Hot oil storage, Heat recovery, Heat exchanger, Temperature, Fuel consumption.